

**GENOME SEQUENCING AND *IN SILICO*
CHARACTERISATION OF *CLADOSPORIUM*
*SPHAEROSPERMUM***

YEW SU MEI

**FACULTY OF MEDICINE
UNIVERSITY OF MALAYA
KUALA LUMPUR**

2017

**GENOME SEQUENCING AND *IN SILICO*
CHARACTERISATION OF *CLADOSPORIUM*
*SPHAEROSPERMUM***

YEW SU MEI

**THESIS SUBMITTED IN FULFILMENT OF THE
REQUIREMENTS FOR THE DEGREE OF DOCTOR OF
PHILOSOPHY**

**FACULTY OF MEDICINE
UNIVERSITY OF MALAYA
KUALA LUMPUR**

2017

UNIVERSITY OF MALAYA
ORIGINAL LITERARY WORK DECLARATION

Name of Candidate: **YEW SU MEI**

Registration/Matric No: **MHA110037**

Name of Degree: **Doctor of Philosophy**

Title of Thesis: **Genome Sequencing and *in silico* Characterisation of *Cladosporium sphaerospermum***

Field of Study: **MEDICAL MICROBIOLOGY**

I do solemnly and sincerely declare that:

- (1) I am the sole author/writer of this Work;
- (2) This Work is original;
- (3) Any use of any work in which copyright exists was done by way of fair dealing and for permitted purposes and any excerpt or extract from, or reference to or reproduction of any copyright work has been disclosed expressly and sufficiently and the title of the Work and its authorship have been acknowledged in this Work;
- (4) I do not have any actual knowledge nor do I ought reasonably to know that the making of this work constitutes an infringement of any copyright work;
- (5) I hereby assign all and every rights in the copyright to this Work to the University of Malaya ("UM"), who henceforth shall be owner of the copyright in this Work and that any reproduction or use in any form or by any means whatsoever is prohibited without the written consent of UM having been first had and obtained;
- (6) I am fully aware that if in the course of making this Work I have infringed any copyright whether intentionally or otherwise, I may be subject to legal action or any other action as may be determined by UM.

Candidate's Signature

Date:

Subscribed and solemnly declared before,

Witness's Signature

Date:

Name:

Designation:

ABSTRACT

Dematiaceous fungi are a taxonomically diverse group of heterogeneous fungi that are present in the environment. Although rare, many species in this group are known to cause diseases in humans and animals. In this study, a collection of 75 fungal isolates were recovered from various clinical specimens. They were identified through morphology and molecular methods using the internal transcribed spacer (ITS)-based phylogenetic analysis. The complementation of the molecular approach enables the identification of 73 isolates at the species level. The most common species isolated were *Cladosporium*, *Cochliobolus*, and *Neoscytalidium*. Also, 16 isolates from the seven species identified have not been reported to cause human infections. Among the *Cladosporium* species that were isolated, the species *C. sphaerospermum* was most frequently isolated. This study was proceeded by whole genome analysis of the *C. sphaerospermum*, using the strain UM 843 as a study model to explore genetic information and its basic biology. *C. sphaerospermum* is a ubiquitous saprophytic fungus that has been documented to cause allergy and other opportunistic diseases in humans. Detail characterisation of this isolate has affirmed the identity of UM 843 and its ability to survive in high salt medium (up to 20% NaCl). The genome of UM 843 was generated by combining 500-bp and 5-kb insert libraries, containing 9,652 predicted gene models in the 26.89 Mb genome. Functional annotation of the predicted genes suggests this fungus has the capability to degrade carbohydrate and protein complexes. The abundance of carbohydrate active enzymes (CAZymes) assists in the degradation of hemicellulose and pectin, thus suggesting the precedence of this fungus towards soft plant tissues. Putative genes encoding peptidases from family A01, S09, and M36 that share similarity with *Aspergillus* peptidases responsible for lung tissue hydrolysis were also identified. UM 843 was also found to carry 16 putative secondary

metabolite backbone genes, three of these are predicted to be responsible for the synthesis of melanin, siderophores, and cladosins. Besides siderophores, UM 843 contains gene encoding proteins that are involved in iron homeostasis via the reductive iron assimilation (RIA) process. In response to salinity, UM 843 was identified to encode 29 ion transporters and the synthesis of various compatible solutes. The analysis of sexual reproduction suggests that UM 843 is a heterothallic fungus. The genome of UM 843 revealed 28 putative genes associated with *C. sphaerospermum* allergy. Orthologous gene analysis on UM 843 with 22 other Dothideomycetes showed 125 genes uniquely present in UM 843. Of these, four genes were predicted to encode class 1 hydrophobins which may be allergens specific to *Cladosporium*. Further analysis showed that the mRNA of the four genes were detected by reverse transcription-polymerase chain reaction (RT-PCR). The genomic analysis of *C. sphaerospermum* UM 843, can significantly contribute to the knowledge of the biology and allergenicity of this species which has not been studied previously.

ABSTRAK

Kulat Dematiaceous merupakan kumpulan kulat heterogenus pelbagai taksonomi hadir dalam persekitaran. Walaupun jarang ditemui, kebanyakan spesies dalam kumpulan ini dikenalpasti berupaya menyebabkan jangkitan pada manusia dan haiwan. Di dalam kajian ini, sebanyak 75 pencilan kulat daripada pelbagai spesimen klinikal telah dikaji. Kulat-kulat ini telah dikenalpasti secara penggunaan kaedah morfologi dan molekul melalui analisis filogenetik berasaskan penjarak transkripsi dalaman (ITS). Pendekatan kaedah pelengkap molekul ini telah berjaya mengenalpasti 73 pencilan pada peringkat spesies. Spesies yang paling lazim dikenalpasti adalah *Cladosporium*, *Cochliobolus* dan *Neoscytalidium*. Selain itu, sebanyak 16 pencilan daripada tujuh spesies yang telah dikenalpasti tidak pernah dilaporkan lagi menyebabkan jangkitan pada manusia. *C. sphaerospermum* merupakan spesies yang paling kerap dipencil di antara spesies *Cladosporium* yang telah dikenalpasti. Kajian analisis keseluruhan genom *C. sphaerospermum* telah dilanjutkan dengan menggunakan strain UM 843 sebagai model kajian untuk meneroka maklumat genetik dan biologi asas pencilan tersebut. *C. sphaerospermum* merupakan kulat saprofitik *ubiquitous* yang sebelum ini telah dilaporkan menyebabkan tindak balas alahan dan penyakit oportunistik pada manusia. Identiti pencilan UM 843 telah disahkan secara pencirian teliti dan ia dikenalpasti mempunyai keupayaan hidup di dalam media yang mengandungi kandungan garam tinggi (sehingga 20% NaCl). Genom UM 843 yang dihasilkan melalui gabungan perpustakaan selitan bersaiz 500-bp dan 5-kb, mengandungi sebanyak 9,652 gen model diramalkan hadir dalam 26.89 Mb genom tersebut. Hasil ramalan kefungsi anotasi gen-gen ramalan menunjukkan kulat ini mempunyai keupayaan untuk mengurai kompleks karbohidrat dan protein. Kulat ini dicadangkan memberikan keutamaan pada tisu-tisu lembut oleh kerana kehadiran kandungan enzim aktif karbohidrat (CAZymes)

yang tinggi berupaya membantu di dalam penguraian hemiselulosa dan pektin. Kehadiran gen-gen putatif mengkodkan kumpulan peptidase A01, S09 dan M36 yang mempunyai persamaan dengan peptidase *Aspergillus* yang berperanan dalam hidrolisis tisu peparu telah berjaya dikenal pasti. UM 843 juga didapati mempunyai 16 gen putatif pengkodan gen tulang belakang metabolit sekunder, di mana tiga daripada gen ramalan tersebut mempunyai peranan di dalam sintesis melanin, siderofor dan kladosin. Selain daripada siderofor, UM 843 mengandungi gen pengkodan protein yang terlibat dalam homeostasis besi melalui proses asimilasi penurunan besi (RIA). Sebanyak 29 gen yang terlibat sebagai pengangkut ion dan sintesis pelbagai bahan larut serasi yang berupaya memberikan gerak balas terhadap kandungan garam tinggi turut dikenalpasti. Hasil analisis pembiakan seksual menunjukkan UM 843 merupakan kulat heterotalik. Sebanyak 28 gen yang berkemungkinan berkaitan dengan tindak balas alahan *C. sphaerospermum* turut didapati hadir dalam genom UM 843. Manakala hasil analisis gen ortolog UM 843 bersama 22 kulat dari kelas Dothideomycetes lain menunjukkan sebanyak 125 gen unik hadir di dalam UM 843. Antaranya adalah empat gen diramalkan mengkod hidrofobin kelas 1 yang bermungkinan merupakan alergen khusus kepada *Cladosporium*. Analisis lanjutan menunjukkan bahawa mRNA daripada empat gen tersebut dapat dikesan melalui tindak balas rantai polimerase transkripsi berbalik (RT-PCR). Analisis genom *C. sphaerospermum* UM 843 dijangka akan menyumbang kepada kefahaman biologi dan tindak balas alahan yang sebelum ini tidak pernah dikaji lagi.

ACKNOWLEDGEMENTS

First and foremost, I would like to express my deepest gratitude to my supervisor, Professor Dr. Ng Kee Peng for his guidance, encouragement throughout my doctoral study, and giving me the freedom to venture into research on my own. I am also thankful for Professor Dr. Ngeow Yun Fong for her suggestion and discussion on my work.

I would like to express my deepest appreciation to Dr. Kuan Chee Sian and collaborators from Codon Genomics Sdn Bhd (especially Dr. Yee Wai Yan and Lee Kok Wei), for their contribution to valuable feedback, assistance, advice and insightful discussion about the research.

I would like to thank all my friends (especially Fan Suet Pin, Kang Wen Tyng, Theresa Yap and Lydia Ong) and fellow colleagues from UM (Na Shiang Ling, Shirley Liew, Toh Yue Fen) for their help and make my time in the PhD pursuit more fun and interesting.

I take this opportunity to sincerely acknowledge the High Impact Research MoE Grant UM.C/625/1/HIR/MOHE/MED/31 (Account no. H-20001-00-E000070) from the Ministry of Education Malaysia and Postgraduate Research Grant (PPP) PV051/2012A from the University of Malaya for the support of this study.

Lastly, I am deeply thankful to my family members (especially my parents) for their unconditional love, sacrifices and for supporting me in everything.

TABLE OF CONTENTS

Abstract	iii
Abstrak	v
Acknowledgements	vii
Table of Contents	viii
List of Figures	xiii
List of Tables	xvi
List of Symbols and Abbreviations	xviii
List of Appendices	xxiii
CHAPTER 1: INTRODUCTION	26
1.0 Background	26
1.1 Hypothesis and objectives	28
CHAPTER 2: LITERATURE REVIEW	31
2.0 Introduction	31
2.1 Clinical mycology	32
2.2 Dematiaceous fungi	33
2.3 <i>Cladosporium</i> species	35
2.3.1 <i>Cladosporium sphaerospermum</i>	41
2.4 Next-generation sequencing (NGS)	42
2.5 Fungal genomes	47
2.6 Fungal nutrients	49
2.6.1 Fungal lifestyles in comparison to distributions of hydrolytic enzymes	53
2.7 Secondary metabolites	55
	viii

2.8	Melanin	59
2.9	Iron regulation	62
2.10	Stress responses	66
2.11	Sexual reproduction	69
2.12	Fungal allergy	70

CHAPTER 3: METHODOLOGY **75**

3.1	Dematiaceous fungal specimens collection and isolation	75
3.1.1	Morphological identification	75
3.1.1.1	Macroscopic observation	75
3.1.1.2	Microscopic observation	75
3.1.2	Molecular identification	76
3.1.2.1	Deoxyribonucleic acid (DNA) extraction	76
3.1.2.2	Polymerase chain reaction (PCR)	78
3.1.2.3	PCR product purification	79
3.1.2.4	DNA sequencing and fungal isolates identification	79
3.1.3	Data mining	80
3.1.4	Phylogenetic analysis	80
3.2	<i>Cladosporium sphaerospermum</i> UM 843	81
3.2.1	Morphological identification	81
3.2.1.1	Scanning electron microscope (SEM)	81
3.2.2	Data mining and phylogenetic tree construction	82
3.2.3	Genomic DNA extraction and sequencing	83
3.2.3.1	Genomic DNA extraction	83
3.2.3.2	Genomic DNA sequencing	84
3.3	<i>C. sphaerospermum</i> UM 843 genome <i>in silico</i> characterisation	85

3.3.1	Sequence pre-processing	85
3.3.2	<i>de novo</i> genome assembly, scaffolding, gap filling and contamination check	85
3.3.3	Gene prediction	87
3.3.4	Functional annotation	88
	3.3.4.1 Primary functional annotation	88
	3.3.4.2 Secondary functional annotation	89
3.3.5	Orthologous genes and genome comparative analysis	93
3.3.6	Phylogenomic analysis	93
3.3.7	Allergen genes in UM 843	94
3.4	Validation of gene sequences and detection of mRNA - hydrophobin genes	94
	3.4.1 mRNA detection	95
	3.4.1.1 RNA extraction	95
	3.4.1.2 Reverse transcription polymerase chain reaction (RT-PCR)	97
3.5	Data availability	98
CHAPTER 4: RESULTS		99
4.1	Fungal collection	99
	4.1.1 Morphological identification	106
	4.1.2 Molecular identification and phylogenetic analysis	110
	4.1.3 Congruence between morphological and molecular identification	111
4.2	<i>C. sphaerospermum</i> UM 843	113
	4.2.1 Morphological description and phylogenetic analysis	113
	4.2.2 Genomic deoxyribonucleic acid (DNA) extraction	117
	4.2.3 <i>C. sphaerospermum</i> UM 843 genome	120
	4.2.3.1 Transposable elements	122

4.2.3.2	Primary functional annotation	122
4.2.3.3	Carbohydrate metabolism	125
4.2.3.4	Peptidases	128
4.2.3.5	Secondary metabolites	133
4.2.3.6	Stress responses	140
4.2.3.7	Sexual reproduction	146
4.3	Phylogenomic analysis	149
4.3.1	Orthologous genes and genome comparative analysis	150
4.4	Fungal allergens	151
4.5	Validation of gene sequences and detection of mRNA	151
CHAPTER 5: DISCUSSION		159
5.1	Fungal collection	159
5.1.1	Molecular identification	162
5.2	<i>C. sphaerospermum</i> UM 843	166
5.2.1	Morphological description and phylogenetic analysis	166
5.2.2	<i>C. sphaerospermum</i> UM 843 genome	166
5.2.2.1	Transposable elements	167
5.2.2.2	Primary functional annotation	168
5.2.2.3	Carbohydrate metabolism	169
5.2.2.4	Peptidases	171
5.2.2.5	Secondary metabolites	172
5.2.2.6	Stress responses	174
5.2.2.7	Sexual reproduction	178
5.3	Phylogenomic analysis	179
5.3.1	Orthologous genes and genome comparative analysis	179

5.4	Fungal allergens	179
5.5	Validation of gene sequences and detection of mRNA	180
5.6	Recommendations for future studies	180
CHAPTER 6: CONCLUSION		182
References		185
List of Publications and Papers Presented		216
APPENDIX		243

University of Malaya

LIST OF FIGURES

Figure 1.1: Overview of this study.....	28
Figure 2.1: Roche 454 sequencing technology.	44
Figure 2.2: Illumina sequencing technology.....	45
Figure 2.3: SMRT bell template.....	46
Figure 2.4: PacBio sequencing technology.....	47
Figure 2.5: Pentaketide DHN-melanin biosynthesis pathway.	60
Figure 2.6: Siderophore biosynthesis pathway.	64
Figure 3.1: Schematic diagram of experimental procedures for dematiaceous fungi identification	77
Figure 3.2: Workflow of <i>C. sphaerospermum</i> UM 843 genome analysis	86
Figure 4.1: Number of isolates collected from the year 2006 to 2011.....	100
Figure 4.2: Number of specimens received in the Mycology Unit from the year 2006 to 2011	101
Figure 4.3: Colonial features of dematiaceous fungi isolated from specimens sent to Mycology Unit, UMMC.	107
Figure 4.4: Micrograph of dematiaceous fungi isolated from specimens sent to Mycology Unit, UMMC.	108
Figure 4.5: Culture and microscopic images of isolates with unidentifiable features. .	110
Figure 4.6: Taxonomic classification of dematiaceous fungi isolates.	112
Figure 4.7: Morphology of <i>C. sphaerospermum</i> UM 843.	115
Figure 4.8: Colonial features of <i>C. sphaerospermum</i> UM 843 grown on various media at 30°C.....	116
Figure 4.9: Colonial features of <i>C. sphaerospermum</i> UM 843 grown on various media at 25°C.....	116
Figure 4.10: Growth of UM 843 in SDB supplemented with various percentage (w/v) of NaCl.	117

Figure 4.11: ITS-based phylogenetic tree of <i>C. sphaerospermum</i> species complex. ...	118
Figure 4.12: Gel image of extracted genomic DNA sent for genome sequencing of the small insert (500-bp) library.	119
Figure 4.13: Gel image of extracted genomic DNA sent for genome sequencing of the large insert (5-kb) library.	119
Figure 4.14: Hash length optimisation graph for optimum assembly	121
Figure 4.15: KOG (a), KEGG (b) and GO (c) classifications of predicted genes in <i>C. sphaerospermum</i> UM 843.....	124
Figure 4.16: Comparison of <i>C. sphaerospermum</i> UM 843 CAZymes with other dematiaceous Dothideomycetes based on CAZyme families.....	127
Figure 4.17: Comparison of <i>C. sphaerospermum</i> UM 843 CAZymes with other dematiaceous Dothideomycetes based on substrate specificities.	127
Figure 4.18: Comparison of peptidases identified in <i>C. sphaerospermum</i> UM 843 with dematiaceous fungi from the class Dothideomycetes.....	128
Figure 4.19: Multiple sequence alignment of predicted DPP IV (UM843_2833) of <i>C. sphaerospermum</i> UM 843 with DPP IV from <i>A. fumigatus</i> (ASPFU_DPPIV; AAC34310.1) and <i>A. oryzae</i> (ASPOR_DPPIV; Q2UH35).	131
Figure 4.20: Multiple sequence alignment of predicted DPP V (UM843_1649) of <i>C. sphaerospermum</i> UM 843 with DPP V from <i>A. fumigatus</i> (ASPFU DPPV; AAB67282) and <i>A. terreus</i> (ASPTN_DPPV; Q0C8V9.1).....	132
Figure 4.21: Putative melanin biosynthesis cluster in UM 843.	135
Figure 4.22: Putative fusarinine-type siderophore biosynthesis cluster in UM 843.	136
Figure 4.23: Putative gene cluster involved in ferrichrome-type siderophore biosynthesis.....	137
Figure 4.24: Putative cluster of genes involved in the transportation of TAFC in UM 843.	137
Figure 4.25: Location of <i>prnC</i> and <i>prnD</i> gene in UM 843.....	141
Figure 4.26: Putative RIA system cluster in UM 843.....	142

Figure 4.27: Taurine biosynthesis pathway of UM 843 predicted via KEGG pathway map	145
Figure 4.28: Multiple sequence alignment of NAD-dependent <i>gpd</i> of <i>C. sphaerospermum</i> UM 843 (UM843_9164) with <i>gpd</i> gene from <i>W. ichthyophaga</i> (WiGpd1; CBW47554), <i>S. cerevisiae</i> (ScGpd1; CAA54189) and <i>H. werneckii</i> (HwGpd1A; AEM44788 and HwGpd1B; AEM44789).....	147
Figure 4.29: Multiple sequence alignment of <i>hog1</i> of <i>C. sphaerospermum</i> UM 843 (UM843_5411) with <i>H. werneckii</i> (HwHog1; AAM64214), <i>S. cerevisiae</i> (ScHog1; P32485) and <i>A. fumigatus</i> (AfSakA; XM_747571).....	148
Figure 4.30: Putative gene organisation of mating type gene cluster in UM 843.....	149
Figure 4.31: Phylogenomic tree of <i>C. sphaerospermum</i> and 22 fungi from the class Dothideomycetes.	150
Figure 4.32: Multiple sequence alignment of putative class I hydrophobin CDS in UM 843 (UM843_3639, UM843_1201, UM843_4115, UM843_6061) with hydrophobin CDS from <i>C. herbarum</i> Cla HCh 1 (Q8NIN9).	152
Figure 4.33: Gel image of extracted RNA.	154
Figure 4.34: Sequence alignment of hydrophobin predicted DNA sequence (1201_g), predicted CDS sequence (1201_t) and cDNA sequence (1201_9A) of <i>C. sphaerospermum</i> UM 843.....	155
Figure 4.35: Sequence alignment of hydrophobin predicted DNA sequence (3639_g), predicted CDS sequence (3639_t) and cDNA sequence (3639_9A) of <i>C. sphaerospermum</i> UM 843.....	156
Figure 4.36: Sequence alignment of hydrophobin predicted DNA sequence (4115_g), predicted CDS sequence (4115_t) and cDNA sequence (4115_9A) of <i>C. sphaerospermum</i> UM 843.....	157
Figure 4.37: Sequence alignment of hydrophobin predicted DNA sequence (6061_g), predicted CDS sequence (6061_t) and cDNA sequence (6061_9A) of <i>C. sphaerospermum</i> UM 843.....	158
Figure 5.1: Micrograph of the <i>Pyrenochaeta</i> (a) and <i>Phoma</i> (b) pycnidia.....	164

LIST OF TABLES

Table 2.1: List of <i>Cladosporium</i> infections collected from the literature.....	37
Table 3.1: Components of PCR master mix.....	78
Table 3.2: List of dematiaceous fungi used in the MEROPS analysis, orthologous genes and genome comparative analysis, and generation of phylogenomic tree	91
Table 3.3: Primer sets designed to be used in amplification of hydrophobin genes in UM 843	95
Table 3.4: Components of PCR master mix.....	95
Table 3.5: Components of reverse transcription process	98
Table 4.1: Details of dematiaceous fungi isolated in this study.....	102
Table 4.2: Isolates with incongruent morphological and molecular identity.....	113
Table 4.3: Genomic DNA quality and quantity assessment of UM 843.....	118
Table 4.4: Small insert library reads statistics of UM 843 genome	120
Table 4.5: Large insert library reads statistics of UM 843 genome	120
Table 4.6: Genome features of <i>C. sphaerospermum</i> UM 843 sequence reads generated from the combined libraries.....	121
Table 4.7: Transposable elements predicted in the <i>C. sphaerospermum</i> UM 843 genome	123
Table 4.8: Plant cell wall and fungal cell wall degrading and modifying CAZyme families predicted in <i>C. sphaerospermum</i> UM 843	125
Table 4.9: Oligopeptide and amino acid transporters identified based on PFAM domain in <i>C. sphaerospermum</i> UM 843	129
Table 4.10: List of homologous peptidase identified via MEROPS batch blast that showed identity to <i>A. fumigatus</i> peptidases that are involved in lung hydrolysis	130
Table 4.11: Secondary metabolite backbone genes predicted in UM 843 and their domain arrangement.....	133

Table 4.12: Putative genes involved in DHN-melanin biosynthesis.....	134
Table 4.13: Putative genes involved in siderophore biosynthesis, transportation and regulation in UM 843	135
Table 4.14: Putative PKS-NRPS hybrid gene cluster of UM 843	138
Table 4.15: Putative genes involved in proline catabolism predicted in UM 843	140
Table 4.16: Putative transporters involved in high salinity survival in UM 843, <i>W. ichthyophaga</i> , <i>H. werneckii</i> , and <i>M. graminicola</i>	143
Table 4.17: Putative genes involved in the synthesis of compatible solutes, transport of glycerol and HOG signalling pathway predicted in UM 843	144
Table 4.19: Gene sequence information of putative class I hydrophobin genes in UM 843	152
Table 4.20: Predicted localisation, protein size, signal peptide and cysteine content of putative hydrophobin genes	152
Table 4.18: Number of genes annotated as allergen (> 50% identity) in UM 843 compared to other members in Dothideomycetes	153
Table 4.21: Quality and quantity of UM 843 extracted RNA.....	154
Table 5.1: Reported human infection cases of dematiaceous species.....	160

LIST OF SYMBOLS AND ABBREVIATIONS

4'PP	:	4'-phosphopantetheine
A	:	adenylation
AA	:	auxiliary activities
ACP	:	acyl carrier protein
AIC	:	Akaike Information Criteria
AT	:	acyltransferase
ATP	:	adenosine triphosphate
BLAST	:	Basic Local Alignment Tool
bp	:	base pair
C	:	condensation
CAZymes	:	carbohydrate-active enzymes
CBM	:	carbohydrate binding module
cDNA	:	complementary DNA
CE	:	carbohydrate esterase
dbCAN	:	database for automated Carbohydrate-active enzyme ANnotation
DH	:	dehydratase
DHN	:	1,8-dihydroxynaphthalene
DMATS	:	dimethylallyl tryptophan synthase
DNA	:	deoxyribonucleic acid
DOE	:	US Department of Energy
DPP	:	dipeptidyl peptidase
EDTA	:	ethylenediamine tetraacetic acid
ER	:	enoyl reductase
FahA	:	fumarylacetoacetate hydrolase

Fe ²⁺	:	ferric ion
Fe ³⁺	:	ferrous ion
FSRD	:	Fungal Stress Response Database
g	:	gravity
GDP	:	glycerol-3-phosphate dehydrogenase
GH	:	glycoside hydrolase
gm	:	gram
GO	:	Gene Ontology
GPP	:	glycerol-3-phosphate
GT	:	glycosyl transferase
GTR	:	general time reversible
H ⁺	:	hydrogen ion
H ₂ O ₂	:	hydrogen peroxide
HIV/AIDS	:	human immunodeficiency virus infection and acquired immune deficiency syndrome
HMG	:	high mobility group
HmgA	:	homogentisate A
HOG	:	high osmolarity signalling
hppD	:	4-hydroxyphenylpyruvate dioxygenase
HR	:	highly reducing
i.e.	:	that is
ITS	:	internal transcribed spacer
JGI	:	Joint Genome Institute
K ⁺	:	potassium ion
kb	:	kilo basepair

KEGG	:	Kyoto Encyclopedia of Genes and Genomes
KOG	:	Eukaryotic Orthologous Group
KOH	:	potassium hydroxide
KR	:	ketoreductase
KS	:	ketosynthase
LCB	:	lactophenol cotton blue
L-DOPA	:	L-3,4-dihydroxyphenylalanine
LSU	:	large subunit
MaiA	:	maleylacetoacetate isomerase
MAPK	:	mitogen-activated protein kinase
Mb	:	Megabase pair
MCMC	:	Markov Chain Monte Carlo
MEA	:	Malt Extract Agar
mg/mL	:	miligram per mililitre
min	:	minute
mL	:	miliiltre
mRNA	:	messenger ribonucleic acid
MSA	:	multiple sequence alignment
mtSSU	:	mitochondrial small subunit
Na ⁺	:	sodium ion
NaCl	:	sodium chloride
NCBI	:	National Centre of Biotechnology Information
NGS	:	next-generation sequencing
NR	:	non-reducing
NRPS	:	nonribosomal peptide synthase

nuLSU	:	nuclear large subunit
OD	:	optical density
OPT	:	oligopeptide transporter
PAH	:	polycyclic aromatic hydrocarbons
PBS	:	phosphate buffered saline
PCR	:	polymerase chain reaction
PFAM	:	Protein families database of alignment and hidden Markov models
Pi	:	inorganic phosphate
PKS	:	polyketide synthase
PL	:	polysaccharide lyase
POT	:	proton-dependent oligopeptide transporter
PP	:	posterior probability
PR	:	partially reducing
PSRF	:	potential scale reduction factor
Qv	:	quality value
RPB2	:	RNA polymerase II
RIA	:	reductive iron assimilation
RNA	:	ribonucleic acid
ROS	:	reactive oxygen species
rRNA	:	ribosomal ribonucleic acid
RT-PCR	:	reverse transcription polymerase chain reaction
SAT	:	Starter unit: ACP transacylase
SDA	:	sabouraud dextrose agar
SDB	:	sabouraud dextrose broth
SDS	:	sodium dodecyl sulfate

sec	:	second
SEM	:	scanning electron microscope
SMRT	:	real-time sequencing technology
SMURF	:	Secondary Metabolite Unknown Region Finders
sp.	:	species
spp.	:	species (plural)
T	:	thiolation
T3HN	:	1,3,8-trihydroxynaphthalene
T4HN	:	1,3,6,8-tetrahydroxynaphthalene
TAFC	:	triacylfusarinine C
TBE	:	Tris-borate-EDTA
TC	:	terpene cyclase
TE	:	thioesterase
TM	:	transmembrane domains
T _m	:	melting temperature
Tris-HCl	:	Tris-hydrochloride
tRNA	:	transfer ribonucleic acid
UMMC	:	Universiti Malaya Medical Centre
UV	:	ultraviolet
V	:	volt
w/v	:	weight per volume
WHO/IUIS	:	World Health Organisation and International Union of Immunological Species
ZMW	:	zero-mode waveguide
μL	:	microlitre

LIST OF APPENDICES

Appendix A: Preparation of media and reagents.....	243
Appendix B: Preparation of agarose gel and electrophoresis workflow.....	246
Appendix C1: List of fungal species and accession number obtained from NCBI GenBank for the phylogenetic tree construction.....	247
Appendix C2: List of species from the <i>C. sphaerospermum</i> species complex obtained from NCBI GenBank for the generation of <i>C.</i> <i>sphaerospermum</i> species complex phylogenetic tree.....	249
Appendix D1: Sequence quality trimming for small insert library of UM 843 genome.....	250
Appendix D2: Sequence quality trimming for large insert library of UM 843 genome.....	254
Appendix D3: CAZyme families predicted in the genome of UM 843.....	258
Appendix D4: Comparison of <i>C. sphaerospermum</i> UM 843 CAZymes with other dematiaceous Dothideomycetes based on substrate specificities.....	260
Appendix D5: Multiple sequence alignment of UM 843 putative IRGF.....	270
Appendix D6: Sequence analysis of fusarinine-type siderophore biosynthesis cluster for identification GATA binding sites.....	271
Appendix D7: Sequence analysis of TAFC transporter cluster for identification of GATA binding sites.....	273
Appendix D8: Sequence analysis of ferrichrome-type siderophore biosynthesis cluster for identification of GATA binding sites.....	274
Appendix D9: Putative genes involved in response to heat predicted in <i>C.</i> <i>sphaerospermum</i> UM843 using FSRD.....	275

Appendix D10: Putative genes involved in starvation predicted in <i>C. sphaerospermum</i> UM843 using FSRD.....	280
Appendix D11: Putative genes involved oxidative stress responses predicted in <i>C. sphaerospermum</i> UM843 using FSRD.....	290
Appendix D12: Sequence analysis of the RIA cluster for identification of GATA binding sites.....	306
Appendix D13: List of putative transporters predicted in UM 843.....	307
Appendix D14: V-type ATPase V ₀ and V ₁ complexes identified in UM 843.....	309
Appendix D15: P-type ATPases identified in UM 843.....	310
Appendix D16: TMpred output of putative glycerol/H ⁺ symporter (Slt1) in UM 843.....	311
Appendix D17: List of UM 843 predicted genes involved in mating, signalling, fruit body development and meiosis.....	312
Appendix D18: <i>C. sphaerospermum</i> UM 843 specific gene families clusters compared to 22 publicly available dematiaceous Dothideomycetes genome.....	315
Appendix D19: Allergen gene homologues predicted in <i>C. sphaerospermum</i> UM 843.....	319
Appendix D20: Gel image of putative hydrophobin genes in UM 843.....	322
Appendix D21: Gel image of putative hydrophobin mRNA in UM 843.....	323
Appendix D22: Sequencing chromatogram of UM843_1201 cDNA by forward primer (a) and reverse primer (b).....	324
Appendix D23: Sequencing chromatogram of UM843_3639 cDNA by forward primer (a) and reverse primer (b).....	325

Appendix D24: Sequencing chromatogram of UM843_4115 cDNA forward primer by (a) and reverse primer (b).....	326
Appendix D25: Sequencing chromatogram of UM843_6061 cDNA by forward primer (a) and reverse primer (b)	327

University of Malaya

CHAPTER 1: INTRODUCTION

1.0 Background

Fungal infections have appeared in the last two decades as the leading cause of infections, especially in immunocompromised patients and, therefore, may be encountered in a wide variety of cases. They are often life-threatening in immunocompromised patients and the mortality rates have increased nearly 4-folds in the last 20 years (Kubak & Hprikar, 2009; Pfaller & Diekema, 2010). As the number of immunodeficient patients is increasing, the list of fungal pathogens is also expanding and many rare fungal pathogens are emerging as etiologic agents of mycoses.

Dematiaceous fungi, is one of the emerging fungal pathogens, comprising both yeasts and filamentous moulds. These are a taxonomically diverse group of heterogeneous fungi characterised by its dark appearance owing to a melanin-containing cell wall that distinguishes this group from other fungi. They are ubiquitous saprophytes that are predominantly found in soil, wood, decaying plant material and are common laboratory contaminants (Revankar, 2007; Rossmann, Cernoch, & Davis, 1996). Infections caused by dematiaceous fungi are rare but these fungi have been increasingly recognised as important pathogens because they can cause diseases in both immunocompetent and immunodeficient patients (Kumar & Hallikeri, 2008; Levin, Baty, Fekete, Truant, & Suh, 2004; Revankar, 2007). Until year 2010, more than 150 species belonging to 70 genera of dematiaceous fungi have been reported as pathogens in humans and animals (Revankar & Sutton, 2010) as compared to 59 species of 28 genera reported by Rossmann et al. in the year 1996. The distribution of dematiaceous fungal pathogens in causing human infections are geographically restricted (Revankar & Sutton, 2010).

In this study, a total of 75 dematiaceous fungi was collected from specimens sent to the Mycology Unit at Universiti Malaya Medical Centre (UMMC) for fungal culture. Of all the isolates identified, *Cladosporium sphaerospermum* was found to be the most frequently isolated species. The project was proceeded by whole genome sequencing and genome analyses using *C. sphaerospermum* UM 843 as the model of study (Figure 1.1). *Cladosporium* is a dematiaceous fungus belonging to the order Capnodiales and family *Davidiellaceae*. It is a saprophyte found in both natural and man-made environments (Bensch, Braun, Groenewald, & Crous, 2012). It has also exhibited the ability to survive in extreme conditions such as hypersaline water (Zalar et al., 2007) and radiation-contaminated wall and soil at the damaged nuclear power plant in Chernobyl (Dadachova et al., 2007). Despite living in the environment, few species of *Cladosporium* including *C. sphaerospermum* has been reported to cause infections in human (Castro, Oliveira, & Lopes, 2013; de Hoog, Guarro, Gene, & Figueras, 2000; Qiu-Xia et al., 2008; Romano, Bilenchi, Alessandrini, & Miracco, 1999).

Apart from causing infections in humans, fungi are also associated with hypersensitive reactions in an estimated 20-30% of atopic cases worldwide (Gioulekas et al., 2004). *Cladosporium* species are among the most common airborne fungi with worldwide distribution (Knutsen et al., 2012). It is also an active aero-allergen causing allergic diseases of the respiratory tract and intrabronchial lesions (Tasic & Tasic, 2007). Although *C. sphaerospermum* has been reported to cause an allergic reaction (Dixit & Kwilinski, 2000), research on *C. sphaerospermum* allergen is currently unavailable. Well-characterised allergen studies were only conducted on *C. herbarum*. In this study, all the potential allergens of *C. sphaerospermum* were identified from its genome.

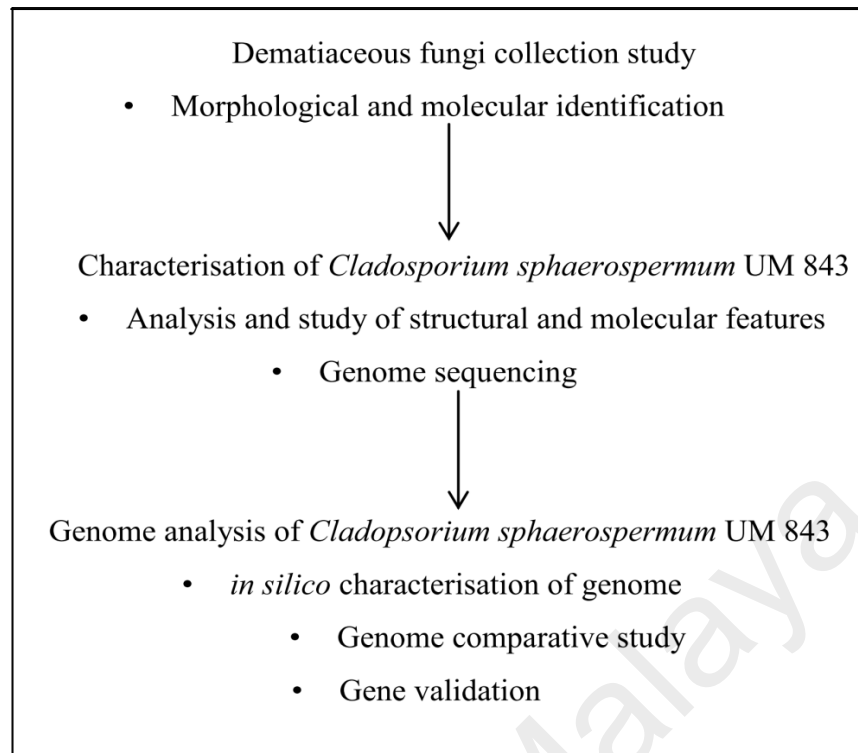


Figure 1.1: Overview of this study

Next-generation sequencing (NGS), also known as massively parallel sequencing, is the second generation of sequencing technology that enables the random reading of DNA templates along the entire genome (Zhang, Chiodini, Badr, & Zhang, 2011). By using bioinformatics methods, the sequences are assembled to generate a whole genome map. From the genome sequence, the genes that are present in a species, particularly those that are involved in pathogenesis, will be revealed. Specific research can then be done to investigate the role of functional proteins of the genes in disease development and the feasibility of using such proteins as genetic markers for diagnosis as well as patient management.

1.1 Hypothesis and objectives

Many studies have reported that dematiaceous fungi were recovered from both immunocompetent and immunocompromised individuals (Kumar & Hallikeri, 2008; Levin et al., 2004, Revankar, 2007). A recent study showed the isolation of numerous

dematiaceous fungi from different human anatomical sites leading to a hypothesis that most of the dematiaceous fungi are emerging pathogens and not merely an environment contaminant. They have evolved to adapt and colonise the human host to cause diseases. In this study, *C. sphaerospermum* is employed as a fungal model to investigate its underlying biology, adaptation and survival in a plethora of niches.

In this study, NGS is used to uncover the underlying genome and regulatory genes in *C. sphaerospermum*. The isolate, UM 843 would be the first reference strain of *C. sphaerospermum* isolated from clinical sample to be sequenced. The findings in this thesis provide a better understanding of the biology of this species and to elucidate potential allergens, and serve as the fundamental for in-depth studies, such as functional characterisation of the genes in future research. The genome is also useful in many different perspectives of fungal genome studies.

The objectives of this study were:

- i. To identify and determine the diversity of the dematiaceous fungi isolated from clinical specimens in Universiti Malaya Medical Centre (UMMC) using morphological examination and internal transcribed spacer (ITS)-based phylogeny
- ii. To morphologically and molecularly characterise *C. sphaerospermum* strain UM 843
- iii. To generate the draft genome of *C. sphaerospermum* UM 843 using next generation sequencing approach
- iv. To analyse the genome content of *C. sphaerospermum* UM 843. *In silico* analyses were conducted to:
 - a) reveal the genome features of *C. sphaerospermum* UM 843

- b) exploit the genomic background that is underlying the biology of *C. sphaerospermum* UM 843 by the study of the genes present in the genome based on functional annotation such as carbohydrate metabolism, peptidases, secondary metabolites, stress responses, sexual reproduction and putative allergens
- c) determine the conserved and specific genes present in UM 843 by comparative genome analysis with other fungi from the class Dothideomycetes
- v. To validate the hydrophobin genes in *C. sphaerospermum* UM 843 genome

CHAPTER 2: LITERATURE REVIEW

2.0 Introduction

Fungi are eukaryotic, non-photosynthetic and heterotrophic organisms that live as saprophytes, parasites or symbionts of animals and plants under nearly all environmental conditions. Out of over 10,000 fungal species reported, a few hundred occur as opportunists and about 100 are known to elicit mycoses in human and animals (de Hoog et al., 2000). Fungal infections have appeared in the last two decades as the leading cause of infections especially in immunocompromised patients and, therefore, may be encountered in a wide variety of cases. They are often life threatening in immunocompromised patients and mortality due to these infections has increased nearly 4-fold in the last 20 years. Immunocompromised individuals include those with neutropenia, haematological malignancies, renal failure, diabetes mellitus and Human Immunodeficiency Virus infection and Acquired Immune Deficiency Syndrome (HIV/AIDS), individuals with inherited immunity disorders, haematopoietic stem cell transplant or solid organ transplant recipients, and even those individual receiving immunosuppressive medications and undergoing chemotherapy (Badiee & Hashemizadeh, 2014; Black & Baden, 2007; Kubak & Huprikar, 2009; Pfaller & Diekema, 2010).

As the number of immunodeficient patients is increasing, the list of fungal pathogens that cause infections is expanding where rare fungal pathogens are emerging as etiologic agents of mycoses. The word 'emerging' is used to depict these fungal agents because they have not yet been discovered, diagnosed or reported as etiological agents of fungal infections (Enoch, Ludlam, & Brown, 2006; Pfaller & Diekema, 2010; Walsh et al., 2004).

2.1 Clinical mycology

Conventionally, pathogens have been categorised into obligate, facultative and opportunistic. Obligate pathogens infect only a narrow range of hosts, and the individual can be immunocompetent. Similarly, facultative pathogens infect a narrow range of hosts, but these pathogens can survive outside the host environment. Lastly, the opportunistic pathogens survive in a wide variety of organic substrates and exhibit low virulence towards a broad range of living hosts. The opportunists attack the host bellicously when the immune system of the host becomes impaired (van Baarlen, van Belkum, Summerbell, Crous, & Thomma, 2007).

The emerging fungal pathogens can be classified into moulds and yeasts as well as, hyaline and dematiaceous (pigmented). Moulds can be further distinguished into opportunistic and endemic (dimorphic); septate or non-septate (zygomycetes) (Groll & Walsh, 2001). Clinical fungi have been categorised into three groups (Guarro, Gené, & Stchigel, 1999a); dermatophytes which infect human skin, nails and hairs; dimorphic fungi which appear in both filamentous and yeast form under the influenced of temperature such as *Penicillium marneffeii* where this group of fungi able to infect immunocompetent individuals and lastly, the opportunistic fungi which are capable of causing diseases in immunocompromised or immunosuppressed individual.

In the mycology laboratory, the identification of fungal isolates is heavily based on the phenotypic characters, which is the morphological appearance of the isolate on the culture and under a microscope. Microscopic determination of fungal identity is done by observing the conidia and types of conidiogenesis. Physiological and biochemical tests are only carried out on yeast samples but not on filamentous moulds due to time constraint, laborious, and poor resolution obtained (Guarro et al., 1999b). The difference in colony appearance on different types of culture media, incubation temperature, the

various forms of a fungal species (synanamorph) and the high similarity of some species have made identification of the fungal isolates difficult especially for an inexperienced mycologist. Moreover, diagnostic morphological characters may not be observed for some isolates which are grouped as mycelia sterilia.

Species identification of causative fungi is essential as species may differ in pathogenicity and antifungal profiles (Boekhout, de Hoog, Samson, Varga, & Walther, 2009). Identification will be difficult if the fungus belongs to species complex, which is a group of distinct species that has very similar morphological appearance (Bickford et al., 2007). Hence, molecular tests offer an alternative approach to the identification of fungal species. Deoxyribonucleic acid (DNA) amplification of the internal transcribed spacers (ITS1 and ITS2) or conserved ribosomal ribonucleic acid (rRNA) genes (18S rRNA, 5.8S rRNA and the 5' end of the 28S rRNA) is the most often used method in fungal identification (Evertsson, Monstein, & Johansson, 2000; Hinrikson, Hurst, Lott, Warnock, & Morrison, 2005; Tsui et al., 2011). With the use of molecular methods, identification and taxonomy study of fungi is progressing drastically (Blackwell, 2011).

2.2 Dematiaceous fungi

The infections caused by dematiaceous fungi are rare but these fungi have been increasingly recognised as important pathogens because they have been reported to cause infections even in immunocompetent individuals who may not have any underlying prerequisite immunodeficiency (Kumar & Hallikeri, 2008; Levin et al., 2004; Revankar, 2007). As reported in a retrospective analysis of 101 cases of central nervous system phaeohyphomycosis, over half of the cases occurred in immunocompetent patients (Revankar, Sutton, & Rinaldi, 2004). Moreover, a clinical-epidemiological and diagnostic study conducted in Brazil reported the increasing trend of phaeohyphomycosis in the last ten years since 2012. The infections caused by non-

human pathogens are emerging as new cases of dematiaceous infections are also reported (Severo, Oliveira, Pilar, & Severo, 2012). In the normal host, dematiaceous fungi usually cause skin lesions in subcutaneous tissues following trauma. In immunocompromised patients, these pathogens have been increasingly recognised to cause sinusitis, pneumonia and disseminated infection (Groll & Walsh, 2001). Thus, rapid detection and accurate identification of fungal pathogens are important in diagnostic laboratories to ensure early and appropriate therapy for infected patients (Revankar & Sutton, 2010; Revankar, 2007; Rossmann et al., 1996).

The extent of diseases associated with dematiaceous fungi ranges from the superficial skin and soft tissue infections to disseminated sepsis with high mortality. The diseases can be distinguished into three types based on histological findings into chromoblastomycosis, eumycetoma and phaeohyphomycosis (de Hoog et al., 2000; Revankar & Sutton, 2010). Chromoblastomycosis is a chronic infection of cutaneous and subcutaneous mycosis which mostly occurs on the extremities, as a result of traumatic implantation of fungi through the skin. It is characterised by localised, slowly expanding sclerotic bodies in tissues. This type of infection is usually seen in tropical areas and associated with *Fonsecaea*, *Phialophora*, *Cladosporium* and *Rhinocladiella* species (Krzyściak, Pindycka-Piaszczyńska, & Piaszczyński, 2014; Queiroz-Telles et al., 2009). Eumycetoma is a chronic subcutaneous mycosis with necrotic pus forming lesions with cavities in tissue. The exudate discharged through multiple fistulae to the surface of skin contains compact grains. Each grain is a hyphal microcolony where the morphology of the species can be observed. The primary causative agent of eumycetoma is *Madurella mycetomatis* and occasionally by *Exophiala jeanselmei*, *Medicopsis romeroi* (formerly known as *Pyrenochaeta romeroi*) and *Curvularia* species (Ahmed, van den Ende, Fahal, van de Sande, & de Hoog, 2014; van Belkum, Fahal, &

van de Sande, 2013). Phaeohyphomycosis is a general term for the infections caused by dematiaceous fungi where the fungus is present in host tissue with melanised filaments. The term 'phaeohyphomycosis' was introduced by Ajello in 1974 to denote the diseases caused by dematiaceous fungi. 'Phaeo' comes from the Greek word meaning 'dark' (Kumar & Hallikeri, 2008). Most of the dematiaceous fungi such as *Exophiala dermatitidis*, *Cladophialophora bantiana*, *Ochroconis gallopava* and *Ramichloridium mackenziei* are opportunistic pathogen although some have been reported to be true neutropenic pathogens with a predilection for nervous tissue which causes cerebral phaeohyphomycosis (Kantarcioğlu & de Hoog, 2004).

The distribution of dematiaceous diseases varies with geographical location. For instance, the most common cause of cerebral phaeohyphomycosis has been reported to be *C. bantiana* in Europe but *R. mackenziei* has been found to be prominent in Middle Eastern countries, including Saudi Arabia, Syria, and Kuwait (Kantarcioğlu & de Hoog, 2004). Chromoblastomycosis has a higher prevalence in tropical and subtropical rural countries (Krzyściak et al., 2014). While eumycetoma is endemic mainly in the tropical areas such as Central Africa, Central America and India (Nenoff, van de Sande, Fahal, Reinel, & Schöfer, 2015). In the tropics, tinea nigra caused by *Hortaea werneckii* is commonly reported in coastal regions while chromoblastomycosis caused by *Cladophialophora carrionii* is commonly reported in subtropical regions (Hsu, Wijaya, Ng, & Gotuzzo, 2012).

2.3 *Cladosporium* species

Cladosporium belongs to the order Capnodiales and family *Davidiellaceae*. Based on the re-examination of comprehensive morphological features and molecular data, the number of *Cladosporium* species has increased from 772 in 2004 (Dugan, Schubert, & Braun, 2004) to 854 in 2012 (Bensch et al., 2012), because numerous taxa have been

placed into new genera. Three major species complexes have been determined in this genus; they are *C. herbarum* (Schubert et al., 2007), *C. sphaerospermum* (Zalar et al., 2007) and *C. cladosporioides* species complexes (Bensch et al., 2010). Species in this genus have a broad ecological niche and are ubiquitous in nature. Some of the species inhabit a particular niche, such as the hypersaline environment, as reported in several species of *C. herbarum* and *C. sphaerospermum*-like species complexes. Also, some species are plant pathogens causing leaf spot, while some live as phylloplane fungi and fungicolous fungi (Bensch et al., 2010; Heuchert, Braun, & Schubert, 2005; Schubert et al., 2007; Zalar et al., 2007).

Occasionally, *Cladosporium* species cause infection in humans. At least 24 cases of *Cladosporium* infections have been reported in the literature (Table 2.1). The diseases caused by *Cladosporium* species are independent of host immune status and most of the infections are either subcutaneous or cutaneous phaeohyphomycosis. Apart from subcutaneous and cutaneous infections, pulmonary phaeohyphomycosis appears to be the most frequent infection. Among the 24 cases, 13 cases were caused by *C. cladosporioides*, followed by *C. sphaerospermum* with six incidences and *C. oxysporum* with three. Also, three species of this genus, namely *C. herbarum*, *C. cladosporioides* and *C. sphaerospermum* have been reported to cause an allergic reaction (Section 2.12).

Table 2.1: List of *Cladosporium* infections collected from the literature

No.	Reference	Pathogen	Gender	Age	Infection and source	Location	Underlying condition	Prognosis
1.	Tamsikar, Naidu, & Singh (2006)	<i>C. cladosporioides</i>	F	24	Cutaneous phaeohyphomycosis, sebaceous cyst lesion	Back	Healthy individual	Healed
2.	Kwon Chung et al. (1975) (as cited in Tamsikar et al., 2006)	<i>C. cladosporioides</i>	-	-	Pulmonary intracavity fungus	Lungs	Immuno-suppressed	Not known
3.	Foster (1975) (as cited in Tamsikar et al., 2006)	<i>C. cladosporioides</i>	-	-	Keratitis, corneal ulcer	Eye	Not known	Healed
4.	Polack (1976) (as cited in Tamsikar et al., 2006)	<i>C. cladosporioides</i>	-	-	Chromomycosis, corneal ulcer	Eye	Antiviral and steroid treatment	Healed
5.	Gugnani (1978) (as cited in Tamsikar et al., 2006)	<i>C. cladosporioides</i>	-	-	Keratitis, corneal ulcer	Eye	Trauma, warm and moist climate and agricultural	Not known
6.	Ramani (1992) (as cited in Tamsikar et al., 2006)	<i>C. cladosporioides</i>	-	-	Not known	Forefoot	Not known	Healed
7.	Annessi, Cimitan, Zambruno, & Di Silverio (1992)	<i>C. cladosporioides</i>	M	54	Cutaneous phaeohyphomycosis, skin lesion	Knee and thigh	Pemphigus vulgaris, steroid induced diabetes	Not known
8.	Gugnani, Sood, Singh, & Makkar (2000)	<i>C. cladosporioides</i>	M	25	Subcutaneous phaeohyphomycosis, skin lesion	Right leg	Healthy individual	Healed

Table 2.1, continued

No.	Reference	Pathogen	Gender	Age	Infection and source	Location	Underlying condition	Prognosis
9.	Vieira, Milheiro, & Pacheco (2001)	<i>C. cladosporioides</i>	M	45	Subcutaneous phaeohyphomycosis	Left thigh	Healthy individual	Healed
10.	Kantarcioglu, Yucel, & de Hoog (2002)	<i>C. cladosporioides</i>	M	30	Cerebral phaeohyphomycosis, cerebrospinal fluid and brain biopsy	Brain	Healthy individual	Death
11.	Chew, Subrayan, Chong, Goh, & Ng (2009)	<i>C. cladosporioides</i>	M	37	Keratomycosis, corneal scraping	Left eye	Corneal laceration	Healed
12.	Aglawe, Tamrakar, Singh, & Sontakke (2013)	<i>C. cladosporioides</i>	M	60	Systemic phaeohyphomycosis, peripheral blood	-	Tuberculosis and gangrene	Not known
13.	Castro et al. (2013)	<i>C. cladosporioides</i>	F	27	Pulmonary phaeohyphomycosis, bronchoalveolar lavage fluid	Lung	Healthy individual	Healed
14.	Shukla et al. (1983) (as cited in de Hoog et al., 2000)	<i>C. sphaerospermum</i>	-	-	Keratitis, corneal ulcer	Eye	Not known	Not known
15.	Bdillet et al. (1982) (as cited in de Hoog et al., 2000)	<i>C. sphaerospermum</i>	-	-	Skin lesions and onychomycoses	Not known	Not known	Not known
16.	Yano, Koyabashi, & Kato (2003)	<i>C. sphaerospermum</i>	F	59	Intrabronchial lesion	Lung	Healthy individual	Not known

Table 2.1, continued

No.	Reference	Pathogen	Gender	Age	Infection and source	Location	Underlying condition	Prognosis
17.	Qiu-Xia et al. (2008)	<i>C. sphaerospermum</i>	-	53	Subcutaneous phaeohyphomycosis, skin biopsy	Right hand	Healthy individual	Not known
18.	Maduri et al. (2015)	<i>C. sphaerospermum</i>	F	65	Subcutaneous phaeohyphomycosis, nodule aspirate	Right hand	Non-Hodgkin's lymphoma, diabetes	Not known
19.	Soumagne, Pana-Katatali, Degano, & Dalphin (2015)	<i>C. sphaerospermum</i>	F	72	Combined pulmonary fibrosis and emphysema in hypersensitivity pneumonitis	Lungs	Healthy	Not known
20.	Forster et al. (1975) (as cited in de Hoog et al., 2000)	<i>C. oxysporum</i>	-	-	Keratitis	Not known	Not known	Not known
21.	Romano et al. (1999)	<i>C. oxysporum</i>	F	66	Cutaneous phaeohyphomycosis, nodular lesion	Right leg	Trauma, immunocompromised Cushing syndrome	Healed
22.	Gugnani et al. (2006)	<i>C. oxysporum</i>	F	30	Cutaneous phaeohyphomycosis, nodular lesion	Left foot	Healthy individual	Healed
23.	de Brevre (1982) (as cited in de Hoog et al., 2000)	<i>C. herbarum</i>	-	-	Skin lesions	Not known	Not known	Not known

Table 2.1, continued

No.	Reference	Pathogen	Gender	Age	Infection and source	Location	Underlying condition	Prognosis
24.	Castro & Gomperta (1984) (as cited in de Hoog et al., 2000)	<i>C. elatum</i>	-	-	Subcutaneous infection	Not known	Not known	Not known

2.3.1 *Cladosporium sphaerospermum*

C. sphaerospermum, belonging to the *C. sphaerospermum* species complex, is a cosmopolitan fungus found in hypersaline water in the Mediterranean and tropics, soil and plants in temperate climates, indoor wet cells, human and indoor and outdoor air (Zalar et al., 2007). The fungi belong to this group are usually identified as airborne contaminants and occupy a wide variety of habitat (Zalar et al., 2007). *C. sphaerospermum* was first described by Penzig in 1882 in decaying Citrus leaves and branches in Italy (Zalar et al., 2007). The species complex in this group includes *C. sphaerospermum*, *C. dominicanum*, *C. psychrotolerans*, *C. velox*, *C. spinulosum*, *C. halotolerans*, *C. langeronii*, *C. salinae* and *C. fusiforme*.

Apart from that, *C. sphaerospermum* has been reported being isolated from the soybean root where it lives as a gibberellins-producing endophyte (Hamayun et al., 2009). It has also been isolated from the soil of an aged gas manufacturing site that was rich in polycyclic aromatic hydrocarbons (PAH), a toxic and carcinogenic compound that is hazardous to public health. The strain was found able to degrade such compounds and serve as a potential bioremediation agent (Potin, Veignie, & Rafin, 2004). *C. sphaerospermum* is the dominant fungal species isolated from the radioactively contaminated wall and soil at the damaged nuclear power plant in Chernobyl (Zhdanova, Zakharchenko, Vember, & Nakonechnaya, 2000). Further study revealed that the radiation enhanced the growth of melanised *C. sphaerospermum* cells under nutrients restrained conditions (Dadachova et al., 2007).

Also, an *in vivo* study of the *C. sphaerospermum* pathogenicity using murine as a model was conducted (Huyan et al., 2012). The study involved inoculation of fungal suspension via dermabrasion, subcutaneous injection and intravenous injection. It

demonstrated that immunocompromised mice were more prone to infection and had delayed healing when compared to the immunocompetent mice. Death even occurred in mice subjected to systemic infection via intravenous injection of the spore suspension. In the systemic infection model, *C. sphaerospermum* was shown to possess tropism towards the lungs, followed by spleen, liver, kidneys and lastly the heart, irrespective of the host immune status. The findings suggested that the lungs were the most susceptible tissue in systemic infection.

2.4 Next-generation sequencing (NGS)

The revelation of DNA as the code of biological life and the sequencing of DNA have led to the effort to unravel its mysteries within an organism. With the advancement in sequencing technology, researchers are now able to decipher the whole genome content of an organism (Zhang et al., 2011). The DNA sequencing performed by Sanger method, the pioneer sequencing technology, provides excellent accuracy and reasonable length (1,000-1,200 bp) but it gives very low throughput. NGS technology provides high throughput of data as it sequences DNA templates in parallel and generates a huge amount of sequencing data. However, the read length of sequence reads is low (35-500 bp). Thus, the parameter coverage is necessary to identify the number of reads that overlap with each other in a specific genomic region, to ensure the assembly is accurate.

Various NGS platforms are available, such as Roche 454, Illumina and the relatively new PacBio. Each of these platforms utilises different approach and chemistry, thus producing different read length, GC bias, output and accuracy of the data. The 454 system by Roche is the first sequencer available and was used to sequence the second complete genome of an individual (D. A. Wheeler et al., 2008). This sequencer employs

sequencing-by-synthesis technology known as pyrosequencing. The amplification of DNA templates is done via emulsion-based clonal polymerase chain reaction (PCR) approach (Margulies et al., 2005), where each single stranded DNA template bound to beads is compartmentalised into aqueous micelles containing PCR reactants (Figure 2.1a). The beads with single stranded DNA are then deposited on a picotitre plate, with one bead in a well (Figure 2.1b). When a nucleotide is incorporated into the DNA strand, pyrophosphate is released and then converted to adenosine triphosphate (ATP) by sulfurylase. This is followed by the reaction of luciferase oxidises luciferin using ATP and generation of chemiluminescence. Each base is added individually and sequentially. Thus, the light signalling of the nucleotide can be correlated with the particular nucleotide being incorporated. The advantage of Roche 454 technology is the ability to generate the longest short reads (500-800 bp) and good raw base accuracy (99%). However, it is prone to insertions and deletions, resulting in the misinterpretation of homopolymers, i.e. sequences with identical bases (Gilles et al., 2011; Hert, Fredlake, & Barron, 2008). The increased read length in other new technologies (e.g. PacBio) has made Roche 454 technology less cost efficient and is in the process of being phased out in mid 2016 (Buermans & den Dunnen, 2014).

The Illumina sequencing technology is the second platform commercially available, and is still commonly used (Zhang et al., 2011). The sequencer uses the sequencing-by-synthesis technology with reversible nucleotide terminator chemistry and bridge amplification to amplify the DNA template before the sequencing process (<http://www.illumina.com/>) (Figure 2.2). The sequencing and imaging steps are done in a flow cell. During sequencing, the mixture of four nucleotides, each fluorescently labelled with specific fluorescent is added. The 3' hydroxyl group of the nucleotides is blocked to ensure incorporation of one nucleotide at a time. The incorporated base

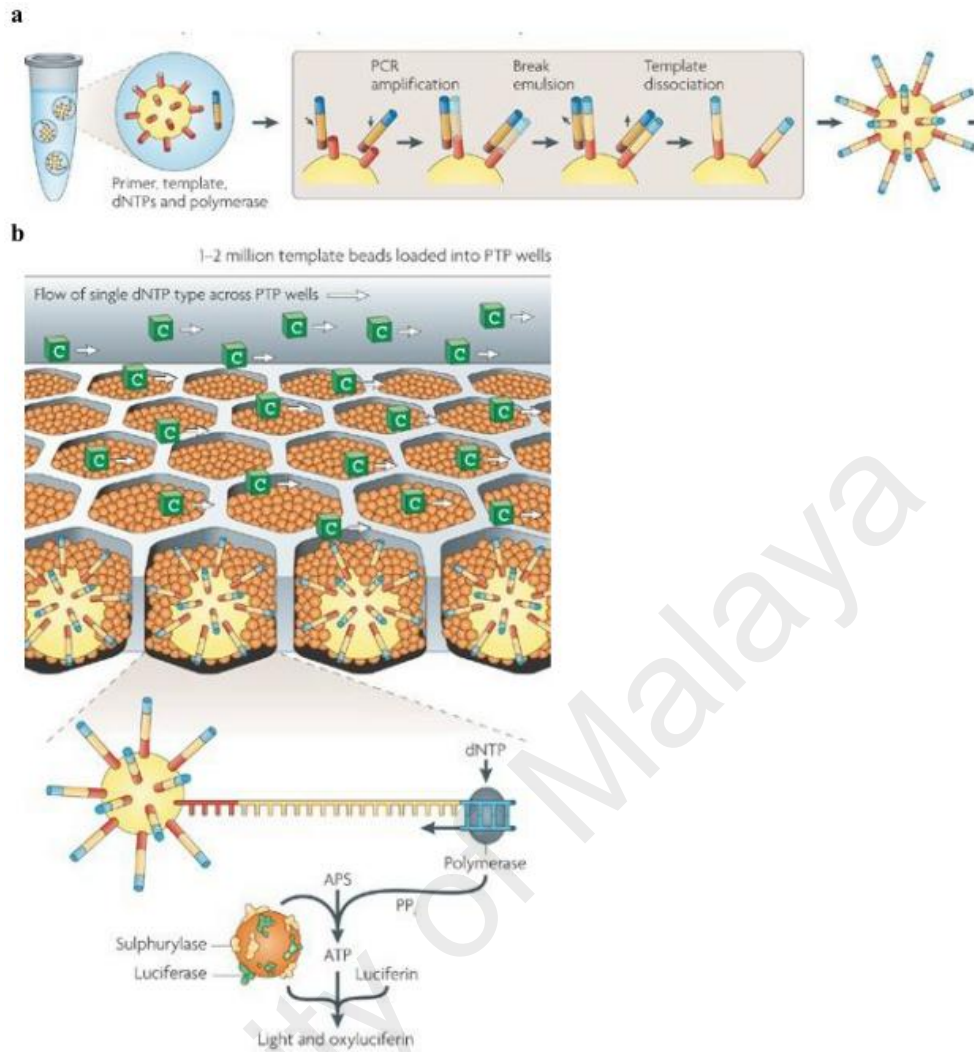


Figure 2.1: Roche 454 sequencing technology. Emulsion based clonal polymerase chain reaction (a) and pyrosequencing (b). Figure was adapted from Metzker (2010)

image is detected and the fluorescent signal emitted is captured, followed by cleavage of the fluorescent label and 3' terminating group to allow incorporation of the next base. The incorporated nucleotide acts as a reversible terminator to prevent extension when it binds to the chain until the imaging and cleavage of the fluorescent are done. The Illumina platform is the most adaptable, the lowest costing and one of the easiest platforms to use (Buermans & den Dunnen, 2014; L. Liu et al., 2012; Zhang et al., 2011).

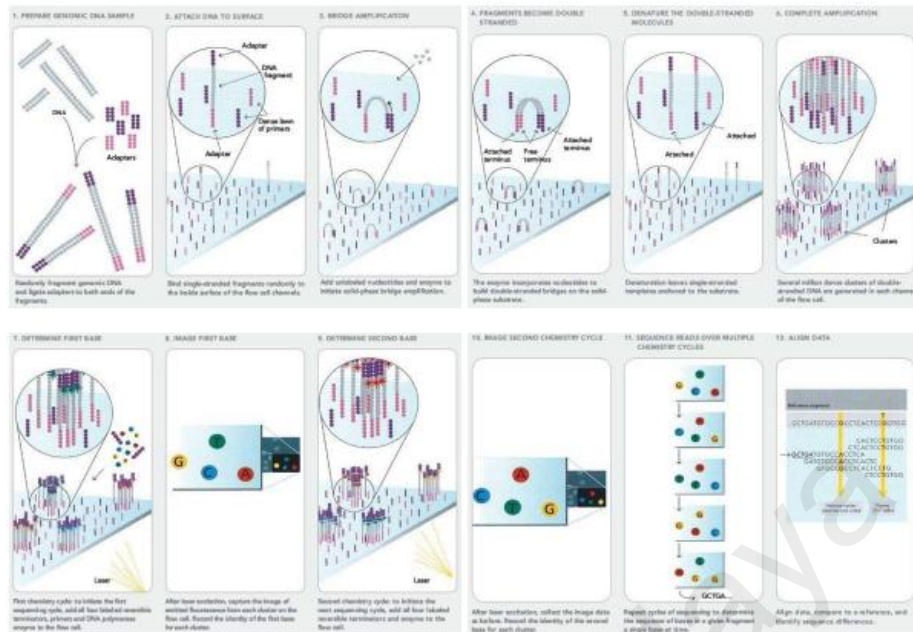


Figure 2.2: Illumina sequencing technology. Figure retrieved from https://www.illumina.com/documents/products/techspotlights/techspotlight_sequencing.pdf

The advancement of NGS technologies comes to a change with the introduction of the PacBio single molecule, real-time sequencing technology (SMRT) (<http://www.pacb.com/>). It is also a sequencing-by-synthesis technology with different features as compared to the last two technologies. Differences are also shown in the library preparation step where two adapters with hairpin structures (SMRT bell adaptors) flank the fragmented double stranded DNA templates, which later becomes circular (Figure 2.3). In addition, no amplification is required to generate a clonal of DNA template owing to the high sensitivity of the detector. During the sequencing process, each of the DNA template-polymerase complexes is immobilised at the bottom of the zero-mode waveguide (ZMW) well on the SMRT cell, in each well (Figure 2.4). The fluorescent signals of the incorporated nucleotide are recorded based on real-time imaging by a powerful optical system that illuminates the individual ZMW from the bottom of the SMRT cell and a parallel confocal recording system detects the signal from the fluorescent nucleotides. The four nucleotides are labelled with different

fluorophores at the terminal phosphate, instead of the bases as in the Illumina technology. This enables the label to be cleaved off during extension, and the cycles are not interrupted as in Illumina and 454 technologies. The main advantage of SMRT technology is the long read data with the average length of 3,000 bp to up to more than 10 kb although the throughput is lower when compared to other technologies, and with more frequent but randomly distributed errors along read length. The long read data, uniform coverage and the ability for detection of modified bases in DNA are the advantages of this technology which cannot be covered by other platforms (Buermans & den Dunnen, 2014; Rhoads & Au, 2015; Roberts, Carneiro, & Schatz, 2013). For instance, the combination of Illumina with PacBio platform complements the deficiency of each platform: the errors of PacBio can be corrected by Illumina data while the long reads of PacBio can serve as a framework for the scaffolding and gap filling between Illumina reads (Grigoriev, 2013).

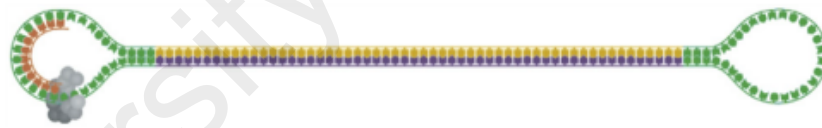


Figure 2.3: SMRT bell template. Double stranded DNA (yellow and purple) were ligated to the hairpin adaptors (green). The polymerase (gray) incorporates bases into the read strand (orange). The image was adapted from Rhoads & Au (2015)

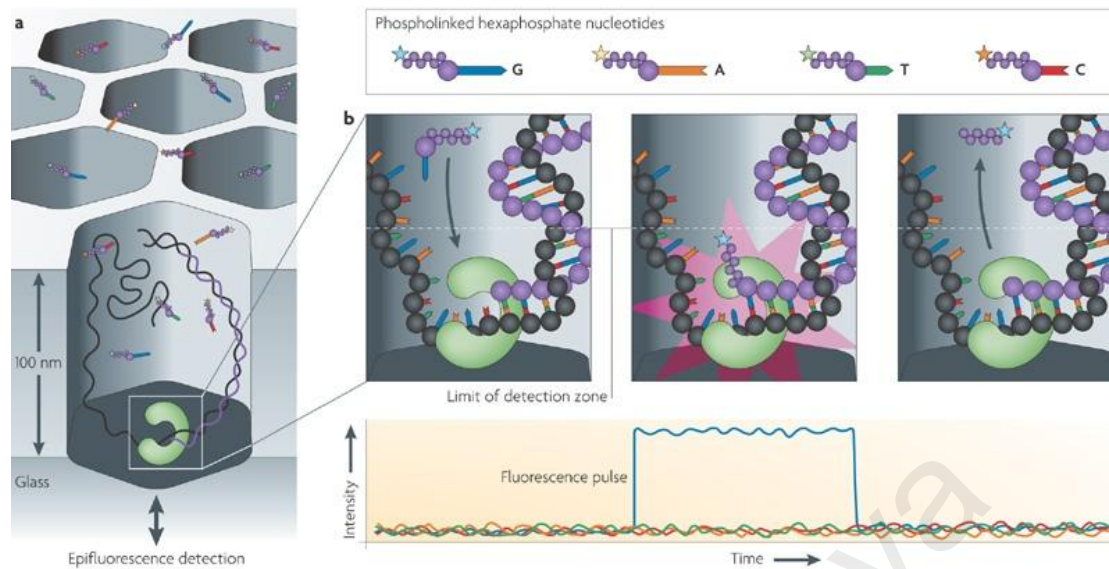


Figure 2.4: PacBio sequencing technology. Zero-mode waveguide (ZMW) (a) and the sequencing mechanism (b). Image was adapted from Metzker (2010)

2.5 Fungal genomes

The first fungal genome was determined in the year 1996 for the baker's yeast, *Saccharomyces cerevisiae* by Goffeau and his co-workers (Grigoriev, 2013). This was followed by the genome of the fission yeast *Schizosaccharomyces pombe* (Wood et al., 2002). The first filamentous fungus genome, *Neurospora crassa*, was published in 2003 (Galagan et al., 2003). The genome of *N. crassa* spurred the sequencing of more filamentous fungi as the biological diversity of filamentous fungi is far more complex than the yeast. The establishment of the Fungal Genome Initiative in the year 2000 by the Broad Institute has nominated fungal genomes to be sequenced based on phylogeny-approach, showing selection towards human health-related fungi and most of the sequenced fungi genomes show bias to the Ascomycota phylum (Cuomo & Birren, 2010). The selection aims to utilise the genomes in comparative, evolutionary, eukaryotic biology and medical studies thoroughly. In 2009, the US Department of

Energy (DOE) Joint Genome Institute (JGI) started the Fungal Genomics Program, focusing on fungi that are important to the environment and energy (Grigoriev, 2013).

Until 2013, more than 250 fungal genomes were publicly available (Grigoriev et al., 2014). A search in the National Centre for Biotechnology Information (NCBI) database showed 805 fungi have been sequenced with 1,508 genomes available. The number of fungal genome sequence will continually progress resulting from the large-scale genome initiative of the 1000 Fungal Genome Project supported by JGI, as well as from other fungal genome consortia such as The Broad Institute.

Studies of fungal genomes enable the discovery and cataloguing of genes in the genome and the metabolites that the enzymes produce, such as the discovery of secondary metabolite biosynthesis cluster of pneumocandin in *Glarea lozoyensis* (Chen et al., 2013) and triterpenes biosynthesis in *Ganoderma lucidum* (D. Liu et al., 2012). This would provide a better understanding of the biology of the fungus. The immense amount of fungal genome sequences allows comparative genomics to be carried out for studies of genomic diversity and evolution of fungal species. For instance, the genome comparison of *Aspergillus nidulans*, *Aspergillus oryzae* and *Aspergillus fumigatus* showed that these three species are distantly related, with genes sharing only 68% amino acid identity (Galagan et al., 2005). The relationship distance between *A. fumigatus* and *A. nidulans*/*A. oryzae* resembles the distance between human and fish (Fedorova et al., 2008).

Comparative genomic analysis enables identification of the genetic differences between fungi, for example, between non-pathogenic and pathogenic fungi to reveal the genetic determinants that may act as virulence factors (Moran, Coleman, & Sullivan, 2011). Moran et al. (2011) summarised that the candidate for comparison should be

between closely related species. The comparison between distantly related species would only provide a broad insight into genome evolution as seen in the comparative analysis on the three *Aspergillus* species mentioned above (Galagan et al., 2005). In a study comparing *A. fumigatus* with the closely related species, *Neosartorya fischeri* and *Aspergillus clavatus*, the genomes of these fungi were shown to be rich with genes involved in transporters, carbohydrate metabolism and synthesis of secondary metabolites (Fedorova et al., 2008). These genes may contribute to the survival of *A. fumigatus* in human hosts. Comparative genomics also enables the discovery of potential drug targets in human pathogens (Abadio et al., 2011). Other examples of the application of fungal genomes are described throughout this chapter.

2.6 Fungal nutrients

As heterotrophs, fungi need to obtain nutrients from the surroundings, but these complexes are too large for direct uptake. Hence, fungi obtain nutrients by secreting extracellular enzymes into the environment and degrading complex polymers such as cellulose and proteins into smaller oligo- or monomers and are then transported into the cells. The trophic mechanism used by fungi is known as osmotrophy (Richards & Talbot, 2013). As a consequence, fungi have become the primary decomposers of biomass in the ecosystem, and pathogens of plant and human.

Carbohydrates can be made up from different poly- and oligosaccharides where the primary monomer is monosaccharide. The variety of monosaccharide and the intersugar linkages result in the formation of the various types of polysaccharides with different strength. The carbohydrate moieties can be glycosylated with other macromolecules such as proteins, nucleic acids, and lipids. The Carbohydrate-active enzymes (CAZymes) involved in the biosynthesis, modification, and degradation of carbohydrate

moieties have been studied extensively and all the information are collected in a database (www.cazy.org).

Plant components, particularly of the cell wall, serve as a source of carbohydrate for fungi as nutrients. The cellulose, hemicellulose and pectin are the major components that make up to 70% of the plant cell wall (Jørgensen, Vibe-Pedersen, Larsen, & Felby, 2007). Cellulose is composed of a linear structure of β -1,4-linked D-glucose which are bundled together into microfibrils and are linked non-covalently to the hemicellulose (van den Brink & de Vries, 2011). Hemicelluloses are mainly composed of xylan (β -1,4-linked D-xylose), mannan (β -1,4-linked D-mannose), and xyloglucan (β -1,4-linked D-glucose). Additional branching occurs on the hemicellulose backbone via monomers such as D-xylose, D-galactose, D-glucuronic acid, and L-arabinose (Scheller & Ulvskov, 2010). Pectins are categorised into homogalacturonan, xylogalacturonan, and rhamnogalacturonan (Caffall & Mohnen, 2009). The composition of these three components are dependent on the plant species and tissue, for instance, pectins are most abundant in plant primary cell walls, the middle lamellae, and in soft tissues such as those found in fruits (Amselem et al., 2011; Caffall & Mohnen, 2009).

Fungi harbour various hydrolytic enzymes for the decomposition of plant cell wall components (Kubicek, Starr, & Glass, 2014). According to the CAZy database, CAZymes are categorised into six families based on the functional domains of experimentally curated proteins (Cantarel et al., 2009; Levasseur, Drula, Lombard, Coutinho, & Henrissat, 2013), responsible for the biosynthesis, modification and degradation of carbohydrate moieties. These are the glycoside hydrolases (GHs), polysaccharide lyases (PLs), carbohydrate esterases (CEs), auxiliary activities (AAs) and glycosyl transferases (GTs), and one associated modules known as carbohydrate

binding modules (CBMs). GHs catalyse the hydrolysis of glycosidic bond between carbohydrates or between carbohydrate and non-carbohydrate moiety while PLs are involved in degradation of glycosaminoglycans and pectin (Cantarel et al., 2009). PLs cleave uronic acid-containing polysaccharide chains via a beta-elimination mechanism to generate an unsaturated hexenuronic acid residue and a new reducing acid. The CEs catalyse the de-O or de-N-acylation of esters or amides and other substituted saccharides (Biely, 2012). CBMs are functional proteins with non-catalytic modules that promote the activities of enzymes in cell wall hydrolysis (Cantarel et al., 2009) while AAs, a newly classified group, include enzymes related to lignocellulose degradation (Levasseur et al., 2013). On the other hand, GTs are responsible for the biosynthesis of glycosidic bonds from phospho-activated sugar donor that are involved in the assembly of fungal cell wall polysaccharides, N- and O-glycoproteins and reserve carbohydrate (Ohm et al., 2012).

As the CAZyme families correlate with its enzyme mechanism, various studies have categorised these families based on the degradation of plant cell wall components (Amselem et al., 2011; de Wit et al., 2012; Kubicek et al., 2014; van den Brink & de Vries, 2011; Zhao, Liu, Wang, & Xu, 2014). Briefly, enzymes involved in cellulose degradation are β -1,4-endoglucanases, cellobiohydrolases and β -glucosidases. The enzymes with β -1,4-endoglucanase activity are located in family GH5, GH7, and GH45, cellobiohydrolase activity in GH6 and GH7 and, β -glucosidases in GH1 and GH3. The degradation of the xyloglucan backbone of hemicellulose is carried out by endo- β -1,4-glucanases from family GH5, GH12, GH16 and GH74 while degradation of xylan backbone is performed by endo- β -1,4-xylanases from family GH10 and GH11, β -xylosidases from family GH3, GH43, and GH54. Mannan degradation is catalysed by β -mannanases (GH5, GH26) and β -mannosidases (GH1, GH2). Enzymes with

polygalacturonidase activity responsible for pectin degradation are accommodated in GH28. As for the pectin degrading enzymes, pectin lyases and pectate lyases are within PL1, PL3, and PL9 families and rhamnogalacturonan lyases in the PL11 family.

The distribution of CAZymes in fungal genome enables correlation of the primary nutrient source for the fungus. A study of *Rhizopus oryzae* genome revealed that it contains enzymes primarily for the degradation of storage polysaccharides (starch and galactomannan), cellulose and pectin. This observation correlates well with the occurrence of this fungus on fruits, vegetables (rich in pectin) and seeds (rich in galactomannan, starch, and inulin) (Battaglia et al., 2011). The deployment of these enzymes is proposed to facilitate invasion on and into the substrate, surpassing other secondary and late coloniser that will have to degrade the more complex components. In addition, the abundance of pectinases in vascular wilt and root pathogens such as *Verticillium albo-atrum*, *Verticillium dahlia*, *Nectria haematococca* and *Fusarium oxysporum* suggests the putative function of pectinases during disease development in the blockage or collapse of vascular bundles (Zhao et al., 2014).

On the contrary, the degradation of protein complexes is carried out by peptidases to provide source of amino acids. Based on the MEROPS database, peptidases are classified into nine classes comprising aspartic, cysteine, glutamic, metallo, asparagines, serine, threonine, mixed, and unknown. These classes are further categorised into families and clans based on the amino acid sequence similarity and catalytic mechanism (Rawlings, Barrett, & Bateman, 2012). Peptidases can also be divided into endopeptidases and exopeptidases, depending on the cleavage site of the peptide bonds in the protein. Endopeptidases cleave the peptide bond within a protein whereas

exopeptidases catalyse the breakdown of peptide bonds terminally, that is at the N- or C-terminal of protein (Yike, 2011).

2.6.1 Fungal lifestyles in comparison to distributions of hydrolytic enzymes

It has been postulated that during the evolution of saprophytes towards pathogen, the ancestral saprophytic fungus first needed to gain traits enabling it to live on various plant species before refining those features and developing additional devices to increase its virulence on individual host species. Fungal pathogens demonstrate enzymic adaptation to the substances present in their particular hosts (St Leger, Joshi, & Roberts, 1997). Plant pathogens would harbour a large amount of CAZymes to act on the components of plant cell wall. In contrary, these fungi possess less or absence of the proteolytic enzymes involved in degradation of animal tissues such as elastin and mucin (St Leger et al., 1997). A study of the fungi from the order Onygenales *Coccidioides immitis* and *Coccidioides posadasii*, which are known to be associated with animal infections were compared to fungi from the order Eurotiales, an order that comprises mostly plant pathogens. The study showed that Onygenales species harboured reduction of genes involved in degradation of plant material such as cellulases, cutinases, and pectinesterases, but had an increase in peptidases such as keratinases and metallopeptidases. This leads to the postulation that *Coccidioides* species are not typical soil saprobes and establishing a close relation with keratin-rich hosts both alive and dead, which is consistent with the previous study demonstrating the association of *Coccidioides* with living animals and the difficulty of isolating *Coccidioides* species from soil (Sharpton et al., 2009).

Plant pathogenic fungi are classified into necrotroph, biotroph and hemibiotroph based on their different strategies in nutritional acquirement. The necrotrophs derive

nutrients from dead host cells while biotrophs derive nutrient from live host cells. The hemibiotrophs establish a biotroph relationship with hosts in the early stage and switch to the necrotrophic growth in the later stage (Zhao et al., 2014). The correlation of the fungal lifestyle with the CAZyme distribution can also be deduced from the comparison of the CAZymes in fungal genome. The different lifestyle of plant pathogen engages different sets of CAZymes to infect the plant host. Zhao et al. (2014) reported that necrotrophic fungi have the highest number of CAZymes followed by hemibiotrophic fungi while biotrophic fungi have the least number of CAZymes.

Studies in peptidases are more related to animal pathogens as peptidases involved in degradation of animal tissues where the main components are proteins. In causing infections in humans and animals, fungal pathogens show a larger amount of peptidases which facilitates the invasion of fungi. For instance, dermatophytes that are known to cause skin infections in animals display an expansion of peptidases involved in the degradation of keratin such as subtilisins (S08 family) and fungalysins (M36 family) (Burmester et al., 2011; Jousson, 2004; Martinez et al., 2012). Other peptidases related to keratin degradation are reported as belonging to the metallocarboxypeptidase from the M14A family and carboxypeptidases from S10 family (Zaugg, Jousson, L  chenne, Staib, & Monod, 2008) and, leucine aminopeptidases from M28 family and dipeptidyl peptidase from S9 family (Monod et al., 2005). The synergism activity of these endo- and exopeptidases are believed to be vital for the dermatophytes in degradation of keratin. The matrix metallopeptidases (M10A) (Chen et al., 2009; Imbert, 2002; Rodier, el Moudni, Kauffmann-Lacroix, Daniault, & Jacquemin, 1999), astacin family zinc metallopeptidases (M12) (Bond & Beynon, 1995) and prolyl aminopeptidases (S33) (Shoulders & Raines, 2009) have been reported to be responsible for collagen and extracellular matrix degradation. Also, some peptidases are allergenic proteins, such as

metallopeptidase Asp f 5 (M36), serine peptidase Asp f 13 (S08) (Namvar et al., 2015) and Pen c 13 (S08) (Chen et al., 2012).

On the other hand, the less specialised nutritional status of saprophytic and opportunistic fungi have a wide variety of protein and carbohydrate degrading enzymes as they obtain nutrients from the environment with a variety of complexes (St Leger et al., 1997). The known opportunistic pathogen, *A. fumigatus* is a saprophyte in nature that lives in soil and decomposes organic materials to release carbon and nitrogen sources into the environment (Sriranganadane et al., 2010). Several studies showed that *A. fumigatus* does not carry specific large gene families encoding secreted peptidases as compared to the obligate pathogens (Sharpton et al., 2009; Sriranganadane et al., 2010). The fungus employs different sets of peptidases to act on different types of protein sources under various conditions (Farnell, Rousseau, Thornton, Bowyer, & Herrick, 2012; Sriranganadane et al., 2010). Thus, the standard nutrient uptake systems that are used in their ecological niche might be utilised by the fungus to cause infection (Abad et al., 2010).

2.7 Secondary metabolites

Secondary metabolites are low molecular mass molecules with heterogeneous structures which are considered not essential for growth. Unlike primary metabolites, these molecules play their roles in communication, defence against competitors, and protection against the stresses (Scharf, Heinekamp, & Brakhage, 2014). Fungal secondary metabolites possess an enormous range of activities, including those that are beneficial and detrimental (Kück, Bloemendal, & Teichert, 2014). The products such as the antibiotic penicillin (Weber, Bovenberg, & Driessen, 2012) and cholesterol-lowering lovastatin (Seenivasan, Subhagar, Aravindan, & Viruthagiri, 2008) are

beneficial to humans while the mycotoxins, such as carcinogenic aflatoxin/sterigmatocystin/dothistromin (Yu, 2012) and, apoptosis inducer and protein synthesis inhibitor trichothecenes (McCormick, Stanley, Stover, & Alexander, 2011) are harmful. The first committed step in the secondary metabolites biosynthesis, which is the synthesis of backbone molecules is carried out by multidomain enzymes comprising polyketide synthases (PKSs), nonribosomal peptide synthases (NRPSs), hybrid PKS-NRPS, dimethylallyl tryptophan synthetase (DMATs) and the terpene cyclase (TCs) (Khaldi et al., 2010).

PKS produces secondary metabolite backbone using mainly acetyl-CoA as a precursor. There are three types of PKSs, which are categorised based on the protein architecture and the way of action. Fungal PKSs belong to the type I iterative PKS, where the domains consist of ketosynthase (KS), acyltransferase (AT), acyl carrier protein (ACP), thioesterase (TE), ketoreductase (KR), dehydratase (DH), and enoyl reductase (ER) domains, of which, KS, AT, and ACP domains are essential. The AT domain selects the extender unit (usually malonyl-CoA) and transfers the acyl to ACP, which loads the extender unit while KS is involved in decarboxylative condensation (Claisen condensation) of the extender unit with acyl thioester. Further reduction of the product may be carried out by KR, DH or ER. This is followed by post-PKS modification of carbon chain via alkylation, acylation and oxygenation to confer additional function to the final product and the diversity of secondary metabolites. The iterative type I PKS reuses the domains during the elongation, unlike the bacterial non-iterative type I PKS. The type I PKS can be classified into non-reducing (NR) PKS, partially reducing (PR) PKS and highly reducing (HR) PKS based on the degree of reduction of their product. The well-known metabolites melanin and aflatoxin are

produced from NR PKS while lovastatin is the product of HR PKS (Cox & Simpson, 2009; Kroken, Glass, Taylor, Yoder, & Turgeon, 2003; Schuemann & Hertweck, 2009).

NRPS synthesises peptides via thio-template mechanism, i.e. thioesterification of amino acids onto an enzyme-bound thiol, without dependence on the ribosome. The precursors, amino acids are activated and bound as thioesters to the enzymes. NRPS consists of three main domains; adenylation (A) domain that function as an amino acid activator, thiolation (T) domain where the peptidyl carrier protein binds to cofactor 4'-phosphopantetheine (4'PP) to activated amino acid and condensation (C) domain which catalyses the formation of a peptide bond. Examples of NRPS products are the well-known antibiotics penicillin, cephalosporin and the iron scavenger siderophores (Brakhage, 2013; Felnagle et al., 2008; Hoffmeister & Keller, 2007).

While the hybrid PKS-NRPS comprises of an iterative reducing PKS followed by an NRPS and an additional module to release the product via reduction or Dieckmann cyclisation (Boettger & Hertweck, 2013; Fisch, 2013). An important feature of hybrid PKS-NRPS is the absence of ER domain (Halo et al., 2008), and it has been suggested that its function is not essential or the function can be carried out by trans-acting ER (Boettger & Hertweck, 2013). The most widely studied hybrid PKS-NRPS are the TenS which produces tenellin by *Beauveria bassiana* but tenellin is not involved in pathogenicity (Eley et al., 2007) and cytochalasins by *Penicillium expansum* (Schümann & Hertweck, 2007) and *A. clavatus* (Qiao, Chooi, & Tang, 2011).

The DMATS is renowned in the biosynthesis of ergot alkaloids by catalysing prenylation of L-tryptophan by *Claviceps purpurea* in the synthesis of ergotamine (Haarmann et al., 2005; Tudzynski et al., 1999). The ergot alkaloids are featured by a tetracycline ergoline ring and divided into three classes based on their structures (Li,

2010; Wallwey & Li, 2011). The enzyme TC catalyses the synthesis of terpenes, including monoterpenes, sesquiterpenes, diterpenes and carotenoids, depending on the starting compound geranyl pyrophosphate, farnesyl pyrophosphate or geranylgeranyl pyrophosphate (Keller, Turner, & Bennett, 2005). The metabolites belonging to this class are the carotenoids (Schmidhauser, Lauter, Russo, & Yanofsky, 1990) and trichothecenes (McCormick et al., 2011).

Most of the secondary metabolite related genes are found in contiguous gene clusters encompassing genes involved in backbone biosynthesis, post-secondary metabolite processing, transcriptional regulation and transport of the metabolites. The gene cluster may be coordinately regulated by a particular Zn₂Cys₆ transcription factor or by the global regulator of secondary metabolism, putative methyltransferase LaeA (Brakhage, 2013; Hoffmeister & Keller, 2007; Keller & Hohn, 1997). The expression of secondary metabolite genes is tightly regulated and is induced by specific environment condition (Brakhage, 2013). Therefore, it is not possible to detect all the secondary metabolite related genes under standard laboratory culture conditions, as demonstrated by the synthesis of aspyridone by *A. nidulans* (Bergmann et al., 2007) and flavipucine derivatives by *Aspergillus terreus* (Gressler, Zaehle, Scherlach, Hertweck, & Brock, 2011).

With the availability of the fungal genome, data mining of secondary metabolite genes that are not expressed enable the discovery of new genes and improves the knowledge of current known metabolites biosynthesis (Van Lanen & Shen, 2006), such as the natural products aspyridone (Bergmann et al., 2007), flavipucine derivatives (Gressler et al., 2011) and ergot alkaloids (Wallwey & Li, 2011). The information of the secondary metabolite gene clusters in genomes provides a convenient genetic locus for

manipulation and has allowed for unique insights into a possible global mechanism underlying the regulation of these clusters (Brakhage, 2013).

2.8 Melanin

Melanin provides various benefits to the organism, such as protection against the effects of ultraviolet (UV) irradiation, desiccation, high temperatures, and oxidants (van Baarlen et al., 2007). The negatively charge insoluble melanin granules are localised to the fungal cell wall where they are likely cross-linked to polysaccharides (Eisenman & Casadevall, 2012). The protection of melanin enables fungi to thrive in harsh environments, such as Antarctica (Rosa, Almeida Vieira, Santiago, & Rosa, 2010), contaminated nuclear reactors (Zhdanova et al., 2000), and even in household dishwashers (Gostinčar, Grube, & Gunde-Cimerman, 2011).

Fungi can synthesise melanin via two pathways, the 1,8-dihydroxynaphthalene (DHN) and L-3,4-dihydroxyphenylalanine (L-DOPA). The dematiaceous fungi synthesise melanin via the DHN biosynthesis pathway (Figure 2.5) (Dadachova et al., 2007; Jacobson, 2000; Langfelder, Streibel, Jahn, Haase, & Brakhage, 2003). In DHN biosynthesis pathway, acetyl-CoA or malonyl-CoA is the starter unit where it forms 1,3,6,8-tetrahydroxynaphthalene (T4HN) catalysed by PKS. The synthesis is followed by a series of reduction and dehydration by tetrahydroxynaphthalene reductase, scytalone dehydratase and trihydroxynaphthalene reductase to produce intermediates scytalone, 1,3,8-trihydroxynaphthalene (T3HN), vermelone and DHN. DHN then undergoes polymerisation to form melanin (Eisenman & Casadevall, 2012; Langfelder et al., 2003). In some fungi, an additional post-modification of polyketide precursor catalysed by yellow-green1 gene (*yg-1*) was reported. The *Wdyg-1* in *Exophiala dermatitidis* deacetylates 2-acetyl-1,3,6,8-tetrahydroxynaphthalene to T4HN (M. H.

Wheeler et al., 2008) while the *A. fumigatus* *Ayg-1* modifies the product of *alb-1* by removing acetoacetic acid to produce T4HN (Fujii et al., 2004; Tsai et al., 2001).

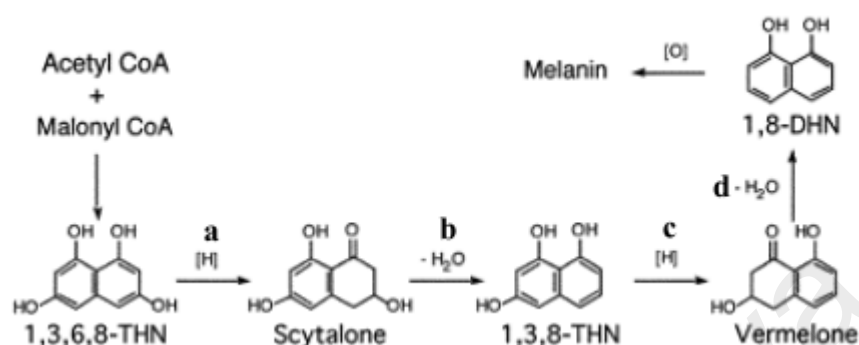


Figure 2.5: Pentaketide DHN-melanin biosynthesis pathway. T4HN reductase (a), scytalone dehydratase (b and d), T3HN reductase (c). Figure was adapted from Tsai et al. (2001)

Whereas in the synthesis of melanin via DOPA pathway, dopaquinone is generated from L-dopa or tyrosine. In the synthesis using L-dopa as a starter, the oxidation of L-dopa is catalysed by laccase to dopaquinone. On the other hand, a reaction involving the conversion of tyrosine to L-dopa followed by oxidation to dopaquinone by tyrosinase occurs if tyrosine is the precursor. The highly reactive dopaquinone will then undergo auto-oxidation and polymerisation to form melanin (Eisenman & Casadevall, 2012; Langfelder et al., 2003).

Besides DHN-melanin and DOPA-melanin, another type of melanin, pyomelanin is produced via L-tyrosine degradation pathway (Keller et al., 2011; Schmalzer-Ripcke et al., 2009). The enzyme 4-hydroxyphenylpyruvate dioxygenase (hppD) converts 4-hydroxyphenylpyruvate to homogentisate, the intermediate of L-tyrosine degradation. The accumulation of homogentisate then oxidises and polymerises to form pyomelanin. Homogentisate can also be further degraded into 4-maleylacetoacetate, 4-

fumarylacetoacetate and lastly to fumarate by homogentisate dioxygenase (HmgA), maleylacetoacetate isomerase (MaiA) and fumarylacetoacetate hydrolase (FahA), respectively. The production of pyomelanin has been described in *A. fumigatus* (Schmaler-Ripcke et al., 2009), *Sporothrix* spp. (Almeida-Paes et al., 2012), *E. dermatitidis* (Chen et al., 2014) and *Penicillium chrysogenum* (Vasanthakumar, DeAraujo, Mazurek, Schilling, & Mitchell, 2015).

It has been postulated that melanin enhances the growth of melanised fungi treated with ionising radiation by harnessing the energy released from radioactive elements and converting it into metabolic energy. It has been reported that cell growth was observed in the irradiated *C. sphaerospermum* isolated in Chernobyl under depleted nutrient and energy sources (Dadachova et al., 2007). This leads to the suggestion that melanin protects the fungus against ionising radiation, UV radiation or extreme temperatures, allowing adaptation to survive in a variety of living conditions.

Apart from protection, fungal melanin also plays a role in pathogenesis (Jacobson, 2000). It is a virulence factor for the known human pathogens such as *Cryptococcus neoformans* and *Sporothrix schenckii* (Madrid et al., 2010; Noverr, Williamson, Fajardo, & Huffnagle, 2004). It has been proposed that the negatively charged melanin is able to quench free radicals such as reactive oxygen species (ROS) produced by the host's immune cells (Cunha et al., 2010; Langfelder et al., 2003; Volling, Thywissen, Brakhage, & Saluz, 2011). In plant pathogenic fungi such as *Magnaporthe grisea*, *Colletotrichum kahawae*, and *Diplocarpon rosae*, melanin is required in the formation of appressorium which is the infection structure for tissue penetration (Chen, Nunes, Silva, & Rodrigues Jr., 2004; Gachomo, Seufferheld, & Kotchoni, 2010; Howard & Valent, 1996).

2.9 Iron regulation

Iron is a stable transition element having ferric (Fe^{2+}) and ferrous (Fe^{3+}) states; it acts as a cofactor for many proteins mediating redox reaction and transfer of electron. This element plays important roles in cellular processes, such as respiration, amino acid metabolism, and dealing with ROS induced by abiotic environments and produced by phagocytic cells during host defence. It is also required for germination, asexual and sexual propagation (Eisendle et al., 2006; Oide, Krasnoff, Gibson, & Turgeon, 2007). However, an excess of free iron is dangerous to the cell through the generation of cell-damaging hydroxyl radicals via Fenton and Haber-Weiss reaction. Although iron is abundant in the Earth, the bioavailability of iron is low as the form of iron exists is the least soluble form of Fe^{3+} . In addition, iron is not freely available in plant and animal hosts. In animals, most of the iron is associated with proteins and appears as ferritin, lactoferrin and transferrin or bound with heme in haemoglobin (Haas, 2014; van Baarlen et al., 2007). Therefore, sophisticated strategies for acquiring iron inside the host are essential for fungal survival. To overcome the bioavailable scarcity and cytotoxic effect of iron, fungi have developed different strategies for iron uptake and regulation.

The major role of iron reduction is solubilisation of this element for cellular processes. There are four iron uptake mechanisms employed by fungi in iron homeostasis, i.e. the high-affinity uptake system of i) siderophore-mediated Fe^{3+} uptake and ii) reductive iron assimilation (RIA); iii) heme uptake which is the utilisation of host iron source and; low-affinity iron uptake system via iv) direct Fe^{2+} uptake. Most fungi employ more than one mechanism, for instance, *A. fumigatus* acquire iron via siderophore, RIA and low-affinity Fe^{2+} uptake (Haas, Eisendle, & Turgeon, 2008).

Siderophore-mediated Fe^{3+} uptake system utilises the secondary metabolite siderophores as iron chelators to form a complex with Fe^{3+} (Haas et al., 2008; Hoffmeister & Keller, 2007). Siderophores can be categorised based on the chemical nature of the moieties donating oxygen ligand for Fe^{3+} , which are aryl caps, carboxylates and hydroxamates. All fungal siderophores belong to the hydroxamates, except the carboxylate-type siderophore rhizoferrin by Zygomycetes. Fungal hydroxamates can further classify into four structural families of rhodotorulic acid, fusarinines, coprogens and ferrichromes (Haas et al., 2008). Most fungi synthesise siderophores, except the yeasts *Saccharomyces*, *Candida* and *Cryptococcus* species. However, these yeasts can utilise siderophores produced by other fungi and this is known as xenosiderophores (Howard, 2004).

In siderophore biosynthesis, the L-ornithine N^5 -oxygenase is responsible for the first committed step to produce N^5 -hydroxyornithine via N^5 -hydroxylation of L-ornithine followed by N^5 -acylation of N^5 -hydroxyornithine (Figure 2.6). The transfer of acyl group from acyl-CoA derivatives to N^5 -hydroxyornithine produces hydroxamate. Different types of hydroxamate will be produced depending on the attached acyl residues. If acetyl is transferred, the products formed are rhodotorulic acid, ferricrocin and ferrichrome, whereas transfer of anhydromevalonyl produces fusarinines and coprogens. The synthesis of hydroxamate is then catalysed by fusarinine-type NRPS (SidD in *A. fumigatus* or its homologue NPS6) or ferrichrome-type NRPS (SidC in *A. fumigatus* or its homologue NPS2) to produce fusarinine C and ferricrocin, respectively. Further N^2 -transacetylation and hydroxylation of the respective product will produce triacetylfusarinine C (TAFC) and hydroxyferricrocin (Haas et al., 2008; Haas, 2014; Schrettl et al., 2007).

In Pezizomycota, fusarinines and coprogens are typically excreted for iron acquisition while ferrichromes are used intracellularly as iron storage (Haas et al., 2008). Fungi such as *A. fumigatus* and *Gibberella zeae* secrete TAFC while coprogen is secreted by *Cochliobolus heterostrophus*, *Cochliobolus miyabeanus* and *Alternaria brassicicola* to acquire iron from the environment. As reported in *A. nidulans*, *C. heterostrophus* and *G. zeae*, these fungi employ ferricrocin as iron storage compound in the cell (Eisendle, Oberegger, Zadra, & Haas, 2003; Oide et al., 2007). In addition to ferricrocin, it was shown that hydroxyferricrocin is also responsible for iron storage in *A. fumigatus* (Schrettl et al., 2007; Wallner et al., 2009).

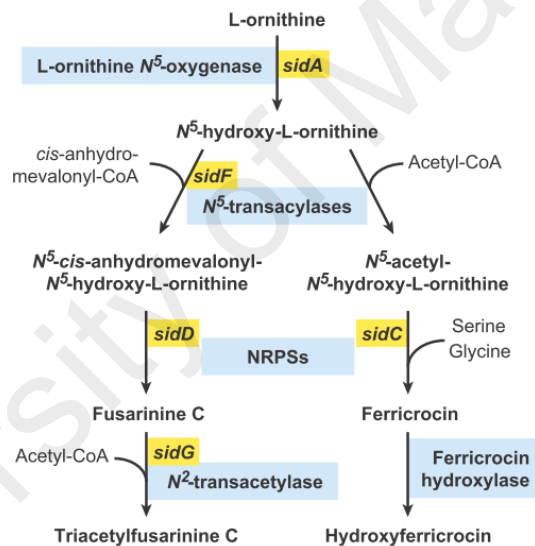


Figure 2.6: Siderophore biosynthesis pathway. Genes are shown in yellow while the product are shown in blue. Image was adapted from Hass et al. (2008)

RIA is another high-affinity iron uptake system whereby the Fe^{3+} is reduced to Fe^{2+} by a reductase prior being transported into the cell across the plasma membrane by an iron permease (Kwok, Severance, & Kosman, 2006). RIA has been shown to be vital for the survival of fungus during iron limitation in the absence of siderophore-mediated iron uptake in *A. fumigatus* (Schrettl et al., 2007), but it is not required for its virulence

(Schrettl et al., 2004a). *A. nidulans* was reported to be lacking this system (Eisendle et al., 2006).

The role of siderophores in the virulence of fungi is species dependent. The SidD of *A. fumigatus* (Schrettl et al., 2004a) and its homologue NPS6 in *F. graminearum*, *C. heterostrophus*, *C. miyabeanus* and *A. brassicicola*, which is involved in the synthesis of extracellular siderophores is reported as the virulence determinant of these fungi (Oide et al., 2006). Deletion of the gene in these fungi results in reduced virulence and hypersensitivity to hydrogen peroxide (H₂O₂). However, the intracellular siderophores of *M. grisea* and *Metarhizium robertsii* are required for the fungal's full virulence (Giuliano Garisto Donzelli, Gibson, & Krasnoff, 2015; Hof et al., 2007). In *C. albicans* and *Ustilago maydis*, the RIA system is an essential virulence factor (Eichhorn et al., 2006; Ramanan & Wang, 2000). Nonetheless, these mechanisms are important in the fungal fitness and complement each other (Oide, Berthiller, Wiesenberger, Adam, & Turgeon, 2014; Schrettl et al., 2007).

Comparative genomics between well-studied fungi enables disclosure of the presence of orthologous genes in the queried genome. For instance, the comparative analysis of *Aspergillus niger* together with *A. fumigatus* and *A. nidulans* genomes revealed the orthologous genes involved in the synthesis of siderophore, reductive iron assimilation and iron regulators *sreA* and *hapX* in *A. niger* (Franken et al., 2014). The analysis also revealed that *sidG* gene that is responsible for synthesis TAFC, the common extracellular siderophore of *A. fumigatus* and *A. nidulans*, is absent in *A. niger*. Further analysis revealed that *A. niger* synthesises coprogen B as an extracellular siderophore.

2.10 Stress responses

Fungi live in virtually all types of habitat for its survival and propagation in the extremes of temperatures, salinity, and acidity (Cantrell, Dianese, Fell, Gunde-Cimerman, & Zalar, 2011; Gostinčar, Grube, de Hoog, Zalar, & Gunde-Cimerman, 2010; Selbmann et al., 2013). They are virtually skilled in colonisation and persist in a novel environment by utilising the available resources and establishing a new association with other species in the novel environment. Fungi can adopt different mechanisms so that it can reproduce. This provides an advantage for the fungi in harbouring new traits (Agosta & Klemens, 2008).

Before 2000, no studies on the isolation of fungi from hypersaline environments were reported until the discovery of fungi that live actively in solar salterns (Gunde-Cimerman, Zalar, de Hoog, & Plemenitas, 2000). Since then, species with unknown habitat previously that cause contamination of food preserved in high salt or have been found to originate from hypersaline environments (Gunde-Cimerman, Ramos, & Plemenitas, 2009).

The dominant halophilic and halotolerant filamentous fungi in Ascomycota are *Hortaea werneckii*, *Phaethotheca triangularis*, *Trimmatostroma salinum* and *Aureobasidium pullulans* from the order Dothideales, *C. sphaerospermum* from Capnodiales and, *A. niger*, *Aspergillus sydowii*, *Eurotium amstelami* and *P. chrysogenum* from Eurotiales (Gunde-Cimerman et al., 2009). The genomes of halophilic yeast *Debaryomyces hansenii* (Kumar, Randhawa, Ganesan, Raghava, & Mondal, 2012), *H. werneckii* (Lenassi et al., 2013) and Basidiomycetes *Wallemia ichthyophaga* (Zajc et al., 2013) have been sequenced with *H. werneckii* and *W. ichthyophaga* being studied intensively in genomic scale.

Hypersaline environments are dominated by sodium (Na^+) ions. However, potassium (K^+) ions are required by the cells for various processes such as osmotic regulation, protein synthesis and enzyme activation (Rodríguez-Navarro, 2000). In order to live in such environments, the cation homeostasis plays a role in maintaining stable K^+ content and low Na^+ ions that are toxic to the cell. The high Na^+ concentrations in the environment may intrude into the cell and replace it with K^+ ions, which leads to osmotic stress and interference of growth (Arino, Ramos, & Sychrova, 2010). The plasma membrane and intracellular cation transporters are involved in cation homeostasis by maintaining low intracellular Na^+ concentration whereas the plasma membrane H^+ -ATPases supply energy to these secondary transporters. Most of the transporters involved in such regulation are well characterised in *S. cerevisiae* and have been identified in the genome of *H. werneckii* and *W. ichthyophaga*, which consist of high affinity K^+ channels Trk1 and Trk2 for K^+ uptake; membrane depolarisation activated K^+ channel Tok1, Ena1-5 ATPases and Na^+/K^+ antiporter Nha1 that function in efflux of K^+ ions. As for the transporters involved in the maintenance of intracellular K^+ concentrations, it encompasses the endosomal Nhx1 and Golgi apparatus Kha1 as Na^+ , H^+ exchangers, vacuolar Vnx1 and mitochondrial Mrs7/Mdm38 as Na^+/K^+ , H^+ exchanger (Arino et al., 2010; Lenassi et al., 2013; Zajc et al., 2013). The Ena ATPase is a P-type ATPase that functions to pump Na^+ out of the cell against the membrane potential via coupling with the hydrolysis of ATP. The P-type ATPases are also responsible for transportation of various ions and phospholipids across plasma membrane such as copper and cadmium type heavy metal (by group IB), sodium (group IID), phospholipids (group IV) and protons (group IIIA) (Kühlbrandt, 2004). The ATPases that are involved in cation transports are from the group IID. In addition, the V-type ATPase complex plays an important role in acidification of vacuolar lumen,

correct functioning of other organelles and maintaining the cytosolic pH homeostasis together with the plasma membrane H^+ -ATPases (Arino et al., 2010). While the Pho89 is a sodium/inorganic phosphate (Na^+/Pi) symporter that imports phosphate into the cell utilising the Na^+ gradient at alkaline pH (Persson et al., 1998).

In adaptation to osmotic stress, the accumulation of compatible solutes is another approach employed by microorganisms. Fungi accumulate different polyols such as glycerol, mannitol and arabitol, free amino acids and derivatives to maintain low intracellular concentrations of Na^+ (Gunde-Cimerman et al., 2009). In *H. werneckii*, *W. ichthyophaga* and *D. hansenii*, glycerol is the primary solute in the maintenance of cell turgor pressure (Jovall, Tunblad-Johansson, & Adler, 1990; Plemenitaš et al., 2014). Moreover, the transport and retention of glycerol in the cell is essential to overcome the rapid change of salt concentration. The sugar/ H^+ symporters and aquaglyceroporins are responsible for the uptake and efflux of glycerol, respectively in *S. cerevisiae* to maintain the osmosis of the cell (Ferreira et al., 2005).

The detection of Na^+ concentrations in the environment is a significant factor for the fungal survival. The high osmolarity glycerol (HOG) pathway, a mitogen-activated protein kinase (MAPK) signalling pathway, is important for osmoregulation and activated under osmotic and cationic stress (Zhao, Mehrabi, & Xu, 2007). This pathway involved a cascade of reactions activated by osmosensors Sho1 and Sln1. In the Sln1 branch, Sln1 form receptor with the phosphorelay molecule Ypd1 and response regulator Ssk1 that activates the MAPK kinase Pbs2. The activated Pbs2 then phosphorylates the MAPK Hog1. While in the activation by Sho1, Pbs2 is activated by Sho1 through Ste11 and Ste20 (Ma & Li, 2013; Zhao et al., 2007).

2.11 Sexual reproduction

Sexual reproduction in fungi produces offsprings that have better survival ability in an environment, by increasing the genetic diversity to increase the fitness and removal of deleterious mutations in the genome. Sexual reproduction contributes to maintaining living organisms during long-term evolution. Sexual reproduction occurs when two compatible partners undergo cell fusion (plasmogamy) and the fusion of their genetic contents (karyogamy) followed by recombination, meiosis and mitosis to produce recombinant offsprings. The Ascomycetes and Basidiomycetes may delay karyogamy and remain in the dikaryotic stage for a long period (Lee, Ni, Li, Shertz, & Heitman, 2010).

Fungal sexual development is choreographed by the genetic locus named as a mating type or MAT locus, with different strategies for the regulation of sexual reproduction. Sexual development may occur via self fertilisation (homothallism) or cross fertilisation (heterothallism). In homothallic fungi, the fungi harbour both *mat* genes, namely *mat1-1* and *mat1-2* containing α box domain and high mobility group (HMG) domain that encode the transcription factor α -factor and a-factor, respectively. Whereas in heterothallic fungi, the fungi only carry either one of the *mat* genes in the MAT locus and require another strain with compatible *mat* gene for mating to occur (Ni, Feretzaki, Sun, Wang, & Heitman, 2011).

Currently, *Cladosporium* species that have known anamorph-teleomorph phase are only reported in *C. herbarum* and *Cladosporium silenes* whereas *Cladosporium grevilleae* is only known with a sexual stage as reviewed by Bensch et al. (2012). However, five species belonging to the *C. herbarum* species complex were reported to have its teleomorph stage, namely *C. herbarum*, *Cladosporium macrocarpum*,

Cladosporium bruhnei, *Cladosporium variabile* and *Cladosporium iridis* by Schubert et al. (2007).

Whole genome sequencing enables discovery of genes involved in pheromone response, mating process, meiosis and fruit body development in fungal with no known sexual phase, such as *A. fumigatus* and *A. oryzae* (Galagan et al., 2005). From the study conducted by Galagan et al. (2005), the *A. fumigatus* and *A. oryzae* are heterothallic fungi, while *A. nidulans* is a homothallic fungus. By comparing the genome, this will help further improve the knowledge of genome evolution in the transition between homothallism and heterothallism that occurs in fungi (Lee et al., 2010).

2.12 Fungal allergy

Allergy is characterised as a hyper response to IgE by environmental allergens such as pollen-food, and fungal spores (Kurup & Banerjee, 2000). An allergen is a molecule that causes allergy, where it harbours the property to sensitise, to elicit an allergic reaction and to bind to IgE antibodies. Upon the sensitisation, the allergens induce the immune system to produce high-affinity antibody and elevation of peripheral and blood lung eosinophilia. Upon re-exposure, the allergen triggers symptoms such as sneezing owing to the interaction of the allergen and IgE on the mast cells. This leads to degranulation and release of mediators such as histamine (Kurup & Banerjee, 2000). The term allergenicity has a few definitions: the capacity of an antigen to induce symptoms or a skin reaction or the ability to induce or bind to IgE antibodies (Aalberse, 2000).

As fungi are ubiquitous and airborne, they can be easily contacted throughout the year. Of all the possible allergens, fungal allergens have the most impact in human apart from causing allergy (Simon-Nobbe, Denk, Pöll, Rid, & Breitenbach, 2008). Unlike

other allergens, fungi may colonise the human body and cause additional damages to the human body. The type I allergy can manifest as allergic rhinitis, allergic asthma and atopic dermatitis (Cramer, Garbani, Rhyner, & Huitema, 2014; Simon-Nobbe et al., 2008). Besides type I allergy, fungal allergy also includes allergic bronchopulmonary mycoses, allergic sinusitis and rhinosinusitis, and hypersensitivity pneumonitis, where these diseases are a result of mixed type I, III and IV fungal hypersensitivity (Cramer et al., 2014; Denning, O'Driscoll, Hogaboam, Bowyer, & Niven, 2006; Glass & Amedee, 2011). Nevertheless, fungal allergens receive the least attention in the field despite their predominant role in causing allergy such as allergic asthma (Kennedy, Heymann, & Platts-Mills, 2012).

More than 80 fungal genera have been shown to induce type I allergies in susceptible persons, whereas allergenic proteins have been identified in 23 fungal genera (Simon-Nobbe et al., 2008). Simon-Nobbe et al. (2008) listed 174 allergens from Ascomycota and 30 from Basidiomycota, with the most important allergy-causing fungal genera belonging to the Ascomycota are *Alternaria*, *Aspergillus*, *Bipolaris*, *Candida*, *Cladosporium*, *Epicoccum* and *Phoma* species.

Currently, there are many databases on allergens, such as Allergome (<http://www.allergome.org/>) and database by the World Health Organisation and International Union of Immunological Species (WHO/IUIS) Allergen Nomenclature Sub-committee (www.allergen.org) (Mari, Rasi, Palazzo, & Scala, 2009). The WHO/IUIS Allergen Sub-committee was established with the aim to maintain and develop a unique, unambiguous and systematic nomenclature for allergens. The committee have agreed on a total of 841 allergens, where allergens from the kingdom Fungi (111) being the least recognised while those in the kingdom Plantae being the

most (389). This amount is far lesser than those allergens described in the literature, as deposited in the other databases. Of the 111 allergens recognised in the kingdom Fungi, 86 are from ascomycetes, with *Alternaria alternata* being to most well characterised.

Fungal allergens consist of various molecular structures, encompassing enzymes, toxins, cell wall components, and highly conserved proteins (Crameri et al., 2014). Cross-reactivity occurs when IgE antibodies initially directed against a given allergen also bind to structurally related allergen from another source (Aalberse, Akkerdaas, & van Ree, 2001). It has been reported that allergenic proteins showing a high degree of sequence homology (>50% identity) are likely to cross-react (Aalberse, 2000). In other words, a patient mounts an allergic reaction upon triggered by proteins from other fungi that are highly homologous to the targeted protein. For instance, the enzyme enolase is a highly conserved protein among fungi that exhibits high IgE cross-reactivity among fungal species such as *A. alternata*, *C. herbarum*, *A. fumigatus* and *P. citrinum* (Breitenbach et al., 1997). The cross-reactivity may also occur irrespective of taxonomic relationship of the fungi as cross-reactivity between vacuolar serine peptidase of *Penicillium oxalicum* and *A. fumigatus* (Pen o 18 and Asp F 18); and peroxisomal protein of *Candida boidini* and *A. fumigatus* (Cand b 2 and Asp f 3) (Hemmann, Blaser, & Crameri, 1997) have been reported.

Among *Cladosporium* species, a list of 16 allergens in *C. herbarum* and two allergens in *C. cladosporioides* have been deposited in Allergome. In contrast, the approved allergens by WHO/IUIS Allergen Sub-Committee are only eight from *C. herbarum* and two from *C. cladosporioides*. Cross-reactivity of *C. herbarum* allergens was observed between mannitol dehydrogenase of *C. herbarum* and *A. alternata* (Cla h 8 and Alt a 8) (Schneider et al., 2006), aldehyde dehydrogenase (Alta 10 and Cla h 10)

and, acidic ribosomal protein P2 (Alt a 7 and Cla h 5) with *S. cerevisiae* YCP4 (Achatz et al., 1995). Although *C. sphaerospermum* has been reported to be an allergy-causing mould, specific allergens have not been identified (Dixit & Kwilinski, 2000). A study by Denis et al. (2012) showed that *C. sphaerospermum* extracts could cross-react with antibodies sensitised by *A. alternata* spores.

The diagnosis of fungal allergy includes *in vivo* skin prick test or by measuring specific IgE levels (Hamilton & Franklin Adkinson, 2004), with the support of patient's clinical history. The commercially available allergens for IgE sensitivity test are in the form of fungal extracts, which composed of both allergenic and non-allergenic molecules. This causes the problem of inconsistent results as the diagnosis is highly dependent on the quality of the fungal extract. The standardisation of crude fungal extracts is difficult, owing to the variation in the protein composition of these extracts, which is influenced by strain variabilities, growth conditions, batch to batch variability, source, protein extraction methods, storage condition, and stability of the extracted protein (Cramer, 2013; Esch, 2004; Vailes et al., 2001).

With the advancement in molecular biology techniques, allergy diagnosis is moving towards the era of molecular allergy, whereby the use of recombinant allergens can overcome the concern on standardisation of fungal extracts as large quantity of pure proteins can be synthesised and protein preparation is reproducible (Simon-Nobbe et al., 2008). The diagnosis uses the pure protein (allergen component) of an allergen, which gives high sensitivity to the specific proteins. This enables clinicians to reveal whether the sensitisation is due to the allergen component. From there, a more accurate diagnosis and better patient management can be done. Identification of allergen component is also critical in providing a successful personalised immunotherapy that

suits the individual (Ferreira, Wolf, & Wallner, 2014b). The advantage of using recombinant allergen compared to crude extracts in allergy diagnosis has been reported in various studies (Schmid-Grendelmeier & Cramer, 2001; Thia & Balfour Lynn, 2009; Thomas, 2011). Currently, the commercially available recombinant allergens are Alt a1, Asp f 1, Asp f 2, Asp f 3 and Asp f 4 from Thermo Scientific (www.phadia.com).

Fungal genomes have also been used in the screening of potential allergens repertoire, to improve the knowledge of fungal allergens and retrieval of the complete coding sequence of allergen-related genes (Fraczek & Bowyer, 2013). Through comparative genome analysis, an estimated 20 well-characterised allergens may be identified from a fungal genome containing 6,000 to 10,000 genes, with another 20 homologous proteins that might cross-react (Bowyer, Fraczek, & Denning, 2006). Hence, the availability of fungal genomes allows homologous protein analysis to be carried out.

CHAPTER 3: METHODOLOGY

3.1 Dematiaceous fungal specimens collection and isolation

The dematiaceous fungal isolates included in this study were collected from the clinical specimens sent to the Mycology Unit of the University Malaya Medical Centre (UMMC) for examination from the period of 2006 to 2011. Clinicians collected patient specimens based on clinical history and suspicion of fungal infection. The samples were sent to Mycology laboratory for direct specimen examination to observe the presence of fungal elements. All specimen examinations were carried out according to the laboratory's standard operating procedures before fungal culturing. The dematiaceous fungi isolated and identified in this study were the result of samples grown from the sub-culturing process. The experimental procedures are depicted in Figure 3.1.

3.1.1 Morphological identification

3.1.1.1 Macroscopic observation

The isolates were cultured on Sabouraud Dextrose Agar (SDA) and incubated at 30°C up to 4 weeks. The cultures were observed for colony characteristics such as colour, texture and topology.

3.1.1.2 Microscopic observation

A cube of Potato Dextrose Agar (PDA) was transferred to the centre of a sterile glass slide in a petri dish. Fungal mycelium was inoculated at the four sides of the agar square followed by placing a cover slide on the surface of the agar. Distilled water was added to the dish without wetting the agar, and the plate was incubated up to a week at 30°C. When sufficient growth was attained, a drop of Lactophenol Cotton Blue (LCB) stain was added on a new glass slide. The cover slip from the culture was removed from the

agar and was placed on top of the drop of LCB on the slide. The structure of hyphae and conidia of each isolate was then observed under light microscope.

3.1.2 Molecular identification

3.1.2.1 Deoxyribonucleic acid (DNA) extraction

A total of 3 mL phosphate buffered saline (PBS, pH 7.4) was added to a full grown fungal culture plate followed by the gentle scraping of the agar surface with an L-shaped glass Pasteur pipette. The suspension was collected into a PBS washed glass beads containing 15 mL tube and was vortexed for 5 mins.

DNA extraction was conducted using ZR Fungal/Bacterial DNA MiniPrep™ kit (Zymo Research, USA). Briefly, 750 µL Lysis Solution and 200 µL of fungal suspension were added into ZR Bashing Beads Lysis Tube. The mixture was vortexed for 5 mins and then centrifuged at $10,000 \times g$ for 1 min. A volume of 400 µL supernatant was transferred into the Zymo-Spin™ IV Filter and was centrifuged at $7000 \times g$ for 1 min. The spin filter was removed, and 1200 µL of Fungal/Bacterial DNA Binding Buffer was added to the collection tube. Next, 800 µL of the mixture was transferred into Zymo-Spin™ IIC Column in a collection tube and was centrifuged at $10,000 \times g$ for 1 min. The flow-through was discarded, and the balance of mixture in collection tube was transferred into the IIC column and centrifuged again. The column was washed with 200 µL of DNA Pre-Wash Buffer and centrifuged at $10,000 \times g$ for 1 min. The column was washed again with 500 µL of Fungal/Bacterial DNA Wash Buffer and centrifuged at $10,000 \times g$ for 1 min. The flow-through was discarded, and the column was reinserted in a collection tube and centrifuged at $10,000 \times g$ for 2 mins to ensure the membrane was thoroughly dry. The IIC column was then transferred to 1.5 mL centrifuge tube, and 100 µL DNA Elution Buffer was added to the column matrix and incubated for 5 mins

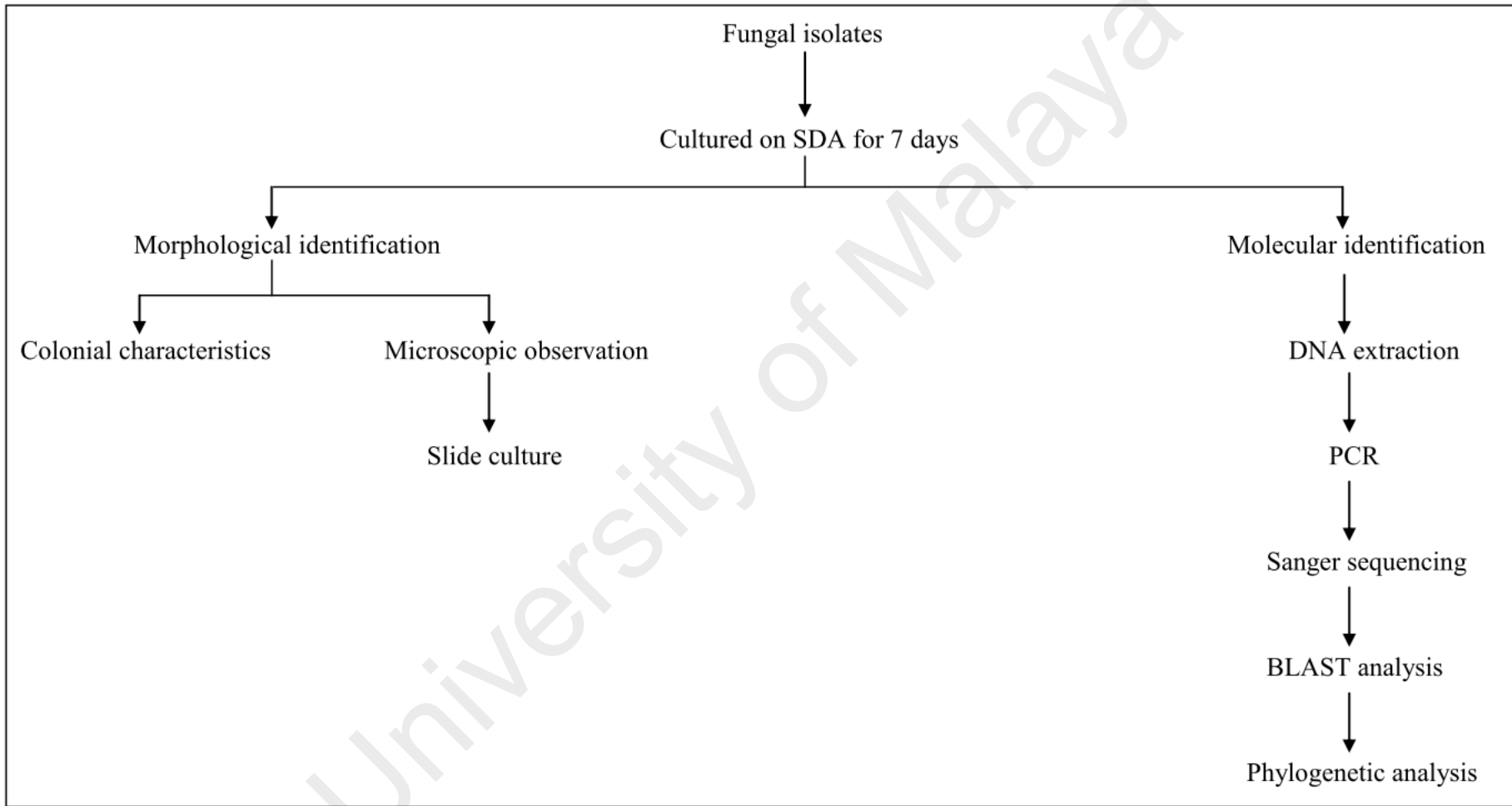


Figure 3.1: Schematic diagram of experimental procedures for dematiaceous fungi identification

at room temperature. The column was centrifuged at $10,000 \times g$ for 2 mins to elute the DNA. The collected elute was stored at -20°C until further process.

3.1.2.2 Polymerase chain reaction (PCR)

For PCR reaction, amplification of the internal transcribed spacer (ITS) region ITS1-5.8SRNA-ITS2 was carried out using HotStarTaq Plus DNA Polymerase (Qiagen, Germany). The primer set ITS1 (5'- TCC GTA GGT GAA CCT GCG G -3') and ITS4 (5'- TCC TCC GCT TAT TGA TAT GC -3') was used as forward and reverse primer, respectively (White, Burns, Lee, & Taylor, 1990). The PCR master mix components were prepared as shown in Table 3.1. The cocktail was then subjected to PCR reaction according to the thermal cycler protocol as follow: initial denaturation at 95°C for 5 mins; 30 cycles of denaturation at 94°C for 30 secs, annealing at 58°C for 30 secs, extension at 72°C for 1 min; and final extension at 72°C for 10 mins.

Table 3.1: Components of PCR master mix

Component	Initial concentration	Final concentration	Volume/reaction (μL)
10 \times Buffer	10 \times	1 \times	2.5
dNTP	10 mM	1 mM	2.5
Forward primer	10 μM	0.2 μM	0.5
Reverse primer	10 μM	0.2 μM	0.5
MgCl ₂	25 mM	1.5 mM	1.5
<i>Taq</i> polymerase	5 U	2.5 U	0.5
Nuclease-free water	-	-	12
Template DNA	-	-	5
Total volume	-	-	25

The fragment size of PCR product was determined by agarose gel electrophoresis using 1% (w/v) agarose gel (Appendix B). A volume of 5 μL PCR product together with 1 μL of loading dye was subjected to electrophoresis at 120 V for 30 mins in 1 \times Tris-Borate-EDTA (TBE) buffer. A total of 1 μL 100 bp DNA ladder was loaded into

another well as a marker (i-DNA, Malaysia). The gel was then photographed under UV light illumination using Syngene InGenius Gel Documentation System (Imgen Technologies, USA).

3.1.2.3 PCR product purification

After obtaining desired PCR product size (600-800 bp) via observation from the agarose gel, the PCR product was purified using Expin™ PCR SV kit (GeneAll Biotechnology, Korea). A total of 100 µL PB Buffer was added to 20 µL of PCR product and then the mixture was transferred into SV Column. The column was centrifuged at $11,000 \times g$ for 30 secs followed by discarding the flow-through. After that, 750 µL of NW Buffer was added to wash the column and was centrifuged at $11,000 \times g$ for 30 secs. The flow-through was discarded, and the column was centrifuged again at $11,000 \times g$ for 2 mins. The SV column was inserted into 1.5 mL centrifuge tube, and 30 µL of EB buffer was added directly to the membrane matrix. The column was incubated for 5 mins at room temperature and centrifuged at $11,000 \times g$ for 2 mins. The eluate was collected and stored at -20°C .

Another gel electrophoresis was carried out after the purification process using 1% (w/v) agarose gel (Appendix B) to ensure the presence of desired product band (Section 3.1.2.2).

3.1.2.4 DNA sequencing and fungal isolates identification

The purified product of each isolate was sent for Sanger sequencing (First Base Laboratories, Malaysia). Base and quality calling was performed on the retrieved sequences using TraceTuner version 3.0.6 (Denisov, Arehart, & Curtin, 2004). The low-quality bases from both ends of the sequence (Phred value < 20) were trimmed using Lucy version 1.20 with the included zapping.awk script (Chou & Holmes, 2001).

Of all the cleaned sequences with the complete ITS1-5.8S-ITS2 region, the consensus sequences of duplicated copies were subjected to further analysis. A search of the unique nucleotide sequences against the National Centre of Biotechnology Information (NCBI) non-redundant database using Nucleotide-Basic Local Alignment Tool (BLAST) program was conducted to identify the fungal species. From the BLAST result, only the top five hits were used for species identification to avoid false identification due to errors deposited in the NCBI GenBank database.

3.1.3 Data mining

The ITS sequences of all species identified from the BLAST result were obtained from the NCBI GenBank, with only sequences containing complete ITS region were selected. In addition, two verified sequences for each identified fungal species were included in the construction of phylogenetic tree unless there was only one record in the database (Appendix C1).

3.1.4 Phylogenetic analysis

The ITS-based phylogenetic tree was constructed using complete ITS sequences obtained from the clinical isolates and the GenBank database, together with two out-group strains of *Saccharomyces boulardii*. Multiple sequence alignment (MSA) was conducted on all ITS sequences using M-Coffee (Moretti et al., 2007). The aligned sequences were combined into a unique final alignment using T-Coffee. The phylogenetic analysis was performed using MrBayes (Huelsenbeck & Ronquist, 2001). Bayesian Markov Chain Monte Carlo (MCMC) analysis was carried out by sampling across the entire general time reversible (GTR) model space. A total of 600,000 generations were run in this analysis, with a sampling frequency of 100 and diagnostics were calculated for every 1,000 generations. A burn-in setting of 25% was used to

discard the first 1,500 trees. The convergence was assessed according to the Draft MrBayes version 3.2 Manual (Ronquist, Huelsenbeck, & Teslenko, 2011). Convergence is achieved when the average standard deviation of split frequencies was below 0.01, the potential scale reduction factor (PSRF) was reasonably close to 1.0 for all parameters and no obvious trend for the plot of the generation versus the log probability of the data (the log likelihood values) was observed.

3.2 *Cladosporium sphaerospermum* UM 843

Based on the study in Section 3.1, *Cladosporium sphaerospermum* UM 843 isolated from blood culture was selected for further morphological and whole genome characterisation.

3.2.1 Morphological identification

The macroscopic and microscopic observation of *C. sphaerospermum* UM 843 was carried out as outlined in Section 3.1.1. Additionally, the isolate was cultured in PDA, Malt Extract Agar (MEA), and MEA supplemented with 5% (w/v) sodium chloride (NaCl) for 14 days at 30°C and 25°C (Appendix A). The isolate was also grown in Sabouraud Dextrose Broth (SDB) supplemented with 5%, 10%, 15%, 20%, 25%, and 30% (w/v) NaCl to observe its ability to grow in salt medium (Appendix A). The growth of fungus was observed up to 14-days.

3.2.1.1 Scanning electron microscope (SEM)

The fungal isolate was grown on SDA at 30°C for a week, and the culture was cut into 1 cm³ slices. The cube was placed into a vial and fixed with 4% glutaraldehyde at 4°C overnight. The specimen was washed three times with 0.1 M sodium cacodylate buffer for 10 mins each and post-fixed in 1% osmium tetroxide at 4°C for 2 hours. The specimen was again washed 3 times with 0.1 M sodium cacodylate buffer for 10 mins

wash each. After washing step, dehydration process was carried out by immersing the specimen in a series of alcohol as followed; 30% alcohol, 50% alcohol, 70% alcohol, 95% alcohol for 10 mins each and 100% alcohol twice for 15 mins each. The specimen was then immersed in 100% acetone twice for 15 mins each.

After the dehydration step, the specimen was transferred into specimen basket and was put into the critical dryer for 30 mins. The specimen was stuck onto stub using double-sided tape and was gold coated in sputter coater. The specimen was viewed by XL-30 ESEM microscope (Philips, Netherlands).

3.2.2 Data mining and phylogenetic tree construction

The ITS sequences of complete ITS region of all *C. sphaerospermum* species complexes were randomly mined from the NCBI GenBank. For each fungal species, the addition of at least two verified sequences was added in the analysis except there was only one record in the database. The ITS sequence of two outgroup strains, *C. salinae* were also obtained from GenBank (Appendix C2).

The construction of ITS-based phylogenetic tree for *C. sphaerospermum* species complexes was conducted similar to that of dematiaceous isolates (Section 3.1.4), with a difference in 150,000 generations were performed using MrBayes (Huelsenbeck & Ronquist, 2001).

3.2.3 Genomic DNA extraction and sequencing

3.2.3.1 Genomic DNA extraction

Large-scale DNA extraction was carried using the method as described (Kuan et al., 2015) to obtain a large amount of high-quality DNA.

The fungal culture was harvested by scraping the colony off the agar and placed in 50 mL tube with PBS buffer. The tube was centrifuged at $4000 \times g$ for 5 mins, and the supernatant was discarded. The harvested fungal culture was crushed into fine powder after freezing in liquid nitrogen using a pestle. The weight of the fungal powder was determined.

A total of 6 mL DNA extraction buffer (200 mM Tris-HCl, pH 8.5, 250 mM NaCl, 25 mM EDTA, 0.6% SDS) (Appendix A) was added for 1 gm of fungal powder and was mixed by inverting the tube several times. The mixture was then incubated at 65°C for 10 mins. After the incubation, 1.4 mL of 3 M sodium acetate (pH 5.3) was added for 1 gm of fungal powder to the mixture and mixed thoroughly. The mixture was incubated at -80°C for 20 mins. The mixture was then centrifuged at $4000 \times g$ for 5 mins, and the supernatant was transferred to a new 50 mL tube. The DNA extract was subjected to isopropanol precipitation by adding an equal volume of isopropanol into the tube and mixed by inverting the tube gently for 30 times. The tube was left to stand at room temperature for 5 mins and centrifuged at $4000 \times g$, 4°C for 30 mins. The supernatant was decanted carefully and proceeded with the washing of DNA pellet. A total of 5 mL 75% ice-cold ethanol was added to the tube followed by inverting the tube 3 to 6 times. The tube was then incubated at -20°C for 10 mins and the alcohol was decanted. This step was repeated twice wherein the third wash; the pellet was

transferred to 1.5 mL centrifuge tube before adding 75% ice cold alcohol. Alcohol was then decanted, and the pellet was dried by placing in a water bath at 65°C.

Lastly, 150 µL of elution buffer (10 mM tris-base, 1 mM EDTA) was added to the tube to dissolve the pellet. The eluate was added with 5 µL of 10 mg/mL Ribonuclease A (Intron Biotechnology, Korea) and incubated at 37°C overnight. Ribonuclease A was then heat inactivated by incubating the eluate at 65°C for 10 mins. The eluate was centrifuged at 4°C, 15,000 × g for 10 mins. The supernatant was transferred to a new tube carefully and stored at -20°C.

The quantity and quality of the extracted DNA were assessed using NanoDrop 2000c spectrophotometer (Thermo Fisher Scientific, USA) and agarose gel electrophoresis. A volume of 1 µL solution was used to measure the quality and quantity of DNA using NanoDrop 2000c. A 0.8% (w/v) agarose gel was prepared for gel electrophoresis (Appendix B). A volume of 1 µL extracted DNA was loaded into the well with 1 µL of loading dye and 4 µL of elution buffer. A volume of 1 µL each of 500 bp DNA ladder (i-DNA, Malaysia) and Lambda DNA/Hind III ladder (Thermo Fisher Scientific, USA) were used as markers. Electrophoresis was conducted at 90 V for 60 mins, and the gel was then photographed under UV light illumination. The integrity of DNA was determined, and the quantity of DNA was estimated based on the gel image.

3.2.3.2 Genomic DNA sequencing

The *C. sphaerospermum* UM 843 genome was sequenced using the Illumina HiSeq 2000 system (Illumina, USA). Two insert size libraries, 500-bp and 5-kb, were prepared using TruSeq v3 Reagent Kits (Illumina, USA). The workflow of *C. sphaerospermum* UM 843 genome analysis is shown in Figure 3.3.

3.3 *C. sphaerospermum* UM 843 genome *in silico* characterisation

3.3.1 Sequence pre-processing

The quality of both libraries sequenced reads was assessed using FastQC (Andrews, 2010). After quality checking, both libraries of sequenced reads were pre-processed using FASTX-Toolkit (http://hannonlab.cshl.edu/fastx_toolkit/). Firstly, two bases from the 5' end of all reads were trimmed. The bases with a Phred quality below quality value (Qv) 20 were trimmed from the 3' end of the reads. The trimmed reads shorter than 30 bp and the reads with 40% bases having $Qv \leq 20$ were filtered. The data produced were subjected to quality re-assessment via FastQC (Andrews, 2010). The unpaired reads as a result of filtering reads were then removed. The paired reads files consisting of forward and reverse sequenced reads were merged into one file as final high quality sequenced read. For the 5-kb sequenced reads, an additional step to reverse complement the reads was performed. The final high-quality reads from both libraries were used for the further process.

3.3.2 *de novo* genome assembly, scaffolding, gap filling and contamination check

The final high quality sequenced reads of the small insert, large insert, and combined insert libraries were assembled individually using Velvet version 1.2.07 (Zerbino & Birney, 2008). The assembly of small and large insert libraries was carried out to ensure the quality of filtered reads for assembly and to estimate the paired reads insert size. Both individual libraries assemblies were done with k-mer setting = 55, with default settings. The combined insert libraries were assembled with k-mer setting = 49, scaffolding = no, insert_length = 465, ins_length_sd = 50, insert_length2 = 5000, ins_length2_sd = 500, min_contig_lgth = 200 and shortMatePaired2 = yes for velvetg parameters. K-mers optimisation was conducted by running velvet with a range of k-mers (39 to 71) to construct the hash table. Assembly with the best k-mer was selected.

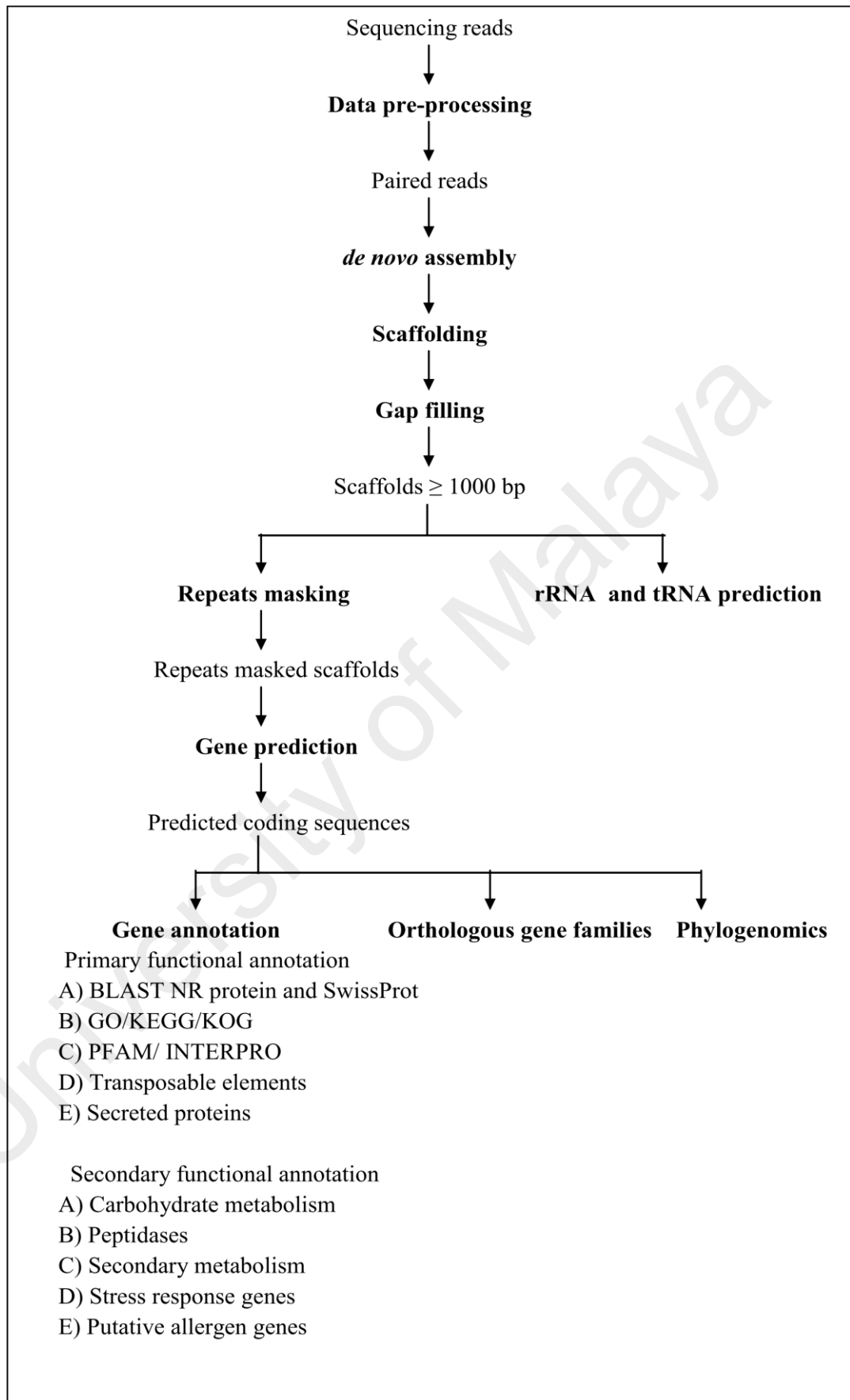


Figure 3.2: Workflow of *C. sphaerospermum* UM 843 genome analysis

The generated contigs were scaffolded using SSPACE Basic version 2.0 [parameters: -z 200, -k 5, -a 0.3, -n 30 and -T 10] (Boetzer, Henkel, Jansen, Butler, & Pirovano, 2011). The scaffolds generated were then gap filled using GapFiller version 1.10 (Boetzer & Pirovano, 2012) [parameters: -m = 60, -o = 15, -r = 0.8, -n = 30, -t = 15 and -T = 10]. The gap filling was performed by utilising paired-end information from both libraries. The final gap-filled sequences were then subjected to contamination check via nucleotide-BLAST against local non-redundant nucleotide database downloaded from NCBI. Sequences that hit to non-fungal species were then manually removed.

3.3.3 Gene prediction

Prior to the gene prediction of *C. sphaerospermum* UM 843, the interspersed repetitive elements, low complexity DNA sequences, rRNAs and tRNAs were masked. The interspersed repetitive elements and low complexity DNA sequences were masked using RepeatMasker version open-3.3.0 (<http://www.repeatmasker.org/>) with the Rebase fungal library version rm-20120418 [parameters: -species = fungi, -norna, -nolow, -pa = 1, -s, -engine = ncbi]. The rRNAs and tRNAs were identified using RNAmmer version 1.2 (Lagesen et al., 2007) and tRNAscan-SE version 1.3.1 (Lowe & Eddy, 1997) respectively. Then, the identified rRNAs and tRNAs were masked using the RepeatMasker output.

Ab initio gene prediction was conducted with GeneMark-ES version 2.3 (Lomsadze, Ter-Hovhannisyan, Chernoff, & Borodovsky, 2005). Frame correction of the stop codons in the translated coding sequences was carried out manually in sequence viewer Artemis version 12.0 (Rutherford et al., 2000). The finalised files of nucleotide and amino acid sequences of the predicted genes were then subjected to annotation. The

visualisation of gene organisation and retrieval of sequence from the genome were performed using Artemis (Rutherford et al., 2000).

3.3.4 Functional annotation

3.3.4.1 Primary functional annotation

Annotation of the putative coding sequences was initiated via local BLAST similarity searches of the nucleotide sequences against NCBI non-redundant and SwissProt databases. The BLAST output from both databases was then subjected to Gene Ontology (GO) and the Kyoto Encyclopedia of Genes and Genomes (KEGG) metabolic pathways match using local BLAST2GO tools (Conesa et al., 2005). The GO assignments were plotted using the web tool WEGO (Ye et al., 2006). On the other hand, the predicted amino acid sequences were classified based on Eukaryotic Orthologous Group (KOG) classifications via RPS-BLAST (Tatusov et al., 2003). Interpro protein domain families match to Pfam database was conducted to annotate predicted proteins based on protein domain families using InterProScan 5 (Quevillon et al., 2005). The putative transposable elements in UM 843 were detected using Transposon-PSI (<http://transposonpsi.sourceforge.net>). The transmembrane regions and orientation of proteins were conducted using TMpred server (http://www.ch.embnet.org/software/TMPRED_form.html).

Secreted proteins were predicted according to the method as described (Ohm et al., 2012). The cleavage sites and signal peptide/non-signal peptide prediction were carried out using SignalP version 4.1 (Petersen, Brunak, von Heijne, & Nielsen, 2011). The presence of transmembrane (TM) domains was identified using TMHMM version 2.0 (Krogh, Larsson, von Heijne, & Sonnhammer, 2001). Secreted proteins were selected on proteins without TM domains and proteins with single TM present at the N-terminal

40 amino acids corresponding to the secretion signals. The percentage of cysteine residues in the secreted proteins were determined to identify high cysteine proteins. According to Ohm et al. (2012), high cysteine protein was determined when the percentage of the cysteine residues in the protein was, at least, two fold the average percentage of cysteine residues in all predicted proteins of that organism. The localisation of the proteins was predicted using Wolf PSORT (Horton et al., 2007).

3.3.4.2 Secondary functional annotation

Annotation of the UM 843 gene models was further conducted to categorise the genes based on functions that involved in carbohydrate metabolism, protein hydrolysis, secondary metabolism and, proteins involved in stress responses.

(a) *Carbohydrate metabolism*

The CAZymes were annotated by searching against the DataBase for automated Carbohydrate-active enzyme ANnotation (dbCAN) (Yin et al., 2012). The annotation was carried out by submitting the predicted protein sequences to the dbCAN website (<http://csbl.bmb.uga.edu/dbCAN/>).

(b) *Peptidases*

The protein models of UM 843 were queried against the MEROPS database via BLASTP (Rawlings et al., 2012). Batch blast was conducted by subjecting the sequences to the MEROPS website (http://merops.sanger.ac.uk/cgi-bin/batch_blast/). Comparison of UM 843 peptidases was carried out by performing MEROPS analysis together with 18 other fungal genomes (Table 3.2). Filtering was performed on sequences where: i) the active site residue and metal-ligand do not match any of those permitted for the active site residue or metal-ligand at that position, and ii) the active site residue or metal ligand is missing.

(c) ***Secondary metabolism***

The putative secondary metabolite biosynthesis backbone genes and its associated gene clusters were analysed using the web-based Secondary Metabolite Unknown Region Finders (SMURF) (Khaldi et al., 2010). A coordinate file consisting of the protein ID, scaffold number, 5' gene start position and 3' gene stop position was prepared. The coordinate file together with the protein sequences file was submitted to the SMURF website (www.jcvi.org/smurf/). Prediction of the transcription factor binding sites of the selected genes was carried out using TFBIND (Tsunoda & Takagi, 1999) by subjecting the upstream region sequence to the website (<http://tfbind.hgc.jp/>).

(d) ***Stress responsive genes***

A local database was built from genes downloaded from the Fungal Stress Response Database (FSRD) (Karányi, Holb, Hornok, Pócsi, & Miskei, 2013). The potential stress responsive genes were identified by performing local BLASTP search against the database. An e-value threshold of $\leq 1e-5$, identity exceeding 50% and subject coverage exceeding 70% were used as the criteria for the genes.

Table 3.2: List of dematiaceous fungi used in the MEROPS analysis, orthologous genes and genome comparative analysis, and generation of phylogenomic tree

Fungal name	Sequencing centre	Reference
<i>Alternaria brassicicola</i> ATCC96866	Washington University Genome Centre (WUGC) (USA)	Cho et al. (2012), Ohm et al. (2012)
<i>Pyrenophora tritici-repentis</i> Pt-1C-BFP	BROAD (USA)	Manning et al. (2013)
<i>Pyrenophora teres f. teres</i> 0-1	Curtin University (Australia)	Ellwood et al. (2010)
<i>Cochliobolus heterostrophus</i> C5	JGI (USA)	Condon et al. (2013), Ohm et al. (2012)
<i>Cochliobolus heterostrophus</i> C4	JGI (USA)	Condon et al. (2013), Ohm et al. (2012)
<i>Cochliobolus carbonum</i> 26-R-13	JGI (USA)	Condon et al. (2013)
<i>Cochliobolus victoriae</i> FI3	JGI (USA)	Condon et al. (2013)
<i>Cochliobolus miyabeanus</i> ATCC 44560	JGI (USA)	Condon et al. (2013)
<i>Cochliobolus sativus</i> ND90Pr	JGI (USA)	Condon et al. (2013), Ohm et al. (2012)
** <i>Cochliobolus lunatus</i> m118	JGI (USA)	Unpublished data
<i>Setosphaeria turcica</i> Et28A	JGI (USA)	Condon et al. (2013), Ohm et al. (2012)
<i>Leptosphaeria maculans</i> JN3	INRA/Genoscope (France)	Ohm et al. (2012), Rouxel et al. (2011)
<i>Hysterium pulicare</i> CBS123377	Oregon State University (USA)	Ohm et al. (2012)
** <i>Botryosphaeria dothidea</i> v 1.1	Oregon State University (USA)	Unpublished data
<i>Macrophomina phaseolina</i> MS6	Bangladesh Jute Research Institute (BJRI) (Dhaka)	Islam et al. (2012)
<i>Neofusicoccum parvum</i> UCRNP2	University of California-Davis (USA)	Blanco-Ulate, Rolshausen, & Cantu (2013)

Table 3.2, continued

Fungal name	Sequencing centre	Reference
** <i>Acidomyces richmondensis</i> v1.0	JGI (USA)	Unpublished data
<i>Baudoinia compniacensis</i> UMAH10762	JGI (USA)	Ohm et al. (2012)
<i>Cladosporium fulvum</i> CBS13901	Wageningen University (The Netherlands)	de Wit et al. (2012), Ohm et al., (2012)
<i>Dothistroma septosporum</i> NZE10	JGI (USA)	de Wit et al., (2012), Ohm et al. (2012)
** <i>Zasmidium cellare</i> ATCC 36951 v1.0	JGI (USA)	Unpublished data
<i>Pseudocercospora fijiensis</i> CIRAD86	JGI(USA)	Ohm et al. (2012)
Outgroup for phylogenomic tree		
** <i>Chaetomium globosum</i> CBS148.51	BROAD (USA)	Ohm et al. (2012)
** <i>Chaetomium thermophilum</i> var. <i>thermophilum</i> DSM 1495	Heideilberg University (Germany)	Amselem et al. (2011)

** fungi not included in peptidase analysis

3.3.5 Orthologous genes and genome comparative analysis

The protein sequences of all current publicly-available dematiaceous Dothideomycetes genomes were downloaded from various databases to identify the UM 843 orthologs (Table 3.2). The analysis of protein sequences clustering (≥ 33 amino acids) was performed using OrthoMCL version 2.02 (Li, Stoeckert, & Roos, 2003). The analysis was executed via all-against-all BLASTP searches of all proteins. Orthologs were recognised by sequences with reciprocal best blast hits from distinct genomes. OrthoMCL applies the Markov Cluster algorithm (Dongen, 2000) with $1e-5$ BLASTP e-value cut-off and 1.5 inflation parameter.

3.3.6 Phylogenomic analysis

The proteome clusters were generated using all the protein sequences shown in Table 3.2. The two Sordariomycetes proteomes are used as outgroup in the construction of the phylogenomic tree. Clustering of protein sequences was carried out as described in Section 3.3.5. A total of 220 single-copy orthologs containing one member of each species was treated with individual sequence alignments using ClustalW version 2.0 (Larkin et al., 2007). Removal of spurious sequences or poorly aligned regions was accomplished using trimAL (with the *automated* option). The filtered multiple alignments were concatenated into a superalignment with 110,781 characters. Eventually, ProtTest version 3.2 (Abascal, Zardoya, & Posada, 2005) with Akaike Information Criteria (AIC) calculation on alignment was carried out to determine the best-fit substitution model. The phylogenomic tree was constructed by using both RAxML version 7.7.9 (Stamatakis, 2006) and MrBayes version 3.2.1 (Huelsenbeck & Ronquist, 2001). The best-scoring maximum likelihood tree was searched by running RAxML with model PROTGAMMALGF, followed by 100 bootstrap replicates. Convergence was observed after 50 replicates using *-I autoMRE* option in RAxML.

MrBayes was run using a mixed amino acid model with gamma-distributed rate variation across sites and a proportion of invariable sites. The MCMC was run with a sampling frequency of 100 for 250,000 generations, and burn-in setting of 25%. The convergence was assessed according to the Draft MrBayes version 3.2 Manual (Ronquist et al., 2011) (Section 3.1.4).

3.3.7 Allergen genes in UM 843

A keyword search using the term 'allergen' was conducted towards the non-redundant and SwissProt BLAST output to search for potential allergen genes in UM 843. Putative genes with <50% identity to the hit were filtered as these proteins are less likely to cross-react in patients sensitised with these fungal allergens (Aalberse, 2000). Further inspection was carried out to identify potential *Cladosporium*-specific allergens.

3.4 Validation of gene sequences and detection of mRNA - hydrophobin genes

DNA extraction was conducted as described (Section 3.1.2.1). PCR was performed using the designed primer sets as shown in Table 3.3. The primer sets were manually designed and primer specificity check was conducted via Primer-BLAST against the *C. sphaerospermum* UM 843 genome (Ye et al., 2012). All primers were synthesised at First Base Laboratories (Malaysia). The PCR master mix components were prepared as shown in Table 3.4. The PCR thermal cycle was performed with the same thermal profile in Section 3.1.2.2. The PCR products were then electrophoresed on 1% (w/v) agarose gel for 30 mins at 90 V to observe the presence of the DNA band. Purification of PCR products was then carried out (Section 3.1.2.3) followed by Sanger sequencing (First Base Laboratories, Malaysia).

Table 3.3: Primer sets designed to be used in amplification of hydrophobin genes in UM 843

Gene ID	Primer	Sequence (5' - 3')
UM843_6061	6061_F	TCAGACATCCCAACACCTTTAC
	6061_R	TTAAAGCGGGATGGAAAGGC
UM843_4115	4115_F	TAAGCAACTCTCCAACCATCAC
	4115_R	TTAAAGCGGGATGGAAAGGC
UM843_3639	3639_F	AGTCAATCCCCCAAACCAAC
	3639_R	TTAGAGAGGGATGGAGACGC
UM843_1201	1201_F	AGTCAACCAACCCAATCAACAC
	1201_R	TTAGAGGGGGAGGGACAGG

F - forward primer

R - reverse primer

Table 3.4: Components of PCR master mix

Component	Initial concentration	Final concentration	Volume/reaction (μL)
10× buffer	10×	1×	5
dNTP	10 mM	0.2 mM	1
Forward primer	10 μM	0.4 μM	2
Reverse primer	10 μM	0.4 μM	2
MgCl ₂	25 mM	1.5 mM	3
<i>Taq</i> polymerase	5 U	2.5 U	0.5
dH ₂ O	-	-	31.5
Template	-	-	5
Total volume	-	-	50

3.4.1 mRNA detection

3.4.1.1 RNA extraction

A week old fungal culture was scrapped off from the agar surface, and 100 mg of the sample was weighed. The sample was then frozen using liquid nitrogen and grounded into fine powder. Total ribonucleic acid (RNA) was extracted from the sample using the RNeasy Plant Mini Kit (Qiagen, Germany).

A volume of 450 μL Buffer RTL was added immediately to the fine powder and mixed vigorously. The lysate was then transferred to the QIAshredder spin column and

was centrifuged at $15,000 \times g$ for 2 mins to homogenise the lysate. The supernatant was transferred carefully to a new 1.5 mL tube followed by addition of 0.5 volume of ethanol (96-100%) to the supernatant. After mixing the mixture via pipetting, the lysate was transferred to the RNeasy spin column and centrifuged at $10,000 \times g$ for 30 secs. The RNeasy column was then transferred to a new collection tube. A total of 350 μL Buffer RW1 was then added to the column and centrifuged at $10,000 \times g$ for 30 secs. The RNeasy column was again transferred to a new collection tube. DNase digestion was carried out by adding a pre-mixture of 10 μL DNase I stock solution with 70 μL Buffer RDD directly on the column membrane and incubated at room temperature for 30 mins.

After incubation, 350 μL of Buffer RW1 was added to the RNeasy column and was centrifuged at $10,000 \times g$ for 30 secs. The RNeasy column was transferred to a new collection tube. A volume of 500 μL Buffer RPE was added to the spin column to wash the column. The tube was centrifuged at $10,000 \times g$ for 30 secs, and the flow-through was discarded. The addition of Buffer RPE was repeated and the tube was centrifuged at $10,000 \times g$ for 2 mins. The RNeasy column was transferred to a new collection tube and spun at $15,000 \times g$ for 1 min. The RNeasy column was then relocated to a 1.5 mL centrifuge tube and 30 μL of RNase-free water was added directly to the column membrane and incubated for 5 mins at room temperature. The column was centrifuged at $10,000 \times g$ for 1 min to elute the RNA. The collected eluate was stored at -80°C until further process.

The quality and integrity of the extracted RNA were assessed using NanoDrop 2000c spectrophotometer (Thermo Fisher Scientific, USA) and via agarose gel electrophoresis, respectively. A volume of 1 μL eluate was used to measure the quality and quantity of

RNA using NanoDrop 2000c. A 1% (w/v) agarose gel was prepared (Appendix B). A volume of 5 μL of RNA with an equal volume of loading dye and 2 μL RiboRuler High Range RNA Ladder (Thermo Fisher Scientific, USA) were loaded into the well. Electrophoresis was conducted at 90 V for 45 mins and the gel was then photographed under UV light illumination. The integrity of the RNA was determined by observing the presence of two intact bands.

3.4.1.2 Reverse transcription polymerase chain reaction (RT-PCR)

(e) *Reverse transcription*

The cDNA was synthesised via reverse transcription process using RevertAid H Minus First Strand cDNA Synthesis Kit (Thermo Fisher Scientific, USA). A primer mixture of 0.5 μL oligo (dT)₁₈ primer and 0.5 μL random hexamer was used in this reaction. The mixture was added to 5 μL template RNA and nuclease-free water was added to achieve a final volume of 12 μL . A no template negative control was prepared by replacing 5 μL RNA template with nuclease-free water. Positive control was prepared by substituting RNA template with 2 μL Control GAPDH RNA supplied by the kit. The tube was then incubated at 65°C for 5 mins. The reaction was terminated by heating at 70°C for 5 mins. The mixture was then chilled immediately on ice, and the components in Table 3.5 were added sequentially to give a final volume of 20 μL . For the reverse transcriptase minus negative control, the 1 μL reverse transcriptase was substituted with nuclease-free water. The mixture was gently mixed and incubated at 25°C for 5 mins followed by 60 mins at 42°C. The product was then kept at -20°C until PCR amplification.

(f) **PCR**

The PCR amplification reaction was conducted as described in Section 3.1.2.2 with the only difference in the amplification cycle of 35. The primers used are the same as shown in Table 3.3. The primers for amplification of control positive was supplied by the manufacturer.

Table 3.5: Components of reverse transcription process

Components	Volume (μL)
5 \times Reaction Buffer	4
RiboLock RNase Inhibitor (20U/ μL)	1
10 mM dNTP Mix	2
RevertAid H Minus M-MulV Reverse Transcriptase (200U/ μL)	1

The amplified PCR products were electrophoresed in the 2% (w/v) agarose gel (Appendix B) for 30 mins at 90 V to observe the presence of the DNA band. Purification of PCR products was then carried out followed by Sanger sequencing (First Base Laboratories, Malaysia).

3.5 Data availability

All the micrographs and ITS sequences of dematiaceous isolates are available at the in-house database, DemaDb (http://www.codoncloud.com:85/FungalGenomeV2_1/). The ITS sequences are also available in NCBI GenBank (refer Table 4.1 for accession No.). The genome data of *C. sphaerospermum* UM 843 is available in DemaDb (Kuan et al., 2016) and the nucleotide sequence of the UM 843 genome can also be retrieved from DDBJ/EMBL/GenBank with accession number AIIA02000000.

CHAPTER 4: RESULTS

4.1 Fungal collection

From 2006 to 2011, a total of 75 dematiaceous fungi was isolated from the collection of 1,250 moulds in the Mycology Unit (Figure 4.1). The fungi were isolated from nails, skins, nasopharyngeal secretions, tissue biopsies and blood (Figure 4.2). The skin scraping has the highest number among all the specimen types received in the lab. Of the 75 isolates, 67 were morphologically identified to the genus level. Based on molecular technique, 73 were identified to the species level. (Table 4.1).

Among the 28 dematiaceous fungi isolated from skin scrapings, 11 genera and one unclassified Herpotrichiellaceae were identified by molecular technique (Table 4.1). There were six isolates of *Cladosporium* spp., comprising *C. cladosporioides* (one), *C. dominicanum* (one) and *C. sphaerospermum* (four). Five isolates of the genus *Cochliobolus* were identified as *C. lunatus* (four) and *C. geniculatus* (one). There were four isolates from the genus *Ochroconis* and were identified as *O. constricta*. Other dematiaceous fungi isolated from the skin scrapings included *Bipolaris* sp. (one), *Curvularia affinis* (three), *Nigrospora oryzae* (three), *Exophiala dermatitidis* (one), *Stagonospora* sp. (one) and *Pyrenochaeta unguis-hominis* (one).

The 24 fungi isolated from nails belonged to ten genera. The 24 isolates included five *Cladosporium*, five *Neoscytalidium*, four *Phoma*, and one *Alternaria*, *Chaetomium*, *Curvularia*, *Exophiala*, *Daldinia*, *Nigrospora*, and Unclassified Ascomycota each. On the other hand, the ten dematiaceous fungi isolated from blood cultures were identified as *Cladosporium* spp. (seven *C. sphaerospermum*, and one *C. cladosporioides*), *Daldinia eschscholtzii*, and *Cochliobolus lunatus* (Table 4.1).

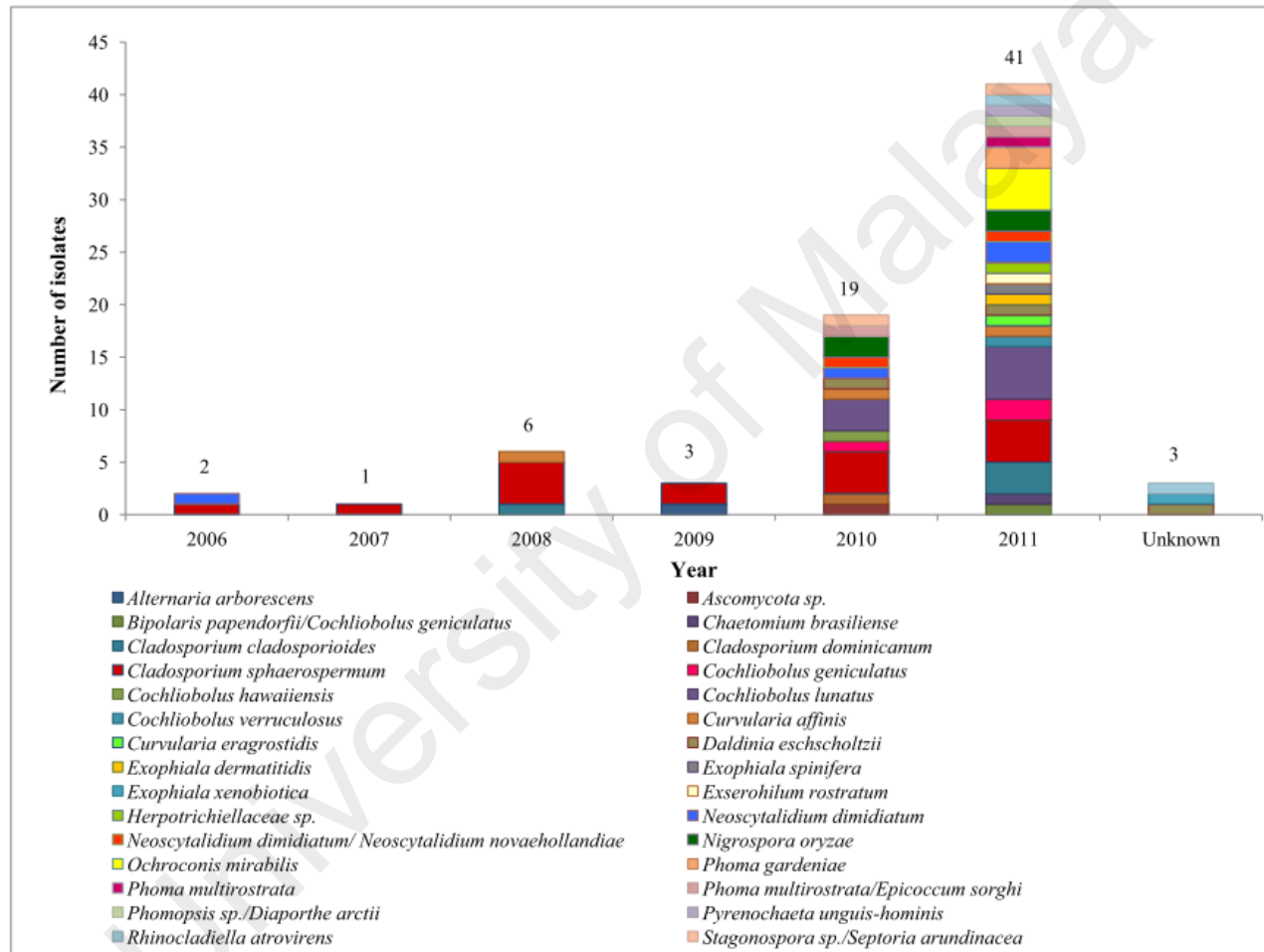


Figure 4.1: Number of isolates collected from the year 2006 to 2011

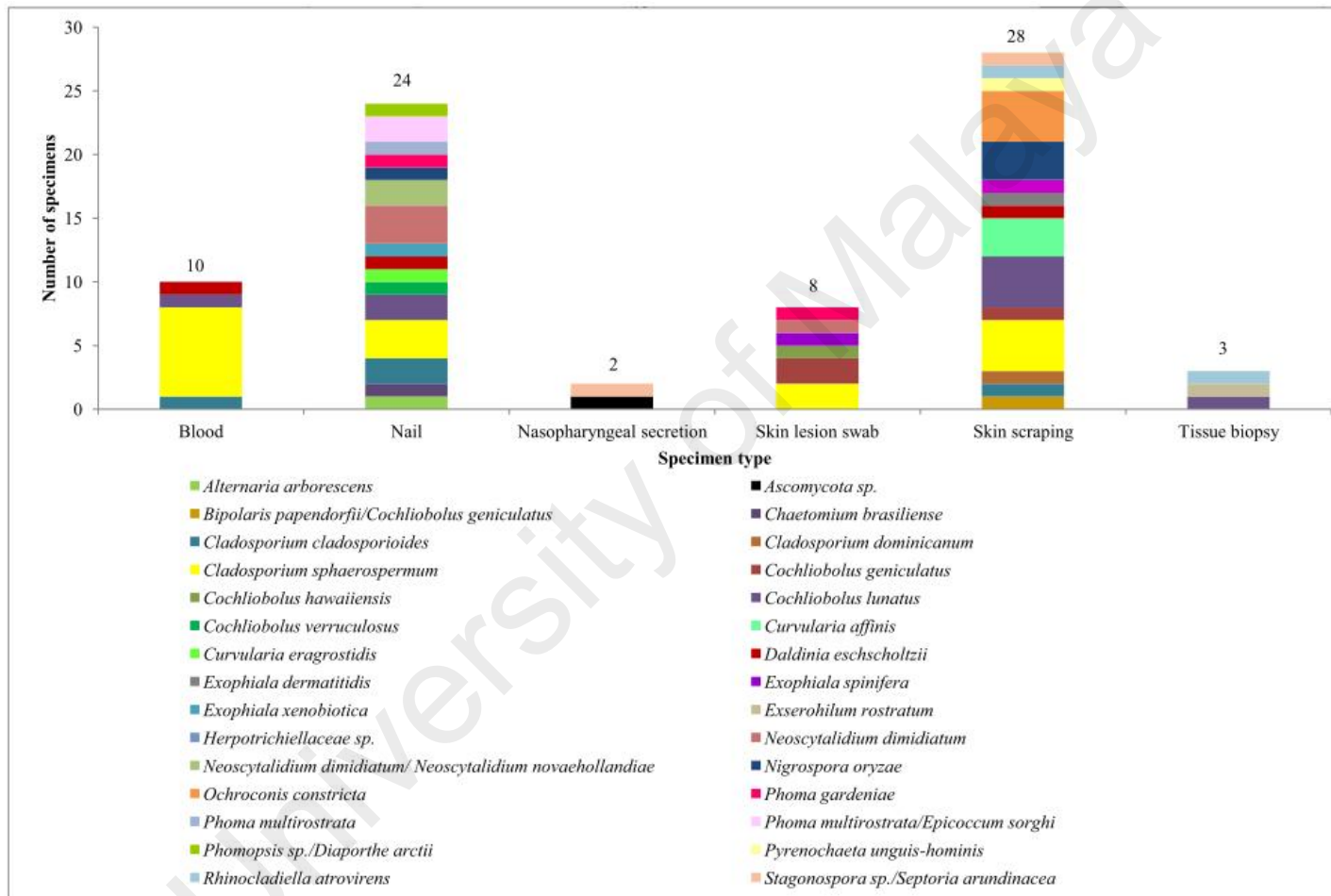


Figure 4.2: Number of specimens received in the Mycology Unit from the year 2006 to 2011

Table 4.1: Details of dematiaceous fungi isolated in this study

No.	Isolate ID	Specimen type	Morphological identity	Molecular identity	Accession No.
1.	UM 75	Nail	<i>Alternaria</i> sp.	<i>Alternaria arborescens</i>	JX966632
2.	UM 221	Nasopharyngeal secretion	No identifiable features	<i>Ascomycota</i> sp.	JX966643
3.	UM 235	Nail	<i>Chaetomium</i> sp.	<i>Chaetomium brasiliense</i>	JX966545
4.	UM 265	Nail	<i>Cladosporium</i> sp.	<i>Cladosporium cladosporioides</i>	JX966584
5.	UM 315	Skin scraping	<i>Cladosporium</i> sp.	<i>Cladosporium cladosporioides</i>	JX966581
6.	UM 318	Nail	<i>Cladosporium</i> sp.	<i>Cladosporium cladosporioides</i>	JX966582
7.	UM 77	Blood	<i>Cladosporium</i> sp.	<i>Cladosporium cladosporioides</i>	JX966583
8.	UM 155	Skin scraping	<i>Cladosporium</i> sp.	<i>Cladosporium dominicanum</i>	JX966585
9.	UM 165	Nail	<i>Cladosporium</i> sp.	<i>Cladosporium sphaerospermum</i>	JX966566
10.	UM 187	Skin lesion Swab	<i>Cladosporium</i> sp.	<i>Cladosporium sphaerospermum</i>	JX966577
11.	UM 225	Skin scraping	<i>Cladosporium</i> sp.	<i>Cladosporium sphaerospermum</i>	JX966565
12.	UM 245	Skin lesion Swab	<i>Cladosporium</i> sp.	<i>Cladosporium sphaerospermum</i>	JX966579
13.	UM 269	Skin scraping	<i>Cladosporium</i> sp.	<i>Cladosporium sphaerospermum</i>	JX966564
14.	UM 333	Skin scraping	<i>Cladosporium</i> sp.	<i>Cladosporium sphaerospermum</i>	JX966574
15.	UM 349	Blood	<i>Cladosporium</i> sp.	<i>Cladosporium sphaerospermum</i>	JX966578
16.	UM 350	Blood	<i>Cladosporium</i> sp.	<i>Cladosporium sphaerospermum</i>	JX966573
17.	UM 351	Blood	<i>Cladosporium</i> sp.	<i>Cladosporium sphaerospermum</i>	JX966575
18.	UM 352	Skin scraping	<i>Cladosporium</i> sp.	<i>Cladosporium sphaerospermum</i>	JX966567
19.	UM 353	Nail	<i>Cladosporium</i> sp.	<i>Cladosporium sphaerospermum</i>	JX966570
20.	UM 354	Nail	<i>Cladosporium</i> sp.	<i>Cladosporium sphaerospermum</i>	JX966569
21.	UM 67	Blood	<i>Cladosporium</i> sp.	<i>Cladosporium sphaerospermum</i>	JX966572

Table 4.1, continued

No.	Isolate ID	Specimen type	Morphological identity	Molecular identity	Accession No.
22.	UM 68	Blood	<i>Cladosporium</i> sp.	<i>Cladosporium sphaerospermum</i>	JX966571
23.	UM 76	Blood	<i>Cladosporium</i> sp.	<i>Cladosporium sphaerospermum</i>	JX966568
24.	UM 843	Blood	<i>Cladosporium</i> sp.	<i>Cladosporium sphaerospermum</i>	JX966576
25.	UM 226	Skin scraping	<i>Bipolaris</i> sp.	<i>Bipolaris papendorfiti/Cochliobolus geniculatus</i>	JX966599
26.	UM 183	Skin lesion Swab	<i>Bipolaris</i> sp.	<i>Cochliobolus geniculatus</i>	JX966589
27.	UM 217	Skin scraping	<i>Bipolaris</i> sp.	<i>Cochliobolus geniculatus</i>	JX966590
28.	UM 236	Skin lesion Swab	<i>Bipolaris</i> sp.	<i>Cochliobolus geniculatus</i>	JX966588
29.	UM 191	Skin lesion Swab	<i>Bipolaris</i> sp.	<i>Cochliobolus hawaiiensis</i>	JX966615
30.	UM 164	Tissue biopsy	<i>Curvularia</i> sp.	<i>Cochliobolus lunatus</i>	JX966621
31.	UM 189	Nail	<i>Curvularia</i> sp.	<i>Cochliobolus lunatus</i>	JX966607
32.	UM 201	Blood	<i>Curvularia</i> sp.	<i>Cochliobolus lunatus</i>	JX966625
33.	UM 239	Skin scraping	<i>Curvularia</i> sp.	<i>Cochliobolus lunatus</i>	JX966622
34.	UM 272	Skin scraping	<i>Curvularia</i> sp.	<i>Cochliobolus lunatus</i>	JX966623
35.	UM 296	Nail	<i>Curvularia</i> sp.	<i>Cochliobolus lunatus</i>	JX966624
36.	UM 313	Skin scraping	<i>Curvularia</i> sp.	<i>Cochliobolus lunatus</i>	JX966628
37.	UM 327	Skin scraping	<i>Bipolaris</i> sp.	<i>Cochliobolus lunatus</i>	JX966626
38.	UM 248	Nail	<i>Bipolaris</i> sp.	<i>Cochliobolus verruculosus</i>	JX966629
39.	UM 193	Skin scraping	<i>Curvularia</i> sp.	<i>Curvularia affinis</i>	JX966612
40.	UM 262	Skin scraping	<i>Curvularia</i> sp.	<i>Curvularia affinis</i>	JX966602
41.	UM 69	Skin scraping	<i>Curvularia</i> sp.	<i>Curvularia affinis</i>	JX966610
42.	UM 297	Nail	<i>Curvularia</i> sp.	<i>Curvularia eragrostidis</i>	JX966616

Table 4.1, continued

No.	Isolate ID	Specimen type	Morphological identity	Molecular identity	Accession No.
43.	UM 1020	Blood	<i>Daldinia</i> sp.	<i>Daldinia eschscholtzii</i>	JX966563
44.	UM 1400	Skin scraping	<i>Daldinia</i> sp.	<i>Daldinia eschscholtzii</i>	JX966561
45.	UM 230	Nail	<i>Daldinia</i> sp.	<i>Daldinia eschscholtzii</i>	JX966562
46.	UM 233	Skin scraping	<i>Exophiala</i> sp.	<i>Exophiala dermatitidis</i>	JX966558
47.	UM 247	Skin lesion Swab	<i>Exophiala</i> sp.	<i>Exophiala spinifera</i>	JX966556
48.	UM 162	Nail	<i>Exophiala</i> sp.	<i>Exophiala xenobiotica</i>	JX966559
49.	UM 241	Tissue biopsy	<i>Exserohilum</i> sp.	<i>Exserohilum rostratum</i>	JX966631
50.	UM 238	Skin scraping	No identifiable features	<i>Herpotrichiellaceae</i> sp.	JX966560
51.	UM 202	Nail	<i>Neoscytalidium</i> sp.	<i>Neoscytalidium dimidiatum</i>	JX966541
52.	UM 231	Nail	<i>Neoscytalidium</i> sp.	<i>Neoscytalidium dimidiatum</i>	JX966544
53.	UM 249	Nail	<i>Neoscytalidium</i> sp.	<i>Neoscytalidium dimidiatum</i>	JX966543
54.	UM 73	Skin lesion Swab	<i>Neoscytalidium</i> sp.	<i>Neoscytalidium dimidiatum</i>	JX966539
55.	UM 153	Nail	<i>Neoscytalidium</i> sp.	<i>Neoscytalidium dimidiatum/ Neoscytalidium novaehollandiae</i>	JX966542
56.	UM 224	Nail	<i>Neoscytalidium</i> sp.	<i>Neoscytalidium dimidiatum/ Neoscytalidium novaehollandiae</i>	JX966540
57.	UM 157	Skin scraping	<i>Nigrospora</i> sp.	<i>Nigrospora oryzae</i>	JX966548
58.	UM 160	Skin scraping	<i>Nigrospora</i> sp.	<i>Nigrospora oryzae</i>	JX966549
59.	UM 244	Skin scraping	<i>Nigrospora</i> sp.	<i>Nigrospora oryzae</i>	JX966547
60.	UM 299	Nail	Mycelia sterilia	<i>Nigrospora oryzae</i>	JX966550
61.	UM 314	Skin scraping	<i>Ochroconis</i> sp.	<i>Ochroconis mirabilis</i> (previous: <i>O. constricta</i>)	JX966647

Table 4.1, continued

No.	Isolate ID	Specimen type	Morphological identity	Molecular identity	Accession No.
62.	UM 324	Skin scraping	<i>Ochroconis</i> sp.	<i>Ochroconis mirabilis</i> (previous: <i>O. constricta</i>)	JX966645
63.	UM 326	Skin scraping	<i>Ochroconis</i> sp.	<i>Ochroconis mirabilis</i> (previous: <i>O. constricta</i>)	JX966646
64.	UM 329	Skin scraping	<i>Ochroconis</i> sp.	<i>Ochroconis mirabilis</i> (previous: <i>O. constricta</i>)	JX966644
65.	UM 228	Skin lesion Swab	<i>Phoma</i> sp.	<i>Phoma gardeniae</i>	JX966640
66.	UM 298	Nail	<i>Phoma</i> sp.	<i>Phoma gardeniae</i>	JX966638
67.	UM 223	Nail	<i>Phoma</i> sp.	<i>Phoma multirostrata</i>	JX966636
68.	UM 186	Nail	Mycelia sterilia	<i>Phoma multirostrata/Epicoccum sorghi</i>	JX966634
69.	UM 255	Nail	Mycelia sterilia	<i>Phoma multirostrata/Epicoccum sorghi</i>	JX966635
70.	UM 254	Nail	Mycelia sterilia	<i>Phomopsis</i> sp./ <i>Diaporthe arctii</i>	JX966551
71.	UM 256	Skin scraping	<i>Phoma</i> sp.	<i>Pyrenochaeta unguis-hominis</i>	JX966641
72.	UM 212	Tissue biopsy	<i>Exophiala</i> sp.	<i>Rhinocladiella atrovirens</i>	JX966554
73.	UM 234	Skin scraping	<i>Exophiala</i> sp.	<i>Rhinocladiella atrovirens</i>	JX966555
74.	UM 1110	Nasopharyngeal secretion	No identifiable features	<i>Stagonospora</i> sp./ <i>Septoria arundinacea</i>	JX966633
75.	UM 259	Skin scraping	Mycelia sterilia	<i>Stagonospora</i> sp./ <i>Septoria arundinacea</i>	JX966642

4.1.1 Morphological identification

According to the criteria described (de Hoog et al., 2000; Ellis, Davis, Alexiou, Handke, & Bartley, 2007; Ju, Rogers, & San Martin, 1997), there are 67 (89.3%) fungal isolates were identified via morphological characteristics to the genus level. The isolates were classified into 11 genera. An isolate, UM 256 was misidentified as *Phoma* species. Overall, the genus *Cladosporium* had the largest number of isolates (21), whereas the genus *Alternaria*, *Chaetomium* and *Exserohilum* had one isolate each. Eleven isolates were identified to the genus *Curvularia*, seven to the genus *Bipolaris*, six to *Neoscytalidium*, five to the genus *Exophiala*, and four species to the genus *Ochroconis*.

On the culture plate, all the dematiaceous isolates displayed colonies with dark brown, olivaceous or black in colour. The reverse of the agar plate is dark in colour. Microscopic observation revealed septate fungal elements and dark colour cell wall. The morphological features of each dematiaceous fungus are shown in Figure 4.3 and Figure 4.4.

Bipolaris, *Curvularia*, *Exserohilum* and *Alternaria* spp. were characterised by the presence of macroconidia. The colonies of *Bipolaris*, *Curvularia* and *Exserohilum* were floccose with brown to black colour. While in *Alternaria*, the colonies were distinguished by greenish black colour with short woolly hyphae. The conidia were thick-walled and fusiform in *Bipolaris* and *Exserohilum*. The conidia of these two fungi were differentiated by the septations in conidia, with *Bipolaris* having three to four septations and *Exserohilum* having seven to 11 septations with cylindrical shaped conidia. The conidia of *Curvularia* were curved in shape, thin cell walls and usually with three narrowed septations. The curved shape of conidia is due to the swelling of the central cells which was darker than the end cells. In *Alternaria*, the conidia were

longitudinally and transversely septate and arranged singly or chained. The conidial were ovate in shape where the part nearest to the conidiophore was round while narrow as it was nearer to the apex.

The genus of *Neoscytalidium* formed densely fluffy colonies with grey to dark grey aerial mycelia. *Neoscytalidium* produced arthroconidia, where the conidia were formed within the hyphae and broken into individual cells. The conidia were arranged in chains and a zig-zag appearance.

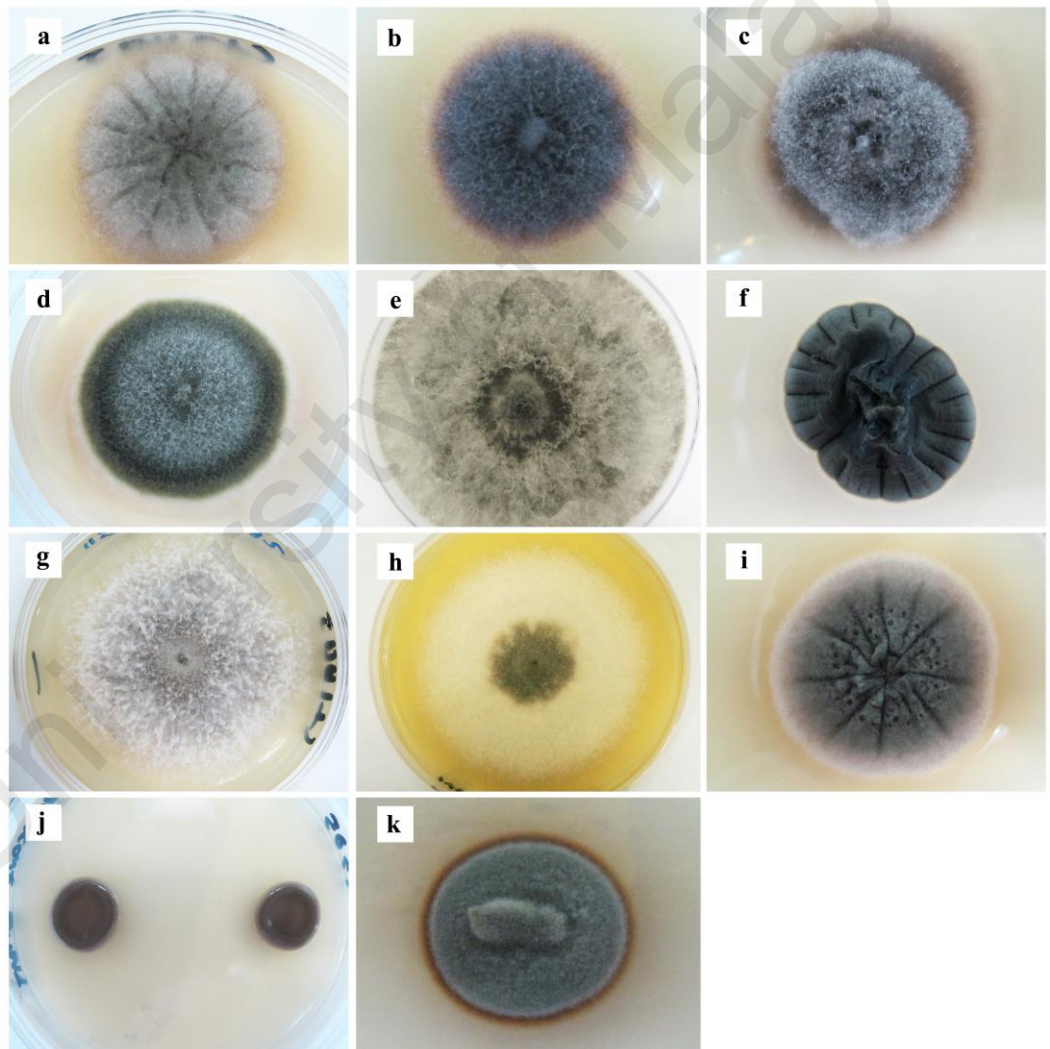


Figure 4.3: Colonial features of dematiaceous fungi isolated from specimens sent to Mycology Unit, UMMC. *Curvularia* (a), *Bipolaris* (b), *Exserohilum* (c), *Alternaria* (d), *Neoscytalidium* (e), *Cladosporium* (f), *Daldinia* (g), *Nigrospora* (h), *Chaetomium* (i), *Exophiala* (j), *Ochroconis* (k)

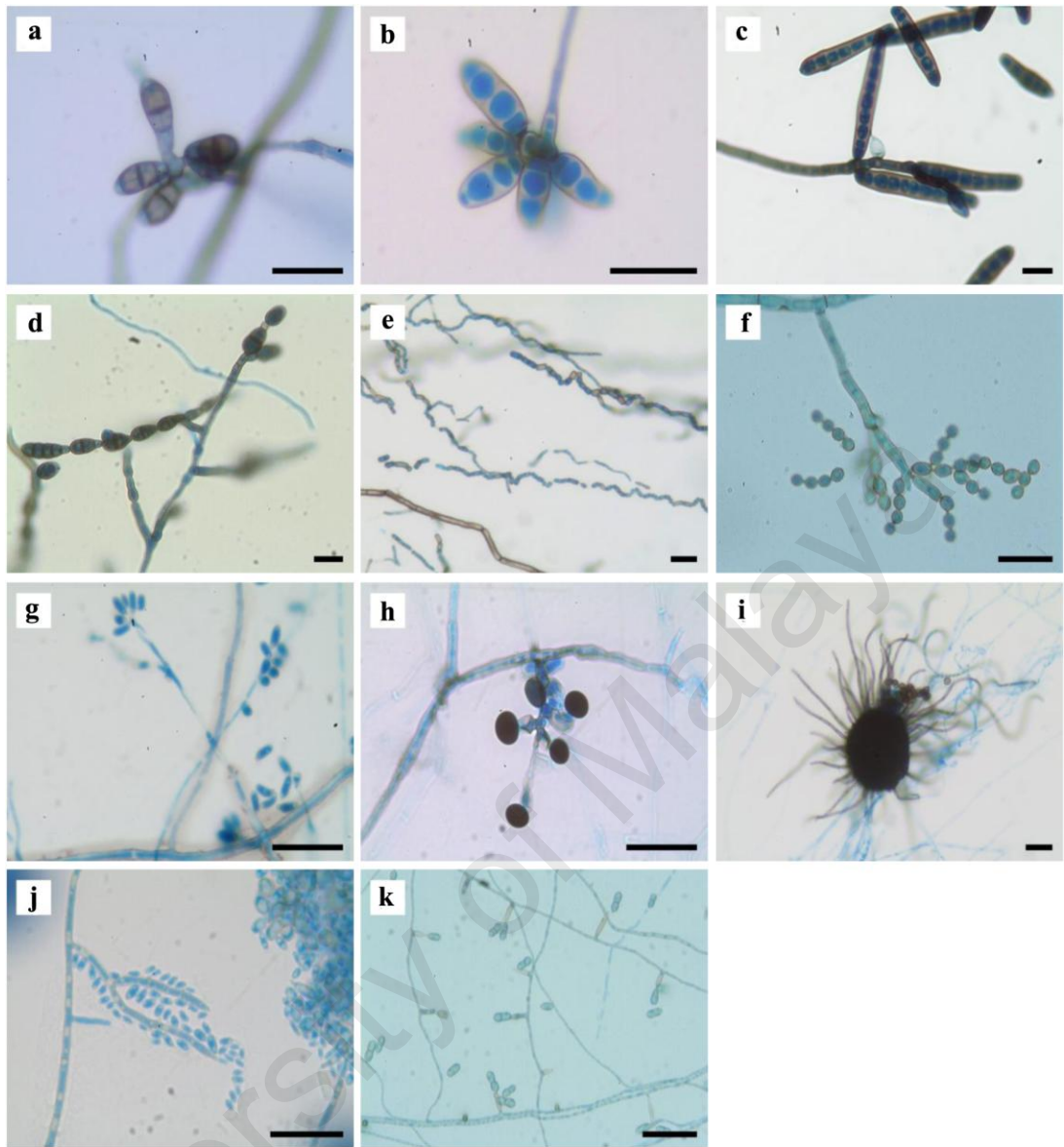


Figure 4.4: Micrograph of dematiaceous fungi isolated from specimens sent to Mycology Unit, UMMC. *Curvularia* (a), *Bipolaris* (b), *Exserohilum* (c) and *Alternaria* (d) macroconidia. *Neoscytalidium* arthroconidia (e), *Cladosporium* conidia and ramoconidia (f). *Daldinia* (g) and *Nigrospora* (h) conidia. Perithecium of *Chaetomium* covered with long setae and dark ascospores (i). Hyaline conidia and spine like conidiophore of *Exophiala* (j). Clavate conidia of *Ochroconis* (k). Bars 20 µm.

Members of *Cladosporium* produced colonies that were velvety. The colonies were olivaceous green to black green in colour. Microscopically, the conidiophores were straight and branched at the apical region, with ovoid to globose conidial shape. The

conidia were typified by the formation of ramoconidia, and dark scoured at both ends of conidia. The conidia were arranged in chains.

Daldinia colonies on the media were felty and whitish in colour. The conidia were ellipsoidal and arose from the terminus, with irregularly branched conidiophores. *Nigrospora* were characterised by woolly and white colonies and becoming black on ageing. The conidiophores were short, narrowing at the apex, bearing a single dark conidium in each conidiophore. The conidium was spherical or oblate with a smooth wall. *Chaetomium* colonies were white colour with aerial mycelium. The colonies turned to greyish when matured. The species in the *Chaetomium* genus were characterised by a dark coloured fruiting body known as perithecium. The perithecium was covered with long setae and ostiolate. The ascospores observed were dark, single-celled and mostly ovoid.

The *Exophiala* colonies observed were olivaceous-black and mucoid. Green colour ariel mycelia were seen at the edge of colonies when matured. The conidiophores were spine-like, erect and simple or branched. The conidia were hyaline, single-celled and subglobose to ellipsoidal in shape. The colonies of species from *Ochroconis* were dry and red-brown in colour. Red-brown exudates were also observed at the edge of the colonies and diffused into the medium. The conidiophores shape was cylindrical, with light brown, clavate 2-celled conidia were noticed at the apex of the conidiogenous cell.

Five isolates did not possess any sporulation structures and were classified as mycelia sterilia. Three isolates (UM 221, UM 238 and UM 1110) could not be identified based on microscopic characteristics (Figure 4.5).

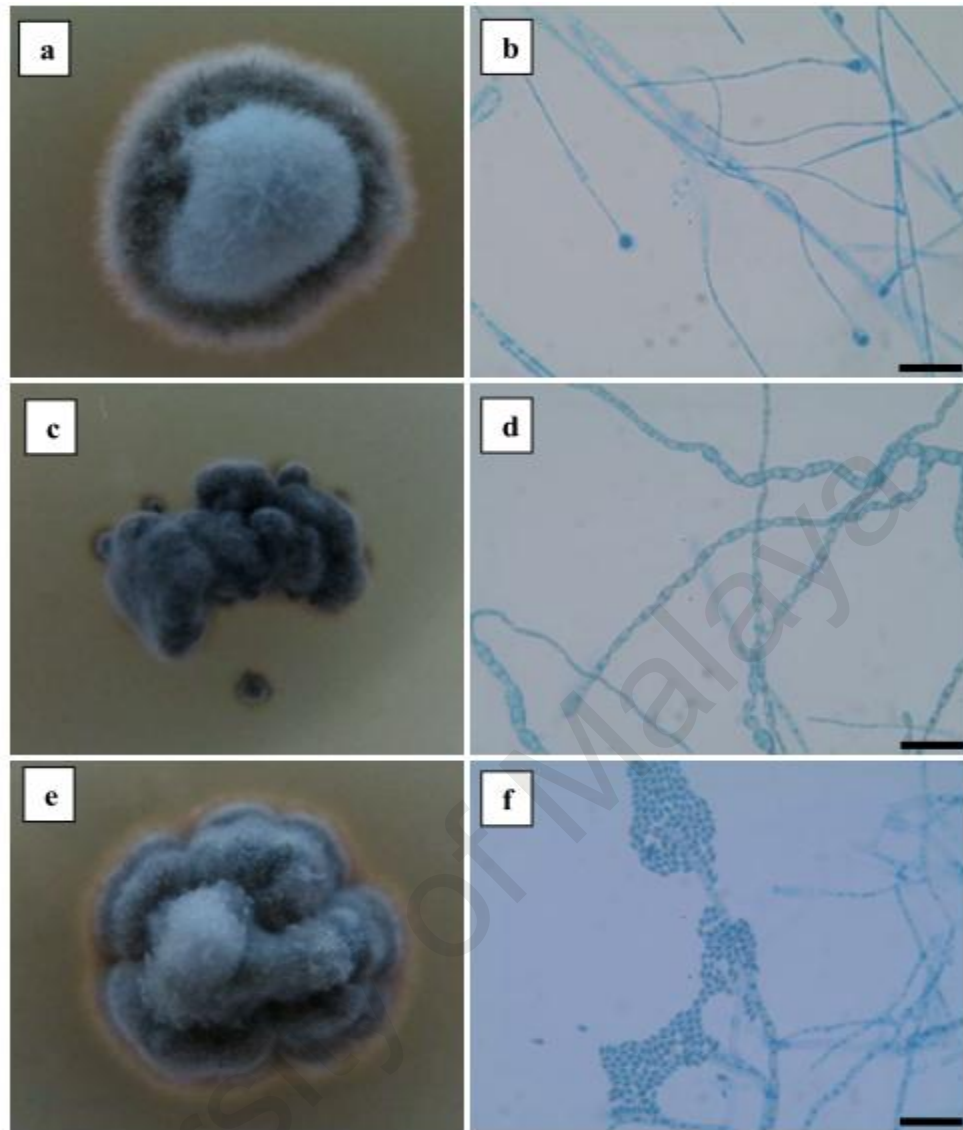


Figure 4.5: Culture and microscopic images of isolates with unidentifiable features. UM 221 culture (a) and micrograph (b), UM 238 culture (c) and micrograph (d), UM 1110 culture (e) and micrograph (f). Bars 20 μ m

4.1.2 Molecular identification and phylogenetic analysis

Molecular identification using internal transcribed spacer (ITS) region identified 97.3% of the fungal isolates (Table 4.1). The isolates were classified into 16 genera comprising 30 species. However, there were eight isolates with two nomenclatures. In the phylogenetic tree, these isolates were found to form a cluster with two fungal

species. There were also two isolates with identity resolved to the taxonomy of family or order level.

Of the 75 ITS sequences, 51 unique sequences were used for the construction of the phylogenetic tree. The Bayesian tree constructed with 120 ITS sequences showed the resolution of the isolates into one unclassified cluster and three distinct classes of Dothideomycetes, Sordariomycetes and Eurotiomycetes (Figure 4.6). The Dothideomycetes made up of 55 (73.3%) of the isolates, forming the largest cluster. The class was further sub-divided into three orders of Pleosporales, Botryosphaeriales and Capnodiales with 28, 6 and 21 isolates being resolved into the respective order. A total of nine (12%) isolates were found in Sordariomycetes while ten (13.3%) isolates in Eurotiomycetes.

The five mycelia sterilia which were unable to be distinguished morphologically were resolved to *Phoma multirostrata*/*Epicoccum sorghi* (UM 186, UM 255), *Stagonospora* sp./*Septoria arundinacea* (UM 259), *Phomopsis* sp./*Diaporthe artcii* (UM 254) and *Nigrospora oryzae* (UM 299). On the other hand, the three isolates with no identifiable features were unable to be identified at the species level and were placed as unclassified fungi. Top BLAST result showed 100% match of UM 221 to Ascomycota sp. (FJ537113), 98% match of UM 1110 to Pleosporales sp. (DQ92531) and 99% match of UM 238 to Herpotrichiellaceae sp. (GU017515). While in phylogenetic analysis, UM 1110 was resolved as *Stagonospora* sp./*S. arundinaceae*.

4.1.3 Congruence between morphological and molecular identification

Congruence between morphological traits and molecular taxonomic groupings was observed for all samples from class Sordariomycetes, class Leotiomycetes, order Botryosphaeriales and order Capnodiales. In Eurotiomycetes, the inconsistent

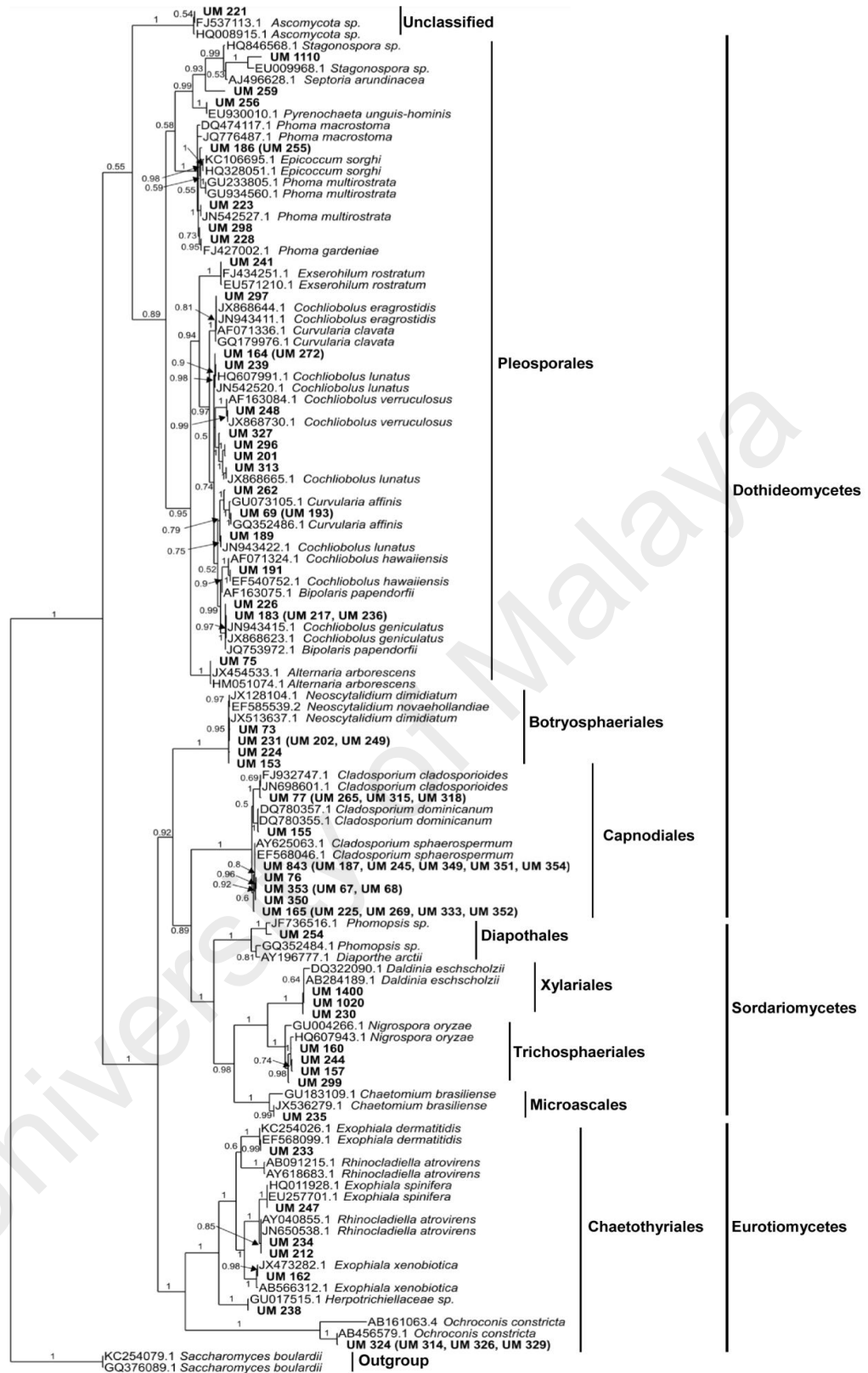


Figure 4.6: Taxonomic classification of dematiaceous fungi isolates. The phylogenetic tree was constructed with general time reversible (GTR) model space using ITS sequences with two *Saccharomyces boulardii* as outgroup strains. The isolates with identical sequence were listed in parentheses next to their representative. Bayesian posterior probability values for every cluster is printed on each node

classification was seen in *Exophiala* while in Pleosporales, this was found in the *Bipolaris*, *Curvularia* and *Phoma* (Table 4.2). UM 212 and UM 234 were identified as *Exophiala* by morphology but *Rhinoctadiella atrovirens* by phylogenetic analysis. Of the seven *Bipolaris* species, six of the isolates were resolved as *Cochliobolus* species whereas seven of the 11 *Curvularia* species were resolved as *Cochliobolus* species. UM 256 that with morphological features of *Phoma* was molecularly identified as *Pyrenochaeta unguis-hominis*.

Table 4.2: Isolates with incongruent morphological and molecular identity

Isolate ID	Morphological identity	Molecular identity
UM 212	<i>Exophiala</i> sp.	<i>Rhinoctadiella atrovirens</i>
UM 234	<i>Exophiala</i> sp.	<i>Rhinoctadiella atrovirens</i>
UM 183	<i>Bipolaris</i> sp.	<i>Cochliobolus geniculatus</i>
UM 217	<i>Bipolaris</i> sp.	<i>Cochliobolus geniculatus</i>
UM 236	<i>Bipolaris</i> sp.	<i>Cochliobolus geniculatus</i>
UM 191	<i>Bipolaris</i> sp.	<i>Cochliobolus hawaiiensis</i>
UM 327	<i>Bipolaris</i> sp.	<i>Cochliobolus lunatus</i>
UM 248	<i>Bipolaris</i> sp.	<i>Cochliobolus verruculosus</i>
UM 164	<i>Curvularia</i> sp.	<i>Cochliobolus lunatus</i>
UM 189	<i>Curvularia</i> sp.	<i>Cochliobolus lunatus</i>
UM 201	<i>Curvularia</i> sp.	<i>Cochliobolus lunatus</i>
UM 239	<i>Curvularia</i> sp.	<i>Cochliobolus lunatus</i>
UM 272	<i>Curvularia</i> sp.	<i>Cochliobolus lunatus</i>
UM 296	<i>Curvularia</i> sp.	<i>Cochliobolus lunatus</i>
UM 313	<i>Curvularia</i> sp.	<i>Cochliobolus lunatus</i>
UM 256	<i>Phoma</i> sp.	<i>Pyrenochaeta unguis-hominis</i>

4.2 *C. sphaerospermum* UM 843

4.2.1 Morphological description and phylogenetic analysis

The UM 843 colony cultured on SDA was flat, radially furrowed and with wrinkled centre forming crater-like structure (Figures 4.7a and b). The colony was olivaceous green and reverse black green in colour. Densely septated hyphae with thick and darkened septa, globose to subglobose, brown to dark brown conidia with prominent

scar were observed under light microscope (Figures 4.7c and d). Ramoconidia were also frequently observed (Figure 4.7d2). Under SEM, the coronate conidia were characterised by protuberant, thickened, darkened with a central convex dome and surrounded by a raised periclinal rim. The conidia and ramoconidia surface ornamentation of UM 843 were verruculose (Figures 4.7e-g).

The colony of UM 843 on different media at 30°C and 25°C were olivaceous green and gray-green in colour (Figures 4.8 and 4.9). The colony was yellowish-green in colour on malt extract agar (MEA) at 25°C (Figures 4.9b and f). On MEA and sabouraud dextrose agar (SDA), white periclinal rim was observed. The colony grew on MEA with 5% sodium chloride (NaCl) was larger compared to MEA for both temperatures. The colony grew at 30°C on MEA with 5% NaCl was slightly hairy while on MEA, the colony was wrinkled in the centre and corrugated. On MEA with 5% NaCl at 25°C, the edge of the colony was radial (Figures 4.9c and g). Also, UM 843 was found able to grow in sabouraud dextrose broth (SDB) supplemented with NaCl up to 20% (w/v) (Figure 4.10).

The ITS1-5.8SRNA-ITS2 region phylogenetic tree comprised of *C. sphaerospermum* species complex and two outgroup sequences was generated (Figure 4.11). The species were well resolved with > 0.70 Bayesian posterior probability (PP) except for *C. langeronii/C. psychrotolerans* group and *C. aphidis/C. fusiforme* group. The isolate was found to resolve well and clustered within the *C. sphaerospermum* cluster with 0.71 PP.

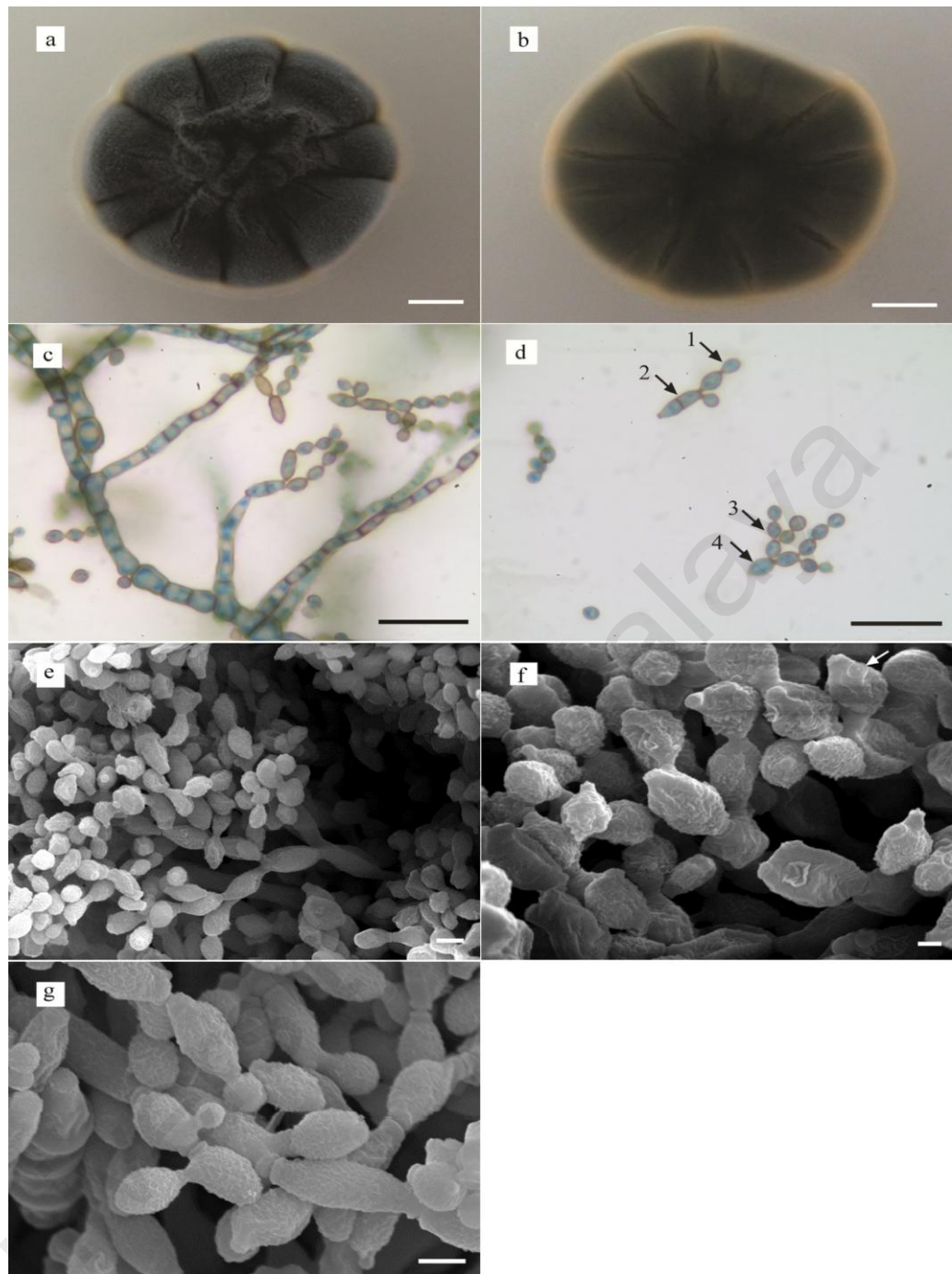


Figure 4.7: Morphology of *C. sphaerospermum* UM 843. Colonial morphology front (a) and reverse (b) of *C. sphaerospermum* UM 843 on SDA after 7-day incubation. Light micrograph showing ramoconidia (d 1 and d 3) and conidia (d 2 and d 4). $\times 630$ magnification, bars $20\ \mu\text{m}$. Observation under scanning electron micrograph showing conidiophores bearing conidium (e, $\times 2000$ magnification, bar $3\ \mu\text{m}$), periclinal rim (f, $\times 5000$ magnification bar $1\ \mu\text{m}$) and verruculose surface of conidia (g, $\times 5000$ magnification, bar $2\ \mu\text{m}$)

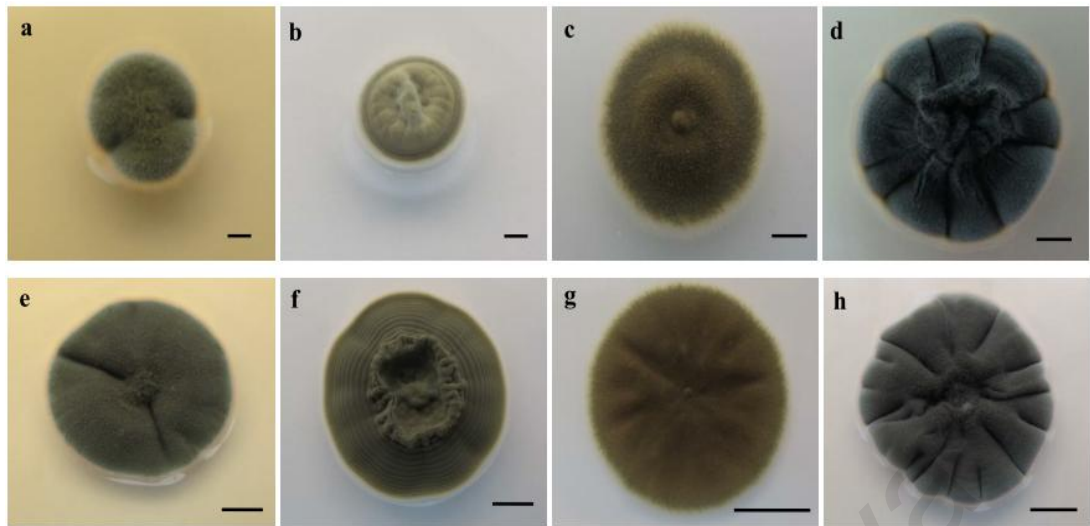


Figure 4.8: Colonial features of *C. sphaerospermum* UM 843 grown on various media at 30°C. PDA (a and e), MEA (b and f), MEA with 5% NaCl (c and g) and, SDA (d and h). Culture grew for 7 days (a-d). Culture grew for 14 days (e-f). Bars 1 cm

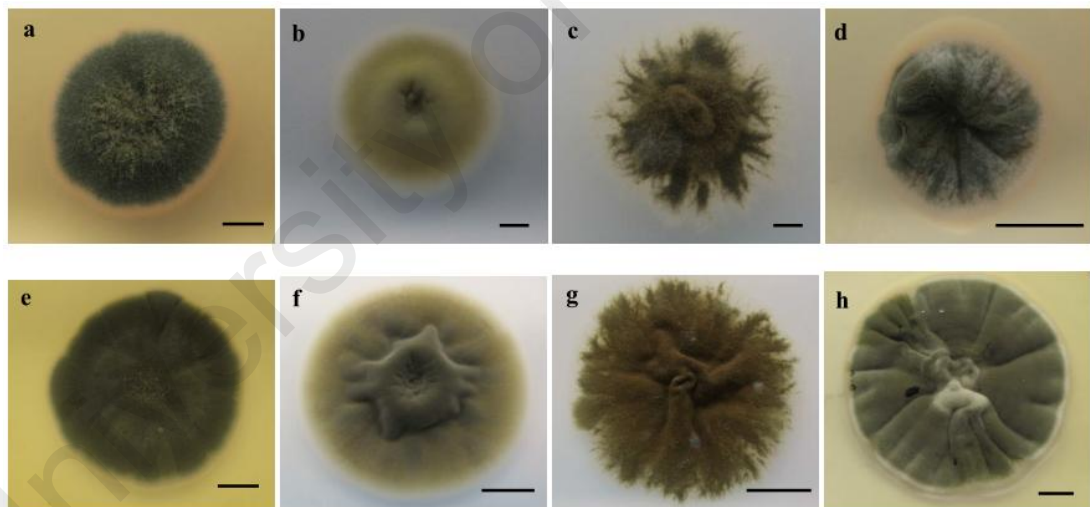


Figure 4.9: Colonial features of *C. sphaerospermum* UM 843 grown on various media at 25°C. PDA (a and e), MEA (b and f), MEA with 5% NaCl (c and g) and, SDA (d and h). Culture grew for 7 days (a-d). Culture grew for 14 days (e-f). Bars 1 cm

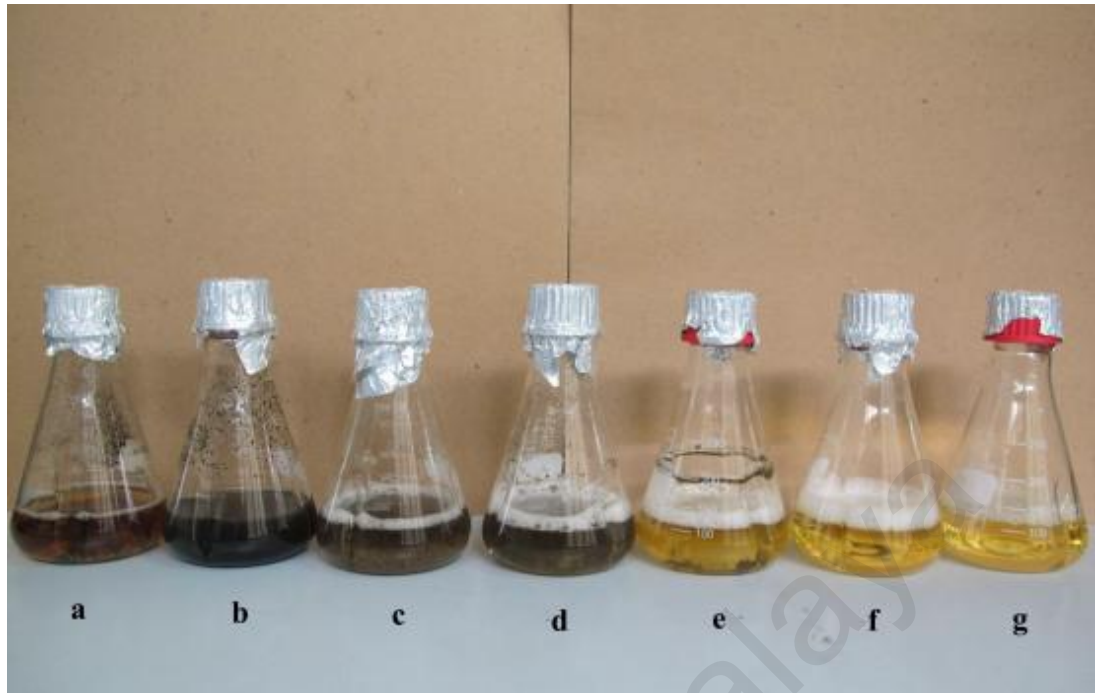


Figure 4.10: Growth of UM 843 in SDB supplemented with various percentage (w/v) of NaCl. 0% (a), 5% (b), 10% (c), 15% (d), 20% (e), 25% (f), and 30% (g) of NaCl in SDB

4.2.2 Genomic deoxyribonucleic acid (DNA) extraction

Two batches of *C. sphaerospermum* UM 843 genomic DNA were extracted and sent for genome sequencing. The quality and quantity assessment of the extracted DNA for the construction of small insert size (500-bp) and large insert size (5-kb) libraries are shown in Table 4.3, Figure 4.12 and Figure 4.13.

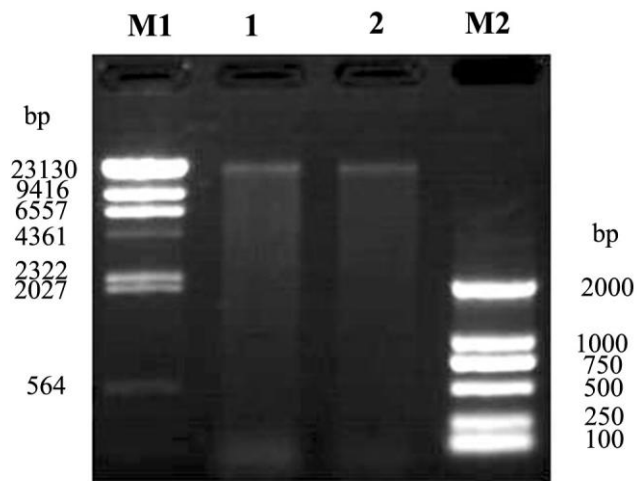


Figure 4.12: Gel image of extracted genomic DNA sent for genome sequencing of the small insert (500-bp) library. Labelling of lane start from left to right: M1: λ -*Hind*III digest (Takara); 1, 2: UM 843 DNA tube 1 and 2; M2: D2000 (Tiagen)

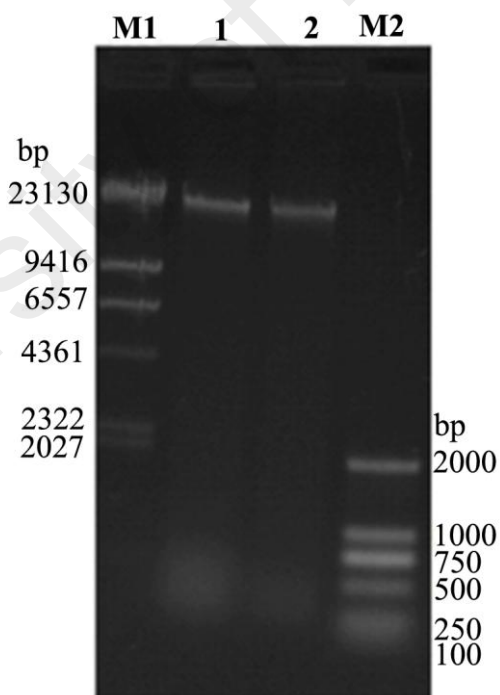


Figure 4.13: Gel image of extracted genomic DNA sent for genome sequencing of the large insert (5-kb) library. Labelling of lane start from left to right: M1: λ -*Hind*III digest (Takara); 1, 2: UM 843 DNA; M2: D2000 (Tiagen)

4.2.3 *C. sphaerospermum* UM 843 genome

The quality assessment and trimming of both small and large insert libraries were carried out as described in the Methodology section (Section 3.2.3.1, Appendix D1 and D2). From the total of 19,253,334 of forward and reverse reads generated from small insert library, 19,194,986 of paired reads were used in the assembly after the trimming and filtering of the low-quality reads (Table 4.4 and Table 4.5). Whereas in the large insert library, 9,943,258 of paired reads from 9,987,556 of total generated reads was obtained. The paired reads from both libraries were combined and proceed with the downstream analysis.

Table 4.4: Small insert library reads statistics of UM 843 genome

	Reads		Bases (bp)	
	Number of reads	Percentage (%)	Total Bases	Percentage (%)
Raw reads				
PE1	9,626,667	-	866,400,030	-
PE2	9,626,667	-	866,400,030	-
Total	19,253,334	100	1,732,800,060	100
Clean reads				
PE1	9,597,493	-	837,225,146	-
PE2	9,597,493	-	834,500,465	-
Total	19,194,986	99.70	1,671,725,611	96.48

Table 4.5: Large insert library reads statistics of UM 843 genome

	Reads		Bases (bp)	
	Number of reads	Percentage (%)	Total Bases	Percentage (%)
Raw reads				
PE1	4,993,778	-	449,440,020	-
PE2	4,993,778	-	449,440,020	-
Total	9,987,556	100	898,880,040	100
Clean reads				
PE1	4,971,629	-	432,744,759	-
PE2	4,971,629	-	416,403,756	-
Total	9,943,258	99.56	849,148,515	94.47

The optimisation of the k-mer length was carried out to optimise the genome assembly. From the graph of N50 length versus hash length (Figure 4.14), it showed that hash 49 is the optimal hash length which would generate an optimum assembly. The combined 2,632 Mb sequence reads represent ~98-fold depth of genome sequence coverage. The reads were assembled into 867 contigs and placed into 155 scaffolds with paired-end information from both libraries. The assembled genome size of UM 843 is 26.89 Mb and the N50 of UM 843 scaffolds was 969,659 bp (Table 4.6).

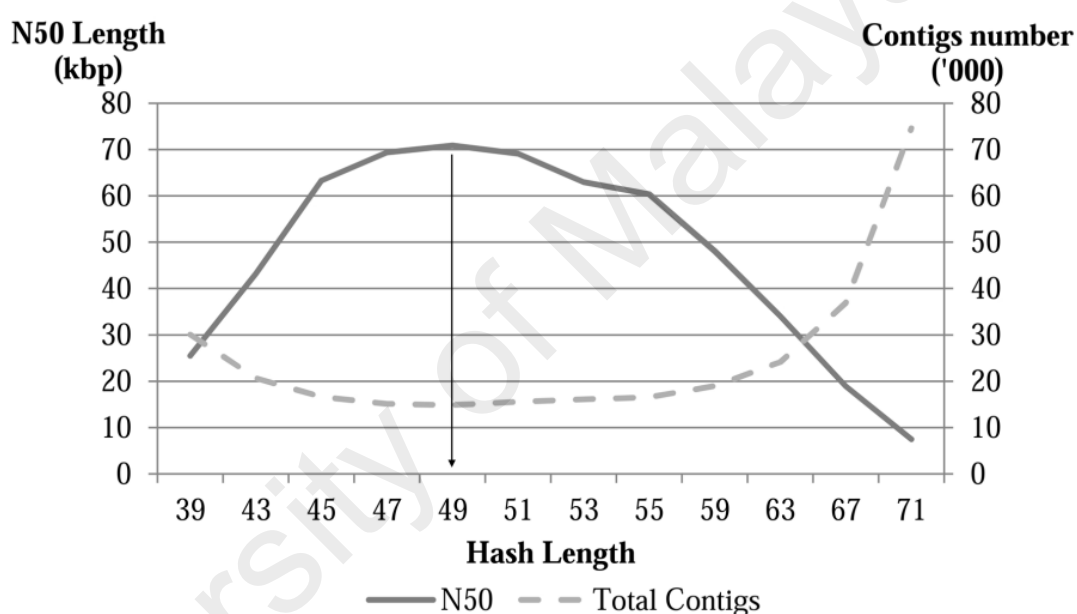


Figure 4.14: Hash length optimisation graph for optimum assembly

Table 4.6: Genome features of *C. sphaerospermum* UM 843 sequence reads generated from the combined libraries

	<i>C. sphaerospermum</i> UM 843
Reads from 500 bp insert library (Mb)	1,733
Reads from 5 kb insert library (Mb)	899
Total Reads (Mb)	2,632
Assembly size (bp)	26,892,198
Number of contigs (≥ 200 bp)	867
Contigs size (N50) (kb)	92,815
Number of scaffolds (≥ 1000 bp)	155

Table 4.6, continued

	<i>C. sphaerospermum</i> UM 843
Scaffolds size (N50) (bp)	969,659
G+C content (%)	55.32
Number of predicted genes (≥ 99 bp)	9,652
Average gene length (bp)	1,482
Average number of exons per gene	2.26
rRNA	42
tRNA	196
KEGG	999
GO	6,065
KOG	5,215
Pfam	6,655

4.2.3.1 Transposable elements

A total of 313 putative transposable elements comprising 284,298 bases (1.06% of the genome size) were identified (Table 4.7). Of these, 231 transposable elements belonging to the class I retrotransposons while 82 transposable elements belonging to class II DNA transposons (Table 4.7). The Gypsy element was the highest (31.95%) among all the elements followed by LINE elements. In the Class II DNA transposons, Crypton element is the smallest element while the hAT element is the largest.

4.2.3.2 Primary functional annotation

A total of 9,652 gene models were predicted in UM 843 with average gene length of 1,482 bp. Of all the predicted gene models, 5,215, 999 and 6,065 genes were annotated in the Eukaryotic Orthologous Group (KOG), Kyoto Encyclopedia of Genes and Genomes (KEGG) and Gene Ontology (GO) classifications, respectively (Figure 4.15). In the KOG, the predicted genes were annotated redundantly into 5,853 KOG classifications (Figure 4.15a). Among the 23 well characterised KOG groups (excluding categories of General functions prediction only [R], Function unknown [S] and Unnamed protein [X]), Posttranslational modification, protein turnover, chaperones [O], Signal transduction mechanisms [T], and Carbohydrate transport and metabolism [G]

were highly annotated. In group O, a total of 69 putative genes encoding chaperone were identified in the genome; that is the highest number of genes found this group. Whereas in group G, 77 genes were annotated as putative permease of the major facilitator superfamily followed by 26 genes encoding monocarboxylate transporter.

Table 4.7: Transposable elements predicted in the *C. sphaerospermum* UM 843 genome

Class	Family name	Total number	Total bases (bp)	Percentage of genome assembled (%)
I	DDE_1	42	43,548	0.16
	gypsy	100	63,804	0.24
	LINE	61	90,510	0.34
	ltr_Roo	2	1,191	0.00
	TY1_Copia	26	24,141	0.09
II	cacta	4	609	0.00
	Crypton	1	258	0.00
	hAT	37	40,137	0.15
	helitronORF	3	2,061	0.01
	mariner	6	2,355	0.01
	mariner_ant1	10	4,890	0.02
	MuDR_A_B	21	10,794	0.04
Total		313	284,298	1.06

In the categorisation of genes based on KEGG pathway, the top five metabolic pathways were carbohydrate metabolism (575 genes), amino acid metabolism (413 genes), lipid metabolism (281 genes), energy metabolism (255 genes) followed by nucleotide metabolism (240 genes) (Figure 4.15b).

Based on the GO classifications, the predicted genes were mainly annotated to Cell, Organelle, Binding, Catalytic, Cellular process and Metabolic process in each GO category (Figure 4.15c). Among these, 1,733 genes were assigned to the response to stimulus category (GO: 0050896). Within this category, 1,080 genes were sub-categorised into the response to stress category (GO: 0006950). The genes were further

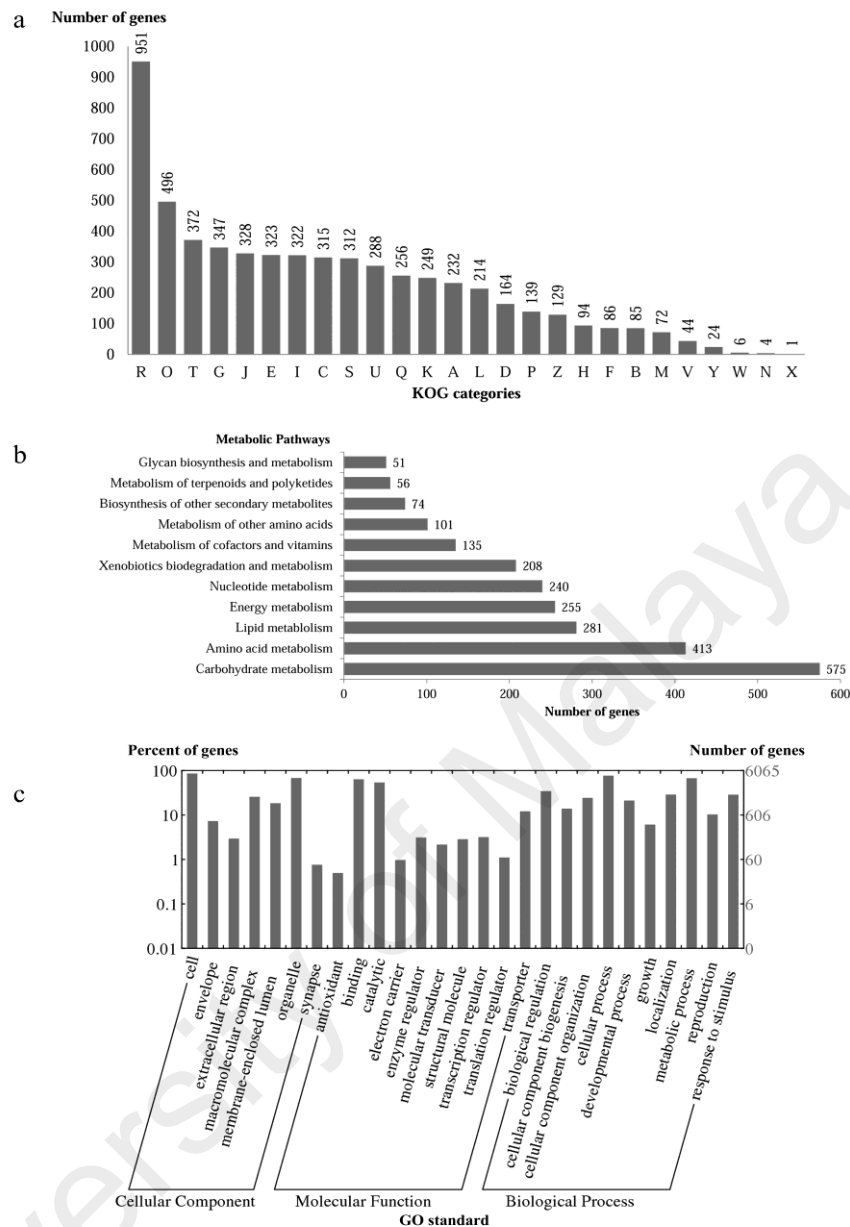


Figure 4.15: KOG (a), KEGG (b) and GO (c) classifications of predicted genes in *C. sphaerospermum* UM 843. KOG classification: A, RNA processing and modification; B, Chromatin structure and dynamics; C, Energy production and conversion; D, Cell cycle control, cell division, chromosome partitioning; E, Amino acid transport and metabolism; F, Nucleotide transport and metabolism; G, Carbohydrate transport and metabolism; H, Coenzyme transport and metabolism; I, Lipid transport and metabolism; J, Translation, ribosomal structure and biogenesis; K, Transcription; L, Replication, recombination and repair; M, Cell wall/membrane/envelope biogenesis; N, Cell motility; O, Posttranslational modification, protein turnover, chaperones; P, Inorganic ion transport and metabolism; Q, Secondary metabolites biosynthesis, transport and catabolism; R, General function prediction only; S, Function unknown; T, Signal transduction mechanisms; U, Intracellular trafficking, secretion, and vesicular transport; V, Defense mechanisms; W, Extracellular structures; X, Unnamed protein and Z, Cytoskeleton.

annotated to various stress responses where the highest number of predicted genes was assigned to the response to osmotic stress category (139 predicted proteins).

4.2.3.3 Carbohydrate metabolism

A total of 605 putative CAZyme catalytic domains belonging to 566 predicted genes were identified. The CAZymes comprised of 261 GHs, 98 GTs, 114 CEs, 14 PLs, 77 AAs, and 41 CBMs (Appendix D3). The putative CAZymes were further classified based on substrate specificity (Table 4.8). Overall, UM 843 consists all of the CAZyme families with at least 171 CAZymes involved in degradation of plant cell wall as previously described (Amselem et al., 2011; van den Brink & de Vries, 2011). Of these, a total of 149 CAZyme modules were identified to engage in hemicellulose and pectin degradation. Only seven CAZyme modules were determined to be involved in cellulose degradation.

Table 4.8: Plant cell wall and fungal cell wall degrading and modifying CAZyme families predicted in *C. sphaerospermum* UM 843

Plant Cell Wall									
Cellulose		Pectin		Hemicellulose		^a HP		CBM family	
Family	No.	Family	No.	Family	No.	Family	No.	Family	No.
GH12	1	CE8	7	CE2	1	GH43	18	CBM1	12
GH45	1	GH105	2	CE1	32	GH51	3	CBM35	2
GH6	1	GH28	10	CE3	1	GH53	2	CBM42	1
GH7	2	GH78	3	CE5	8	GH54	1	CBM63	2
GH74	2	GH88	2	CE16	2	GH62	3		
		GH95	1	GH10	4	GH93	3		
		PL1	8	GH11	5	CE12	2		
		^b PL22	1	GH27	4				
		PL3	4	GH29	1				
		PL9	1	GH31	11				
				GH35	4				
				GH36	1				
				GH67	1				
				^c GH115	3				
Total	7	Total	39	Total	78	Total	32	Total	17

Table 4.8, continued

Fungal cell wall		Plant and fungal cell wall		Energy storage and recovery	
Family	No.	Family	No.	Family	No.
CBM14	2	GH1	4	CBM20	5
CBM18	2	GH2	8	CBM21	1
CBM43	1	GH3	19	CBM48	1
CBM52	1	GH5	17	GH13	16
CE4	6	^c GH64	5	GH15	2
GH16	12			GH32	5
GH17	7			GH37	2
GH18	6			GH65	1
GH20	1				
GH55	3				
GH71	1				
GH72	6				
GH76	9				
GH81	1				
GH92	4				
^c GH30	3				
Total	65	Total	53	Total	33

^aHP: enzymes involved in hemicellulose or pectin side chain degradation

Putative functions of families allocate according to Amselem et al. (2011) unless specified:

^bGarron and Cygler (2010)

^cZhao et al. (2014)

GH: glycoside hydrolases; CE: carbohydrate esterases; PL: polysaccharide lyases; CBM: carbohydrate-binding modules

A comparison of CAZymes predicted in UM 843 to all available dematiaceous Dothideomycetes was constructed (Figure 4.16). UM 843 has a comparable number of CAZyme modules with the other Dothideomycetes. Also, the comparison was made based on the degradation of plant cell wall principal components (cellulose, hemicellulose and pectin) (Figure 4.17). All the Capnodiales fungi have lesser cellulose degradation CAZymes as compared to Pleosporales. The fungi from this order have a lower number of CBM18 and lack of GH94 family but more abundant of GH64 family than Pleosporales. However, UM 843 has the highest number of predicted CBM1,

GH10, GH11, PL1 and PL3 among the Capnodiales. The number of these CAZymes is closer to that of Pleosporales (Appendix D4).

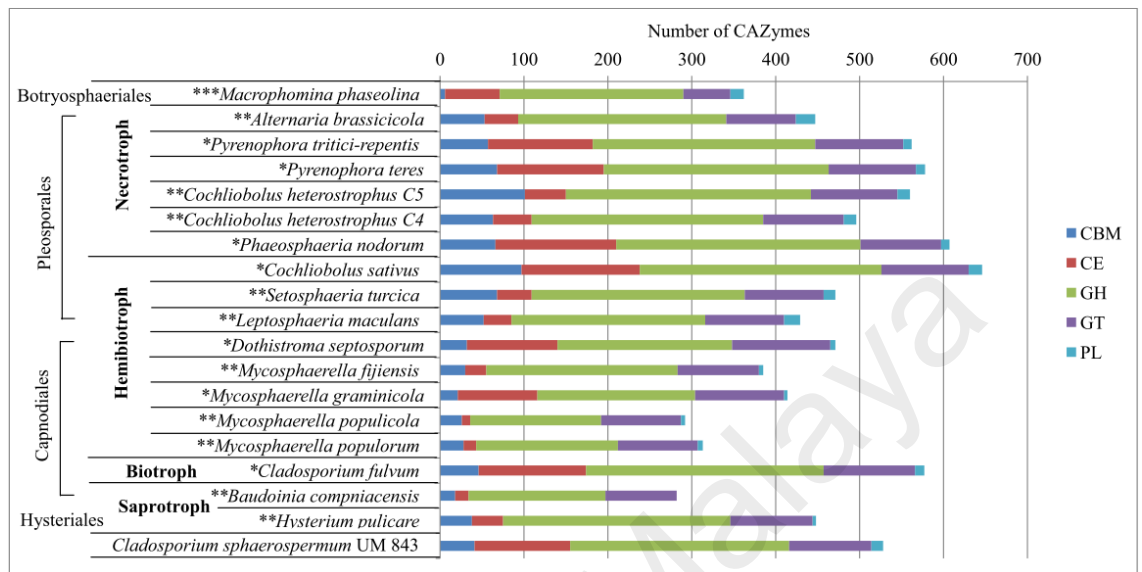


Figure 4.16: Comparison of *C. sphaerospermum* UM 843 CAZymes with other dematiaceous Dothideomycetes based on CAZyme families. CBM, carbohydrate-binding modules; CE, carbohydrate esterases; GH, glycoside hydrolases; GT, glycosyltransferases; PL, polysaccharide lyases. Data were obtained from *Zhao et al. (2014), **Ohm et al. (2012) and ***Islam et al. (2012)

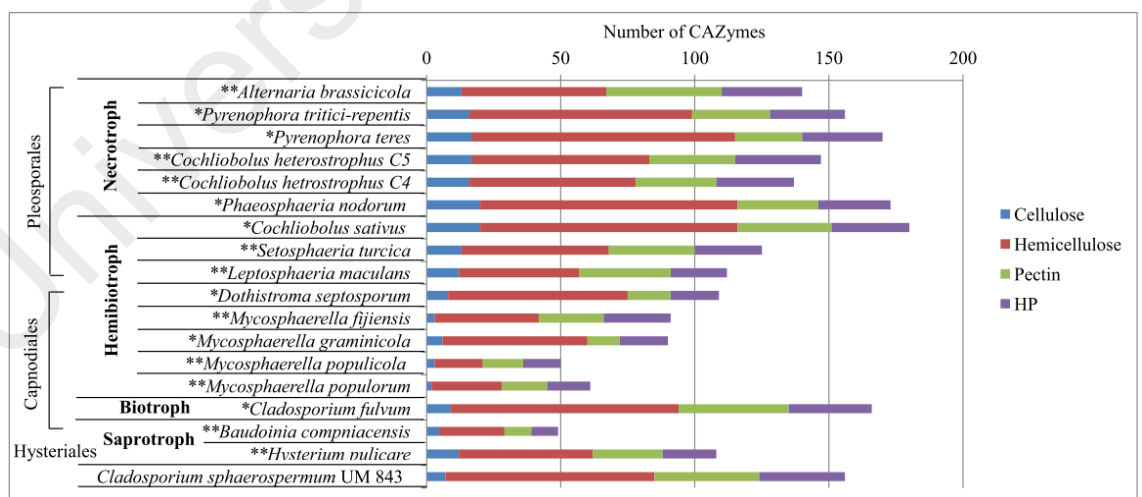


Figure 4.17: Comparison of *C. sphaerospermum* UM 843 CAZymes with other dematiaceous Dothideomycetes based on substrate specificities. HP: Hemicellulose-pectin. HP: Hemicellulose-pectin. Data were obtained from *Zhao et al. (2014) and **Ohm et al. (2012)

4.2.3.4 Peptidases

A total of 130 predicted peptidases were identified in UM 843 encompassing seven aspartic peptidases, 22 carboxypeptidases, 53 metallopeptidases, 38 serine peptidases, nine threonine peptidases and one unknown peptidase. Comparison of peptidases among the Dothideomycetes did not reveal the predominance of any particular enzyme family in UM 843 (Figure 4.18). In addition, a total of 30 genes encoding amino acid permease domain, six genes encoding proton-dependent oligopeptide transporter (POT) family domain and three genes encoding oligopeptide transporter (OPT) family domain were identified (Table 4.9).

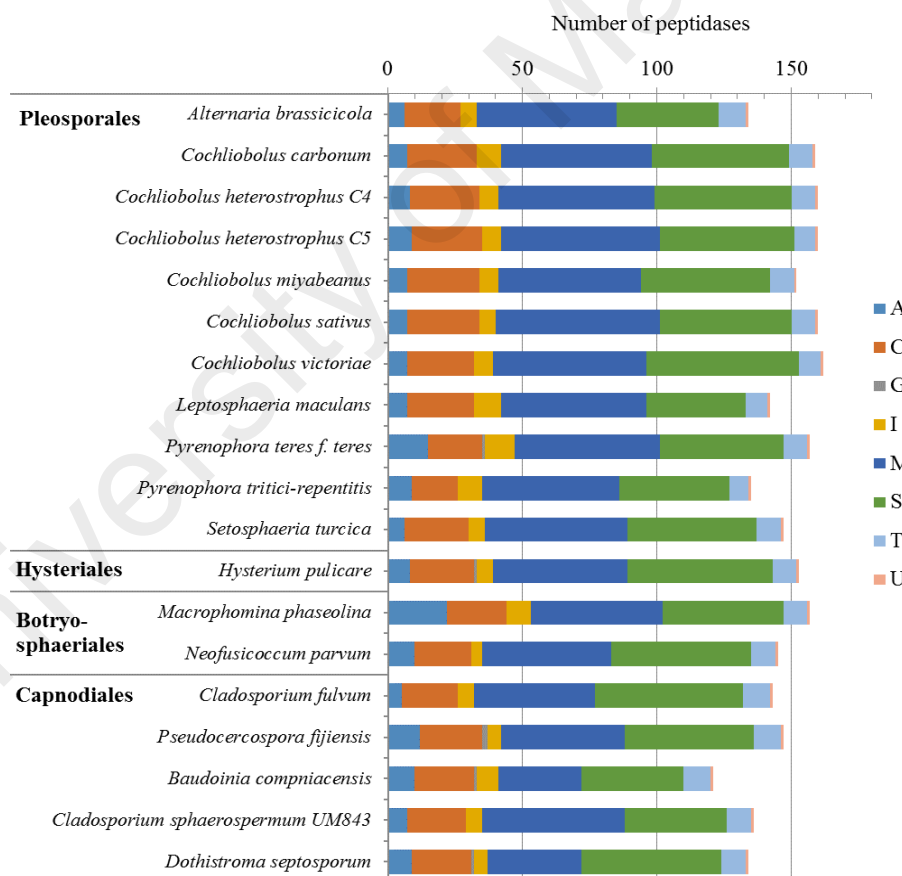


Figure 4.18: Comparison of peptidases identified in *C. sphaerospermum* UM 843 with dematiaceous fungi from the class Dothideomycetes. A: aspartic; C: cysteine; G: glutamic; I: inhibitor; M: metallo; S: serine; T: threonine; U: unknown.

Table 4.9: Oligopeptide and amino acid transporters identified based on PFAM domain in *C. sphaerospermum* UM 843

Gene ID	Matched gene accession No.	Identity (%)
PF00854//POT family		
UM843_2289	EFY95632	72.83
UM843_2544	EFQ34161	71.24
UM843_2808	EIM80418	47.39
UM843_3028	XP_001939496	74.26
UM843_4385	XP_001934967	71.85
UM843_5149	EFY96635	80.10
PF03169//OPT oligopeptide transporter protein		
UM843_3093	EGP82613	69.18
UM843_7124	EGP92571	66.28
UM843_7500	EFY94602	69.59
PF13520//Amino acid permease		
UM843_43	EGX93903	52.54
UM843_645	CCD50912	56.67
UM843_944	XP_001939969	64.30
UM843_1183	XP_001262458	66.67
UM843_1423	CBY00789	61.26
UM843_1457	CBY00789	55.38
UM843_2153	CCD34211	63.08
UM843_2575	XP_001934055	67.17
UM843_2668	XP_002481734	59.72
UM843_2676	EGR51024	61.26
UM843_2975	EFQ25870	59.47
UM843_3026	EJB10542	67.19
UM843_3217	XP_001271885	52.11
UM843_3391	XP_001263641	65.13
UM843_4086	CCD34211	60.27
UM843_4421	EJD40859	60.08
UM843_4967	CCD48924	61.00
UM843_5693	XP_001481438	59.60
UM843_5832	XP_001827651	62.82
UM843_6274	XP_002480702	74.45
UM843_7503	ABS57481	82.65
UM843_8185	CCD34211	57.88
UM843_8594	EGX90158	51.86
UM843_8664	EFQ27312	60.23
UM843_8741	EIT80604	63.59
UM843_8909	CBY00789	59.52
UM843_8956	XP_002481020	72.08
UM843_9543	XP_001934830	50.00

Table 4.9, continued

Gene ID	Matched gene accession No.	Identity (%)
PF13520//Amino acid permease		
UM843_9675	CCD34432	71.46
UM843_9729	XP_001933856	78.07

Five of the total 31 secreted peptidases (two from A01, two from S09 and one from M36) and one non-secreted peptidase from the A01 family were related to lung tissue hydrolysis (Table 4.10). Inspection of the two serine peptidases (UM843_2883 and UM843_1649) sequence alignment showed the Gly-X-Ser-X-Gly conserved sequence motif and catalytic triad Ser 631, Asp 711, His 746 and Ser 565, Asp 646, His 678 in UM843_2883 and UM843_1649, respectively (Figure 4.19 and 4.20).

Table 4.10: List of homologous peptidase identified via MEROPS batch blast that showed identity to *A. fumigatus* peptidases that are involved in lung hydrolysis

Gene ID	Family	MEROPS ID	Holotype	Matched gene accession No.	Identity (%)
UM843_1326	A01A	MER001437	peptidase F	Q06902	51.70
UM843_4966	A01A	MER001438	peptidase F	A1DDK1	61.99
*UM843_5823	A01A	MER000941	saccharopepsin	O42630	76.05
UM843_2925	M36	MER001400	fungalsin	Q0UC19	67.86
UM843_2883	S09B	MER004504	dipeptidyl peptidase IV	Q2UH35	56.24
UM843_1649	S09X	MER000263	dipeptidyl peptidase V	Q9Y8E3	50.07

All the genes are predicted to be secreted, except for UM843_5823

```

UM843_2883 1 MTAVSLACAATLLIGSSIAIDPPREFFVAPTGGAGNESLTFNNTVVSPOFRASLISVDWLPD
ASPFU_DPPIV 1 ---MKWS---ILLVGCAAAIDVPRQFPYAPTGGSKKRLTFNETVVKRAISPSAISVEWIST
ASPOR_DPPIV 1 ---MKYSKLILLVSVVQAIDVPRQFPYAPTGGSKKRLTFNETVVKRAITPISRSVQWLSG

UM843_2883 61 EEDGLVYVQADDGALIFENYATGENDTQVAADLIPF--EYVEYVIRSRQEKVLSSTNYTQ
ASPFU_DPPIV 56 SEDGDVYVQDQDGLKIQSIVTNIHQTLVPAKQVPE--DAYSYWIHFNLSVWLWATNYTK
ASPOR_DPPIV 58 AEDGSYVYVAFDGLSITENIVTNEVRTLIPADKIPTGKFAFNWYIHPDLSSVWLWASNHTK

UM843_2883 119 NYRHSYNSNIIVLDWASGEQTPLDQDQDGIQYAOQAPFTGDLIAFVRANNLYTKVATICE
ASPFU_DPPIV 114 QYRHSYFADYFIDVQVSNKLRPLAPDQSGDIQYQWSPTGDATAFVRGNNVFVWT--NAS
ASPOR_DPPIV 118 QYRHSYFADYVQDWESLKSVPLMPDQSGDIQYQWSFVGNITAFVRENDLYVWL--NGT

UM843_2883 179 ISQITNDGGEDMFHGVDPDWYEEEIFGDRYTLWFSPDARLISFLSFNETGVGTFVQYEM
ASPFU_DPPIV 172 TSQITNDGGPDLFNGVDPDWIYEEELGDRFALWFSPDGAYLAFRFNETGVPTFTVFPYEM
ASPOR_DPPIV 176 VTRITDGGPDMFHGVDPDWIYEEELGDRYALWFSPDGAYLALFSFNETGVPTFTVQYEM

UM843_2883 239 NDSDIAPFYSQNLIRYPKVGTTNPTVSLTLLLESMQLSPVSAADAFPEELIIGEVAVW
ASPFU_DPPIV 232 DNDEIAPFYSRELEIRYPKVSQTNPTVSLNLLLRNGRFPVPIDAFPAKELIIGEVAVW
ASPOR_DPPIV 236 DNDEIAPFYSRELEIRYPKVSQTNPTVSLNLLLRNGRFPVPIDAFPAKELIIGEVAVW

UM843_2883 299 TDTHESTIYFAVNRVQDTEKIVTVSWPFSASTVHRRERDGDGWLNLNLIQYVGVGFGNS
ASPFU_DPPIV 292 TGRHFWVAMKAFNRVQDTEKIVTVSWPFSASTVHRRERDGDGWLNLNLIQYVGVGFGNS
ASPOR_DPPIV 296 TDTHTIWAAKAFNRVQDQKVVAVDTASNKATVISDRDGTGWLNLNLSMKYIGPIKPS-

UM843_2883 359 TYSGSNTTYLIDLSASGWAHLYLFPVNGPASNNITLTSGEWEVRSILSIDQERQLVYYT
ASPFU_DPPIV 351 -----KLEYYIDISDQSGWAHLNLFVAVGG--EPIPLTKGEWEVTNLSIDKPRQLVYIL
ASPOR_DPPIV 355 ----DKLQYYIDISDQSGWAHLYLFPVSGG--EPIPLTKGEWEVTSILSIDQERQLVYYL

UM843_2883 419 STERHSTESHLYSVSFAHLAKKALVDDSPAGNWSASFSSNNGYIILYGGPDPVYQELYA
ASPFU_DPPIV 404 STERHSTERHLYSVSKTKETPLVDDTVAAMWSASFSSGGGYIILYRGPDPVYQELYA
ASPOR_DPPIV 409 STQHHSTERHLYSVSYSTFAVPLVDDTVAAMWSASFSSNNGYIILYGGPDPVYQELMT

UM843_2883 479 VNSSEPHSTVTSNCAVLRICDYNLENTIYTCIGPVHDTEYMLNVKVTYPPNEDFSKKYP
ASPFU_DPPIV 464 INSTAPLRTITSNAAVLNALKRYTLPNITYFELAL-PS-GETLNVMQRLPQVFSKPKYP
ASPOR_DPPIV 469 TNSTKPLRTITDIAKVLQIKDYALPNITYFELPL-PS-GETLNVMQRLPQVFSKPKYP

UM843_2883 539 VLFPTPGGPGNSRWTKAMTTFNNIYVAAPPELQYILYTDNRCGLYQGRFRFRAVTRQL
ASPFU_DPPIV 522 VLFPTPGGPGAQEVSKPQALDFKAYIASDPELEYITWTVDNRGTGYKGRFRCQVASRL
ASPOR_DPPIV 527 VLFPTPGGPGAQEVTKRQALNFKAYVADSELEYITWTVDNRGTGKGRFRFRAVTRQL

UM843_2883 599 GLEAKDQIYAAQQAADYILISQHDYIDADHIALWGSFSGGLTKVLETQGSIAEFTLGLITA
ASPFU_DPPIV 582 GLEAADQVYAAQQA--AKLPYDAQHIAIWGWSYGGYLTQKVLK---DSGAFSLGVYTA
ASPOR_DPPIV 587 GLEAADQIYAAQQA--ANIPYIDADHIALWGSFSGGLTKVLEK---DSGAFSLGVYTA

UM843_2883 659 PVSDWRFPYDSMYTERYMTPAINARGYEAIAIRDTTSEKIVSGGESTQHGLEDNVHGH
ASPFU_DPPIV 638 PVSDWRFPYDSMYTERYMTLEINAGYASAIRKVAEIKNVRGCVLIQHGTDGDDNVHFGN
ASPOR_DPPIV 643 PVSDWRFPYDSMYTERYMTLSTNEGYEISAIRKTDGPKNVEGGFLIQHGTDGDDNVHFGN

UM843_2883 719 TAALVDLLVGDGVTPKMDWRVYVTDSDHSTAVNCAVNHLYKYLSKKLYDEKNREAGLVFQ
ASPFU_DPPIV 698 AAALVDLLVGAAGVTPEKIQVQWFTDSDHGIRYHGGNVFLYQLSKRLEYEKRRKEK-GFA
ASPOR_DPPIV 703 SAALVDLLVGDGVPEKIHSDWFTDSDHGISYHGGVFLYKQIAEKLYQEKNEQTO-VLM

UM843_2883 779 HWSKRGLELFFK
ASPFU_DPPIV 757 HWSKRSVY---
ASPOR_DPPIV 762 HWTKKLEL---

```

Figure 4.19: Multiple sequence alignment of predicted DPP IV (UM843_2883) of *C. sphaerospermum* UM 843 with DPP IV from *A. fumigatus* (ASPFU_DPPIV; AAC34310.1) and *A. oryzae* (ASPOR_DPPIV; Q2UH35). The consensus motif Gly-X-Ser-X-Gly is indicated with circle (•) and the catalytic triad Ser 631, Asp 711, His 746 are indicated with asterisk (*)

```

UM843_1649 1 MVAGQIAAAALLLPLAAITPEQMLSAAPVSAASSNPSGGEAVYVSTNYSFETQAAAV
ASPFU_DPPV 1 MGARRWLSIAAA-ASTALAITPEQLITAPRRSEALPDPGKVAVFSLSQYSFETHKRTSW
ASPTN_DPPV 1 MAARRWLSAVVAVSITVLAITPEQMLSAAPRRAEAI PNPSGNVALFSAQYSFDTKEKSSS

UM843_1649 61 WKLLNFKTGDIDLPFADDVSEVWVGNNTNSVLYINGTNDLIPGGVILWITDIAISPIV
ASPFU_DPPV 60 WSLIDLKTKGQTKVLTNDSSVSEIVWLSDD--DSILYVNSTNADIPGGVELWVTAQAS-SFAK
ASPTN_DPPV 61 WNLNFKTGDITLLTDDANVSEIVWLGDDTSLLYINGTNAEIPGGVELWVSSIK-DESK

UM843_1649 121 GTQVASLDAPFSGLKASNTPSGGINEVFNAAKAYANNGSAYNEEFASIPATTCQLYDNVWV
ASPFU_DPPV 117 GYKAASLDAPFSGLKAAKTSAGDINFAVYQSYPNGTAYNEELATAHLSARIYDSIYV
ASPTN_DPPV 120 GYKAASLDAPFSGLKAVETPSGDIKFAVNAQSYA--NGTAYNEELATKYASTARIYDSIYV

UM843_1649 181 RHWDTYVITQERFSVFGSLAQSNS--SLSLSCNVTNLLGIDAPITRFEIPYQPFGGSSD
ASPFU_DPPV 176 RHWDTYVITQERFSVFGSLAQSNS--SLSLSCNVTNLLGIDAPITRFEIPYQPFGGSSD
ASPTN_DPPV 179 RHWDTYVITQERFSVFGSLAQSNS--SLSLSCNVTNLLGIDAPITRFEIPYQPFGGSSD

UM843_1649 239 YDLSPDGSCQVVEMTKAPELPKANFTASYLYLVPHDGSVVERINGENST-APEEAKGASA
ASPFU_DPPV 232 YDLSPDGKVVAFKSKAPELPKANFTTSYIYLPHDSETPARPINGPDSPGTGGKGGDS
ASPTN_DPPV 233 YDLSPDGKVVAFKSKAPVFRANVTTAVIYLAIPHDSSTATIPINGPDSPGTPEGVGGAN

UM843_1649 298 NPVWSPDGKRIAYQMDGINYESDRAKLYADVASGE--ITLAAADWVSVSGSLKWSHDCD
ASPFU_DPPV 292 SPVFSFNGDKLAYFQMRDEYIESDRAILYVYVLSGSKKTIKSVAGDWRSPDSKVVTPGK
ASPTN_DPPV 293 YPVFSFNGDKLAYFQMAHKSYESDRRLYVYVLSGSKTITKAVAGDWRSPDSKVVLD-NK

UM843_1649 357 ELYVTGTYIGSTRLEFI-VPADAADYKFNVDSTVVDENVLNGDSLISAVWSSRM
ASPFU_DPPV 352 TLIVGSEDEHGRTRLES-IPANAKDDYKFNFTDGGSVSAYYFLPDSILLVTGSAIWTNN
ASPTN_DPPV 352 HLIIGSEDEHGRTRLES-IPANAKDDYKFNFTDGGSVSAYYFLPDKIIVLVTGSAIWTNN

UM843_1649 416 IYTVVPSKST-TYLYKADVDABLAGLGPDDISFEVYTFELGQQQMLVIYIEGTHKNT
ASPFU_DPPV 411 VYTAKPKKGVIRKIASANKIDPELKGLGSDISEFYFQGNFTDI-HANVIYENFDKSKK
ASPTN_DPPV 412 VYTAKPKKGVIRKIASANKIDPELGLAGLGPDISSEFYFDGNVTKI-QSWLIYENFDKSKK

UM843_1649 475 YDLAFIHHGGPQGLHANSWSTRWNEKVVADQGYVVVAPNPTGTSYGOALTDRIQGRWST
ASPFU_DPPV 470 YPLFFIHHGGPQGNWADGWSTRWNEKVVADQGYVVVAPNPTGSTGFGQALTTAIQNNWGG
ASPTN_DPPV 471 YPLFFIHHGGPQSATEDSWSTRWNAKVVADQGYVVVAPNPTGSTGFGQELTDAIANNWGG

...

UM843_1649 535 WPYEDLVNNAFHVRTYFVNTSNAPAGASYGGMTNWIQGGDLGRKFKALVAHDGVTT
ASPFU_DPPV 530 APYEDLVKQWEYVHNLVYVDTFNGVAAGASYGGFMINWIQGGDLGRKFKALVSHDGTFF
ASPTN_DPPV 531 APYEDLVKAWEVVDKNLVYVDTFNGVAAGASYGGFMINWIQGGDLGRKFKALVSHDGTFF

UM843_1649 595 TFSDFGTEELFMLHDQNGTLWENRETVAMNDPFFTHA--RNFSTPQLIHNLDYRLPVS
ASPFU_DPPV 590 ADAKSTEEELWFMQRNENGTFFWDARDNYRRWDPSAPERILQFDFEMLVIHSEKDYRLPVA
ASPTN_DPPV 591 ADAKSTEEELWFMQRNENGTFFWDARDNYRRWDPSAPERILQFDFEMLVIHSDQDYRLPVA

UM843_1649 653 EGLAMFNALQLLGVPSRFTFFPDENHWVLRNENSLWFHTFDNINNYTGKTESLSLEGV
ASPFU_DPPV 650 EGLSIFNVLQERGVPSRFLNFPDENHWVLRNENSLVWHQALGWINNYSGEKSDFNAVS
ASPTN_DPPV 651 EGLAMFNVLQERGVPSRFLNFPDENHWVLRNENSLVWHQALGWLNRYSGEENPDAVS

UM843_1649 713 ITQ-----
ASPFU_DPPV 710 LDDTIVPVVNYN-
ASPTN_DPPV 711 LDDTIVPVVNYNP

```

Figure 4.20: Multiple sequence alignment of predicted DPP V (UM843_1649) of *C. sphaerospermum* UM 843 with DPP V from *A. fumigatus* (ASPFU DPPV; AAB67282) and *A. terreus* (ASPTN_DPPV; Q0C8V9.1). The consensus motif Gly-X-Ser-X-Gly is indicated with circle (•) and the catalytic triad Ser 565, Asp 646, His 678 are indicated with asterisk (*)

4.2.3.5 Secondary metabolites

A total of 16 secondary metabolite backbone genes were predicted (Table 4.11) by using Secondary Metabolite Unknown Region Finders (SMURF). Of these, one of the non-reducing polyketide synthase (PKS) (UM843_1729) was found likely to be involved in pigment synthesis, two nonribosomal peptide synthase (NRPS) (UM843_7306 and UM843_8410) are likely to be responsible for siderophore biosynthesis and a hybrid PKS-NRPS (UM843_7284) likely to be involved in the synthesis of cladosins.

Table 4.11: Secondary metabolite backbone genes predicted in UM 843 and their domain arrangement

Gene ID	Backbone gene prediction	Domain arrangement
UM843_3397	NRPS	A-T-C-C-A-T-C-A-T-C-C-T-C-T
UM843_549	NRPS	A-T-C
UM843_7306	NRPS	A-T-C-T-C
UM843_8410	NRPS	A-T-C-A-T-C-T-C-A-T-C-T-C-T-C
UM843_3304	NRPS-Like	A-T-R-R
UM843_3629	NRPS-Like	A-T-R
UM843_8241	NRPS-Like	A-T-R
UM843_826	NRPS-Like	A-T-R-P loop containing nucleoside triphosphate hydrolase
UM843_8532	NRPS-Like	A-T-Trimeric LxpA-like
UM843_9473	NRPS-Like	A-T-R
UM843_1729	PKS	SAT-KS-AT-DH-ACP-ACP-TE
UM843_7344	PKS	KS-AT-DH-MT-ER-KR-ACP
UM843_9325	PKS	KS-AT-DH-ER-KR-ACP
UM843_4619	PKS-Like	KS-AT-DH
UM843_6793	PKS-Like	GTPase binding domain-KS
UM843_7284	PKS-NRPS	KS-AT-KR-ACP-C-A-T-R

NRPS: nonribosomal peptide synthase; PKS: polyketide synthase; A: adenylation; T: thiolation; C: condensation; R: reduction; SAT: starter unit:ACP transacylase; KS: ketosynthase; AT: acyltransferase; ACP: acyl carrier protein; TE: thioesterase; KR: ketoreductase

Similarity search showed that gene UM843_1729 is best matched to a characterised conidial yellow pigment biosynthesis PKS from *A. fumigatus* (*alb-1*) (GenBank accession: Q03149) and showed a significantly high identity to a predicted *Cladosporium phlei* Cppks1 protein (GenBank accession: AFP89389) (Table 4.12). The genes encoding enzymes that are involved in the 1,8-dihydroxynaphthalene (DHN)-melanin biosynthesis, scytalone dehydratase (UM843_148) and tetrahydroxynaphthalene reductase genes (UM843_1726; UM843_7560) were also identified in the genome. The PKS gene was found to be preceded by a tetrahydroxynaphthalene reductase (UM843_1726) and transcription factor Cmr1 (UM843_1727) encoding genes (Figure 4.21). In addition, two *yg-1* like genes annotated as *Wdyg-1* (UM843_912) and *Ayg-1* (UM843_6732) were identified in the UM 843 genome.

Table 4.12: Putative genes involved in DHN-melanin biosynthesis

Gene description	Gene ID	Matched gene accession No.	Identity (%)
polyketide synthase	UM843_1729	AFP89389	90.00
yellowish green-1	UM843_912	AAT81166	61.02
	UM843_6732	AAF03354	54.00
scytalone dehydratase	UM843_148	BAC79365	73.48
tetrahydroxynaphthalene reductase (T4HN)	UM843_1726	EHY60769	78.24
	UM843_7560	ACA52027	81.20

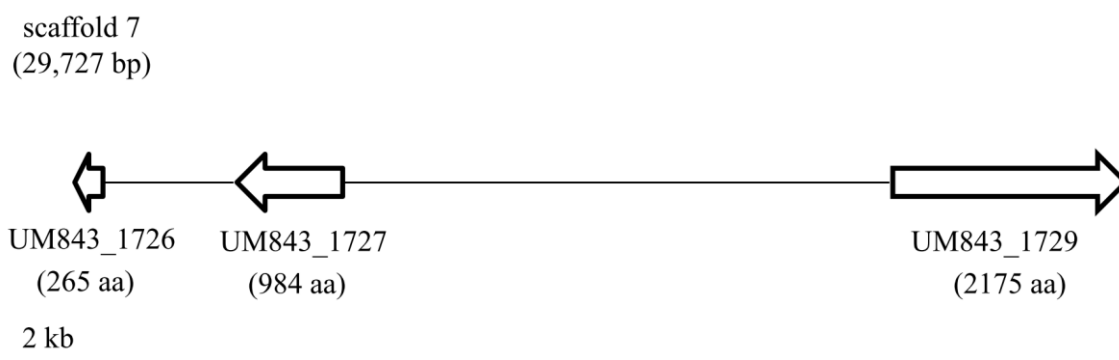


Figure 4.21: Putative melanin biosynthesis cluster in UM 843. The genes are predicted to encode tetrahydroxynaphthalene reductase (UM843_1726), transcription factor Cmr1 (UM843_1727) and PKS (UM843_1729). The direction of transcription is depicted by the arrow for each gene

As for the genes involved in siderophore biosynthesis, all the genes predicted to be involved in the biosynthesis and transportation of siderophores were identified (Table 4.13). The genes nearby the gene encoding fusarinine-type NRPS (UM843_7306) encompass L-ornithine-N⁵-monooxygenase, esterase, ABC transporter SitT, carnitiny-CoA dehydratase and acetyltransferase SidF encoding genes (Figure 4.22). However, the ortholog of *A. fumigatus sidG* gene was absent in UM 843 genome. Likewise, the predicted ferrichrome-type NRPS encoding gene (UM843_8410) is located in adjacent to ABC transporter and L-ornithine-N⁵-monooxygenase (Figure 4.23).

Table 4.13: Putative genes involved in siderophore biosynthesis, transportation and regulation in UM 843

Putative gene description	Gene ID	Matched gene accession No.	Identity (%)
L-ornithine N ⁵ -oxygenase	UM843_8412	EGP90755	62.27
	UM843_7304	XP_002796674	28.04
N ⁵ - transacyclase SidF	UM843_7309	GAA92776	76.03
NRPS SidD (Fusarinine)	UM843_7306	Q4WF53	59.56
NRPS SidC (Ferrichrome)	UM843_8410	XP_001267711	38.54

Table 4.13, continued

Putative gene description	Gene ID	Matched gene accession No.	Identity (%)
Transporter (MirB)	UM843_1516	Q870L2	56.54
	UM843_1642	EFY92978	61.18
	UM843_7063	EDP53308	64.65
	UM843_6538	XP_001826761	56.15
	UM843_9659	XP_001247665	50.85
	UM843_9664	XP_002628804	53.34
Transporter (MirC)	UM843_6757	EGP89386	67.01
Transporter (Sit1/Arn3)	UM843_5791	EHY59937	64.55
Iron-responsive GATA factor (IRGF)	UM843_1371	CAC36427	53.91
Transcription factor Hap-X	UM843_5128	XP_002848863	29.76
CCAAT-binding complex Hap-B	UM843_2106	EFX04486	79.57
CCAAT-binding complex Hap-C	UM843_5496	XP_001265272	57.41
CCAAT-binding complex Hap-E	UM843_475	EEQ85865	78.72

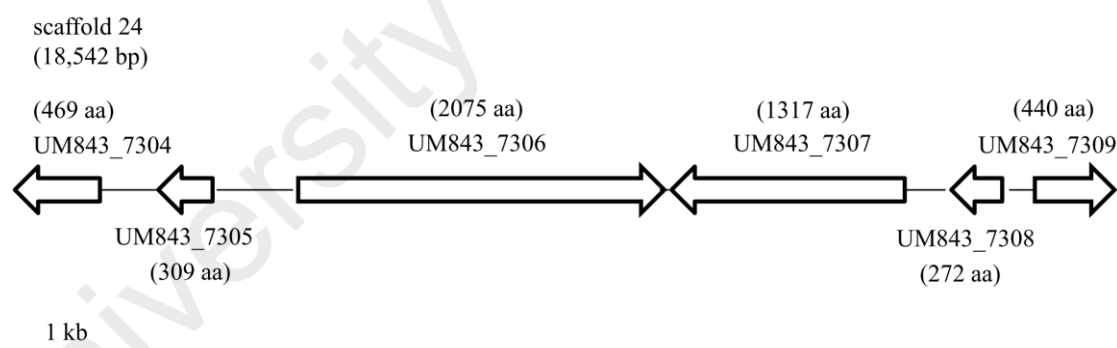


Figure 4.22: Putative fusarinine-type siderophore biosynthesis cluster in UM 843. The genes are predicted to encode L-ornithine-N⁵-monooxygenase (UM843_7304), esterase (UM843_7305), NRPS SidD (UM843_7306), transporter SitT (UM843_7307), carnitinyI-CoA dehydratase (UM843_7308), acetyltransferase SidF (UM843_7309). The direction of transcription is depicted by the arrow for each gene

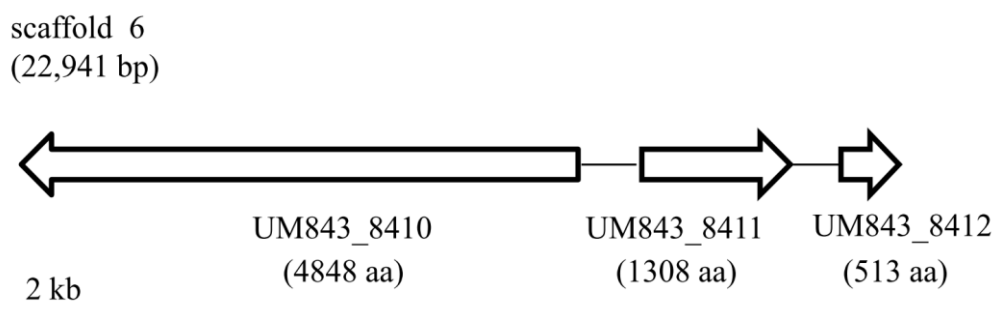


Figure 4.23: Putative gene cluster involved in ferrichrome-type siderophore biosynthesis. The genes are predicted to encode ferrichrome-type NRPS (UM843_8410), ABC transporter (UM843_8411) and L-ornithine-N⁵-monooxygenase (UM843_8412). The direction of transcription is depicted by the arrow for each gene

A total of nine siderophore transporters similar to the siderophore transporters MirB, MirC and Sit1, were determined (Table 4.13). A gene encoding siderophore esterase (UM843_1515) similar to *estB* of *A. fumigatus* (GenBank accession: XP748686) was found adjacent to the UM 843 putative *mirB* (UM843_1516). UM843_1516 has 56.54% identity with *A. nidulans mirB* (Figure 4.24).

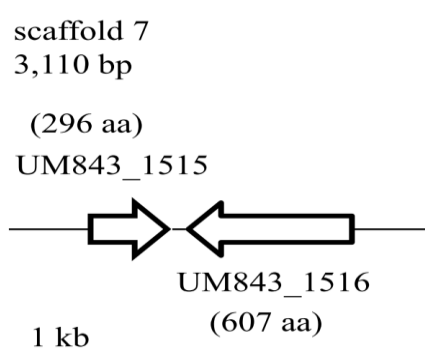


Figure 4.24: Putative cluster of genes involved in the transportation of TAFC in UM 843. The genes are predicted to encode siderophore esterase (UM843_1515) and siderophore transporter (UM843_1516). The direction of transcription is depicted by the arrow for each gene

Additionally, putative genes involved in regulation of iron homeostasis were identified in the genome such as the iron-responsive GATA factor (IRGF) (UM843_1371), transcription factor Hap-X (UM843_5128) and the monomers of CCAAT-binding complex, Hap-B (UM843_2106), Hap-C (UM843_5496) and Hap-E (UM843_475) (Table 4.13). The sequence alignment of IRGFs from UM 843, *A. fumigatus*, *A. nidulans*, *Ustilago maydis* and *Penicillium chrysogenum* showed two GATA-type zinc fingers flanking a highly conserved cysteine-rich region (Appendix D5). Further inspection in the 5'-upstream region of the siderophore gene clusters and transporter genes revealed several GATA binding elements (Appendix D6-D8).

The gene UM843_7284, the only PKS-NRPS hybrid predicted in UM 843, is shown to share 40% and 41% identity with *Talaromyces stipitatus* putative PKS (GenBank accession: XP_002478535) and *Aspergillus clavatus* PKS-NRPS cytochalasin (GenBank accession: A1CY8), respectively. Unlike the *T. stipitatus* and *A. clavatus* PKS-NRPS, the DH and MT domains were missing in UM843_7284. The predicted gene cluster disclosed neighbouring genes such as genes encoding transporters, cytochrome P450, alpha beta hydrolase, thioesterase and transcription factor domain containing proteins (Table 4.14).

Table 4.14: Putative PKS-NRPS hybrid gene cluster of UM 843

Gene ID	PFAM ID//Functional annotation	Annotated gene function (non-redundant; SwissProt)
UM843_7295	PF07690//Major Facilitator Superfamily	MFS monocarboxylate; uncharacterized transporter esbp6
UM843_7294	PF07859//alpha/beta hydrolase fold	Alpha beta-hydrolase
UM843_7293	-	Hypothetical protein
UM843_7292	-	Hypothetical protein
UM843_7291	-	gpi-anchored cell wall beta- - endoglucanase;laminarinase eglc
UM843_7290	PF00168//C2 domain	c2 domain-containing protein

Table 4.14, continued

Gene ID	PFAM ID//Functional annotation	Annotated gene function (non-redundant; SwissProt)
UM843_7289	PF00493//MCM2/3/5 family PF14551//MCM N-terminal domain	DNA replication licensing factor mcm7;minichromosome maintenance protein 7
UM843_7288	PF00083//Sugar (and other) transporter PF03962//Mnd1 family	Hexose transporter protein;lactose permease
UM843_7287	PF00067//Cytochrome P450	Cytochrome p450;cytochrome p450-4
UM843_7286	PF07690//Major Facilitator Superfamily	MFS multidrug transporter; protein zinc-induced facilitator-like 2
UM843_7285	-	Hypothetical protein
UM843_7284	PF00109//Beta-ketoacyl synthase, N-terminal domain PF02801//Beta-ketoacyl synthase, C-terminal domain PF16197//Beta-ketoacyl synthase, C-terminal extension PF00698//Acyl transferase domain PF08659//KR domain PF00668//Condensation domain PF00501//AMP-binding enzyme PF13193//AMP-binding enzyme, C-terminal domain PF13745//HxxPF-repeated domain PF00550//Phosphopantetheine attachment site PF07993//Male sterility protein	Putative PKS; PKS-NRPS cytochalasin
UM843_7281	PF04082//Fungal specific transcription factor	c6 transcription factor
UM843_7280	PF00975//Thioesterase domain	thioesterase domain containing protein
UM843_7279	PF07690//Major Facilitator Superfamily	mfs drug efflux transporter; hc-toxin efflux carrier toxa
UM843_7278	PF01019//Gamma-glutamyltranspeptidase	gamma-glutamyltranspeptidase; gamma-glutamyltranspeptidase 2 light chain
UM843_7277	PF00067//Cytochrome P450	Cytochrome p450; cytochrome p450 57a2
UM843_7276	-	Peroxin pex22-like protein
UM843_7275	PF00501//AMP-binding enzyme PF13193//AMP-binding enzyme C-terminal domain	Phenylacetyl-; 4-coumaroyl-synthase 2

Table 4.14, continued

Gene ID	PFAM ID//Functional annotation	Annotated gene function (non-redundant; SwissProt)
UM843_7274	PF06644//ATP11 protein	f1f0 atp synthase assembly protein atp11; protein mitochondrial
UM843_7273	PF00005//ABC transporter PF00664//ABC transporter transmembrane region	ABC multidrug; leptomycin b resistance protein pmc1
UM843_7272	PF13302//Acetyltransferase (GNAT) domain	gcn5-related n-acetyltransferase

4.2.3.6 Stress responses

Fungal Stress Respond Database (FSRD) analysis identified a total of 340 genes related to stress responses such as amino acid starvation, nitrogen starvation, iron starvation, osmotic stress, oxidative stress, and heat stress. Based on the FSRD GO annotations, there are 29, 39 and 75 gene models assigned in response to heat stress, starvation and oxidative stress, respectively (Appendix D9-D11).

Three proline catabolism associated genes (UM843_6340, UM843_4194 and UM843_2468) were grouped under the category of response to amino acid starvation (Appendix D10 and Table 4.15). Search in the UM 843 genome revealed the full set of genes involved proline catabolism (Table 4.15). Two of the genes encoding product of PrnC and PrnD were located in adjacent (Figure 4.25).

Table 4.15: Putative genes involved in proline catabolism predicted in UM 843

Putative gene description (A. <i>nidulans</i> homologue)	Gene ID	Matched gene accession No.	Identity (%)
Proline permease (<i>prnB</i>)	UM843_6340	ANID_01732T0	54.63
Delta-1-pyrroline-5-carboxylate dehydrogenase (<i>prnC</i>)	UM843_4194	ANID_01733T0	68.35
	UM843_2468	ANID_01733T0	53.35
Proline oxidase (<i>prnD</i>)	UM843_2469	EHY60587	54.28
Transcription factor (<i>prnA</i>)	UM843_7253	XP_001936226	40.00
Proline utilisation protein (<i>prnX</i>)	UM843_6979	XP_001388763	41.87

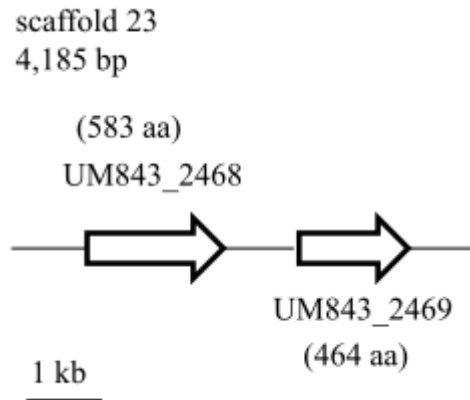


Figure 4.25: Location of *prnC* and *prnD* gene in UM 843. The genes are located in scaffold 23 encompassing 4,185 bp in length. The genes were predicted to encode delta-1-pyrroline-5-carboxylate dehydrogenase (UM843_2468) and proline oxidase (UM843_2469). The direction of transcription is depicted by the arrow for each gene

Genes encoding a ferroxidase and iron permease similar to *fetC* (UM843_5150, 69.12% identity to P38993) and *ftr1* (UM843_5151, 59.69% identity to P40088), respectively were determined. These two genes are involved in reductive iron assimilation (RIA) and were located adjacent to each other in the genome (Figure 4.26). Similar to the regulation of siderophore biosynthesis genes, RIA genes are also regulated by GATA factor. The GATA-binding elements were predicted in the upstream of putative *fetC* and *ftr1* genes (Appendix D12).

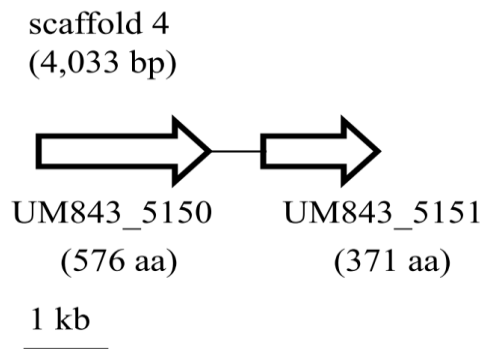


Figure 4.26: Putative RIA system cluster in UM 843. The genes are predicted to encode ferroxidase FetC (UM843_5150) and iron permease Ftr1 (UM843_5151). The direction of transcription is depicted by the arrow for each gene

(a) ***Response to high salinity***

In this study, a total of 29 genes encoding plasma membrane and intracellular transporters that are involved in cation regulation were determined in UM 843 (Appendix D13). Also, all the subunits of V-type ATPase complex were identified (Appendix D14). A total of 20 P-type ATPases were predicted and were classified according to the subfamilies based on the domains present (Appendix D15). Additionally, the fungus contains a higher number of *ena* genes than *nhal* genes. Table 4.16 shows a comparison of the number of transporters in UM 843, with halotolerant *H. werneckii*, halophilic *W. ichthyophaga*, and non-halotolerant *M. graminicola*.

The genes involved in the synthesis of compatible solutes glycerol, trehalose, d-mannitol and arabitol; transportation of glycerol and signalling components involved in high osmolarity glycerol (HOG) signalling pathway were predicted in UM 843 (Table 4.17). The genes involved in taurine synthesis pathway were also found in KEGG map (Figure 4.27).

Table 4.16: Putative transporters involved in high salinity survival in UM 843, *W. ichthyophaga*, *H. werneckii*, and *M. graminicola*

Cellular location	Transporter type	Substrate specificity	^a <i>Sc</i> homologue	UM 843	^b <i>Wi</i> ¹	^c <i>Hw</i> ²	^d <i>Mg</i> ²
Plasma membrane	Uniporter	K ⁺ uptake	Trk1, 2	2	1	8	1
	Channel	K ⁺ efflux	Tok1	2	0	4	1
	P-type ATPase	K ⁺ influx	Acu	1	2	0	1 ³
	Symporter	K ⁺ influx	Hak	1	0	0	2 ³
	Antiporter	Na ⁺ /H ⁺ exchange	-	3	1	-	-
	Antiporter	Na ⁺ , (K ⁺)/H ⁺ exchange	Nha1	2	2	8	3
	P-type ATPase	Na ⁺ (and Li ⁺) efflux	Ena1,2,5	4	2	4	3
	P-type ATPase	H ⁺ export	Pma1	1	3	4	-
	Symporter	Na ⁺ /Pi cotransporter	Pho89	3	1	6	2
Vacuole	V-type ATPase	H ⁺ uptake	Vma1	1	1	2	-
	Antiporter	Na ⁺ , K ⁺ /H ⁺ exchange	Vnx1	0	1	2	1
Endosomal	Antiporter	Na ⁺ /H ⁺ exchange	Nhx1	1	1	2	1
Golgi apparatus	Antiporter	K ⁺ /H ⁺ exchange	Kha1	1	2	2	1
Mitochondria	Antiporter	K ⁺ /H ⁺ exchange	Mrs7/Mdm38	1	1	2	1

^a*S. cerevisiae*

^b*W. ichthyophaga*

^c*H. werneckii*

^d*M. graminicola*

¹ Data were obtained from Zajc et al. (2013)

² Data were obtained from Lenassi et al. (2013)

³ Data were obtained from Benito, Garciadeblás, Fraile-Escanciano, & Rodríguez-Navarro (2011)

Table 4.17: Putative genes involved in the synthesis of compatible solutes, transport of glycerol and HOG signalling pathway predicted in UM 843

FSRD protein description	Gene ID	Matched gene accession No.	Identity (%)
Glycerol synthesis			
NAD-dependent glycerol-3-phosphate dehydrogenase GfdB	UM843_9164	ANID_06792T0	55.12
Glycerol-3-phosphate phosphatase GPP	UM843_7180	EER42892	61.2
NADP ⁺ -dependent glycerol dehydrogenase GldB	UM843_8216	ANID_05563T0	71.56
Trehalose synthesis			
trehalose-6-phosphate synthase TpsA	UM843_5932	Afu6g12950	74.41
Trehalose 6-phosphate phosphatase Or1A	UM843_772	Afu3g05650	65.75
D-mannitol synthesis			
*NADP-dependent mannitol dehydrogenases	UM843_6416	P0C0Y5	94.00
	UM843_1976	XP_003709497	57.85
Arabitol synthesis			
*D-arabinitol-2-dehydrogenase	UM843_3559	EGY14085	63.45
	UM843_3572	EGY22408	57.55
	UM843_7702	CBY02077	63.82
Cell membrane regulation			
Plasma membrane proteolipid Pmp3	UM843_3575	SPBC713_11c.1	53.19
	UM843_7922	SPBC713_11c.1	55.56
	UM843_5517	SPBC713_11c.1	59.09
	UM843_7985	SPBC713_11c.1	79.17
*sugar/H ⁺ symporters St11	*UM843_186	EGP92429	76.68
	UM843_4858	EGY23675	63.35
	UM843_5382	XP_001932938	59.50
	UM843_8200	EGY21476	67.86
	UM843_8407	XP_001935208	65.27
	UM843_8680	XP_001935331	66.86
	UM843_8814	XP_001934931	65.49
*Aquaglyceroporin	UM843_5638	EHY54199	69.75
	UM843_4817	EIT81294	48.79
	UM843_4886	XP_002377303	53.59
HOG signalling pathway components			
Putative MAPK Saka	UM843_5411	Afu1g12940	92.24
MAPK kinase PbsA	UM843_2812	ANID_00931T0	52.18
Putative transmembrane osmosensor Sho1	UM843_8679	Afu5g08420	56.12
Histidine-containing phosphotransfer protein YpdA	UM843_8084	ANID_02005T0	57.78

Table 4.17, continued

FSRD protein description	Gene ID	Matched gene accession No.	Identity (%)
HOG signalling pathway components			
*osmolarity two-component system protein Sln1	UM843_4487	XP_001934856	51.83
*Two-component response regulator Ssk1	UM843_8730	EGP88949	61.42
*Serine/threonine-protein kinase PakA (Ste20 homologue)	UM843_3491	Q2VWQ3	81.40

The genes were annotated from FRDS unless specified

*gene search in UM 843 genome data

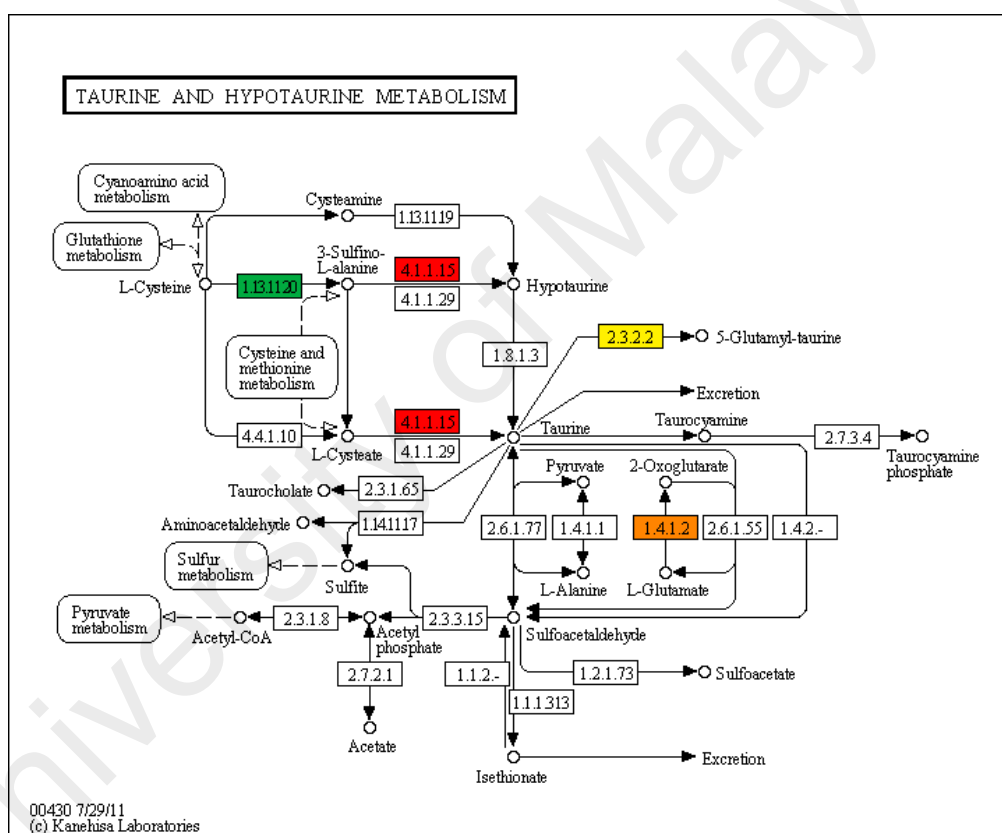


Figure 4.27: Taurine biosynthesis pathway of UM 843 predicted via KEGG pathway map

The predicted UM 843 glycerol-3-phosphate dehydrogenase (*gpd*) gene involved in glycerol biosynthesis, UM843_9164 shared 74.22% and 73.29% identity with *H. werneckii gpd1A* and *gpd1B*, respectively. Sequence alignment of *gpd* genes from *S.*

cerevisiae, UM 843, *H. werneckii* and *W. ichthyophaga* showed that the latter three species do not have the N-terminal type 2 peroxisomal targeting sequence (PTS2) compared to *S. cerevisiae gpd* (Figure 4.28). The six putative sugar/H⁺ symporters St11 appeared to contain 12 transmembrane domains (Appendix D16). The *hog1* gene of UM843 (UM843_5411) shared 92.48% identity with *H. werneckii hog1*. The multiple sequence alignment of UM 843, *H. werneckii*, *A. fumigatus* and *S. cerevisiae hog1* showed a conserved T-G-Y phosphorylation motif in the activation loop and a common docking domain-containing conserved YHDP[T/S]DEP motif (Figure 4.29).

4.2.3.7 Sexual reproduction

The genes involved in the mating process and signalling, fruit body development and meiosis of fungi were determined in UM 843 (Appendix D17). A putative *mat1-2* gene was identified in UM 843. The gene (UM843_3044) containing high mobility group (HMG) domain shared 65.05% identity with *Dothistroma septosporum mat1-2* gene (GenBank accession: ABK91354). The putative DNA lyase *apn2* gene, anaphase promoting complex protein encoding gene and cytochrome c oxidase subunit VIa *cox13* gene were determined adjoining to the putative *mat1-2* gene as shown in Figure 4.30.

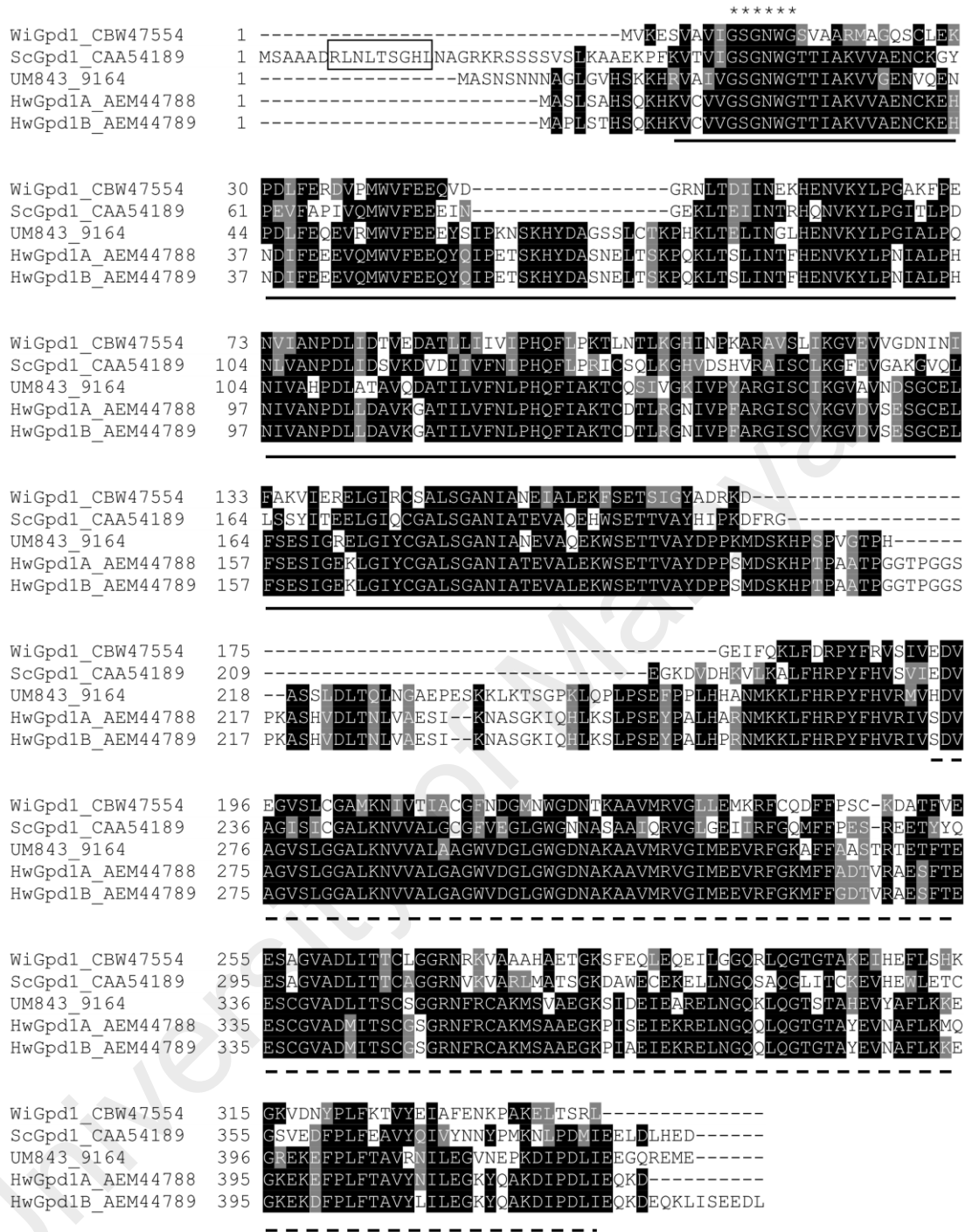


Figure 4.28: Multiple sequence alignment of NAD-dependent *gpd* of *C. sphaerospermum* UM 843 (UM843_9164) with *gpd* gene from *W. ichthyophaga* (WiGpd1; CBW47554), *S. cerevisiae* (ScGpd1; CAA54189) and *H. werneckii* (HwGpd1A; AEM44788 and HwGpd1B; AEM44789). The peroxisomal targeting signal type 2 (PTS2) is indicated in box and the consensus NAD(P)/NAD(P)H binding site GXGXXG is indicated in asterisk (*). The Gpd N-terminus domain (PF01210) and C-terminus domain (PF07479) are shown in solid and dash line, respectively

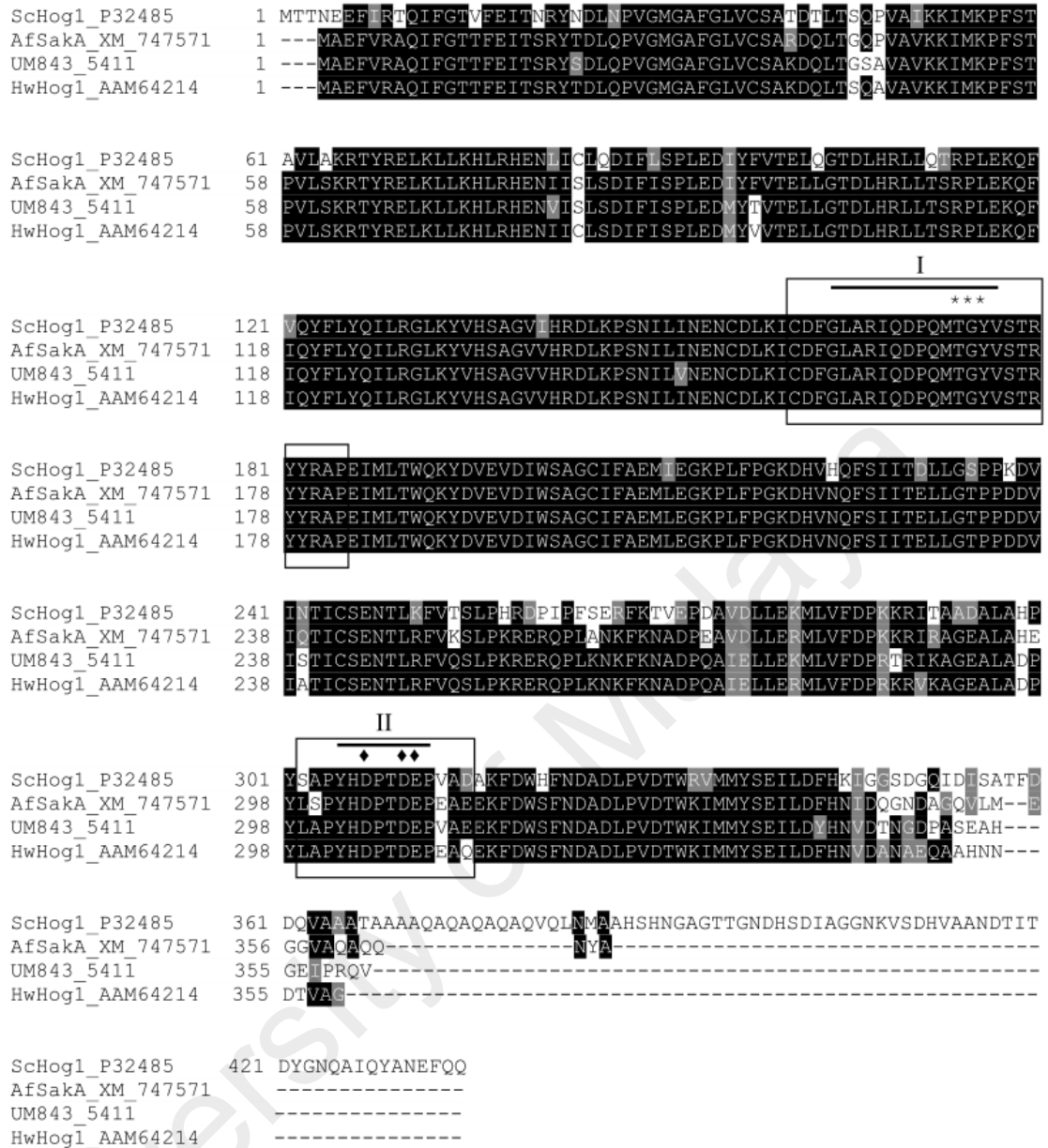


Figure 4.29: Multiple sequence alignment of *hog1* of *C. sphaerospermum* UM 843 (UM843_5411) with *H. werneckii* (HwHog1; AAM64214), *S. cerevisiae* (ScHog1; P32485) and *A. fumigatus* (AfSakA; XM_747571). The activation loop and common docking domain are indicated in the box I and II, respectively. The conserved phosphorylation Lip is indicated in line while the asterisk (*) indicates the TYG phosphorylation site motif. The YHDP[T/S]DEP motif is indicated in line in the second box with rhombus (♦) showing the negatively charged amino acid residues

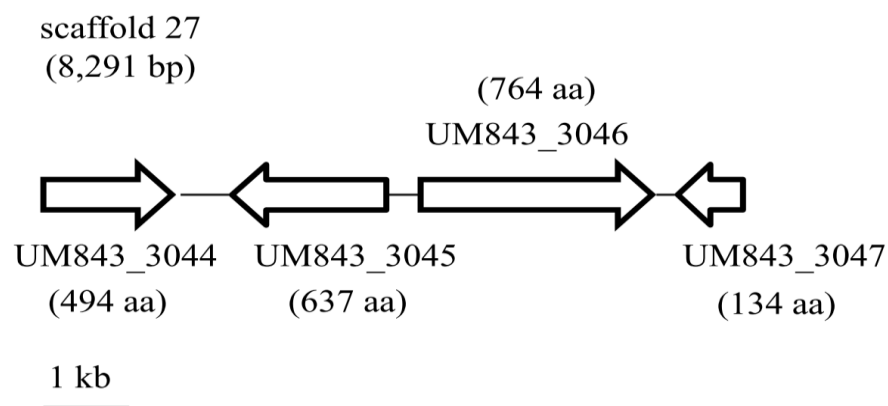


Figure 4.30: Putative gene organisation of mating type gene cluster in UM 843. The neighbouring genes of the high-mobility domain containing gene (UM843_3044) encompass the DNA lyase *apn2* gene (UM578_3045), anaphase promoting complex subunit 5 gene (UM843_3046) and cytochrome C oxidase VIa *cox13* gene (UM843_3047). The direction of transcription is depicted by the arrow for each gene

4.3 Phylogenomic analysis

A total of 303,264 predicted protein sequences were used in all-against-all BLASTP for all the selected fungal genomes, including the outgroup (Table 3.2). A total of 24,581 orthologous clusters with 2,203 single-copy orthologues (one copy of gene from each species) were generated. A concatenated alignment generated from 10% (approximately 220 single-copy orthologue) of the single-copy orthologues was used to construct the Maximum likelihood and Bayesian trees. Both trees have the same topology (Figure 4.31). The Dothideomycetes were categorised into four orders encompassing Pleosporales (12 members), Capnodiales (7 members), Botryosphaerales (3 members) and Hysteriales (1 member). The UM 843 genome forms a sister-group relationship with two clusters within the order Capnodiales; the first cluster consisting of *Acidomyces richmondensis* and *Baudoinia compniacensis* and the second cluster comprising four species, *Cladosporium fulvum*, *Dothistroma septosporum*, *Zasmidium cellare* and *Pseudocerospora fijiensis*.

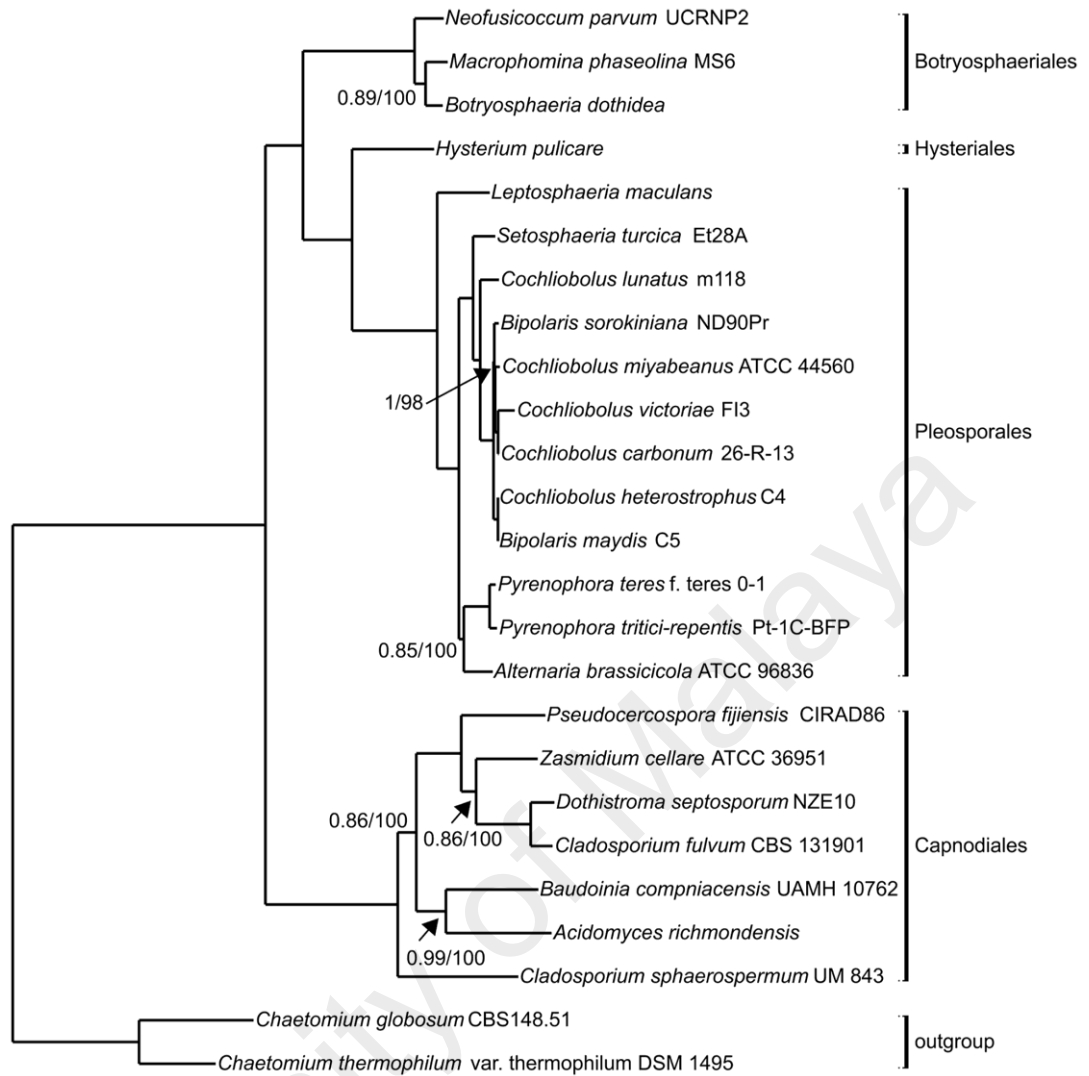


Figure 4.31: Phylogenomic tree of *C. sphaerospermum* and 22 fungi from the class Dothideomycetes. The phylogenomic tree was constructed with two outgroups from Sordariomycetes using Bayesian and maximum likelihood analysis. The first number at the node is Bayesian posterior probability followed by the maximum likelihood bootstrap number. Values less than 1 or 100 for posterior probability and maximum likelihood bootstrap number, respectively, were shown on branches

4.3.1 Orthologous genes and genome comparative analysis

From the 23 dematiaceous Dothideomycetes genomes, a total of 23,800 orthologous clusters were generated. Of these, 14% (3,333 clusters) were conserved among the 23 genomes whereas 51 clusters encompassing 125 UM 843 unique genes were identified (Appendix D18). Among the UM 843 specific genes were putative genes related to

hydrophobins (DOTH 13561), mitogen-activated protein kinases (MAPKs) (DOTH 14960), as well as proteins involved in carbohydrate and protein hydrolysis, amino acid transportation, signal transduction, helicase activity, peroxidase activity, and reverse transcription. In the cluster DOTH 14960, three genes sharing $\geq 60\%$ similarity with MAPK *spk1* from *Schizosaccharomyces pombe* (GenBank accession: P27638) were identified.

4.4 Fungal allergens

A search for the annotated genes in the UM 843 genome revealed 28 genes for allergens with $> 50\%$ identity to the respective allergen match (Appendix D19). In addition, Table 4.18 lists the number of genes annotated as allergens from data derived from the comparative analysis from the previous section (Section 4.3.1).

Interestingly, allergen Cla h HCh1 from the family DOTH 13561 encoding class I hydrophobin was noted only in UM 843. The genes in this family, UM843_1201, UM843_6061, UM843_4115 and UM843_3639, showed 70.48%, 73.33%, 70.48% and 69.14% identity to the hydrophobin gene from *Cladosporium herbarum* (GenBank accession: Q8NIN9), respectively. Also, the sequence alignment of the predicted coding DNA sequences (CDS) with *C. herbarum* Cla h HCh1 showed the eight conserved cysteine residue codons in the genes (Figure 4.32).

4.5 Validation of gene sequences and detection of mRNA

The information of the four putative class I hydrophobin genes is listed in Table 4.19. All the genes were predicted to be secreted and were high cysteine-containing proteins (Table 4.20). The quality and quantity of the RNA extracted are shown in Table 4.21 and Figure 4.33. The sequence alignment of the predicted gene sequence, predicted CDS together with cDNA sequence for each gene are shown in Figure 4.34 to

Figure 4.37. The gel image and electrogram of the cDNA sequences were shown in Appendix D20-D25.

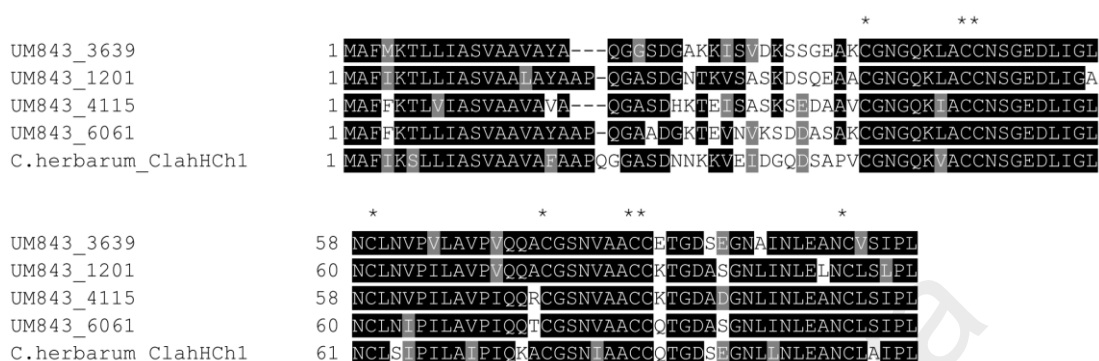


Figure 4.32: Multiple sequence alignment of putative class I hydrophobin CDS in UM 843 (UM843_3639, UM843_1201, UM843_4115, UM843_6061) with hydrophobin CDS from *C. herbarum* Cla HCh 1 (Q8NIN9). The eight conserved cysteine (C) residues were marked with asterisk (*)

Table 4.18: Gene sequence information of putative class I hydrophobin genes in UM 843

Gene ID	Location (scaffold)	Gene length (bp)	No. of intron	Intron length (bp)	Intron position (bp)
UM843_1201	4	384	1	69	200-268
UM843_3639	22	371	1	62	194-255
UM843_4115	13	424	2	61	194-254, 324-377
UM843_6061	9	368	1	53	200-252

Table 4.19: Predicted localisation, protein size, signal peptide and cysteine content of putative hydrophobin genes

Gene ID	Localisation	Protein size (aa)	Signal start	Signal end	Cysteine content
UM843_1201	Extracellular	104	1	18	high cysteine
UM843_3639	Extracellular	102	1	18	high cysteine
UM843_4115	Extracellular	102	1	18	high cysteine
UM843_6061	Extracellular	104	1	18	high cysteine

Table 4.20: Number of genes annotated as allergen (> 50% identity) in UM 843 compared to other members in Dothideomycetes

Families Name	Related allergens	Ab	Ptr	Pt	ChC5	ChC4	Cc	Cv	Cm	Cs	St	Lm	Hp	Mp	Np	843	Bc	Cf	Ds	Pf
DOTH542	Cla h 10	2	1	1	1	1	1	1	1	1	1	1	1	1	1	2	1	1	1	1
DOTH109	Cla h 10	1	2	2	2	2	2	2	2	2	2	1	1	2	2	3	1	1	1	1
DOTH17	Cla h HSP70	2	3	3	3	3	3	3	3	3	3	3	3	3	3	3	3	3	3	2
DOTH13561	Cla h HCh1	-	-	-	-	-	-	-	-	-	-	-	-	-	-	4	-	-	-	-
DOTH5316	Cla h 7	1	1	1	1	1	1	1	1	1	1	-	1	-	1	1	1	1	1	1
DOTH5884	Cla h 8	1	1	1	1	1	1	1	1	1	1	1	1	-	-	1	1	1	1	1
DOTH4756	Cla h 5	1	1	1	1	1	1	1	1	1	1	1	1	1	1	1	1	1	1	1
DOTH5001	Cla h 12	1	1	1	1	1	1	1	1	1	1	1	1	1	1	1	1	-	1	1
DOTH3626	Cla h 6	1	1	1	1	1	1	1	1	1	1	1	1	1	1	1	1	1	1	1
DOTH4659	Cla h NTF2	1	1	-	1	1	1	1	1	1	1	1	1	1	1	1	1	1	1	1
DOTH2993	Asp f 18	1	1	1	1	1	1	1	1	1	1	1	1	1	1	1	1	1	1	1
DOTH2082	Asp f 23	1	1	1	1	1	1	1	1	1	1	1	1	1	1	1	1	1	1	1
DOTH5943	Asp f 2	1	1	1	1	1	1	1	1	1	1	1	-	1	1	2	-	1	-	1
DOTH3212	Fus c 2	1	1	1	1	1	1	1	1	1	1	1	1	1	1	1	1	1	1	1
DOTH1840	Alt a 4	1	1	1	1	1	1	1	1	1	1	1	1	1	1	1	1	1	1	1
DOTH1586	Asp f 12	1	1	1	1	1	1	1	1	1	1	1	1	1	1	1	1	1	1	1
DOTH883	Cand a 1	1	1	1	1	1	1	1	1	1	1	1	1	1	1	2	1	1	1	1
DOTH2261	37 kDa major allergen	1	1	1	1	1	1	1	1	1	1	1	1	1	1	1	1	1	1	1

Ab: *Alternaria brassicicola*; Ptr: *Pyrenophora tritici-repentis*; Pt: *Pyrenophora teres f. teres*; ChC5: *Cochliobolus heterostrophus* C5; ChC4: *Cochliobolus heterostrophus* C4; Cc: *Cochliobolus carbonum*; Cv: *Cochliobolus victoriae*; Cm: *Cochliobolus miyabeanus*; Cs: *Cochliobolus sativus*; St: *Setosphaeria turcica*; Lm: *Leptosphaeria maculans*; Hp: *Hysterium pulicare*; Mp: *Macrophomina phaseolina*; Np: *Neofusicoccum parvum*; 843: UM843; Bc: *Baudoinia compniacensis*; Cf: *Cladosporium fulvum*; Ds: *Dothistroma septosporum*; Pf: *Pseudocercospora fijiensis*

Table 4.21: Quality and quantity of UM 843 extracted RNA

Sample	Concentration (ng/ μ L)	OD 260/280	OD 260/230
9A_843	93.9	2.16	1.6
9B_843	30.7	2.12	1.78

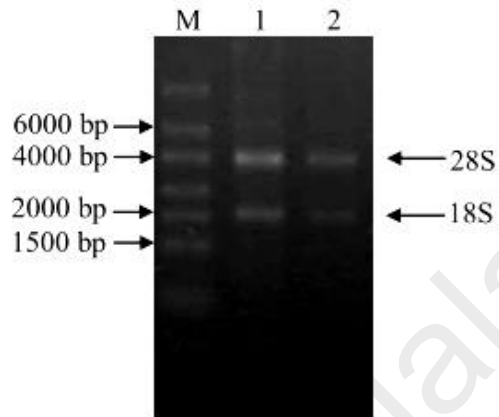


Figure 4.33: Gel image of extracted RNA. Labelling of lane start from left to right: M: High range riboRulerTM RNA ladder; 1, 2: total RNA extracted from *C. sphaerospermum* UM 843.

```

1201_g   1  -----ATGGCCTTCATCAAGACTCTCCTCATCGCCTCCGTGGCCGCCCTTG
1201_t   1  -----ATGGCCTTCATCAAGACTCTCCTCATCGCCTCCGTGGCCGCCCTTG
1201_9A  1  ACCCAATCAACACAATGGCCTTCATCAAGACTCTCCTCATCGCCTCCGTGGCCGCCCTTG

1201_g  47  CCTACGCGCCCCCAGGGCGCCTCTGACGGCAACACCAAGGTCTCCGCCTCCAAGGACT
1201_t  47  CCTACGCGCCCCCAGGGCGCCTCTGACGGCAACACCAAGGTCTCCGCCTCCAAGGACT
1201_9A 61  CCTACGCGCCCCCAGGGCGCCTCTGACGGCAACACCAAGGTCTCCGCCTCCAAGGACT

1201_g  107  CCCAGGAGGCTGCCTGCGGCAACGGCCAGAAGCTCGCTGCTGCAACAGCGGCGAGGACC
1201_t  107  CCCAGGAGGCTGCCTGCGGCAACGGCCAGAAGCTCGCTGCTGCAACAGCGGCGAGGACC
1201_9A 121  CCCAGGAGGCTGCCTGCGGCAACGGCCAGAAGCTCGCTGCTGCAACAGCGGCGAGGACC

1201_g  167  TCATCGGCGCCAACACTGCCTGAACGTCCCCATCCGTACGTTTCCACGATTCTCCAAACAT
1201_t  167  TCATCGGCGCCAACACTGCCTGAACGTCCCCATCC-----
1201_9A 181  TCATCGGCGCCAACACTGCCTGAACGTCCCCATCC-----

1201_g  227  TTTATCGCTCCTTATCACTCCTTTACTGACACTCAAACACAGTGGCCGTCCCCGTCCAGC
1201_t  200  -----TGGCCGTCCCCGTCCAGC
1201_9A 214  -----TGGCCGTCCCCGTCCAGC

1201_g  287  AGGCCTGCGGCTCCAACGTGCGCGGTGCTGCAAGACCGGCGATGCCTCCGGCAACCTCA
1201_t  218  AGGCCTGCGGCTCCAACGTGCGCGGTGCTGCAAGACCGGCGATGCCTCCGGCAACCTCA
1201_9A 232  AGGCCTGCGGCTCCAACGTGCGCGGTGCTGCAAGACCGGCGATGCCTCCGGCAACCTCA

1201_g  347  TCAACCTCGAGCTCAACTGCCTGTCCCTCCCCCTCTAA
1201_t  278  TCAACCTCGAGCTCAACTGCCTGTCCCTCCCCCTCTAA
1201_9A 292  TCAACCTCGAGCTCAACTGCCTGTCCCTCCCCCTCTAA

```

Figure 4.34: Sequence alignment of hydrophobin predicted DNA sequence (1201_g), predicted CDS sequence (1201_t) and cDNA sequence (1201_9A) of *C. sphaerospermum* UM 843. The start codon is in box and the intron region shaded in yellow

```

3639_g 1 -----ATGGCCTTCATGAAGACTCTCCTCATCGCCTCCG
3639_t 1 -----ATGGCCTTCATGAAGACTCTCCTCATCGCCTCCG
3639_9A 1 -----AAAACCAACAAATGGCCTTCATGAAGACTCTCCTCATCGCCTCCG

3639_g 35 TGGCTGCTGTTGCCTACGCCAGGGCGGCTCTGACGGCGCCAAGAAGATCTCCGTCGACA
3639_t 35 TGGCTGCTGTTGCCTACGCCAGGGCGGCTCTGACGGCGCCAAGAAGATCTCCGTCGACA
3639_9A 47 TGGCTGCTGTTGCCTACGCCAGGGCGGCTCTGACGGCGCCAAGAAGATCTCCGTCGACA

3639_g 95 AGAGCTCCGGCGAGGCCAAGTGC GGCAACGGCCAGAAGCTCGCTTGCTGCAACAGCGGCG
3639_t 95 AGAGCTCCGGCGAGGCCAAGTGC GGCAACGGCCAGAAGCTCGCTTGCTGCAACAGCGGCG
3639_9A 107 AGAGCTCCGGCGAGGCCAAGTGC GGCAACGGCCAGAAGCTCGCTTGCTGCAACAGCGGCG

3639_g 155 AGGACCTCATCGGTCTCAACTGCCTGAACGTCCCCGTCCGTACGTATCCCTCTCGAGCT
3639_t 155 AGGACCTCATCGGTCTCAACTGCCTGAACGTCCCCGTCC-----
3639_9A 167 AGGACCTCATCGGTCTCAACTGCCTGAACGTCCCCGTCC-----

3639_g 215 CCCATCTTCCAAACGGACCTCGAGGCTAACAATCACAACAGTGGCCGTCCCCGTCCAGCA
3639_t 194 -----TGGCCGTCCCCGTCCAGCA
3639_9A 206 -----TGGCCGTCCCCGTCCAGCA

3639_g 275 GGCCTGCGGCTCCAACGTGCGCGGTGCTGCGAGACTGGCGACTCCGAGGGCAACGCCAT
3639_t 213 GGCCTGCGGCTCCAACGTGCGCGGTGCTGCGAGACTGGCGACTCCGAGGGCAACGCCAT
3639_9A 225 GGCCTGCGGCTCCAACGTGCGCGGTGCTGCGAGACTGGCGACTCCGAGGGCAACGCCAT

3639_g 335 CAACCTCGAGGCCAACTGCGTCTCCATCCCTCTCTAA
3639_t 273 CAACCTCGAGGCCAACTGCGTCTCCATCCCTCTCTAA
3639_9A 285 CAACCTCGAGGCCAACTGCGTCTCCATCCCTCTCTAA

```

Figure 4.35: Sequence alignment of hydrophobin predicted DNA sequence (3639_g), predicted CDS sequence (3639_t) and cDNA sequence (3639_9A) of *C. sphaerospermum* UM 843. The start codon is in box and the intron region shaded in yellow

```

4115_g      1  .  -----ATGGCCTTCTTCAAGACTCTCGTCATCGCCTCCGTGG
4115_t      1  1  -----ATGGCCTTCTTCAAGACTCTCGTCATCGCCTCCGTGG
4115_9A     1  1  AAGCAACTCTCCAACCATCACATGGCCTTCTTCAAGACTCTCGTCATCGCCTCCGTGG

4115_g     38  CTGCCGTCGCTGTCGCCCAGGGCGCTTCTGACCACAAGACCGAGATCTCCGCCTCCAAGA
4115_t     38  CTGCCGTCGCTGTCGCCCAGGGCGCTTCTGACCACAAGACCGAGATCTCCGCCTCCAAGA
4115_9A    60  CTGCCGTCGCTGTCGCCCAGGGCGCTTCTGACCACAAGACCGAGATCTCCGCCTCCAAGA

4115_g     98  GCGAGGACGCTGCCGTCTGCGGCAACGGCCAGAAGATCGCCTGCTGCAACAGCGGCGAGG
4115_t     98  GCGAGGACGCTGCCGTCTGCGGCAACGGCCAGAAGATCGCCTGCTGCAACAGCGGCGAGG
4115_9A   120  GCGAGGACGCTGCCGTCTGCGGCAACGGCCAGAAGATCGCCTGCTGCAACAGCGGCGAGG

4115_g    158  ACCTCATCGGTCTTAACTGCCTGAACGTCCCCATCCGTACGTTCCACCATCAATCTATTC
4115_t    158  ACCTCATCGGTCTTAACTGCCTGAACGTCCCCATCC-----
4115_9A   180  ACCTCATCGGTCTTAACTGCCTGAACGTCCCCATCC-----

4115_g    218  GATCGACTAGACCCTTTTAGCTGACAACCTCCAAACAGTCGCTGTCCCCATCCAGCAGCGC
4115_t    194  -----TCGCTGTCCCCATCCAGCAGCGC
4115_9A   216  -----TCGCTGTCCCCATCCAGCAGCGC

4115_g    278  TGCGGTTCCAACGTTGCCGCTTGCTGCAAGACTGGCGATGCCGATGTAAGTATCGATCGA
4115_t    217  TGCGGTTCCAACGTTGCCGCTTGCTGCAAGACTGGCGATGCCGATG-----
4115_9A   239  TGCGGTTCCAACGTTGCCGCTTGCTGCAAGACTGGCGATGCCGATG-----

4115_g    338  TCATTGACAATTCTGACCATCAGCTAACATACTTCTCAGGGCAACCTCATCAACCTCGAG
4115_t    263  -----GCAACCTCATCAACCTCGAG
4115_9A   285  -----GCAACCTCATCAACCTCGAG

4115_g    398  GCCAACTGCCTTTCCATCCCGCTTTAA
4115_t    283  GCCAACTGCCTTTCCATCCCGCTTTAA
4115_9A   305  GCCAACTGCCTTTCCATCCCGCTTTAA

```

Figure 4.36: Sequence alignment of hydrophobin predicted DNA sequence (4115_g), predicted CDS sequence (4115_t) and cDNA sequence (4115_9A) of *C. sphaerospermum* UM 843. The start codon is in box and the intron region shaded in yellow

6061_g	1	-----	ATG	GCCTTCTTCAAGACTCTCCTCATCGCCTCCGTG
6061_t	1	-----	ATG	GCCTTCTTCAAGACTCTCCTCATCGCCTCCGTG
6061_9A	1	-----	CCAACACCTTTAC	ATG GCCTTCTTCAAGACTCTCCTCATCGCCTCCGTG
6061_g	37	GCTGCCGTGCGCTACGCCGCCCCCAGGGTGCCGCTGATGGCAAGACCGAGGTCAACGTC		
6061_t	37	GCTGCCGTGCGCTACGCCGCCCCCAGGGTGCCGCTGATGGCAAGACCGAGGTCAACGTC		
6061_9A	51	GCTGCCGTGCGCTACGCCGCCCCCAGGGTGCCGCTGATGGCAAGACCGAGGTCAACGTC		
6061_g	97	AAGTCCGACGACGCCTCCGCCAAGTGCGGCAACGGCCAGAAGCTTGCCTGCTGCAACAGC		
6061_t	97	AAGTCCGACGACGCCTCCGCCAAGTGCGGCAACGGCCAGAAGCTTGCCTGCTGCAACAGC		
6061_9A	111	AAGTCCGACGACGCCTCCGCCAAGTGCGGCAACGGCCAGAAGCTTGCCTGCTGCAACAGC		
6061_g	157	GCGGAGGACCTCATCGCCTGAACTGCCTGAACATCCCCATCC	GTGAGTTGACCATTTC	
6061_t	157	GCGGAGGACCTCATCGCCTGAACTGCCTGAACATCCCCATCC	-----	
6061_9A	171	GCGGAGGACCTCATCGCCTGAACTGCCTGAACATCCCCATCC	-----	
6061_g	217	CATACCACCGAAAGCGCAACGCTGACAGTGCAACAG	TTGCTGTCCCCATCCAGCAGACCT	
6061_t	200	-----	TTGCTGTCCCCATCCAGCAGACCT	
6061_9A	214	-----	TTGCTGTCCCCATCCAGCAGACCT	
6061_g	277	GCGGCTCCAACGTCGCTGCGTGCTGCCAGACTGGCGACGCCTCCGGCAACCTCATCAACC		
6061_t	224	GCGGCTCCAACGTCGCTGCGTGCTGCCAGACTGGCGACGCCTCCGGCAACCTCATCAACC		
6061_9A	238	GCGGCTCCAACGTCGCTGCGTGCTGCCAGACTGGCGACGCCTCCGGCAACCTCATCAACC		
6061_g	337	TTGAGGCCAACTGCCTTTCCATCCCGCTTTAA		
6061_t	284	TTGAGGCCAACTGCCTTTCCATCCCGCTTTAA		
6061_9A	298	TTGAGGCCAACTGCCTTTCCATCCCGCTTTAA		

Figure 4.37: Sequence alignment of hydrophobin predicted DNA sequence (6061_g), predicted CDS sequence (6061_t) and cDNA sequence (6061_9A) of *C. sphaerospermum* UM 843. The start codon is in box and the intron region shaded in yellow

CHAPTER 5: DISCUSSION

5.1 Fungal collection

During the 5-year period of sample collection, an increase of dematiaceous isolates received in Mycology Unit was observed. However, the prevalence of dematiaceous fungal infections among patients could not be determined because fungal culture is not a routine laboratory procedure and it is only performed on clinician's request. It is not surprising that the skin scraping and nail specimens consist of the largest variety of fungal species as these anatomical sites are frequently exposed to the natural habitats of fungi.

In this study, most of the isolated dematiaceous fungi were previously reported to cause human infections (Table 5.1). In line with the clinical guidelines compiled by the European Society of Clinical Microbiology and Infectious Diseases (ESCMID) and European Confederation of Medical Mycology (ECMM) (Chowdhary et al., 2014), 11 of the 16 dematiaceous fungi genera identified were listed as important disease-causing fungi. These include species of the genus *Alternaria*, *Bipolaris*, *Chaetomium*, *Curvularia*, *Exophiala*, *Exserohilum*, *Neoscytalidium*, *Ochroconis*, *Phoma*, *Pyrenochaeta* and *Rhinocladiella*. Although *Alternaria* has been reported as a common causative agent in fungal infections and hypersensitivity (Pastor & Guarro, 2008), only one isolate was recovered in this study. The species identified in this study, *A. arborescens*, is a rare causative agent as this species has only a recent reported case of causing cutaneous alternariosis in a healthy individual (Hu, Ran, Zhuang, Lama, & Zhang, 2015).

Table 5.1: Reported human infection cases of dematiaceous species

Genus	Species	Case reported by
<i>Alternaria</i>	<i>A. arborescens</i>	Hu et al. (2015)
<i>Chaetomium</i>	<i>C. brasiliense</i>	Hubka, Mencl, Skorepova, Lyskova, & Zalabska (2011)
<i>Cladosporium</i>	<i>C. cladosporioides</i>	As cited in Table 2.1
	<i>C. sphaerospermum</i>	As cited in Table 2.1
<i>Bipolaris</i>	<i>Cochliobolus hawaiiensis</i>	de Hoog et al. (2000), Mikosz et al. (2014)
	<i>B. papendorfii</i> / <i>Cochliobolus geniculatus</i>	da Cunha et al. (2012), de Hoog et al. (2000)
<i>Curvularia</i>	<i>Cochliobolus geniculatus</i> (<i>C. senegalensis</i>)	Chowdhary et al. (2014), de Hoog et al. (2000), Guarro et al. (1999a)
	<i>Cochliobolus lunatus</i>	Carter & Boudreaux (2004), Chowdhary et al. (2014), de Hoog et al. (2000)
	<i>Cochliobolus verruculosus</i>	de Hoog et al. (2000)
<i>Exophiala</i>	<i>E. dermatitidis</i>	Chowdhary et al. (2014), de Hoog et al. (2000), Oztas et al. (2009)
	<i>E. spinifera</i>	de Hoog et al. (2000), Rajendran et al. (2003), Wang et al. (2013)
	<i>E. xenobiotica</i>	Aoyama, Nomura, Yamanaka, Ogawa, & Kitajima (2009), Morio et al. (2012)
<i>Exserohilum</i>	<i>E. rostratum</i>	Andes & Casadevall (2013), de Hoog et al. (2000), Hsu & Lee (1993), Pappas, Kontoyiannis, Perfect, & Chiller (2013), Saint-jean, St-germain, Laferrière, & Tapiero (2007)
<i>Neoscytalidium</i>	<i>N. dimidiatum</i>	Chowdhary et al. (2014), Khan, Ahmad, Joseph, & Chandy (2009), Mani et al. (2008), Tendolkar, Tayal, Baveja, & Shinde (2015)
<i>Ochroconis</i>	<i>O. mirabilis</i>	Samerpitak et al. (2013)
<i>Phoma</i>	<i>P. multirostrata</i>	Singh & Barde (1990)
	<i>P. multirostrata</i> / <i>Epicoccum sorghi</i>	de Hoog et al. (2000)
<i>Phomopsis</i>	<i>Phomopsis sp./Diaporthe articii</i>	Sutton, Timm, Morgan-Jones, & Rinaldi (1999)
<i>Pyrenochaeta</i>	<i>P. unguis-hominis</i>	de Hoog et al. (2000), English (1980)
<i>Rhinocladiella</i>	<i>R. atrovirens</i>	Del Palacio-Hernanz, Moore, Campbell, Del Palacio-Perez-Medel, & Del Castillo-Cantero (1989), Ellis et al. (2007), Rajput, Mehrotra, Srivastav, Kumar, & Rao (2011)

The high number of *Cladosporium* isolates showed that this species is an important fungus encounter in this study. Interestingly, 80% of the fungi isolated from blood specimens were *Cladosporium* species. Of the *Cladosporium* species identified, *C. sphaerospermum* is the most frequent isolate and often recovered from blood samples. The common presence of *C. sphaerospermum* as an airborne fungus has made this fungus being recognised as contaminant rather than the etiological agent (Zalar et al., 2007). Nevertheless, it has been reported that *C. sphaerospermum* can cause infection (Huyan et al., 2012).

Apart from reported pathogenic fungi, 16 isolates from seven species are not known to be associated with human diseases (Table 4.1). These included *Cladosporium dominicanum* and *Curvularia affinis* (from skin scrapings), *Curvularia eragrostidis* (from nails), *Daldinia eschscholtzii* (from blood, skin and nail samples), *Phoma gardeniae* (from skin lesion swab and nails), *Nigrospora oryzae* (from nail and skin scrapings) and *Stagonospora* sp./*S. arundinacea* (from nasopharyngeal secretion and skin scrapings). *C. dominicanum* was reported to live in plant material and hypersaline water (Zalar et al., 2007) while *C. affinis*, *C. eragrostidis* (Ferreira, Pinho, Machado, & Pereira, 2014a), *N. oryzae*, *P. gardeniae* (Gade, Rai, Duran, & Ingle, 2015) and *Stagonospora/Septoria* sp. are known plant pathogens. *C. affinis* is a soil fungus that causes leaf spot disease in plants (Huang, Zheng, & Hsiang, 2004; Sharma, Singh, & Verma, 2012). Unlike *Nigrospora sphaerica* that has been reported to cause onychomycosis (Fan, Huang, Li, & Zhang, 2009) and corneal ulcer (Ananya, Kindo, Subramanian, & Suresh, 2014), *N. oryzae* has been reported to cause stem blight in mustard plants (Sharma, Meena, & Chauhan, 2013) and leaf spots in herb plants (Wu, Zhang, Mao, Qian, & Wang, 2014b). The anamorphs of Phaeosphaeriaceae in the Pleoporales order are mostly saprobes or plant pathogens of herbaceous plants (Zhang,

Crous, Schoch, & Hyde, 2012) with *Stagonospora nodorum* as the most intensively studied plant pathogen that causes disease in wheat (Solomon, Lowe, Tan, Waters, & Oliver, 2006). *Septoria* species represent a plant pathogen genus associated with leaf spots and stem canker (Quaedvlieg et al., 2013).

As these isolates have never been reported to be associated with human infections, it cannot be excluded that the isolates might be contaminants. However, the recovery of these isolates was from symptomatic patients that were suspected to have fungal infections. The skin scraping and nail specimens were examined for fungal elements via direct examination using potassium hydroxide (KOH) under light microscope to confirm the diagnosis. This further strengthens that the isolates are not solely contaminants.

5.1.1 Molecular identification

The internal transcribed spacer (ITS) sequence-based phylogenetic results in this study showed good congruence with morphological identification. Molecular approach enabled the isolates to be identified up to species level.

The ITS region comprising the ITS1, ITS2, and, 5.8S rRNA was selected for molecular determination of a fungus. This region is the most commonly sequenced region for systematics and taxonomy and is widely accepted for species identification in mycology (Nilsson, Ryberg, Abarenkov, Sjökvist, & Kristiansson, 2009). This 500-700 bp region was used as a universal marker due to the ease of this region to be amplified because of the presence of this region in multiple copies in the fungal genome. Also, this region provides sufficient taxonomic resolution for most fungi due to its high interspecific variation combined with low intraspecific variation, and the high number of sequences deposited in public databases such as GenBank

(<http://www.ncbi.nlm.nih.gov>), European Molecular Biology Laboratory nucleotide sequence data (<http://www.ebi.ac.uk/embl/>) and DNA Data Bank Japan (<http://www.ddbj.nig.ac.jp/>). This enables comparison of sequence from an unknown isolate (Balajee et al., 2009).

The inadequate diagnostic expertise of the medical microbiologist and the rarity of fungus recovered from human specimens cause the morphological identification of fungus become difficult (Varga, Houbraken, Van Der Lee, Verweij, & Samson, 2008). Laboratory technicians will only familiar and able to identify fungal species commonly isolated from samples. When encounter with a rare fungal species, the use of molecular technique will reveal the identity of the fungus and the technician may cross-examine the morphological characteristics of the fungus to confirm its identity.

The use of molecular techniques to determine the identity of mycelia sterilia and isolates with unidentifiable cultural characteristics (as shown in Figure 4.5) would enable accurate diagnosis and treatment to the patient. This is also especially helpful for the fungi with similar microscopic features. For instance, the species *Phoma* and *Pyrenochaeta* are two coelomycetes having fruit bodies known as pycnidia and produce hyaline conidia (Figure 5.1). Their pycnidia, conidia and cultural characters are very similar (de Gruyter et al., 2010; Revankar & Sutton, 2010). The isolate UM 256 was initially misidentified as *Phoma* sp. due to the overlapping characters and the identity was confirmed as *Pyrenochaeta unguis-hominis* via the ITS sequencing. Some fungal species may appear in a different form known as synanamorph. In the Chaetothyriales order, the *Exophiala* synanamorph of *Rhinocladiella* was observed in strain UM 212 and UM 234. Thus, the molecular approach is a better option for their identification (Arzanlou et al., 2007; de Hoog et al., 2011).

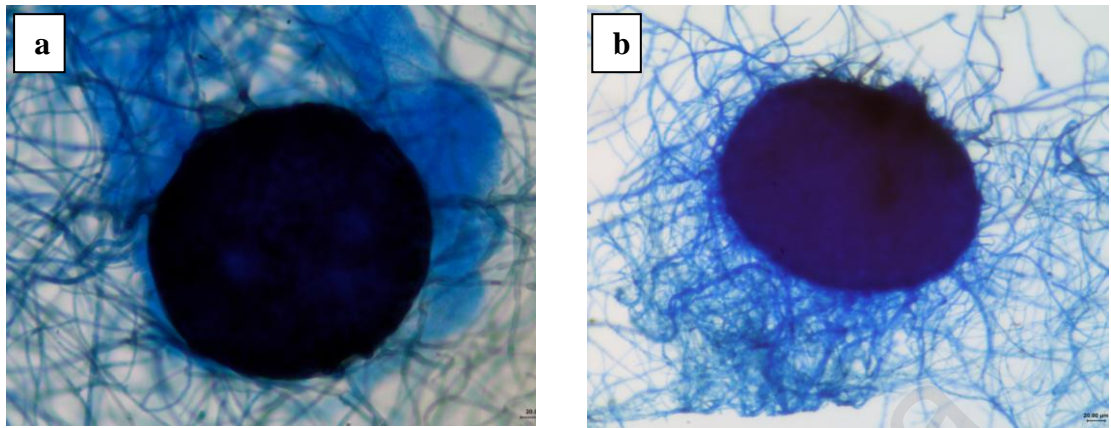


Figure 5.1: Micrograph of the *Pyrenochaeta* (a) and *Phoma* (b) pycnidia

In the phylogenetic analysis, most of the *Bipolaris* and *Curvularia* species were identified molecularly as *Cochliobolus*. *Cochliobolus* is a pleomorphic fungus having both the *Bipolaris* and *Curvularia* as its anamorph (Manamgoda et al., 2012). Even though the morphology of *Bipolaris* and *Curvularia* species are distinguishable, some of the isolates were shown to have intermediate morphology. Recent molecular studies revealed that the *Bipolaris* species cluster in several clades, with some of the *Bipolaris* species, showed to form a cluster within the *Curvularia* subgroup (Manamgoda, Cai, Bahkali, Chukeatirote, & Hyde, 2011).

Nevertheless, the ability to identify a fungal species using molecular technique is dependent on the deposition of fungal sequences into the public databases, where the identity is dependent on morphological examination. Two isolates were not identified to the genus or species level by the ITS sequence analysis due to the lack of information in the current GenBank database (Ryberg, Kristiansson, Sjökvist, & Nilsson, 2009). In addition, eight species identity were unresolved. The unresolved identity of isolates may be improved by conducting more extensive sampling and using multi-locus phylogeny. For instance, UM 226 which was identified as *Bipolaris papendorffii*/ *Cochliobolus*

geniculatus was further confirmed as *B. papendorfii* using multi-locus phylogeny comprising large subunit (LSU)- small subunit (SSU)-ITS sequences (Kuan et al., 2015). It should also be noted that the reliability of the deposited sequences in the database also influences the identification of isolates.

As fungal taxonomy is progressing, this may lead to changes in the naming of fungi and the introduction of new fungal species. The taxonomy of *Ochroconis* has been suggested to be placed within Chaetothyriales order (Revankar & Sutton, 2010) or as unclassified anamorphic ascomycetes (Lian & de Hoog, 2010). Until recently, this genus has been re-classified into the Pleosporales order in the family Sympoventuriaceae (Machouart, Samerpitak, de Hoog, & Gueidan, 2013) by multi-locus phylogenetic analysis comprised of mitochondrial small subunit (mtSSU), nuclear large subunit (nuLSU), RNA polymerase II (RPB2) region 5-7 and RPB2 region 7-11 sequences. In the study by Samerpitak et al. (2013), nine new species have been introduced into the *Ochroconis* genus from the original of four species, and the thermophilic oligotrophs *O. gallopava*, *O. verruculosa* and *O. calidifluminalis* have been suggested to a new genus *Verruconis*. By employing the reported new classification, UM 314, UM 324, UM 326 and UM 329 were re-classified as *O. mirabilis* (Yew et al., 2016).

As *C. sphaerospermum* had the largest number of isolates and mostly recovered from blood specimens, a *C. sphaerospermum* strain, UM 843 was subjected to genome sequencing.

5.2 *C. sphaerospermum* UM 843

5.2.1 Morphological description and phylogenetic analysis

Prior to whole genome sequencing, the isolate UM 843 was subjected to detail characterisation to affirm its identity. The presence of a scar, also known as hilum at the end of conidia and ramoconidia is one of the characteristics of *Cladosporium* species (Schubert et al., 2007). Ramoconidia (Figures 4.7 d1 and d3) are conidia with more than one conidial hilum which typically accumulated at the tip of these conidia. The colony and microscopic features of UM 843 were concordant with reported description of this species (Zalar et al., 2007). The characteristics of coronate conidia under scanning electron microscope (SEM) (Figure 4.7f) correlated with the finding of David (1997) as described by Dugan et al. (2004). Zalar et al. (2007) reported that the morphology of *Cladosporium halotolerans* strongly resembles that of *C. sphaerospermum* with a subtle difference. The *C. halotolerans* has verrucose ornamented conidia while *C. sphaerospermum* has slightly verruculose ornamented conidia. The UM 843 verruculose ornamentation of conidia and ramoconidia corresponded to the morphology of *C. sphaerospermum* were observed (Figure 4.7g). In addition, the clustering of UM 843 with *C. sphaerospermum* clade (Figure 4.11) further strengthened the identity of UM 843 as *C. sphaerospermum*. With the combination of morphological and molecular approach, the identity of UM 843 was ascertained.

5.2.2 *C. sphaerospermum* UM 843 genome

As shown in Table 4.4 and 4.5, the high percentage of usable clean reads indicates that the sequencing processes are good. The use of different insert size libraries has been reported to improve genome assembly (Ekblom & Wolf, 2014; van Heesch et al., 2013). Particularly, the use of mate-pair library significantly improves *de novo* assembly, as

the method could reduce gap regions and extend scaffold length by establishing long-range continuity (Henson, Tischler, & Ning, 2012; Liu et al., 2012).

5.2.2.1 Transposable elements

Transposable elements are one of the interspersed repeats that able to move about in the genome and to insert into another region of the host's DNA. By studying the diversity of transposable elements present in a genome, it would provide an understanding on the evolution, genetic diversity and stress adaptation of the fungus (Amyotte et al., 2012; Chadha & Sharma, 2014). The Gypsy and Copia elements of class I retrotransposons are the most abundant transposable elements in fungal genomes whereas the Tc1-Mariner is the most abundant class II DNA transposons (Santana & Queiroz, 2015). The largest number of Gypsy element predicted in UM 843 (Table 4.7) corroborated with previous findings. The large number of hAT superfamily of class II elements in UM 843 (Table 4.7) also corroborated with previous findings that this family is well represented in Ascomycetes and Basidiomycetes (Fávaro, Araújo, Azevedo, & Paccola-Meirelles, 2005). The Crypton element is a rare transposable element that was originally identified in *Cryptococcus neoformans* (Goodwin, Butler, & Poulter, 2003). To date, only eleven fungal species containing this element have been identified (Goodwin et al., 2003; Kojima & Jurka, 2011) and UM 843 is the only Dothideomycetes so far predicted to contain this element.

It should be noted that owing to the limitation of Illumina technology, the predicted transposable elements identified in this isolate may be underrepresented (Ohm et al., 2012). This is due to the difficulties in the assembly of short repetitive reads into long repeat regions. However, the availability of such data provides an idea of the type of

transposable elements present in the genome and enables the design of the best strategy for sequencing the whole genome (Li et al., 2014).

5.2.2.2 Primary functional annotation

Among the types of metabolism, carbohydrate metabolism has the highest number of genes being annotated in Eukaryotic Orthologous Group (KOG) and Kyoto Encyclopedia of Genes and Genomes (KEGG) (Figures 4.15a and b). As carbon source is an essential nutrient for fungal growth, conidiation, and virulence (Safavi et al., 2007; Shah, Wang, & Butt, 2005), it is not surprising that UM 843 contained a high number of genes involved in carbohydrate metabolism. The monocarboxylate transporters in group G of KOG are required in the transportation of monocarboxylates across the plasma membrane into the cell. Monocarboxylates such as pyruvate and lactate play important roles in energy utilisation, intracellular pH regulation and virulence in certain pathogenic fungi (Cássio, Côrte-Real, & Leão, 1993; Cui et al., 2015; Jin et al., 2010).

Posttranslational modifications of proteins are important in cellular regulation, development and adaptation to stress (Leach & Brown, 2012). Chaperones are associated with stress adaptation, directory of misfolded proteins to degradation via the ubiquitin-proteasome system, regulatory degradation of metabolic enzymes and cell viability (Glover & Lindquist, 1998; Imai, Yashiroda, Maruya, Yahara, & Tanaka, 2003; Leach & Brown, 2012; Lim et al., 2010). Meanwhile, signal transduction plays a major role in responding to external stimuli whereby changes in the external environment can trigger an appropriate cellular response (Alonso-Monge, Román, Arana, Pla, & Nombela, 2009; Zhao et al., 2007).

In KEGG, the pathways involved in xenobiotic degradation and metabolism has the fifth highest number of genes. The distribution of Gene Ontology (GO) genes related to osmotic stress (Figure 4.15c) might be reflective of the habitats of *C. sphaerospermum* in which the fungus has to combat with osmotic imbalance (Zalar et al., 2007). All these proteins work in concert to provide the fungus the response and adjustment in cellular conditions to live in the fluctuating environment.

5.2.2.3 Carbohydrate metabolism

The presence of all CAZyme families required to degrade plant cell wall ensures the complete degradation of these components by UM 843 (Table 4.8). The larger number of CAZymes responsible for hemicellulose and pectin degradation in UM 843 suggests the preference of this fungus towards soft plant tissues such as flower and fruit (Amselem et al., 2011), as reported in *R. oryzae* (Battaglia et al., 2011).

The CAZymes of families GH55, GH64 and GH81 exhibit β -1,3-glucanase activity that acts on β -1,3-glucan, the primary substrate of fungal cell wall and plant cell wall callose (Zhao et al., 2014). UM 843 was observed to have more abundant CAZyme of the GH64 family, which is similar to other Capnodiales (Ohm et al., 2012) (Appendix D4). In addition, the lower number of CAZymes involved in cellulose degradation in UM 843 is similarly seen in other Capnodiales species (Ohm et al., 2012). The GH94 family, which was absent in UM 843, is reported to encode carbohydrate phosphorylase involved in cellulose degradation (O'Neill & Field, 2015). Nevertheless, the high number of CBM1 (11) in UM 843, compared to the other members of Capnodiales, may assist in the degradation of cellulose. CBM1 has been shown to be able to disrupt the crystalline structure of cellulose by non-hydrolytic cleavage of inter- and intra-hydrogen bonds of polysaccharide chains, besides aiding cellulases in contact between

the substrate and catalytic domain (Banka, Mishra, & Ghose, 1998; Xiao, Gao, Qu, & Wang, 2001). The weakened cellulose structure allows easy accessibility of other enzymes such as hemicellulolytic enzymes to carry out catalytic reactions. The GH10 and GH11 display xylanase activity in the degradation of hemicellulose of the xylan (van den Brink & de Vries, 2011) whereas PL1 and PL3 display pectate lyases activity involve in pectin degradation of the polygalacturonan (Garron & Cygler, 2010).

A comparison of CAZymes in UM 843 with other dematiaceous Dothideomycetes was conducted to correlate the possible lifestyles of UM 843 (Figures 4.16 and 4.17). However, no conclusive inference can be drawn that UM 843 belongs to the saprophytic group. Zhao et al., (2014) revealed that saprophytic fungi lack CAZyme families CE11, GH73, GH80 and GH82. This was observed in UM 843 that suggested it to be a saprophyte. Therefore, the presence of large CAZyme families in this fungus, together with the observation by Zhao et al. (2014), suggests the possible lifestyle of UM 843 as a saprophyte in nature.

The study by Zhao et al. (2014) has also correlated the absence and reduction of certain CAZyme families such as GH16, GH78, PL1, PL3, GH76, CBM1 and CBM18 families to the biotrophic lifestyle of fungi. However, the lower number of PL1, PL3, CBM18 and CBM1 is shown to be more related to the taxonomic division as reported by Ohm et al. (2012) (Appendix D4). Thus, the taxonomic classification of a fungus should be taken into consideration in correlating the lifestyle of a fungus with the abundance of CAZymes.

5.2.2.4 Peptidases

Similar to the abundance of CAZymes (Section 4.2.3.3), the broad spectrum of peptidases in UM 843 without any predominance of any particular family is consistent with the saprophytic nature of fungi (St Leger et al., 1997) (Figure 4.18). The peptidases act synergistically to digest proteins into amino acids and oligopeptides which are then assimilated via membrane transporters into the cells.

The small size ($2\text{-}5 \times 2\text{-}4 \mu\text{m}$) *C. sphaerospermum* conidia are easily disseminated and found in indoor and outdoor air (Knutsen et al., 2012). Thus, the conidia may be inhaled by humans to reach lung alveoli. The tropism of *C. sphaerospermum* towards lungs (Huyan et al., 2012) leads to the postulation of peptidases involved in lung tissue hydrolysis which enables the fungus to degrade the complexes present in the niche. Studies have suggested that hyphal penetration through protein-rich tissue layers and vessels walls containing elastin and collagen might be achieved by simple mechanical forces, strictly localised proteolysis brought by fungal cell wall-associated proteinases, or by more generalised proteolysis caused by proteinases secreted from the fungal hyphae (Reichard, Cole, Ruchel, & Monod, 2000). Referring to Table 4.10, the secreted aspartic endopeptidases (UM843_1326 and UM843_4966) similar to the family A01 peptidase F was reported to involve in the hydrolysis of lung components elastin and laminin (Lee & Kolattukudy, 1995) while cell wall associated aspartic peptidase (UM843_5823) facilitates the penetration of young hyphae into the connective tissue (Reichard et al., 2000; Reichard, Monod, Odds, & Ruchel, 1997). Moreover, metallopeptidase M36 hydrolyses the elastin (Markaryan, Morozova, Yu, & Kolattukudy, 1994). The secreted serine peptidase DPPIV facilitates colonisation of the lung by binding to the collagen and subsequently degrading the dipeptide of collagen, whereas DPPV is the elicitor of host defence mechanisms (Beauvais et al., 1997a;

Beauvais et al., 1997b). Both the predicted DPPIV and DPPV have the conserved predicted catalytic sites with other reported DPPs (Figures 4.19 and 4.20). These peptidases might work in concert to disrupt lung tissues. However, previous *in vivo* experiments have found no loss of virulence in enzyme-negative mutants of *A. fumigatus* (Monod et al., 2002) which may be due to the presence of cross-reacting peptidases conducting the similar function (Sriranganadane et al., 2011). The functions of these peptidases in pathologic behaviour thus remain to be elucidated.

5.2.2.5 Secondary metabolites

C. sphaerospermum has been demonstrated to synthesise DHN-melanin where the fungus in medium containing tricyclazole, the DHN-melanin biosynthesis inhibitor produced melanin-deficient colony (Dadachova et al., 2007). The gene UM843_1729 matched to both *alb-1* from *A. fumigatus* (Tsai et al., 2001) and *C. phlei cppks1* (So et al., 2012) that has been reported to be responsible for pigment synthesis. The gene contains a SAT domain (PF16073), which is typical of non-reducing PKS (Huitt-Roehl et al., 2015). The domain arrangement of UM843_1729 was similar to the PKS involved in melanin biosynthesis (Kroken et al., 2003). The gene organisation of melanin PKS cluster in UM 843 was similar to that of *C. heterostrophus* and *A. brassicicola* DHN-melanin cluster (Eliahu, Igbaria, Rose, Horwitz, & Lev, 2007), but in different gene orientation and organisation (Figure 4.21). The presence of two *yg-1* genes in UM 843 (Table 4.12) suggests that the synthesis of DHN-melanin may involve an additional polyketide precursor post-modification step as reported in *E. dermatitidis* and *A. fumigatus* (Tsai et al., 2001; M. H. Wheeler et al., 2008).

The domain arrangement of NRPS UM843_7306 was similar to that of *A. fumigatus* SidD responsible for fusarinine-type siderophore biosynthesis (Schrettl et al., 2007).

The presence of different neighbouring genes in UM 843 (Figure 4.22) compared to other reported gene clusters may be due to rearrangement during genome evolution and speciation (Kragl et al., 2007; Schrettl, Winkelmann, & Haas, 2004b; Schrettl et al., 2008; Yuan, Gentil, Budde, & Leong, 2001). Also, UM843 lacks the orthologue of *sidG* gene that is involved in the synthesis of TAFC. In fungi, *sidG* is only found in *A. fumigatus*, *A. nidulans*, *A. clavatus*, *A. oryzae* and *Giberella zeae* (Haas et al., 2008; Schrettl et al., 2007). Thus, this fungus may synthesise only fusarinine C, the precursor of TAFC.

Ferrichrome-type NRPSs have a diversity of domain architectures consisting of two to four complete A-T-C modules which are usually followed by a T-C repeat (Haas et al., 2008). Compared to the ferrichrome-type NRPS NPS2 of *C. heterostrophus*, the UM843 NRPS has one adenylation domain less than NPS2. The predicted cluster of ferrichrome-type biosynthesis genes is similar to that of *C. heterostrophus* (Haas et al., 2008) (Figure 4.23).

Siderophore transporter MirB has been reported to be involved in the transportation of TAFC in *A. nidulans* but the function of MirC is unknown (Haas et al., 2003). A gene encoding an esterase EstB (UM843_1515) involved in the hydrolysis of TAFC was identified next to the *mirB* gene (UM843_1516) (Figure 4.24). Hence, UM 843 may utilise TAFC produced by other fungi despite its inability to produce TAFC. The Sit1/Arn3 transporter has been reported to facilitate the transportation of ferrioxamine B in *S. cerevisiae* (Yun et al., 2000) and *C. neoformans* (Tangen, Jung, Sham, Lian, & Kronstad, 2007). The possession of multiple siderophore transporters reflects the ability of UM 843 to utilise different types of siderophores, including xenosiderophores for iron uptake (Table 4.13).

Iron regulation is carried out by iron-responsive GATA factors (IRGFs), Hap-X and CCAAT-binding complex in the function of iron availability (Franken et al., 2014; Schrettl et al., 2008). The putative IRGF, UM843_1371 possessed the common characteristics of fungal IRGFs (Haas, Angermayr, & Stöffler, 1997) (Appendix D5). The presence of GATA binding elements upstream of the siderophore synthesis genes (Appendix D6-D8) further strengthens the predicted function of the genes as IRGFs recognise and bind to *cis*-acting binding elements HGATAR and modified ATCWGATAA sequences in genes involved in iron regulation (Hwang, Seth, Gilmore, & Sil, 2012; Schrettl et al., 2008). Collectively, the concerted action of potential transcriptional regulatory elements, along with their targeted genes that are orchestrated in the cluster could play a role in the biosynthesis of siderophore.

Recently, an isolate of *C. sphaerospermum* was reported to synthesise polyketide hybrid cladosins such as Cladosin C showing mild antiviral activity (Wu et al., 2014a; Yu, Wu, Zhu, Gu, & Li, 2015). However, the synthesis pathway of cladosins has not been studied. As UM843_7284 is the only PKS-NRPS hybrid identified in the genome (Table 4.11), this gene might be involved in cladosins synthesis. The genes identified in the predicted cluster of PKS-NRPS hybrid may be associated with the synthesis and transport of the product (Table 4.14).

5.2.2.6 Stress responses

The pre-adaptation that fungi harbour from the external environment may serve to withstand pressures and survival in animal hosts, as the host represents an extreme condition for the fungi (Cooney & Klein, 2008). Thus, the presence of genes responsible for heat and oxidative stresses may provide an advantage for UM 843 to survive in the host. The heat shock proteins function to stabilise the membrane and

proteins and ensure correct folding of proteins to function (Brown et al., 2014). Five heat shock proteins were identified in the UM 843 genome, namely, genes encoding Hsp78, Pss1, Hsp104, Hsp80 and Hsp70 (Appendix D9). Enzymes such as superoxide dismutase (SodA), catalase (Cat-1, Cat-2 and Cat4), laccase (Lcc1) and thioredoxin reductase (TrxR) shown in Appendix D11 may protect the fungus the killing effect of ROS produced by phagocytic cells (Dantas et al., 2015).

In order to be able to live inside the animal host, fungi have to adapt to the low nutrient in the host. Fungi, such as *C. neoformans* are able to utilise proline, a multifunctional amino acid as nitrogen or carbon source (Lee et al., 2013). In *A. nidulans*, the proline catabolism-associated genes form a cluster (Cubero, Gómez, & Scazzocchio, 2000), while the genes are dispersed in *C. neoformans*. Overall, UM 843 has the potential to catabolise proline with a different arrangement of genes (Figure 4.25) compared to the two species.

The presence of genes involved in reductive iron assimilation (RIA) suggests that UM 843 may employ another high-affinity iron acquisition system, apart from the siderophores. The ferroxidase and iron permease-encoding gene cluster is also found in other fungi (Haas et al., 2008) and the presence of GATA binding element in the upstream of these genes (Appendix D12) strengthen the functionality of the genes.

(a) ***Response to high salinity***

UM 843 was observed to have more genes encoding Ena (4) than Nha1 (2) (Table 4.16). This may render the capability of this fungus to survive in the near neutral to alkaline pH of a hypersaline environment. Ena is important in the export of Na⁺ ions at alkaline pH (Bañuelos, Sychrová, Bleykasten-Grosshans, Souciet, & Potier, 1998).

Notwithstanding, Nha1 is also required by the fungus as this gene is essential for the immediate response to osmotic shock (Proft & Struhl, 2004).

Comparative analysis in Table 4.16 showed that UM 843 contained more *trk*, *tok*, *ena* and *pho89* genes compared to *M. graminicola* despite it has lesser genes compared to *H. werneckii*. *H. werneckii* was reported to have undergone recent whole genome duplication (Lenassi et al., 2013), thereby confers a large set of genes. The Pho89 is proposed to facilitate the uptake of phosphate under alkaline pH where the H⁺ gradient cannot efficiently energise the phosphate import (Lenassi et al., 2013). Interestingly, the genes encoding K⁺(Na⁺)-ATPase (alkali cation uptake, Acu transporters) and K⁺-H⁺ symporter (Hak symporters) were found in UM 843 but absent in *H. werneckii*. The presence of these transporters might be an advantage for the fungus to adapt to a hypersaline environment owing to its high affinity for K⁺ ions uptake (Benito et al., 2011). However, UM 843 does not contain vacuolar *vnx1* genes for Na⁺, K⁺/H⁺ exchange, but has six genes encoding Ca²⁺, K⁺/H⁺ antiporter Vcx1 (Appendix D13). The presence of vacuolar Vcx1 would facilitate the maintenance of cytosolic K⁺ in the vacuole (Cagnac, Aranda-Sicilia, Leterrier, Rodriguez-Rosales, & Venema, 2010). Studies have shown that the halotolerant species, *H. werneckii* and *W. ichthyophaga*, use different strategies to counteract high salinity (Lenassi et al., 2013; Zajc et al., 2013). The diversity of cation transporters found in UM 843 demonstrates the possibility that this fungus uses strategies in response to dynamic changes in salinity that are different from those employed by *H. werneckii* and *W. ichthyophaga*.

The genome also indicates the ability of UM 843 to synthesise glycerol, mannitol, arabitol and trehalose as compatible solutes (Table 4.17). Glycerol is produced by the reaction of NAD-dependent glycerol-3-phosphate dehydrogenase (Gpd) and glycerol-3-

phosphate phosphatase (Gpp) on the glycolysis intermediate dihydroxyacetone phosphate. Mannitol is produced via reduction of fructose by NADP-dependent mannitol dehydrogenase while arabitol is synthesised via reduction of D-ribulose-5-phosphate by D-arabinitol-2-dehydrogenase (Zajc et al., 2013). The absence of peroxisomal targeting signal type 2 (PTS2) in UM 843 putative *gpd* gene which is similar to the *H. werneckii* and *W. ichthyophaga gpd* (Figure 4.28) suggests the ability of this fungus to survive in high salinity environments (Lenassi et al., 2011). The production of taurine by UM 843 might be used as osmoregulant, which has been proposed in the acidophile *Acidomyces richmondensis* (Mosier et al., 2013).

The large number of sugar/H⁺ symporters and aquaglyceroporins present in UM 843 suggest that this fungus might act rapidly to a highly dynamic concentration of external NaCl. The glycerol/H⁺ symporter with the typical characteristic of 12 transmembrane domains (Appendix D16) function to import glycerol into the cell actively under hyperosmotic shock (Ferreira et al., 2005). In contrast, the aquaglyceroporin was reported to be involved in the efflux of glycerol when the fungus under hypoosmotic shock.

The UM 843 Hog1 is similar to that of Hog1 of other fungi, containing both the conserved TGY phosphorylation motif and common docking domain (Figure 4.29). The common docking domain YHDP[T/S]DEP motif with negatively charge amino acids (underlined) is critical for the interaction of mitogen-activated proein kinase (MAPK) with downstream effectors (Lenassi, Vaupotic, Gunde-Cimerman, & Plemenitas, 2007). As a result from the activation of high osmolarity glycerol (HOG) signalling pathway, several responses that lead to osmotic adaptation such as the regulation of *still*, *nha1*, *tok1* and *ena1* expression and the synthesis of glycerol via activation of *gpd1*, are

activated (Proft & Struhl, 2004; Proft et al., 2006). HOG also regulates Pmp3 that is responsible for cationic stress response by modulating the cell membrane potential (Wang & Shiozaki, 2006). Altogether, the mediation of salt tolerance in UM 843 might involve the activation of the HOG signalling pathway, regulation of transporters and synthesis of various compatible solutes.

5.2.2.7 Sexual reproduction

As listed in Appendix D17, most of the genes involved in sexual reproduction were identified in UM 843. Only one mating type gene was identified in the genome, thus, isolate UM 843 might be a heterothallic fungus, which is different from all the known teleomorph of *C. herbarum* species complex (Schubert et al., 2007). Besides that, the presence of *apn2* and *cox13* genes near the *mat1-2* gene (Figure 4.30) is also found in fungi from Eurotiomycetes such as *Aspergillus*, *Coccidioides*, *Histoplasma* (Fraser et al., 2007) and dermatophytes (Burmester et al., 2011), and in the *O. mirabilis* UM 578 (Yew et al., 2016), with differences in gene content and organisation. However, no pheromone gene was identified in UM 843. As pheromone is required to activate the pheromone receptor that leads to activation of G protein complex to initiate Fus3 MAPK signalling pathway which subsequently causes stimulation of genes involve in mating and cell cycle (Jones & Bennett, 2011), this indicates that UM 843 might not be able to carry out mating process. Nevertheless, *C. neoformans* has been shown to undergo sexual reproduction without ligand activation of the pheromone response pathway (Hsueh, Xue, & Heitman, 2009). Therefore, UM 843 may still possesses the ability to carry out sexual reproduction without pheromone activation.

5.3 Phylogenomic analysis

The placement of UM 843 in the Capnodiales order in Figure 4.31 is congruent with previous single gene based phylogenetic analysis (Section 5.2.1). The genome-based phylogenetic analysis provides a more accurate evaluation of the relationships as more information is used in generating the result (Nishida, Beppu, & Ueda, 2011). However, the number of fungal genomes available in public data sets the limitation of this powerful tool in the identification of UM 843 into a lower taxonomy level.

5.3.1 Orthologous genes and genome comparative analysis

The MAPK Spk1 (Fus3/Kaa1 orthologue) is important in the pathogenicity of certain plant pathogenic fungi, sexual/asexual reproduction, hyphal growth, conidial germination and pigment synthesis (Eliahu et al., 2007; Zhao et al., 2007). However, the typical T-X-Y motif in the activation loop of MAPK was absent in the predicted genes of UM 843, which suggests that these genes are putative atypical MAPK. Eight atypical MAPKs have been reported in the wheat scab fungus *Fusarium graminearum* (Wang et al., 2011). However, the exact role of these proteins remains to be elucidated.

5.4 Fungal allergens

The 28 putative genes with >50% identity to known allergens indicate a high potential for cross-reactivity in patients sensitised with these fungal allergens (Appendix D19), despite the fact that not all these genes encode allergenic proteins. The comparison of allergen genes across Dothideomycetes revealed UM 843 having a higher copy number of genes encoding allergens Cla h 10, Cla h HCh 1, Asp f 23 and Cand a 1, with Cla h HCh1 only found in UM 843 (Table 4.18). The allergen Cla h HCh1 encodes hydrophobin, a class of small secreted protein with low sequence similarity between species. The important characteristic of hydrophobin, i.e. the

conserved pattern of eight cysteine residues which is involved in the formation of four disulphide bridges (Bayry, Aimanianda, Guijarro, Sunde, & Latgé, 2012), is shown in Figure 4.32.

The study of Weichel et al. (2003) showed that the hydrophobin Cla h HCh1 from *C. herbarum* was the only protein that elicited a specific IgE-dependent allergic reaction; the homolog of this allergen, HYP1 from *A. fumigatus* with 28% identity to Cla HCh1, did not trigger an allergic reaction. However, no further characterisation of this protein on its allergenicity has been reported after the study. Hence, study on these putative hydrophobin allergenicity would be of great interest as it might be a *Cladosporium*-specific allergen.

5.5 Validation of gene sequences and detection of mRNA

As Cla HCh1 might be a potential allergen biomarker for diagnosis of *Cladosporium*-specific allergy, sequence validation and mRNA detection of the genes were conducted to check whether the genes were expressed. All the genes were successfully amplified and were expressed (Appendix D20-D25). In addition, the alignment of the sequences showed identity to the predicted coding DNA sequences (CDS), indicating the merit of the genome assembly.

5.6 Recommendations for future studies

This thesis studies the genome content of a *C. sphaerospermum* isolate which provides basic biology of this fungus. There are plenty of future projects can be performed for this study. For instance, UM 843 may synthesise the bioactive compound cladosins that has antiviral activity. Detection and characterisation of the bioactive compound cladosins in culture can be conducted via high performance liquid chromatography and isolate the compound via chromatography method.

In this study, UM 843 was shown able to grow at a high concentration of NaCl (20% w/v). The result is comparable with the genomic analysis that UM 843 harbours various genes encoding transporters confer to the ability of UM 843 to survive in high salinity environment. Comparative genomic analysis with the genomes of halotolerant *H. werneckii*, halophilic *W. ichthyophaga*, and non-halotolerant *M. graminicola* further demonstrated that UM 843 possibly uses different strategies in response to dynamic changes in salinity. Further studies may be conducted by performing differential high throughput sequencing of transcriptome to search for genes that are differentially expressed between conditions to validate the predicted genes involved in osmoregulation are functional. By comparing the expression of genes under two conditions, additional genes that showed changes in expression may be discovered. This would give a complete picture on how the regulation in salt environment is carried out by this fungus. Phenotype profiles of the isolate may also be done using a Biolog phenotypic microarray to examine the utilisation of nutrient sources and adaptation of this isolate to the ranges of osmotic and pH environments.

CHAPTER 6: CONCLUSION

In this study, a total of 75 dematiaceous fungal isolates were recovered from various clinical sites, including dermatological specimens, tissues, and blood. The identification of dematiaceous fungi is traditionally based on the observation of differentiating morphological structures, including the differentiation of conidiophores, septation of macroconidia, the presence or absence of collarettes on adelophialides. The main challenge in managing fungal infections is the lack of fast-accurate fungal identification. The lack of familiarity in dematiaceous infection among clinicians in Malaysia coupled with the inadequate sensitivity and specificity tests make these black mould difficult to be rapidly identified. In this work, a total of 30 species from 16 genera were identified using integrated morphological-molecular approach. The molecular test can reduce diagnostic uncertainty enough to make optimal decision for subsequent clinical management.

The ubiquitous presence of dematiaceous fungi in the environment makes it very difficult to gauge their clinical significance when they are isolated from patient samples. The majority of isolates in this study are not contaminants or colonisers as all isolates were from symptomatic patients, most of whom had a physician's diagnosis of fungal infection or were started on antifungal therapy. Although there are 16 isolates (from seven species) not reported to be involved in human disease, but they may be emerging pathogens to cause real infection. In addition, their positive cultures correlated well with signs of fungal proliferation or tissue invasion under direct potassium hydroxide (KOH) microscopic examination. However, at this stage of knowledge, the pathogenic role(s) of these fungi in human infections remains unknown, although it is believe that they are low-virulence human pathogen.

The study reported increased isolation of *Cladosporium sphaerospermum* from blood specimens in the Universiti Malaya Medical Centre (UMMC), a tertiary hospital in Kuala Lumpur, the capital of Malaysia from 2006 to 2011. This evidence suggests an increasing of *C. sphaerospermum* isolation trend in human in Malaysia. *C. sphaerospermum* was thus used as a fungal model for this study to elucidate its basic biology and provide a valuable platform for future fungal research.

In this study, a high-quality draft genome sequence of *C. sphaerospermum* was successfully generated. This is the first genome assembly of *C. sphaerospermum*, which allows comparative genomic analyses to be carried out. The genomic analysis in this study has uncovered the underlying genes that might contribute to the biology and lifestyle of UM 843. The 26.89 Mb genome of UM 843 was predicted to have a rare Class II DNA transposons Crypton element, which currently only found in eleven fungi. Study of the genome revealed UM 843 is a heterothallic fungus which may reproduce sexually in the field. The diversity of carbohydrate-active enzymes (CAZymes) and peptidases in the genome suggests the ecological role of UM 843 as a saprophyte, enabling this fungus to degrade various types of complexes available in the environment as a nutrient source. The classification of CAZymes based on substrate specificity proposed predominance towards hemicellulose and pectin components of plant cell wall. This non-specialised pattern of enzymes present in the genome would also allow the fungus to cause opportunistic infection, as shown by the presence of lung tissue hydrolytic peptidases. UM 843 contains genes that shared similarity to *Aspergillus* peptidases responsible in the degradation of lung components such as the aspartic peptidases (A01 family), metallopeptidases (M36 family) and dipeptidyl peptidases (S09 family). Given that the conidia of *C. sphaerospermum* can easily reach the lungs, the presence of these peptidases suggests the capability of this fungus in causing lung

tissues damage. Nevertheless, further studies on the function of these putative genes are required to reveal their role.

UM 843 encodes an array of secondary metabolites such as 1,8-dihydroxynaphthalene (DHN)-melanin, fusarinine- and ferrichrome-type siderophores, and cladosins. The DHN-melanin would protect the fungus from extreme conditions while the siderophores, together with the reductive iron assimilation (RIA) system regulate the iron uptake in UM 843. The hybrid polyketide synthase-non ribosomal peptide synthase (PKS-NRPS) cladosins isolated recently showing antiviral activity would be a new drug for treatment. The genome of UM 843 allows targeted experimental study on the biosynthesis of cladosins. The presence of genes enables adaptation towards various stresses such as heat stress, oxidation stress and nutrient depletion may aid in the survival of UM 843 in hosts. Also, the ability of UM 843 to grow under high salinity medium might be contributed by the cation transporters identified in the genome. The comparison of cation transporters in UM 843 with the other halophilic fungi showed that UM 843 may harbour different strategies to combat with high salinity condition.

Genome search on allergenic proteins revealed 28 genes are likely able to cross-react. The comparison of the UM 843 genome with the 22 Dothideomycetes genomes revealed genes unique to UM 843, i.e. the class I hydrophobin. The genes were found matched to the allergen Cla h HCh 1 produced by *Cladosporium herbarum*, showing the potential of this protein to be *Cladosporium*-specific allergen. Validation of the gene sequences and detection of the mRNA products showed that the genes are expressed. This indicates the potential of the genes to be functional and as a candidate for *Cladosporium*-specific allergen marker.

REFERENCES

- Aalberse, R. C. (2000). Structural biology of allergens. *The Journal of Allergy and Clinical Immunology*, 106(2), 228–238.
- Aalberse, R. C., Akkerdaas, J., & van Ree, R. (2001). Cross-reactivity of IgE antibodies to allergens. *Allergy*, 56(6), 478–490.
- Abad, A., Fernández-Molina, J. V., Bikandi, J., Ramírez, A., Margareto, J., Sendino, J., ... Rementeria, A. (2010). What makes *Aspergillus fumigatus* a successful pathogen? Genes and molecules involved in invasive aspergillosis. *Revista Iberoamericana de Micología*, 27(4), 155–182.
- Abadio, A. K. R., Kioshima, E. S., Teixeira, M. M., Martins, N. F., Maigret, B., & Felipe, M. S. S. (2011). Comparative genomics allowed the identification of drug targets against human fungal pathogens. *BMC Genomics*, 12, 75.
- Abascal, F., Zardoya, R., & Posada, D. (2005). ProtTest: selection of best-fit models of protein evolution. *Bioinformatics*, 21(9), 2104–2105.
- Achatz, G., Oberkofler, H., Lechenauer, E., Simon, B., Unger, A., Kandler, D., ... Breitenbach, M. (1995). Molecular cloning of major and minor allergens of *Alternaria alternata* and *Cladosporium herbarum*. *Molecular Immunology*, 32(3), 213–227.
- Aglawe, V., Tamrakar, M., Singh, S. M., & Sontakke, H. (2013). Systemic phaeohyphomycosis caused by *Cladosporium cladosporioides*: *in vitro* sensitivity and its serological diagnosis. *Advances in Life Science and Technology*, 8, 16–21.
- Agosta, S. J., & Klemens, J. A. (2008). Ecological fitting by phenotypically flexible genotypes: implications for species associations, community assembly and evolution. *Ecology Letters*, 11(11), 1123–1134.
- Ahmed, S. A., van den Ende, B. H. G. G., Fahal, A. H., van de Sande, W. W. J., & de Hoog, G. S. (2014). Rapid identification of black grain eumycetoma causative agents using rolling circle amplification. *PLoS Neglected Tropical Diseases*, 8(12), e3368.
- Almeida-Paes, R., Frases, S., Araújo, G. de S., de Oliveira, M. M. E., Gerfen, G. J., Nosanchuk, J. D., & Zancopé-Oliveira, R. M. (2012). Biosynthesis and functions of a melanoid pigment produced by species of the sporothrix complex in the presence of L-tyrosine. *Applied and Environmental Microbiology*, 78(24), 8623–8630.
- Alonso-Monge, R., Román, E., Arana, D. M., Pla, J., & Nombela, C. (2009). Fungi sensing environmental stress. *Clinical Microbiology and Infection*, 15(SUPPL. 1), 17–19.

- Amselem, J., Cuomo, C. A., van Kan, J. A. L., Viaud, M., Benito, E. P., Couloux, A., ... Dickman, M. (2011). Genomic analysis of the necrotrophic fungal pathogens *Sclerotinia sclerotiorum* and *Botrytis cinerea*. *PLoS Genetics*, 7(8), e1002230.
- Amyotte, S. G., Tan, X., Pennerman, K., del Mar Jimenez-Gasco, M., Klosterman, S. J., Ma, L.-J., ... Veronese, P. (2012). Transposable elements in phytopathogenic *Verticillium* spp.: insights into genome evolution and inter- and intra-specific diversification. *BMC Genomics*, 13(1), 314.
- Ananya, T. S., Kindo, A. J., Subramanian, A., & Suresh, K. (2014). *Nigrospora sphaerica* causing corneal ulcer in an immunocompetent woman: A case report. *International Journal of Case Reports and Images*, 5(10), 675-679.
- Andes, D., & Casadevall, A. (2013). Insights into fungal pathogenesis from the iatrogenic epidemic of *Exserohilum rostratum* fungal meningitis. *Fungal Genetics and Biology*, 61, 143-145.
- Andrews, S. (2010). FastQC A Quality Control Tool for High Throughput Sequence Data. Retrieved from <http://www.bioinformatics.babraham.ac.uk/projects/fastqc/>
- Annessi, G., Cimitan, A., Zambruno, G., & Di Silverio, A. (1992). Cutaneous phaeohyphomycosis due to *Cladosporium cladosporioides*. *Mycoses*, 35(9-10), 243-246.
- Aoyama, Y., Nomura, M., Yamanaka, S., Ogawa, Y., & Kitajima, Y. (2009). Subcutaneous phaeohyphomycosis caused by *Exophiala xenobiotica* in a non-Hodgkin lymphoma patient. *Medical Mycology*, 47(1), 95-99.
- Arino, J., Ramos, J., & Sychrova, H. (2010). Alkali metal cation transport and homeostasis in yeasts. *Microbiology and Molecular Biology Reviews*, 74(1), 95-120.
- Arzanlou, M., Groenewald, J. Z., Gams, W., Braun, U., Shin, H.-D., & Crous, P. W. (2007). Phylogenetic and morphotaxonomic revision of *Ramichloridium* and allied genera. *Studies in Mycology*, 58, 57-93.
- Badiee, P., & Hashemizadeh, Z. (2014). Opportunistic invasive fungal infections: diagnosis & clinical management. *The Indian Journal of Medical Research*, 139(2), 195-204.
- Balajee, S. A., Borman, A. M., Brandt, M. E., Cano, J., Cuenca-Estrella, M., Dannaoui, E., ... Wickes, B. L. (2009). Sequence-based identification of *Aspergillus*, *Fusarium*, and mucorales species in the clinical mycology laboratory: where are we and where should we go from here? *Journal of Clinical Microbiology*, 47(4), 877-884.
- Banka, R. R., Mishra, S., & Ghose, T. K. (1998). Fibril formation from cellulose by a novel protein from *Trichoderma reesei*: A non-hydrolytic cellulolytic component? *World Journal of Microbiology and Biotechnology*, 14, 551-558.

- Bañuelos, M. A., Sychrová, H., Bleykasten-Grosshans, C., Souciet, J. L., & Potier, S. (1998). The Nha1 antiporter of *Saccharomyces cerevisiae* mediates sodium and potassium efflux. *Microbiology*, *144*, 2749–2758.
- Battaglia, E., Benoit, I., van den Brink, J., Wiebenga, A., Coutinho, P. M., Henrissat, B., & de Vries, R. P. (2011). Carbohydrate-active enzymes from the zygomycete fungus *Rhizopus oryzae*: a highly specialized approach to carbohydrate degradation depicted at genome level. *BMC Genomics*, *12*(1), 38.
- Bayry, J., Aïmanianda, V., Guijarro, J. I., Sunde, M., & Latgé, J.-P. (2012). Hydrophobins-unique fungal proteins. *PLoS Pathogens*, *8*(5), e1002700.
- Beauvais, A., Monod, M., Debeaupuis, J.-P., Diaquin, M., Kobayashi, H., & Latgé, J.-P. (1997a). Biochemical and antigenic characterization of a new dipeptidyl-peptidase isolated from *Aspergillus fumigatus*. *Journal of Biological Chemistry*, *272*(10), 6238–6244.
- Beauvais, A., Monod, M., Wyniger, J., Debeaupuis, J. P., Grouzmann, E., Brakch, N., ... Latgé, J. P. (1997b). Dipeptidyl-peptidase IV secreted by *Aspergillus fumigatus*, a fungus pathogenic to humans. *Infection and Immunity*, *65*(8), 3042–3047.
- Benito, B., Garciadeblás, B., Fraile-Escanciano, A., & Rodríguez-Navarro, A. (2011). Potassium and sodium uptake systems in fungi. The transporter diversity of *Magnaporthe oryzae*. *Fungal Genetics and Biology*, *48*(8), 812–822.
- Bensch, K., Braun, U., Groenewald, J. Z., & Crous, P. W. (2012). The genus *Cladosporium*. *Studies in Mycology*, *72*, 1–401.
- Bensch, K., Groenewald, J. Z., Dijksterhuis, J., Starink-Willemse, M., Andersen, B., Summerell, B. A., ... Crous, P. W. (2010). Species and ecological diversity within the *Cladosporium cladosporioides* complex (Davidiellaceae, Capnodiales). *Studies in Mycology*, *67*, 1–94.
- Bergmann, S., Schumann, J., Scherlach, K., Lange, C., Brakhage, A. a, & Hertweck, C. (2007). Genomics-driven discovery of PKS-NRPS hybrid metabolites from *Aspergillus nidulans*. *Nature Chemical Biology*, *3*(4), 213–217.
- Bickford, D., Lohman, D. J., Sodhi, N. S., Ng, P. K. L., Meier, R., Winker, K., ... Das, I. (2007). Cryptic species as a window on diversity and conservation. *Trends in Ecology & Evolution*, *22*(3), 148–155.
- Biely, P. (2012). Microbial carbohydrate esterases deacetylating plant polysaccharides. *Biotechnology Advances*, *30*(6), 1575–1588.
- Black, K. E., & Baden, L. R. (2007). Fungal infections of the CNS: treatment strategies for the immunocompromised patient. *CNS Drugs*, *21*(4), 293–318.

- Blackwell, M. (2011). The Fungi: 1, 2, 3 ... 5.1 million species? *American Journal of Botany*, 98(3), 426–438.
- Blanco-Ulate, B., Rolshausen, P., & Cantu, D. (2013). Draft genome sequence of *Neofusicoccum parvum* isolate UCR-NP2, a fungal vascular pathogen associated with grapevine cankers. *Genome Announcements*, 1(3), 5–6.
- Boekhout, T., de Hoog, S., Samson, R., Varga, J., & Walther, G. (2009). Fungal taxonomy: new developments in medically important fungi. *Current Fungal Infection Reports*, 3, 170–178.
- Boettger, D., & Hertweck, C. (2013). Molecular diversity sculpted by fungal PKS-NRPS hybrids. *Chembiochem*, 14(1), 28–42.
- Boetzer, M., Henkel, C. V, Jansen, H. J., Butler, D., & Pirovano, W. (2011). Scaffolding pre-assembled contigs using SSPACE. *Bioinformatics*, 27(4), 578–579.
- Boetzer, M., & Pirovano, W. (2012). Toward almost closed genomes with GapFiller. *Genome Biology*, 13(6), R56.
- Bond, J. S., & Beynon, R. J. (1995). The astacin family of metalloendopeptidases. *Protein Science*, 4(7), 1247–1261.
- Bowyer, P., Fraczek, M., & Denning, D. W. (2006). Comparative genomics of fungal allergens and epitopes shows widespread distribution of closely related allergen and epitope orthologues. *BMC Genomics*, 7, 251.
- Brakhage, A. A. (2013). Regulation of fungal secondary metabolism. *Nature Reviews. Microbiology*, 11(1), 21–32.
- Breitenbach, M., Simon, B., Probst, G., Oberkofler, H., Ferreira, F., Briza, P., ... Hirschwehr, R. (1997). Enolases are highly conserved fungal allergens. *International Archives of Allergy and Immunology*, 113, 114–117.
- Brown, A. J. P., Budge, S., Kaloriti, D., Tillmann, A., Jacobsen, M. D., Yin, Z., ... Leach, M. D. (2014). Stress adaptation in a pathogenic fungus. *The Journal of Experimental Biology*, 217, 144–155.
- Buermans, H. P. J., & den Dunnen, J. T. (2014). Next generation sequencing technology: Advances and applications. *Biochimica et Biophysica Acta*, 1842(10), 1932–1941.
- Burmester, A., Shelest, E., Glöckner, G., Heddergott, C., Schindler, S., Staib, P., ... Brakhage, A. A. (2011). Comparative and functional genomics provide insights into the pathogenicity of dermatophytic fungi. *Genome Biology*, 12(1), R7.
- Caffall, K. H., & Mohnen, D. (2009). The structure, function, and biosynthesis of plant cell wall pectic polysaccharides. *Carbohydrate Research*, 344(14), 1879–1900.

- Cagnac, O., Aranda-Sicilia, M. N., Leterrier, M., Rodriguez-Rosales, M.-P., & Venema, K. (2010). Vacuolar cation/H⁺ antiporters of *Saccharomyces cerevisiae*. *The Journal of Biological Chemistry*, 285(44), 33914–33922.
- Cantarel, B. L., Coutinho, P. M., Rancurel, C., Bernard, T., Lombard, V., & Henrissat, B. (2009). The Carbohydrate-Active EnZymes database (CAZy): an expert resource for glycogenomics. *Nucleic Acids Research*, 37, D233–D238.
- Cantrell, S. A., Dianese, J. C., Fell, J., Gunde-Cimerman, N., & Zalar, P. (2011). Unusual fungal niches. *Mycologia*, 103(6), 1161–1174.
- Carter, E., & Boudreaux, C. (2004). Fatal cerebral phaeohyphomycosis due to *Curvularia lunata* in an immunocompetent patient. *Journal of Clinical Microbiology*, 42(11), 5419–5423.
- Cássio, F., Côrte-Real, M., & Leão, C. (1993). Quantitative analysis of proton movements associated with the uptake of weak carboxylic acids. The yeast *Candida utilis* as a model. *Biochimica et Biophysica Acta*, 1153(1), 59–66.
- Castro, A. S., Oliveira, A., & Lopes, V. (2013). Pulmonary phaeohyphomycosis: a challenge to the clinician. *European Respiratory Review*, 22(128), 187–188.
- Chadha, S., & Sharma, M. (2014). Transposable elements as stress adaptive capacitors induce genomic instability in fungal pathogen *Magnaporthe oryzae*. *PloS One*, 9(4), e94415.
- Chen, J.-C., Chiu, L.-L., Lee, K.-L., Huang, W.-N., Chuang, J.-G., Liao, H.-K., & Chow, L.-P. (2012). Identification of critical amino acids in an immunodominant IgE epitope of Pen c 13, a major allergen from *Penicillium citrinum*. *PloS One*, 7(4), e34627.
- Chen, L., Yue, Q., Zhang, X., Xiang, M., Wang, C., Li, S., ... An, Z. (2013). Genomics-driven discovery of the pneumocandin biosynthetic gene cluster in the fungus *Glarea lozoyensis*. *BMC Genomics*, 14(1), 339.
- Chen, X.-L., Xie, B.-B., Bian, F., Zhao, G.-Y., Zhao, H.-L., He, H.-L., ... Zhang, Y.-Z. (2009). Ecological function of myroilysin, a novel bacterial M12 metalloprotease with elastinolytic activity and a synergistic role in collagen hydrolysis, in biodegradation of deep-sea high-molecular-weight organic nitrogen. *Applied and Environmental Microbiology*, 75(7), 1838–1844.
- Chen, Z., Martinez, D. A., Gujja, S., Sykes, S. M., Zeng, Q., Szaniszló, P. J., ... Cuomo, C. A. (2014). Comparative genomic and transcriptomic analysis of *Wangiella dermatitidis*, a major cause of phaeohyphomycosis and a model black yeast human pathogen. *G3 (Bethesda, Md.)*, 4(4), 561–578.
- Chen, Z., Nunes, M. A., Silva, M. C., & Rodrigues Jr., C. J. (2004). Appressorium turgor pressure of *Colletotrichum kahawae* might have a role in coffee cuticle penetration. *Mycologia*, 96(6), 1199–1208.

- Chew, F. L. M., Subrayan, V., Chong, P. P., Goh, M. C., & Ng, K. P. (2009). *Cladosporium cladosporioides* keratomycosis: a case report. *Japanese Journal of Ophthalmology*, *53*(6), 657–659.
- Cho, Y., Srivastava, A., Ohm, R. A., Lawrence, C. B., Wang, K.-H., Grigoriev, I. V., & Marahatta, S. P. (2012). Transcription factor Amr1 induces melanin biosynthesis and suppresses virulence in *Alternaria brassicicola*. *PLoS Pathogens*, *8*(10), e1002974.
- Chou, H.-H., & Holmes, M. H. (2001). DNA sequence quality trimming and vector removal. *Bioinformatics*, *17*(12), 1093–1104.
- Chowdhary, A., Meis, J. F., Guarro, J., de Hoog, G. S., Kathuria, S., Arendrup, M. C., ... Cuenca-Estrella, M. (2014). ESCMID and ECMM joint clinical guidelines for the diagnosis and management of systemic phaeohyphomycosis: diseases caused by black fungi. *Clinical Microbiology and Infection*, *20*, 47–75.
- Condon, B. J., Leng, Y., Wu, D., Bushley, K. E., Ohm, R. A., Otilar, R., ... Turgeon, B. G. (2013). Comparative genome structure, secondary metabolite, and effector coding capacity across *Cochliobolus* pathogens. *PLoS Genetics*, *9*(1), e1003233.
- Conesa, A., Götz, S., García-Gómez, J. M., Terol, J., Talón, M., & Robles, M. (2005). Blast2GO: a universal tool for annotation, visualization and analysis in functional genomics research. *Bioinformatics*, *21*(18), 3674–3676.
- Cooney, N. M., & Klein, B. S. (2008). Fungal adaptation to the mammalian host: it is a new world, after all. *Current Opinion in Microbiology*, *11*(6), 511–516.
- Cox, R. J., & Simpson, T. J. (2009). Fungal type I polyketide synthases. *Methods in Enzymology*, *459*, 49–78.
- Cramer, R. (2013). The crux with a reliable *in vitro* and *in vivo* diagnosis of allergy. *Allergy*, *68*(6), 693–694.
- Cramer, R., Garbani, M., Rhyner, C., & Huitema, C. (2014). Fungi: the neglected allergenic sources. *Allergy*, *69*(2), 176–185.
- Cubero, B., Gómez, D., & Scazzocchio, C. (2000). Metabolite repression and inducer exclusion in the proline utilization gene cluster of *Aspergillus nidulans*. *Journal of Bacteriology*, *182*(1), 233–235.
- Cui, Z., Gao, N., Wang, Q., Ren, Y., Wang, K., & Zhu, T. (2015). BcMctA, a putative monocarboxylate transporter, is required for pathogenicity in *Botrytis cinerea*. *Current Genetics*, *61*(4), 545–553.
- Cunha, M. M. L., Franzen, A. J., Seabra, S. H., Herbst, M. H., Vugman, N. V., Borba, L. P., ... Rozental, S. (2010). Melanin in *Fonsecaea pedrosoi*: a trap for oxidative radicals. *BMC Microbiology*, *10*, 80.

- Cuomo, C. A., & Birren, B. W. (2010). The fungal genome initiative and lessons learned from genome sequencing. *Methods in Enzymology*, 470, 833–855.
- da Cunha, K. C., Sutton, D. A., Fothergill, A. W., Cano, J., Gené, J., Madrid, H., ... Guarro, J. (2012). Diversity of *Bipolaris* species in clinical samples in the United States and their antifungal susceptibility profiles. *Journal of Clinical Microbiology*, 50(12), 4061–4066.
- Dadachova, E., Bryan, R. A., Huang, X., Moadel, T., Schweitzer, A. D., Aisen, P., ... Casadevall, A. (2007). Ionizing radiation changes the electronic properties of melanin and enhances the growth of melanized fungi. *PloS One*, 2(5), e457.
- Dantas, A. da S., Day, A., Ikeh, M., Kos, I., Achan, B., & Quinn, J. (2015). Oxidative stress responses in the human fungal pathogen, *Candida albicans*. *Biomolecules*, 5(1), 142–165.
- de Gruyter, J., Woudenberg, J. H. C., Aveskamp, M. M., Verkley, G. J. M., Groenewald, J. Z., & Crous, P. W. (2010). Systematic reappraisal of species in *Phoma* section *Paraphoma*, *Pyrenochaeta* and *Pleurophoma*. *Mycologia*, 102(5), 1066–1081.
- de Hoog, G. S., Guarro, J., Gene, J., & Figueras, M. J. (2000). *Atlas of clinical fungi* (2nd ed.). Netherlands: Centraalbureau voor Schimmekulture.
- de Hoog, G. S., Vicente, V. A., Najafzadeh, M. J., Harrak, M. J., Badali, H., & Seyedmousavi, S. (2011). Waterborne *Exophiala* species causing disease in cold-blooded animals. *Persoonia*, 27, 46–72.
- de Wit, P. J. G. M., van der Burgt, A., Ökmen, B., Stergiopoulos, I., Abd-Elsalam, K. A., Aerts, A. L., ... Bradshaw, R. E. (2012). The genomes of the fungal plant pathogens *Cladosporium fulvum* and *Dothistroma septosporum* reveal adaptation to different hosts and lifestyles but also signatures of common ancestry. *PLoS Genetics*, 8(11), e1003088.
- Del Palacio-Hernanz, A., Moore, M. K., Campbell, C. K., Del Palacio-Perez-Medel, A., & Del Castillo-Cantero, R. (1989). Infection of the central nervous system by *Rhinocladiella atrovirens* in a patient with acquired immunodeficiency syndrome. *Medical Mycology*, 27(2), 127–130.
- Denis, O., Van Cauwenberge, A., Treutens, G., Es Saadi, B., Symoens, F., Popovic, N., & Huygen, K. (2012). Characterization of new *Alternaria alternata*-specific rat monoclonal antibodies. *Mycopathologia*, 173, 151–162.
- Denisov, G. A., Arehart, A. B., & Curtin, M. D. (2004). System and method for improving the accuracy of DNA sequencing and error probability estimation through application of a mathematical model to the analysis of electropherograms. US Patent 6681186.

- Denning, D. W., O'Driscoll, B. R., Hogaboam, C. M., Bowyer, P., & Niven, R. M. (2006). The link between fungi and severe asthma: a summary of the evidence. *The European Respiratory Journal*, 27(3), 615–626.
- Dixit, A., & Kwilinski, K. (2000). 969 *Cladosporium sphaerospermum* - A new allergic species. *Journal of Allergy and Clinical Immunology*, 105(1), S328.
- Dongen, S. Van. (2000). Graph clustering by flow simulation. Phd thesis, University of Utrecht, Netherlands.
- Dugan, F. M., Schubert, K., & Braun, U. (2004). Check-list of *Cladosporium* names. *Schlechtendalia*, 11, 1–103.
- Eichhorn, H., Lessing, F., Winterberg, B., Schirawski, J., Kämper, J., Müller, P., & Kahmann, R. (2006). A ferroxidation/permeation iron uptake system is required for virulence in *Ustilago maydis*. *The Plant Cell*, 18(11), 3332–3345.
- Eisendle, M., Oberegger, H., Zadra, I., & Haas, H. (2003). The siderophore system is essential for viability of *Aspergillus nidulans*: functional analysis of two genes encoding L-ornithine N⁵-monooxygenase (*sidA*) and a non-ribosomal peptide synthetase (*sidC*). *Molecular Microbiology*, 49(2), 359–375.
- Eisendle, M., Schrettl, M., Kragl, C., Müller, D., Illmer, P., & Haas, H. (2006). The intracellular siderophore ferricrocin is involved in iron storage, oxidative-stress resistance, germination, and sexual development in *Aspergillus nidulans*. *Eukaryotic Cell*, 5(10), 1596–1603.
- Eisenman, H. C., & Casadevall, A. (2012). Synthesis and assembly of fungal melanin. *Applied Microbiology and Biotechnology*, 93(3), 931–940.
- Eklblom, R., & Wolf, J. B. W. (2014). A field guide to whole-genome sequencing, assembly and annotation. *Evolutionary Applications*, 2014, 1026-1042.
- Eley, K. L., Halo, L. M., Song, Z., Powles, H., Cox, R. J., Bailey, A. M., ... Simpson, T. J. (2007). Biosynthesis of the 2-pyridone tenellin in the insect pathogenic fungus *Beauveria bassiana*. *ChemBioChem*, 8(3), 289–297.
- Eliahu, N., Igbaria, A., Rose, M. S., Horwitz, B. a, & Lev, S. (2007). Melanin biosynthesis in the maize pathogen *Cochliobolus heterostrophus* depends on two mitogen-activated protein kinases, Chk1 and Mps1, and the transcription factor Cmr1. *Eukaryotic Cell*, 6(3), 421–429.
- Ellis, D., Davis, S., Alexiou, H., Handke, R., & Bartley, R. (2007). *Descriptions of medical fungi* (2nd ed.). Australia: Adelaide Medical Centre for Women and Children.
- Ellwood, S. R., Liu, Z., Syme, R. A., Lai, Z., Hane, J. K., Keiper, F., ... Friesen, T. L. (2010). A first genome assembly of the barley fungal pathogen *Pyrenophora teres f. teres*. *Genome Biology*, 11(11), R109.

- English, M. P. (1980). Infection of the finger-nail by *Pyrenochaeta unguis-hominis*. *British Journal of Dermatology*, *103*, 91–94.
- Enoch, D. A., Ludlam, H. A., & Brown, N. M. (2006). Invasive fungal infections: a review of epidemiology and management options. *Journal of Medical Microbiology*, *55*, 809–818.
- Esch, R. E. (2004). Manufacturing and standardizing fungal allergen products. *The Journal of Allergy and Clinical Immunology*, *113*(2), 210–215.
- Evertsson, U., Monstein, H. J., & Johansson, A. G. (2000). Detection and identification of fungi in blood using broad-range 28S rDNA PCR amplification and species-specific hybridisation. *APMIS*, *108*(5), 385–392.
- Fan, Y.-M., Huang, W.-M., Li, W., & Zhang, G.-X. (2009). Onychomycosis caused by *Nigrospora sphaerica* in an immunocompetent man. *Archives of Dermatology*, *145*(5), 611–612.
- Farnell, E., Rousseau, K., Thornton, D. J., Bowyer, P., & Herrick, S. E. (2012). Expression and secretion of *Aspergillus fumigatus* proteases are regulated in response to different protein substrates. *Fungal Biology*, *116*(9), 1003–1012.
- Fávaro, L., Araújo, W., Azevedo, J., & Paccola-Meirelles, L. (2005). The biology and potential for genetic research of transposable elements in filamentous fungi. *Genetics and Molecular Biology*, *28*(4), 804–813.
- Fedorova, N. D., Khaldi, N., Joardar, V. S., Maiti, R., Amedeo, P., Anderson, M. J., ... Nierman, W. C. (2008). Genomic islands in the pathogenic filamentous fungus *Aspergillus fumigatus*. *PLoS Genetics*, *4*(4), e1000046.
- Felnagle, E. A., Jackson, E. E., Chan, Y. A., Podevels, A. M., Berti, A. D., McMahon, M. D., & Thomas, M. G. (2008). Nonribosomal peptide synthetases involved in the production of medically relevant natural products. *Molecular Pharmaceutics*, *5*(2), 191–211.
- Ferreira, A. P. S., Pinho, D. B., Machado, A. R., & Pereira, O. L. (2014a). First report of *Curvularia eragrostidis* causing postharvest rot on pineapple in Brazil. *Plant Disease*, *98*(9), 1277.
- Ferreira, C., van Voorst, F., Martins, A., Neves, L., Oliveira, R., Kielland-Brandt, M. C., ... Brandt, A. (2005). A member of the sugar transporter family, Stl1p is the glycerol/H⁺ symporter in *Saccharomyces cerevisiae*. *Molecular Biology of the Cell*, *16*(4), 2068–2076.
- Ferreira, F., Wolf, M., & Wallner, M. (2014b). Molecular approach to allergy diagnosis and therapy. *Yonsei Medical Journal*, *55*(4), 839–852.
- Fisch, K. M. (2013). Biosynthesis of natural products by microbial iterative hybrid PKS–NRPS. *RSC Advances*, *3*(40), 18228–18247.

- Fraczek, M. G., & Bowyer, P. (2013). Genomics of Fungal Allergens. *Fungal Genomics & Biology*, 3(2), 1–3.
- Franken, A. C. W., Lechner, B. E., Werner, E. R., Haas, H., Lokman, B. C., Ram, A. F. J., ... Punt, P. J. (2014). Genome mining and functional genomics for siderophore production in *Aspergillus niger*. *Briefings in Functional Genomics*, 13(6), 482–492.
- Fraser, J. A., Stajich, J. E., Tarcha, E. J., Cole, G. T., Inglis, D. O., Sil, A., & Heitman, J. (2007). Evolution of the mating type locus: Insights gained from the dimorphic primary fungal pathogens *Histoplasma capsulatum*, *Coccidioides immitis*, and *Coccidioides posadasii*. *Eukaryotic Cell*, 6(4), 622–629.
- Fujii, I., Yasuoka, Y., Tsai, H. F., Chang, Y. C., Kwon-Chung, K. J., & Ebizuka, Y. (2004). Hydrolytic polyketide shortening by Ayg1p, a novel enzyme involved in fungal melanin biosynthesis. *Journal of Biological Chemistry*, 279(43), 44613–44620.
- Gachomo, E. W., Seufferheld, M. J., & Kotchoni, S. O. (2010). Melanization of appressoria is critical for the pathogenicity of *Diplocarpon rosae*. *Molecular Biology Reports*, 37(7), 3583–3591.
- Gade, A., Rai, M., Duran, N., & Ingle, A. P. (2015). Synthesis of silver nanoparticles by *Phoma gardeniae* and *in vitro* evaluation of their efficacy against human disease-causing bacteria and fungi. *IET Nanobiotechnology*, 9(2), 71–75.
- Galagan, J. E., Calvo, S. E., Borkovich, K. A., Selker, E. U., Read, N. D., Jaffe, D., ... Birren, B. (2003). The genome sequence of the filamentous fungus *Neurospora crassa*. *Nature*, 422(6934), 859–868.
- Galagan, J. E., Calvo, S. E., Cuomo, C., Ma, L., Wortman, J. R., Batzoglou, S., ... Birren, B. W. (2005). Sequencing of *Aspergillus nidulans* and comparative analysis with *Aspergillus fumigatus* and *Aspergillus oryzae*. *Nature*, 438(7071), 1105–1115.
- Garron, M.-L., & Cygler, M. (2010). Structural and mechanistic classification of uronic acid-containing polysaccharide lyases. *Glycobiology*, 20(12), 1547–1573.
- Gilles, A., Megléc, E., Pech, N., Ferreira, S., Malausa, T., & Martin, J.-F. (2011). Accuracy and quality assessment of 454 GS-FLX Titanium pyrosequencing. *BMC Genomics*, 12, 245.
- Gioulekas, D., Damialis, A., Papakosta, D., Spieksma, F., Giouleka, P., & Patakas, D. (2004). Allergenic fungi spore records (15 years) and sensitization in patients with respiratory allergy in Thessaloniki-Greece. *Journal of Investigational Allergology and Clinical Immunology*, 14(3), 225–231.
- Giuliano Garisto Donzelli, B., Gibson, D. M., & Krasnoff, S. B. (2015). Intracellular siderophore but not extracellular siderophore is required for full virulence in *Metarhizium robertsii*. *Fungal Genetics and Biology*, 82, 56–68.

- Glass, D., & Amedee, R. G. (2011). Allergic fungal rhinosinusitis: a review. *The Ochsner Journal*, *11*(3), 271–275.
- Glover, J. R., & Lindquist, S. (1998). Hsp104, Hsp70, and Hsp40: A novel chaperone system that rescues previously aggregated proteins. *Cell*, *94*(1), 73–82.
- Goodwin, T. J. D., Butler, M. I., & Poulter, R. T. M. (2003). Cryptons: A group of tyrosine-recombinase-encoding DNA transposons from pathogenic fungi. *Microbiology*, *149*(11), 3099–3109.
- Gostinčar, C., Grube, M., de Hoog, S., Zalar, P., & Gunde-Cimerman, N. (2010). Extremotolerance in fungi: evolution on the edge. *FEMS Microbiology Ecology*, *71*(1), 2–11.
- Gostinčar, C., Grube, M., & Gunde-Cimerman, N. (2011). Evolution of fungal pathogens in domestic environments? *Fungal Biology*, *115*(10), 1008–1018.
- Gressler, M., Zaehle, C., Scherlach, K., Hertweck, C., & Brock, M. (2011). Multifactorial induction of an orphan PKS-NRPS gene cluster in *Aspergillus terreus*. *Chemistry & Biology*, *18*(2), 198–209.
- Grigoriev, I. V. (2013). A changing landscape of fungal genomics. In *The Ecological Genomics of Fungi* (pp. 1–20). Hoboken, NJ: John Wiley & Sons, Inc.
- Grigoriev, I. V., Nikitin, R., Haridas, S., Kuo, A., Ohm, R., Otilar, R., ... Shabalov, I. (2014). MycoCosm portal: gearing up for 1000 fungal genomes. *Nucleic Acids Research*, *42*, D699–D704.
- Groll, A. H., & Walsh, T. J. (2001). Uncommon opportunistic fungi: new nosocomial threats. *Clinical Microbiology and Infection*, *7*, 8–24.
- Guarro, J., Akiti, T., Horta, R. A., Morizot Leite-Filho, L. A., Gené, J., Ferreira-Gomes, S., ... Ortoneda, M. (1999a). Mycotic keratitis due to *Curvularia senegalensis* and in vitro antifungal susceptibilities of *Curvularia* spp. *Journal of Clinical Microbiology*, *37*(12), 4170–4173.
- Guarro, J., Gené, J., & Stchigel, A. M. (1999b). Developments in fungal taxonomy. *Clinical Microbiology Reviews*, *12*(3), 454–500.
- Gugnani, H. C., Ramesh, V., Sood, N., Guarro, J., Moin-Ul-Haq, Paliwal-Joshi, A., & Singh, B. (2006). Cutaneous phaeohyphomycosis caused by *Cladosporium oxysporum* and its treatment with potassium iodide. *Medical Mycology*, *44*(3), 285–288.
- Gugnani, H. C., Sood, N., Singh, B., & Makkar, R. (2000). Case report. Subcutaneous phaeohyphomycosis due to *Cladosporium cladosporioides*. *Mycoses*, *43*, 85–87.
- Gunde-Cimerman, N., Ramos, J., & Plemenitas, A. (2009). Halotolerant and halophilic fungi. *Mycological Research*, *113*, 1231–1241.

- Gunde-Cimerman, N., Zalar, P., de Hoog, S., & Plemenitas, A. (2000). Hypersaline waters in salterns- natural ecological niches for halophilic black yeasts. *FEMS Microbiology Ecology*, 32(3), 235–240.
- Haarmann, T., Machado, C., Lübbe, Y., Correia, T., Schardl, C. L., Panaccione, D. G., & Tudzynski, P. (2005). The ergot alkaloid gene cluster in *Claviceps purpurea*: Extension of the cluster sequence and intra species evolution. *Phytochemistry*, 66(11), 1312–1320.
- Haas, H. (2014). Fungal siderophore metabolism with a focus on *Aspergillus fumigatus*. *Natural Product Reports*, 31(10), 1266–1276.
- Haas, H., Angermayr, K., & Stöffler, G. (1997). Molecular analysis of a *Penicillium chrysogenum* GATA factor encoding gene (*sreP*) exhibiting significant homology to the *Ustilago maydis urbs1* gene. *Gene*, 184(1), 33–37.
- Haas, H., Eisendle, M., & Turgeon, B. G. (2008). Siderophores in fungal physiology and virulence. *Annual Review of Phytopathology*, 46, 149–187.
- Haas, H., Schoeser, M., Lesuisse, E., Ernst, J. F., Parson, W., & Abt, B. (2003). Characterization of the *Aspergillus nidulans* transporters for the siderophores enterobactin and triacetylfusarinine C. *Biochemical Society*, 513, 505–513.
- Halo, L. M., Marshall, J. W., Yakasai, A. A., Song, Z., Butts, C. P., Crump, M. P., ... Cox, R. J. (2008). Authentic heterologous expression of the tenellin iterative polyketide synthase nonribosomal peptide synthetase requires coexpression with an enoyl reductase. *Chembiochem*, 9(4), 585–594.
- Hamayun, M., Khan, S. A., Ahmad, N., Tang, D.-S., Kang, S.-M., Na, C.-I., ... Lee, I.-J. (2009). *Cladosporium sphaerospermum* as a new plant growth-promoting endophyte from the roots of *Glycine max* (L .) Merr. *World Journal of Microbiology and Biotechnology*, 25, 627–632.
- Hamilton, R. G., & Franklin Adkinson, N. (2004). *In vitro* assays for the diagnosis of IgE-mediated disorders. *The Journal of Allergy and Clinical Immunology*, 114(2), 213–225.
- Hemmann, S., Blaser, K., & Cramer, R. (1997). Allergens of *Aspergillus fumigatus* and *Candida boidinii* share IgE-binding epitopes. *American Journal of Respiratory and Critical Care Medicine*, 156(6), 1956–1962.
- Henson, J., Tischler, G., & Ning, Z. (2012). Next-generation sequencing and large genome assemblies. *Pharmacogenomics*, 13(8), 901–915.
- Hert, D. G., Fredlake, C. P., & Barron, A. E. (2008). Advantages and limitations of next-generation sequencing technologies: a comparison of electrophoresis and non-electrophoresis methods. *Electrophoresis*, 29(23), 4618–4626.
- Heuchert, B., Braun, U., & Schubert, K. (2005). Morphotaxonomic revision of fungicolous *Cladosporium* species (hyphomycetes). *Schlechtendalia*, 13, 1–78.

- Hinrikson, H. P., Hurst, S. F., Lott, T. J., Warnock, D. W., & Morrison, C. J. (2005). Assessment of ribosomal large-subunit D1-D2, internal transcribed spacer 1, and internal transcribed spacer 2 regions as targets for molecular identification of medically important *Aspergillus* species. *Journal of Clinical Microbiology*, *43*(5), 2092–2103.
- Hof, C., Eisfeld, K., Welzel, K., Antelo, L., Foster, A. J., & Anke, H. (2007). Ferricrocin synthesis in *Magnaporthe grisea* and its role in pathogenicity in rice. *Molecular Plant Pathology*, *8*(2), 163–172.
- Hoffmeister, D., & Keller, N. P. (2007). Natural products of filamentous fungi: enzymes, genes, and their regulation. *Natural Product Reports*, *24*(2), 393–416.
- Horton, P., Park, K.-J., Obayashi, T., Fujita, N., Harada, H., Adams-Collier, C. J., & Nakai, K. (2007). WoLF PSORT: protein localization predictor. *Nucleic Acids Research*, *35*, W585–W587.
- Howard, D. H. (2004). Iron gathering by zoopathogenic fungi. *FEMS Immunology and Medical Microbiology*, *40*(2), 95–100.
- Howard, R. J., & Valent, B. (1996). Breaking and entering: host penetration by the fungal rice blast pathogen *Magnaporthe grisea*. *Annual Review of Microbiology*, *50*, 491–512.
- Hsu, L. Y., Wijaya, L., Shu-Ting Ng, E., & Gotuzzo, E. (2012). Tropical fungal infections. *Infectious Disease Clinics of North America*, *26*(2), 497–512.
- Hsu, M. M., & Lee, J. Y. (1993). Cutaneous and subcutaneous phaeohyphomycosis caused by *Exserohilum rostratum*. *Journal of the American Academy of Dermatology*, *28*, 340–344.
- Hsueh, Y.-P., Xue, C., & Heitman, J. (2009). A constitutively active GPCR governs morphogenic transitions in *Cryptococcus neoformans*. *The EMBO Journal*, *28*(9), 1220–1233.
- Hu, W., Ran, Y., Zhuang, K., Lama, J., & Zhang, C. (2015). *Alternaria arborescens* infection in a healthy individual and literature review of cutaneous Alternariosis. *Mycopathologia*, *179*, 147–152.
- Huang, J. B., Zheng, L., & Hsiang, T. (2004). First report of leaf spot caused by *Curvularia affinis* on *Festuca arundinacea* in Hubei, China. *Plant Disease*, *88*(9), 1048.
- Hubka, V., Mencl, K., Skorepova, M., Lyskova, P., & Zalabska, E. (2011). Phaeohyphomycosis and onychomycosis due to *Chaetomium* spp., including the first report of *Chaetomium brasiliense* infection. *Medical Mycology*, *49*(7), 724–733.
- Huelsenbeck, J. P., & Ronquist, F. (2001). MRBAYES: Bayesian inference of phylogenetic trees. *Bioinformatics*, *17*(8), 754–755.

- Huitt-Roehl, C. R., Hill, E. A., Adams, M. M., Vagstad, A. L., Li, J. W., & Townsend, C. A. (2015). Starter unit flexibility for engineered product synthesis by the nonreducing polyketide synthase PksA. *ACS Chemical Biology*, *10*(6), 1443–1449.
- Huyan, X.-H., Yang, Y.-P., Fan, Y.-M., Huang, W.-M., Li, W., & Zhou, Y. (2012). Cutaneous and systemic pathogenicity of a clinical isolate of *Cladosporium sphaerospermum* in a murine model. *Journal of Comparative Pathology*, *147*, 354–359.
- Hwang, L. H., Seth, E., Gilmore, S. a., & Sil, A. (2012). SRE1 regulates iron-dependent and -independent pathways in the fungal pathogen *Histoplasma capsulatum*. *Eukaryotic Cell*, *11*(1), 16–25.
- Imai, J., Yashiroda, H., Maruya, M., Yahara, I., & Tanaka, K. (2003). Proteasomes and Molecular Chaperones. *Cell Cycle*, *2*(6), 585–589.
- Imbert, C. (2002). Effect of matrix metalloprotease inhibitors on the 95 kDa metallopeptidase of *Candida albicans*. *Journal of Antimicrobial Chemotherapy*, *49*(6), 1007–1010.
- Islam, M. S., Haque, M. S., Islam, M. M., Emdad, E. M., Halim, A., Hossen, Q. M. M., ... Alam, M. (2012). Tools to kill: genome of one of the most destructive plant pathogenic fungi *Macrophomina phaseolina*. *BMC Genomics*, *13*(1), 493.
- Jacobson, E. S. (2000). Pathogenic roles for fungal melanins. *Clinical Microbiology Reviews*, *13*(4), 708–717.
- Jin, K., Zhang, Y., Fang, W., Luo, Z., Zhou, Y., & Pei, Y. (2010). Carboxylate transporter gene JEN1 from the entomopathogenic fungus *Beauveria bassiana* is involved in conidiation and virulence. *Applied and Environmental Microbiology*, *76*(1), 254–263.
- Jones, S. K., & Bennett, R. J. (2011). Fungal mating pheromones: choreographing the dating game. *Fungal Genetics and Biology*, *48*(7), 668–676.
- Jørgensen, H., Vibe-Pedersen, J., Larsen, J., & Felby, C. (2007). Liquefaction of lignocellulose at high-solids concentrations. *Biotechnology and Bioengineering*, *96*(5), 862–870.
- Jousson, O. (2004). Multiplication of an ancestral gene encoding secreted fungalsin preceded species differentiation in the dermatophytes *Trichophyton* and *Microsporium*. *Microbiology*, *150*(2), 301–310.
- Jovall, P. A., Tunblad-Johansson, I., & Adler, L. (1990). ¹³C NMR analysis of production and accumulation of osmoregulatory metabolites in the salt-tolerant yeast *Debaryomyces hansenii*. *Archives of Microbiology*, *154*(3), 209–214.
- Ju, Y. M., Rogers, J. D., & San Martin, F. (1997). A revision of the genus *Daldinia*. *Mycotaxon*, *61*, 243–293.

- Kantarcioğlu, A. S., & de Hoog, G. S. (2004). Infections of the central nervous system by melanized fungi: a review of cases presented between 1999 and 2004. *Mycoses*, *47*, 4–13.
- Kantarcioğlu, A. S., Yücel, A., & Hoog, G. S. (2002). Case report. Isolation of *Cladosporium cladosporioides* from cerebrospinal fluid. *Mycoses*, *45*, 500–503.
- Karányi, Z., Holb, I., Hornok, L., Pócsi, I., & Miskei, M. (2013). FSRD: Fungal stress response database. *Database*, *2013*, 1–6.
- Keller, N., & Hohn, T. (1997). Metabolic pathway gene clusters in filamentous fungi. *Fungal Genetics and Biology*, *21*(1), 17–29.
- Keller, N. P., Turner, G., & Bennett, J. W. (2005). Fungal secondary metabolism - from biochemistry to genomics. *Nature Reviews. Microbiology*, *3*(12), 937–947.
- Keller, S., Macheleidt, J., Scherlach, K., Schmalzer-Ripcke, J., Jacobsen, I. D., Heinekamp, T., & Brakhage, A. A. (2011). Pyomelanin formation in *Aspergillus fumigatus* requires HmgX and the transcriptional activator HmgR but is dispensable for virulence. *PLoS One*, *6*(10), e26604.
- Kennedy, J. L., Heymann, P. W., & Platts-Mills, T. A. E. (2012). The role of allergy in severe asthma. *Clinical and Experimental Allergy*, *42*(5), 659–669.
- Khaldi, N., Seifuddin, F. T., Turner, G., Haft, D., Nierman, W. C., Wolfe, K. H., & Fedorova, N. D. (2010). SMURF: genomic mapping of fungal secondary metabolite clusters. *Fungal Genetics and Biology*, *47*(9), 736–741.
- Khan, Z. U., Ahmad, S., Joseph, L., & Chandy, R. (2009). Cutaneous phaeohyphomycosis due to *Neoscytalidium dimidiatum*: First case report from Kuwait. *Journal of Medical Mycology*, *19*(2), 138–142.
- Knutsen, A. P., Bush, R. K., Demain, J. G., Denning, D. W., Dixit, A., Fairs, A., ... Wardlaw, A. J. (2012). Fungi and allergic lower respiratory tract diseases. *Journal of Allergy and Clinical Immunology*, *129*(2), 280–291.
- Kojima, K. K., & Jurka, J. (2011). Crypton transposons: identification of new diverse families and ancient domestication events. *Mobile DNA*, *2*(1), 12.
- Kragl, C., Schrettl, M., Abt, B., Sarg, B., Lindner, H. H., & Haas, H. (2007). EstB-mediated hydrolysis of the siderophore triacetylfusarinine C optimizes iron uptake of *Aspergillus fumigatus*. *Eukaryotic Cell*, *6*(8), 1278–1285.
- Krogh, A., Larsson, B., von Heijne, G., & Sonnhammer, E. L. (2001). Predicting transmembrane protein topology with a hidden Markov model: application to complete genomes. *Journal of Molecular Biology*, *305*(3), 567–580.

- Kroken, S., Glass, N. L., Taylor, J. W., Yoder, O. C., & Turgeon, B. G. (2003). Phylogenomic analysis of type I polyketide synthase genes in pathogenic and saprobic ascomycetes. *Proceedings of the National Academy of Sciences of the United States of America*, *100*(26), 15670–15675.
- Krzyściak, P. M., Pindycka-Piaszczyńska, M., & Piaszczyński, M. (2014). Chromoblastomycosis. *Advances in Dermatology and Allergology*, *5*, 310–321.
- Kuan, C. S., Yew, S. M., Chan, C. L., Toh, Y. F., Lee, K. W., Cheong, W.-H., ... Ng, K. P. (2016). DemaDb: an integrated dematiaceous fungal genomes database. *Database*, *2016*, baw008.
- Kuan, C. S., Yew, S. M., Toh, Y. F., Chan, C. L., Ngeow, Y. F., Lee, K. W., ... Ng, K. P. (2015). Dissecting the fungal biology of *Bipolaris papendorffii*: from phylogenetic to comparative genomic analysis. *DNA Research*, *22*(3), 219–232.
- Kubak, B. M., & Huprikar, S. S. (2009). Emerging & rare fungal infections in solid organ transplant recipients. *American Journal of Transplantation*, *9*, S208–S226.
- Kubicek, C. P., Starr, T. L., & Glass, N. L. (2014). Plant cell wall-degrading enzymes and their secretion in plant-pathogenic fungi. *Annual Review of Phytopathology*, *52*(1), 427–451.
- Kück, U., Bloemendal, S., & Teichert, I. (2014). Putting fungi to work: harvesting a cornucopia of drugs, toxins, and antibiotics. *PLoS Pathogens*, *10*(3), e1003950.
- Kühlbrandt, W. (2004). Biology, structure and mechanism of P-type ATPases. *Nature Reviews Molecular Cell Biology*, *5*(4), 282–295.
- Kumar, K. K., & Hallikeri, K. (2008). Phaeohyphomycosis. *Indian Journal of Pathology and Microbiology*, *51*(4), 556–558.
- Kumar, S., Randhawa, A., Ganesan, K., Raghava, G. P. S., & Mondal, A. K. (2012). Draft genome sequence of salt-tolerant yeast *Debaryomyces hansenii* var. *hansenii* MTCC 234. *Eukaryotic Cell*, *11*(7), 961–962.
- Kurup, V. P., & Banerjee, B. (2000). Fungal allergens and peptide epitopes. *Peptides*, *21*(4), 589–599.
- Kwok, E. Y., Severance, S., & Kosman, D. J. (2006). Evidence for iron channeling in the Fet3p-Ftr1p high-affinity iron uptake complex in the yeast plasma membrane. *Biochemistry*, *45*(20), 6317–6327.
- Lagesen, K., Hallin, P., Rødland, E. A., Staerfeldt, H.-H., Rognes, T., & Ussery, D. W. (2007). RNAmmer: consistent and rapid annotation of ribosomal RNA genes. *Nucleic Acids Research*, *35*(9), 3100–3108.

- Langfelder, K., Streibel, M., Jahn, B., Haase, G., & Brakhage, A. A. (2003). Biosynthesis of fungal melanins and their importance for human pathogenic fungi. *Fungal Genetics and Biology*, 38(2), 143–158.
- Larkin, M. A., Blackshields, G., Brown, N. P., Chenna, R., McGettigan, P. A., McWilliam, H., ... Higgins, D. G. (2007). Clustal W and Clustal X version 2.0. *Bioinformatics*, 23(21), 2947–2948.
- Leach, M. D., & Brown, A. J. P. (2012). Posttranslational modifications of proteins in the pathobiology of medically relevant fungi. *Eukaryotic Cell*, 11(2), 98–108.
- Lee, I. R., Lui, E. Y. L., Chow, E. W. L., Arras, S. D. M., Morrow, C. A., & Fraser, J. A. (2013). Reactive oxygen species homeostasis and virulence of the fungal pathogen *Cryptococcus neoformans* requires an intact proline catabolism pathway. *Genetics*, 194(2), 421–433.
- Lee, J. D., & Kolattukudy, P. E. (1995). Molecular cloning of the cDNA and gene for an elastinolytic aspartic proteinase from *Aspergillus fumigatus* and evidence of its secretion by the fungus during invasion of the host lung. *Infection and Immunity*, 63(10), 3796–3803.
- Lee, S. C., Ni, M., Li, W., Shertz, C., & Heitman, J. (2010). The evolution of sex: a perspective from the fungal kingdom. *Microbiology and Molecular Biology Reviews*, 74(2), 298–340.
- Lenassi, M., Gostinčar, C., Jackman, S., Turk, M., Sadowski, I., Nislow, C., ... Plemenitaš, A. (2013). Whole genome duplication and enrichment of metal cation transporters revealed by *de novo* genome sequencing of extremely halotolerant black yeast *Hortaea werneckii*. *PloS One*, 8(8), e71328.
- Lenassi, M., Vaupotic, T., Gunde-Cimerman, N., & Plemenitas, A. (2007). The MAP kinase HwHog1 from the halophilic black yeast *Hortaea werneckii*: coping with stresses in solar salterns. *Saline Systems*, 3(1), 3.
- Lenassi, M., Zajc, J., Gostinčar, C., Gorjan, A., Gunde-Cimerman, N., & Plemenitaš, A. (2011). Adaptation of the glycerol-3-phosphate dehydrogenase Gpd1 to high salinities in the extremely halotolerant *Hortaea werneckii* and halophilic *Wallemia ichthyophaga*. *Fungal Biology*, 115(10), 959–970.
- Levasseur, A., Drula, E., Lombard, V., Coutinho, P. M., & Henrissat, B. (2013). Expansion of the enzymatic repertoire of the CAZy database to integrate auxiliary redox enzymes. *Biotechnology for Biofuels*, 6(1), 41.
- Levin, T. P., Baty, D. E., Fekete, T., Truant, A. L., & Suh, B. (2004). *Cladophialophora bantiana* brain abscess in a solid-organ transplant recipient: Case report and review of the literature. *Journal of Clinical Microbiology*, 42(9), 4374–4378.
- Li, L., Stoeckert, C. J., & Roos, D. S. (2003). OrthoMCL: identification of ortholog groups for eukaryotic genomes. *Genome Research*, 13(9), 2178–2189.

- Li, S.-F., Gao, W.-J., Zhao, X.-P., Dong, T.-Y., Deng, C.-L., & Lu, L.-D. (2014). Analysis of transposable elements in the genome of *Asparagus officinalis* from high coverage sequence data. *PLoS ONE*, 9(5), e97189.
- Li, S.-M. (2010). Prenylated indole derivatives from fungi: structure diversity, biological activities, biosynthesis and chemoenzymatic synthesis. *Nat. Prod. Rep.*, 27(1), 57–78.
- Lian, X., & de Hoog, G. S. (2010). Indoor wet cells harbour melanized agents of cutaneous infection. *Medical Mycology*, 48(4), 622–628.
- Lim, J., Lee, J., Kim, J., Park, J., Park, S., Yang, M., & Kim, D. (2010). A DnaJ-like homolog from *Cryphonectria parasitica* is not responsive to hypoviral infection but is important for fungal growth in both wild-type and hypovirulent strains, 30(3), 235–243.
- Liu, D., Gong, J., Dai, W., Kang, X., Huang, Z., Zhang, H.-M., ... Xiong, X. (2012). The genome of *Ganoderma lucidum* provides insights into triterpenes biosynthesis and wood degradation. *PLoS One*, 7(5), e36146.
- Liu, L., Li, Y., Li, S., Hu, N., He, Y., Pong, R., ... Law, M. (2012). Comparison of next-generation sequencing systems. *Journal of Biomedicine and Biotechnology*, 2012, 1–11.
- Lomsadze, A., Ter-Hovhannisyan, V., Chernoff, Y. O., & Borodovsky, M. (2005). Gene identification in novel eukaryotic genomes by self-training algorithm. *Nucleic Acids Research*, 33(20), 6494–6506.
- Lowe, T. M., & Eddy, S. R. (1997). tRNAscan-SE: a program for improved detection of transfer RNA genes in genomic sequence. *Nucleic Acids Research*, 25(5), 955–964.
- Ma, D., & Li, R. (2013). Current understanding of HOG-MAPK pathway in *Aspergillus fumigatus*. *Mycopathologia*, 175, 13–23.
- Machouart, M., Samerpitak, K., de Hoog, G. S., & Gueidan, C. (2013). A multigene phylogeny reveals that *Ochroconis* belongs to the family Symptoventuriaceae (Venturiales, Dothideomycetes). *Fungal Diversity*, 65(1), 77–88.
- Madrid, I. M., Xavier, M. O., Mattei, A. S., Fernandes, C. G., Guim, T. N., Santin, R., ... Araújo Meireles, M. C. (2010). Role of melanin in the pathogenesis of cutaneous sporotrichosis. *Microbes and Infection*, 12(2), 162–165.
- Maduri, A., Patnayak, R., Verma, A., Mudgeti, N., Kalawat, U., & Asha, T. (2015). Subcutaneous infection by *Cladosporium sphaerospermum*- A rare case report. *Indian Journal of Pathology and Microbiology*, 58(3), 406–407.
- Manamgoda, D. S., Cai, L., Bahkali, A. H., Chukeatirote, E., & Hyde, K. D. (2011). *Cochliobolus*: an overview and current status of species. *Fungal Diversity*, 51(1), 3–42.

- Manamgoda, D. S., Cai, L., McKenzie, E. H. C., Crous, P. W., Madrid, H., Chukeatirote, E., ... Hyde, K. D. (2012). A phylogenetic and taxonomic re-evaluation of the *Bipolaris* - *Cochliobolus* - *Curvularia* Complex. *Fungal Diversity*, 56(1), 131–144.
- Mani, R. S., Chickabasaviah, Y. T., Nagarathna, S., Chandramuki, A., Shivprakash, M. R., Vijayan, J., ... Kovoov, J. (2008). Cerebral phaeohyphomycosis caused by *Scytalidium dimidiatum*: a case report from India. *Medical Mycology*, 46(7), 705–711.
- Manning, V. A., Pandelova, I., Dhillon, B., Wilhelm, L. J., Goodwin, S. B., Berlin, A. M., ... Ciuffetti, L. M. (2013). Comparative genomics of a plant-pathogenic fungus, *Pyrenophora tritici-repentis*, reveals transduplication and the impact of repeat elements on pathogenicity and population divergence. *G3 (Bethesda, Md)*, 3(1), 41–63.
- Margulies, M., Egholm, M., Altman, W. E., Attiya, S., Bader, J. S., Bembien, L. A., ... Rothberg, J. M. (2005). Genome sequencing in microfabricated high-density picolitre reactors. *Nature*, 437(7057), 376–380.
- Mari, A., Rasi, C., Palazzo, P., & Scala, E. (2009). Allergen databases: current status and perspectives. *Current Allergy and Asthma Reports*, 9(5), 376–383.
- Markaryan, A., Morozova, I., Yu, H., & Kolattukudy, P. E. (1994). Purification and characterization of an elastinolytic metalloprotease from *Aspergillus fumigatus* and immunoelectron microscopic evidence of secretion of this enzyme by the fungus invading the murine lung. *Infection and Immunity*, 62(6), 2149–2157.
- Martinez, D. A., Oliver, B. G., Gräser, Y., Goldberg, J. M., Li, W., Martinez-Rossi, N. M., ... White, T. C. (2012). Comparative genome analysis of *Trichophyton rubrum* and related dermatophytes reveals candidate genes involved in infection. *mBio*, 3(5), e00259–12.
- McCormick, S. P., Stanley, A. M., Stover, N. A., & Alexander, N. J. (2011). Trichothecenes: from simple to complex mycotoxins. *Toxins*, 3(7), 802–814.
- Metzker, M. L. (2010). Sequencing technologies - the next generation. *Nature Reviews Genetics*, 11(1), 31–46.
- Mikosz, C. A., Smith, R. M., Kim, M., Tyson, C., Lee, E. H., Adams, E., ... Park, B. J. (2014). Fungal endophthalmitis associated with compounded products. *Emerging Infectious Diseases*, 20(2), 248–256.
- Monod, M., Capoccia, S., Léchenne, B., Zaugg, C., Holdom, M., & Jousson, O. (2002). Secreted proteases from pathogenic fungi. *International Journal of Medical Microbiology*, 292, 405–419.
- Monod, M., Léchenne, B., Jousson, O., Grand, D., Zaugg, C., Stöcklin, R., & Grouzmann, E. (2005). Aminopeptidases and dipeptidyl-peptidases secreted by the dermatophyte *Trichophyton rubrum*. *Microbiology*, 151(1), 145–155.

- Moran, G. P., Coleman, D. C., & Sullivan, D. J. (2011). Comparative genomics and the evolution of pathogenicity in human pathogenic fungi. *Eukaryotic Cell*, 10(1), 34–42.
- Moretti, S., Armougom, F., Wallace, I. M., Higgins, D. G., Jongeneel, C. V., & Notredame, C. (2007). The M-Coffee web server: a meta-method for computing multiple sequence alignments by combining alternative alignment methods. *Nucleic Acids Research*, 35, W645–W648.
- Morio, F., Berre, J.-Y. Le, Garcia-Hermoso, D., Najafzadeh, M. J., de Hoog, S., Benard, L., & Michau, C. (2012). Phaeohyphomycosis due to *Exophiala xenobiotica* as a cause of fungal arthritis in an HIV-infected patient. *Medical Mycology*, 50(5), 513–517.
- Mosier, A. C., Justice, N. B., Bowen, B. P., Baran, R., Thomas, B. C., Northen, T. R., & Banfield, J. F. (2013). Metabolites associated with adaptation of microorganisms to an acidophilic, metal-rich environment identified by stable-isotope-enabled metabolomics. *mBio*, 4(2), e00484–12.
- Namvar, S., Warn, P., Farnell, E., Bromley, M., Fraczek, M., Bowyer, P., & Herrick, S. (2015). *Aspergillus fumigatus* proteases, Asp f 5 and Asp f 13, are essential for airway inflammation and remodelling in a murine inhalation model. *Clinical and Experimental Allergy*, 45(5), 982–993.
- Nenoff, P., van de Sande, W. W. J., Fahal, A. H., Reinel, D., & Schöfer, H. (2015). Eumycetoma and actinomycetoma - an update on causative agents, epidemiology, pathogenesis, diagnostics and therapy. *Journal of the European Academy of Dermatology and Venereology*, 29(10), 1873–1883.
- Ni, M., Feretzaki, M., Sun, S., Wang, X., & Heitman, J. (2011). Sex in Fungi. *Annual Review of Genetics*, 45(1), 405–430.
- Nilsson, R. H., Ryberg, M., Abarenkov, K., Sjökvist, E., & Kristiansson, E. (2009). The ITS region as a target for characterization of fungal communities using emerging sequencing technologies. *FEMS Microbiology Letters*, 296(1), 97–101.
- Nishida, H., Beppu, T., & Ueda, K. (2011). Whole-genome comparison clarifies close phylogenetic relationships between the phyla Dictyoglomi and Thermotogae. *Genomics*, 98(5), 370–375.
- Noverr, M. C., Williamson, P. R., Fajardo, R. S., & Huffnagle, G. B. (2004). CNLAC1 is required for extrapulmonary dissemination of *Cryptococcus neoformans* but not pulmonary persistence. *Infection and Immunity*, 72(3), 1693–1699.
- O'Neill, E. C., & Field, R. A. (2015). Enzymatic synthesis using glycoside phosphorylases. *Carbohydrate Research*, 403, 23–37.

- Ohm, R. A., Feau, N., Henrissat, B., Schoch, C. L., Horwitz, B. A., Barry, K. W., ... Grigoriev, I. V. (2012). Diverse lifestyles and strategies of plant pathogenesis encoded in the genomes of eighteen Dothideomycetes fungi. *PLoS Pathogens*, 8(12), e1003037.
- Oide, S., Berthiller, F., Wiesenberger, G., Adam, G., & Turgeon, B. G. (2014). Individual and combined roles of malonichrome, ferricrocin, and TAFC siderophores in *Fusarium graminearum* pathogenic and sexual development. *Frontiers in Microbiology*, 5, 759.
- Oide, S., Krasnoff, S. B., Gibson, D. M., & Turgeon, B. G. (2007). Intracellular siderophores are essential for ascomycete sexual development in heterothallic *Cochliobolus heterostrophus* and homothallic *Gibberella zeae*. *Eukaryotic Cell*, 6(8), 1339–1353.
- Oide, S., Moeder, W., Krasnoff, S., Gibson, D., Haas, H., Yoshioka, K., & Turgeon, B. G. (2006). NPS6, encoding a nonribosomal peptide synthetase involved in siderophore-mediated iron metabolism, is a conserved virulence determinant of plant pathogenic ascomycetes. *The Plant Cell*, 18(10), 2836–2853.
- Oztas, E., Odemis, B., Kekilli, M., Kurt, M., Dinc, B. M., Parlak, E., ... Sasmaz, N. (2009). Systemic phaeohyphomycosis resembling primary sclerosing cholangitis caused by *Exophiala dermatitidis*. *Journal of Medical Microbiology*, 58, 1243–1246.
- Pappas, P. G., Kontoyiannis, D. P., Perfect, J. R., & Chiller, T. M. (2013). Real-time treatment guidelines: considerations during the *Exserohilum rostratum* outbreak in the United States. *Antimicrobial Agents and Chemotherapy*, 57(4), 1573–1576.
- Pastor, F. J., & Guarro, J. (2008). *Alternaria* infections: Laboratory diagnosis and relevant clinical features. *Clinical Microbiology and Infection*, 14(8), 734–746.
- Persson, B. L., Berhe, A., Fristedt, U., Martinez, P., Pattison, J., Petersson, J., & Weinander, R. (1998). Phosphate permeases of *Saccharomyces cerevisiae*. *Biochimica et Biophysica Acta*, 1365, 23–30.
- Petersen, T. N., Brunak, S., von Heijne, G., & Nielsen, H. (2011). SignalP 4.0: discriminating signal peptides from transmembrane regions. *Nature Methods*, 8(10), 785–786.
- Pfaller, M. A., & Diekema, D. J. (2010). Epidemiology of invasive mycoses in North America. *Critical Reviews in Microbiology*, 36(1), 1–53.
- Plemenitaš, A., Lenassi, M., Konte, T., Kejžar, A., Zajc, J., Gostinčar, C., & Gunde-Cimerman, N. (2014). Adaptation to high salt concentrations in halotolerant/halophilic fungi: a molecular perspective. *Frontiers in Microbiology*, 5(5), 199.

- Potin, O., Veignie, E., & Rafin, C. (2004). Biodegradation of polycyclic aromatic hydrocarbons (PAHs) by *Cladosporium sphaerospermum* isolated from an aged PAH contaminated soil. *FEMS Microbiology Ecology*, *51*(1), 71–78.
- Proft, M., Mas, G., de Nadal, E., Vendrell, A., Noriega, N., Struhl, K., & Posas, F. (2006). The stress-activated Hog1 kinase is a selective transcriptional elongation factor for genes responding to osmotic stress. *Molecular Cell*, *23*(2), 241–250.
- Proft, M., & Struhl, K. (2004). MAP kinase-mediated stress relief that precedes and regulates the timing of transcriptional induction. *Cell*, *118*(3), 351–361.
- Qiao, K., Chooi, Y.-H., & Tang, Y. (2011). Identification and engineering of the cytochalasin gene cluster from *Aspergillus clavatus* NRRL 1. *Metabolic Engineering*, *13*(6), 723–732.
- Qiu-Xia, C., Chang-Xing, L., Wen-Ming, H., Jiang-Qiang, S., Wen, L., & Shun-Fang, L. (2008). Subcutaneous phaeohyphomycosis caused by *Cladosporium sphaerospermum*. *Mycoses*, *51*(1), 79–80.
- Quaedvlieg, W., Verkley, G. J. M., Shin, H.-D., Barreto, R. W., Alfenas, A. C., Swart, W. J., ... Crous, P. W. (2013). Sizing up *Septoria*. *Studies in Mycology*, *75*(1), 307–390.
- Queiroz-Telles, F., Esterre, P., Perez-Blanco, M., Vitale, R. G., Salgado, C. G., & Bonifaz, A. (2009). Chromoblastomycosis: an overview of clinical manifestations, diagnosis and treatment. *Medical Mycology*, *47*(1), 3–15.
- Quevillon, E., Silventoinen, V., Pillai, S., Harte, N., Mulder, N., Apweiler, R., & Lopez, R. (2005). InterProScan: protein domains identifier. *Nucleic Acids Research*, *33*, W116–W120.
- Rajendran, C., Khaitan, B. K., Mittal, R., Ramam, M., Bhardwaj, M., & Datta, K. K. (2003). Phaeohyphomycosis caused by *Exophiala spinifera* in India. *Medical Mycology*, *41*(5), 437–441.
- Rajput, D. K., Mehrotra, A., Srivastav, A. K., Kumar, R., & Rao, R. N. (2011). Cerebral phaeohyphomycosis mimicking glioma. *Pan Arab Journal of Neurosurgery*, *15*(1), 87–90.
- Ramanan, N., & Wang, Y. (2000). A high-affinity iron permease essential for *Candida albicans* virulence. *Science*, *288*(5468), 1062–1064.
- Rawlings, N. D., Barrett, A. J., & Bateman, A. (2012). MEROPS: the database of proteolytic enzymes, their substrates and inhibitors. *Nucleic Acids Research*, *40*, D343–D350.

- Reichard, U., Cole, G. T., Röchel, R., & Monod, M. (2000). Molecular cloning and targeted deletion of PEP2 which encodes a novel aspartic proteinase from *Aspergillus fumigatus*. *International Journal of Medical Microbiology*, 290(1), 85–96.
- Reichard, U., Monod, M., Odds, F., & Röchel, R. (1997). Virulence of an aspergillopepsin-deficient mutant of *Aspergillus fumigatus* and evidence for another aspartic proteinase linked to the fungal cell wall. *Journal of Medical and Veterinary Mycology*, 35(3), 189–196.
- Revankar, S. G. (2007). Dematiaceous fungi. *Mycoses*, 50(2), 91–101.
- Revankar, S. G., & Sutton, D. A. (2010). Melanized fungi in human disease. *Clinical Microbiology Reviews*, 23(4), 884–928.
- Revankar, S. G., Sutton, D. A., & Rinaldi, M. G. (2004). Primary central nervous system phaeohyphomycosis: a review of 101 cases. *Clinical Infectious Diseases*, 38(2), 206–216.
- Rhoads, A., & Au, K. F. (2015). PacBio sequencing and its applications. *Genomics, Proteomics & Bioinformatics*, 13(5), 278–289.
- Richards, T. A., & Talbot, N. J. (2013). Horizontal gene transfer in osmotrophs: playing with public goods. *Nature Reviews Microbiology*, 11(10), 720–727.
- Roberts, R. J., Carneiro, M. O., & Schatz, M. C. (2013). The advantages of SMRT sequencing. *Genome Biology*, 14(7), 405.
- Rodier, M. H., el Moudni, B., Kauffmann-Lacroix, C., Daniault, G., & Jacquemin, J. L. (1999). A *Candida albicans* metallopeptidase degrades constitutive proteins of extracellular matrix. *FEMS Microbiology Letters*, 177(2), 205–210.
- Rodríguez-Navarro, A. (2000). Potassium transport in fungi and plants. *Biochimica et Biophysica Acta*, 1469(1), 1–30.
- Romano, C., Bilenchi, R., Alessandrini, C., & Miracco, C. (1999). Case report. Cutaneous phaeohyphomycosis caused by *Cladosporium oxysporum*. *Mycoses*, 42, 111–115.
- Ronquist, F., Huelsenbeck, J., & Teslenko, M. (2011). *Draft MrBayes version 3.2 Manual : Tutorials and Model Summaries*.
- Rosa, L. H., Almeida Vieira, M. D. L., Santiago, I. F., & Rosa, C. A. (2010). Endophytic fungi community associated with the dicotyledonous plant *Colobanthus quitensis* (Kunth) Bartl. (Caryophyllaceae) in Antarctica. *FEMS Microbiology Ecology*, 73(1), 178–189.
- Rossmann, S. N., Cernoch, P. L., & Davis, J. R. (1996). Dematiaceous fungi are an increasing cause of human disease. *Clinical Infectious Diseases*, 22(1), 73–80.

- Rouxel, T., Grandaubert, J., Hane, J. K., Hoede, C., van de Wouw, A. P., Couloux, A., ... Howlett, B. J. (2011). Effector diversification within compartments of the *Leptosphaeria maculans* genome affected by Repeat-Induced Point mutations. *Nature Communications*, 2, 202.
- Rutherford, K., Parkhill, J., Crook, J., Horsnell, T., Rice, P., Rajandream, M. A., & Barrell, B. (2000). Artemis: sequence visualization and annotation. *Bioinformatics*, 16(10), 944–945.
- Ryberg, M., Kristiansson, E., Sjökvist, E., & Nilsson, R. H. (2009). An outlook on the fungal internal transcribed spacer sequences in GenBank and the introduction of a web-based tool for the exploration of fungal diversity. *New Phytologist*, 181(2), 471–477.
- Safavi, S. A., Shah, F. A., Pakdel, A. K., Reza Rasoulia, G., Bandani, A. R., & Butt, T. M. (2007). Effect of nutrition on growth and virulence of the entomopathogenic fungus *Beauveria bassiana*. *FEMS Microbiology Letters*, 270(1), 116–123.
- Saint-jean, M., St-germain, G., Laferrière, C., & Tapiero, B. (2007). Hospital-acquired phaeohyphomycosis due to *Exserohilum rostratum* in child with leukemia. *Canadian Journal of Infection Diseases Medical Microbiology*, 18(3), 200–202.
- Samerpitak, K., Van der Linde, E., Choi, H.-J., Gerrits van den Ende, A. H. G., Machouart, M., Gueidan, C., & de Hoog, G. S. (2013). Taxonomy of *Ochroconis*, genus including opportunistic pathogens on humans and animals. *Fungal Diversity*, 65(1), 89–126.
- Santana, M. F., & Queiroz, M. V. (2015). Transposable elements in fungi: A genomic approach. *Scientific Journal of Genetics and Gene Therapy*, 1(1), 12–16.
- Scharf, D. H., Heinekamp, T., & Brakhage, A. A. (2014). Human and plant fungal pathogens: The role of secondary metabolites. *PLoS Pathogens*, 10(1), e1003859.
- Scheller, H. V., & Ulvskov, P. (2010). Hemicelluloses. *Annual Review of Plant Biology*, 61(1), 263–289.
- Schmaler-Ripcke, J., Sugareva, V., Gebhardt, P., Winkler, R., Kniemeyer, O., Heinekamp, T., & Brakhage, A. A. (2009). Production of pyomelanin, a second type of melanin, via the tyrosine degradation pathway in *Aspergillus fumigatus*. *Applied and Environmental Microbiology*, 75(2), 493–503.
- Schmid-Grendelmeier, P., & Cramer, R. (2001). Recombinant allergens for skin testing. *International Archives of Allergy and Immunology*, 125(2), 96–111.
- Schmidhauser, T. J., Lauter, F. R., Russo, V. E., & Yanofsky, C. (1990). Cloning, sequence, and photoregulation of *al-1*, a carotenoid biosynthetic gene of *Neurospora crassa*. *Molecular and Cellular Biology*, 10(10), 5064–5070.

- Schneider, P. B., Denk, U., Breitenbach, M., Richter, K., Schmid-Grendelmeier, P., Nobbe, S., ... Simon-Nobbe, B. (2006). *Alternaria alternata* NADP-dependent mannitol dehydrogenase is an important fungal allergen. *Clinical and Experimental Allergy*, 36(12), 1513–1524.
- Schrettl, M., Bignell, E., Kragl, C., Joechl, C., Rogers, T., Arst, H. N., ... Haas, H. (2004a). Siderophore biosynthesis but not reductive iron assimilation is essential for *Aspergillus fumigatus* virulence. *The Journal of Experimental Medicine*, 200(9), 1213–1219.
- Schrettl, M., Bignell, E., Kragl, C., Sabiha, Y., Loss, O., Eisendle, M., ... Haas, H. (2007). Distinct roles for intra- and extracellular siderophores during *Aspergillus fumigatus* infection. *PLoS Pathogens*, 3(9), 1195–1207.
- Schrettl, M., Kim, H. S., Eisendle, M., Kragl, C., Nierman, W. C., Heinekamp, T., ... Haas, H. (2008). SreA-mediated iron regulation in *Aspergillus fumigatus*. *Molecular Microbiology*, 70(1), 27–43.
- Schrettl, M., Winkelmann, G., & Haas, H. (2004b). Ferrichrome in *Schizosaccharomyces pombe* – an iron transport and iron storage compound. *Biometals*, 17(6), 647–654.
- Schubert, K., Groenewald, J. Z., Braun, U., Dijksterhuis, J., Starink, M., Hill, C. F., ... Crous, P. W. (2007). Biodiversity in the *Cladosporium herbarum* complex (Davidiellaceae, Capnodiales), with standardisation of methods for *Cladosporium* taxonomy and diagnostics. *Studies in Mycology*, 58, 105–156.
- Schuemann, J., & Hertweck, C. (2009). Biosynthesis of fungal polyketides. In *Physiology and Genetics* (pp. 331–351). Berlin, Heidelberg: Springer Berlin Heidelberg.
- Schümann, J., & Hertweck, C. (2007). Molecular basis of cytochalasan biosynthesis in fungi: gene cluster analysis and evidence for the involvement of a PKS-NRPS hybrid synthase by RNA silencing. *Journal of the American Chemical Society*, 129(31), 9564–9565.
- Seenivasan, A., Subhagar, S., Aravindan, R., & Viruthagiri, T. (2008). Microbial production and biomedical applications of lovastatin. *Indian Journal of Pharmaceutical Sciences*, 70(6), 701–709.
- Selbmann, L., Egidi, E., Isola, D., Onofri, S., Zucconi, L., de Hoog, G. S., ... Varese, G. C. (2013). Biodiversity, evolution and adaptation of fungi in extreme environments. *Plant Biosystems*, 147(1), 237–246.
- Severo, C. B., Oliveira, F. de M., Pilar, E. F. S., & Severo, L. C. (2012). Phaeohyphomycosis: a clinical-epidemiological and diagnostic study of eighteen cases in Rio Grande do Sul, Brazil. *Memórias Do Instituto Oswaldo Cruz*, 107(7), 854–858.

- Shah, F. A., Wang, C. S., & Butt, T. M. (2005). Nutrition influences growth and virulence of the insect-pathogenic fungus *Metarhizium anisopliae*. *FEMS Microbiology Letters*, 251(2), 259–266.
- Sharma, P., Meena, P. D., & Chauhan, J. S. (2013). First Report of *Nigrospora oryzae* (Berk. & Broome) Petch Causing Stem Blight on *Brassica juncea* in India. *Journal of Phytopathology*, 161(6), 439–441.
- Sharma, P., Singh, N., & Verma, O. P. (2012). First report of *Curvularia* leaf spot, caused by *Curvularia affinis* on *Dalbergia sissoo*. *Forest Pathology*, 42(3), 265–266.
- Sharpton, T. J., Stajich, J. E., Rounsley, S. D., Gardner, M. J., Wortman, J. R., Jordan, V. S., ... Taylor, J. W. (2009). Comparative genomic analyses of the human fungal pathogens *Coccidioides* and their relatives. *Genome Research*, 19(10), 1722–1731.
- Shoulders, M. D., & Raines, R. T. (2009). Collagen structure and stability. *Annual Review of Biochemistry*, 78, 929–958.
- Simon-Nobbe, B., Denk, U., Pöll, V., Rid, R., & Breitenbach, M. (2008). The spectrum of fungal allergy. *International Archives of Allergy and Immunology*, 145(1), 58–86.
- Singh, S. M., & Barde, A. K. (1990). Non- dermatophytes as emerging opportunistic causal agents of superficial mycoses at Balaghat (M.P). *Indian Journal of Dermatology, Venereology and Leprology*, 56(4), 289–292.
- So, K.-K., Kim, J.-M., Nguyen, N.-L., Park, J.-A., Kim, B.-T., Park, S.-M., ... Kim, D.-H. (2012). Rapid screening of an ordered fosmid library to clone multiple polyketide synthase genes of the phytopathogenic fungus *Cladosporium phlei*. *Journal of Microbiological Methods*, 91(3), 412–419.
- Solomon, P. S., Lowe, R. G. T., Tan, K.-C., Waters, O. D. C., & Oliver, R. P. (2006). *Stagonospora nodorum*: cause of *Stagonospora nodorum* blotch of wheat. *Molecular Plant Pathology*, 7(3), 147–156.
- Soumagne, T., Pana-Katatali, H., Degano, B., & Dalphin, J.-C. (2015). Combined pulmonary fibrosis and emphysema in hypersensitivity pneumonitis. *BMJ Case Reports*, 2015, bcr2015211560.
- Sriranganadane, D., Reichard, U., Salamin, K., Fratti, M., Jousson, O., Waridel, P., ... Monod, M. (2011). Secreted glutamic protease rescues aspartic protease Pep deficiency in *Aspergillus fumigatus* during growth in acidic protein medium. *Microbiology*, 157, 1541–1550.
- Sriranganadane, D., Waridel, P., Salamin, K., Reichard, U., Grouzmann, E., Neuhaus, J.-M., ... Monod, M. (2010). *Aspergillus* protein degradation pathways with different secreted protease sets at neutral and acidic pH. *Journal of Proteome Research*, 9(7), 3511–3519.

- St Leger, R. J., Joshi, L., & Roberts, D. W. (1997). Adaptation of proteases and carbohydrates of saprophytic, phytopathogenic and entomopathogenic fungi to the requirements of their ecological niches. *Microbiology*, *143*, 1983–1992.
- Stamatakis, A. (2006). RAxML-VI-HPC: maximum likelihood-based phylogenetic analyses with thousands of taxa and mixed models. *Bioinformatics*, *22*(21), 2688–2690.
- Sutton, D. A., Timm, W. D., Morgan-Jones, G., & Rinaldi, M. G. (1999). Human phaeohyphomycotic osteomyelitis caused by the coelomycete *Phomopsis saccardo* 1905: criteria for identification, case history, and therapy. *Journal of Clinical Microbiology*, *37*(3), 807–811.
- Tamsikar, J., Naidu, J., & Singh, S. M. (2006). Phaeohyphomycotic sebaceous cyst due to *Cladosporium cladosporioides*: case report and review of literature. *Journal of Medical Mycology*, *16*(1), 55–57.
- Tangen, K. L., Jung, W. H., Sham, A. P., Lian, T., & Kronstad, J. W. (2007). The iron- and cAMP-regulated gene SIT1 influences ferrioxamine B utilization, melanization and cell wall structure in *Cryptococcus neoformans*. *Microbiology*, *153*, 29–41.
- Tasic, S. ., & Tasic, N. (2007). *Cladosporium* spp.- cause of opportunistic mycoses. *Acta Fac Med Naiss*, *24*(1), 15–19.
- Tatusov, R. L., Fedorova, N. D., Jackson, J. D., Jacobs, A. R., Kiryutin, B., Koonin, E. V, ... Natale, D. A. (2003). The COG database: an updated version includes eukaryotes. *BMC Bioinformatics*, *4*, 41.
- Tendolkar, U., Tayal, R., Baveja, S., & Shinde, C. (2015). Mycotic keratitis due to *Neoscytalidium dimidiatum*: A rare case. *Community Acquired Infection*, *2*(4), 142–144.
- Thia, L. P., & Balfour Lynn, I. M. (2009). Diagnosing allergic bronchopulmonary aspergillosis in children with cystic fibrosis. *Paediatric Respiratory Reviews*, *10*(1), 37–42.
- Thomas, W. R. (2011). The advent of recombinant allergens and allergen cloning. *The Journal of Allergy and Clinical Immunology*, *127*(4), 855–859.
- Tsai, H. F., Fujii, I., Watanabe, A., Wheeler, M. H., Chang, Y. C., Yasuoka, Y., ... Kwon-Chung, K. J. (2001). Pentaketide melanin biosynthesis in *Aspergillus fumigatus* requires chain-length shortening of a heptaketide precursor. *The Journal of Biological Chemistry*, *276*(31), 29292–29298.
- Tsui, C. K. M., Woodhall, J., Chen, W., Andrélévesque, C., Lau, A., Schoen, C. D., ... de Hoog, S. G. (2011). Molecular techniques for pathogen identification and fungus detection in the environment. *IMA Fungus*, *2*(2), 177–189.

- Tsunoda, T., & Takagi, T. (1999). Estimating transcription factor bindability on DNA. *Bioinformatics*, *15*, 622–630.
- Tudzynski, P., Hölter, K., Correia, T., Arntz, C., Grammel, N., & Keller, U. (1999). Evidence for an ergot alkaloid gene cluster in *Claviceps purpurea*. *Molecular and General Genetics*, *261*(1), 133–141.
- Vailes, L., Sridhara, S., Cromwell, O., Weber, B., Breitenbach, M., & Chapman, M. (2001). Quantitation of the major fungal allergens, Alt a 1 and Asp f 1, in commercial allergenic products. *The Journal of Allergy and Clinical Immunology*, *107*(4), 641–646.
- van Baarlen, P., van Belkum, A., Summerbell, R. C., Crous, P. W., & Thomma, B. P. H. J. (2007). Molecular mechanisms of pathogenicity: how do pathogenic microorganisms develop cross-kingdom host jumps? *FEMS Microbiology Reviews*, *31*(3), 239–277.
- van Belkum, A., Fahal, A., & van de Sande, W. W. J. (2013). Mycetoma caused by *Madurella mycetomatis*: a completely neglected medico-social dilemma. *Advances in Experimental Medicine and Biology*, *764*, 179–189.
- van den Brink, J., & de Vries, R. P. (2011). Fungal enzyme sets for plant polysaccharide degradation. *Applied Microbiology and Biotechnology*, *91*(6), 1477–1492.
- van Heesch, S., Kloosterman, W. P., Lansu, N., Ruzius, F.-P., Levandowsky, E., Lee, C. C., ... Cuppen, E. (2013). Improving mammalian genome scaffolding using large insert mate-pair next-generation sequencing. *BMC Genomics*, *14*, 257.
- Van Lanen, S. G., & Shen, B. (2006). Microbial genomics for the improvement of natural product discovery. *Current Opinion in Microbiology*, *9*(3), 252–260.
- Varga, J., Houbraeken, J., Van Der Lee, H. A. L., Verweij, P. E., & Samson, R. A. (2008). *Aspergillus calidoustus* sp. nov., causative agent of human infections previously assigned to *Aspergillus ustus*. *Eukaryotic Cell*, *7*(4), 630–638.
- Vasanthakumar, A., DeAraujo, A., Mazurek, J., Schilling, M., & Mitchell, R. (2015). Pyomelanin production in *Penicillium chrysogenum* is stimulated by L-tyrosine. *Microbiology*, *161*(6), 1211–1218.
- Vieira, M. R., Milheiro, A., & Pacheco, F. A. (2001). Phaeohyphomycosis due to *Cladosporium cladosporioides*. *Medical Mycology*, *39*(1), 135–137.
- Volling, K., Thywissen, A., Brakhage, A. A., & Saluz, H. P. (2011). Phagocytosis of melanized *Aspergillus* conidia by macrophages exerts cytoprotective effects by sustained PI3K/Akt signalling. *Cellular Microbiology*, *13*(8), 1130–1148.

- Wallner, A., Blatzer, M., Schrettl, M., Sarg, B., Lindner, H., & Haas, H. (2009). Ferricrocin, a siderophore involved in intra- and transcellular iron distribution in *Aspergillus fumigatus*. *Applied and Environmental Microbiology*, 75(12), 4194–4196.
- Wallwey, C., & Li, S.-M. (2011). Ergot alkaloids: structure diversity, biosynthetic gene clusters and functional proof of biosynthetic genes. *Natural Product Reports*, 28(3), 496–510.
- Walsh, T. J., Groll, A., Hiemenz, J., Fleming, R., Roilides, E., & Anaissie, E. (2004). Infections due to emerging and uncommon medically important fungal pathogens. *Clinical Microbiology and Infection*, 1, 48–66.
- Wang, C., Zhang, S., Hou, R., Zhao, Z., Zheng, Q., Xu, Q., ... Xu, J.-R. (2011). Functional analysis of the kinome of the wheat scab fungus *Fusarium graminearum*. *PLoS Pathogens*, 7(12), e1002460.
- Wang, L., She, X., Lv, G., Shen, Y., Cai, Q., Zeng, R., ... Liu, W. (2013). Cutaneous and mucosal phaeohyphomycosis caused by *Exophiala spinifera* in a pregnant patient: case report and literature review. *Mycopathologia*, 175, 331–338.
- Wang, L. Y., & Shiozaki, K. (2006). The fission yeast stress MAPK cascade regulates the *pmp3⁺* gene that encodes a highly conserved plasma membrane protein. *FEBS Letters*, 580(10), 2409–2413.
- Weber, S. S., Bovenberg, R. A. L., & Driessen, A. J. M. (2012). Biosynthetic concepts for the production of β -lactam antibiotics in *Penicillium chrysogenum*. *Biotechnology Journal*, 7(2), 225–236.
- Weichel, M., Schmid-Grendelmeier, P., Rhyner, C., Achatz, G., Blaser, K., & Cramer, R. (2003). Immunoglobulin E-binding and skin test reactivity to hydrophobin HCh-1 from *Cladosporium herbarum*, the first allergenic cell wall component of fungi. *Clinical and Experimental Allergy*, 33(1), 72–77.
- Wheeler, D. A., Srinivasan, M., Egholm, M., Shen, Y., Chen, L., McGuire, A., ... Rothberg, J. M. (2008). The complete genome of an individual by massively parallel DNA sequencing. *Nature*, 452(7189), 872–876.
- Wheeler, M. H., Abramczyk, D., Puckhaber, L. S., Naruse, M., Ebizuka, Y., Fujii, I., & Szaniszlo, P. J. (2008). New biosynthetic step in the melanin pathway of *Wangiella (Exophiala) dermatitidis*: evidence for 2-acetyl-1,3,6,8-tetrahydroxynaphthalene as a novel precursor. *Eukaryotic Cell*, 7(10), 1699–1711.
- White, T. J., Burns, T., Lee, S., & Taylor, J. (1990). Amplification and direct sequencing of fungal ribosomal RNA genes for phylogenetics. In M. A. Innis, D. H. Gelfand, J. J. Sninsky, & T. J. White (Eds.), *PCR protocols: A guide to methods and applications* (1st ed., pp. 315–322). New York: Academic Press.

- Wood, V., Gwilliam, R., Rajandream, M.-A., Lyne, M., Lyne, R., Stewart, A., ... Cerrutti, L. (2002). The genome sequence of *Schizosaccharomyces pombe*. *Nature*, *415*(6874), 871–880.
- Wu, G., Sun, X., Yu, G., Wang, W., Zhu, T., Gu, Q., & Li, D. (2014a). Cladosins A–E, hybrid polyketides from a deep-sea-derived fungus, *Cladosporium sphaerospermum*. *Journal of Natural Products*, *77*(2), 270–275.
- Wu, J. B., Zhang, C. L., Mao, P. P., Qian, Y. S., & Wang, H. Z. (2014b). First report of leaf spot caused by *Nigrospora oryzae* on *Dendrobium candidum* in China. *Plant Disease*, *98*(7), 996.
- Xiao, Z., Gao, P., Qu, Y., & Wang, T. (2001). Cellulose-binding domain of endoglucanase III from *Trichoderma reesei* disrupting the structure of cellulose. *Biotechnology Letters*, *220*, 711–715.
- Yano, S., Koyabashi, K., & Kato, K. (2003). Intrabronchial lesion due to *Cladosporium sphaerospermum* in a healthy, non-asthmatic woman. *Mycoses*, *46*(8), 348–350.
- Ye, J., Coulouris, G., Zaretskaya, I., Cutcutache, I., Rozen, S., & Madden, T. L. (2012). Primer-BLAST: a tool to design target-specific primers for polymerase chain reaction. *BMC Bioinformatics*, *13*(1), 134.
- Ye, J., Fang, L., Zheng, H., Zhang, Y., Chen, J., Zhang, Z., ... Wang, J. (2006). WEGO: A web tool for plotting GO annotations. *Nucleic Acids Research*, *34*, 293–297.
- Yew, S. M., Chan, C. L., Kuan, C. S., Toh, Y. F., Ngeow, Y. F., Na, S. L., ... Ng, K. P. (2016). The genome of newly classified *Ochroconis mirabilis*: Insights into fungal adaptation to different living conditions. *BMC Genomics*, *17*(1), 91.
- Yike, I. (2011). Fungal proteases and their pathophysiological effects. *Mycopathologia*, *171*(5), 299–323.
- Yin, Y., Mao, X., Yang, J., Chen, X., Mao, F., & Xu, Y. (2012). dbCAN: a web resource for automated carbohydrate-active enzyme annotation. *Nucleic Acids Research*, *40*, W445–W451.
- Yu, G.-H., Wu, G.-W., Zhu, T.-J., Gu, Q.-Q., & Li, D.-H. (2015). Cladosins F and G, two new hybrid polyketides from the deep-sea-derived *Cladosporium sphaerospermum* 2005-01-E3. *Journal of Asian Natural Products Research*, *17*(2), 120–124.
- Yu, J. (2012). Current understanding on aflatoxin biosynthesis and future perspective in reducing aflatoxin contamination. *Toxins*, *4*(12), 1024–1057.
- Yuan, W. M., Gentil, G. D., Budde, A. D., & Leong, S. A. (2001). Characterization of the *Ustilago maydis* *sid2* gene, encoding a multidomain peptide synthetase in the ferrichrome biosynthetic gene cluster. *Journal of Bacteriology*, *183*(13), 4040–4051.

- Yun, C. W., Ferea, T., Rashford, J., Ardon, O., Brown, P. O., Botstein, D., ... Philpott, C. C. (2000). Desferrioxamine-mediated iron uptake in *Saccharomyces cerevisiae*. Evidence for two pathways of iron uptake. *The Journal of Biological Chemistry*, 275(14), 10709–10715.
- Zajc, J., Liu, Y., Dai, W., Yang, Z., Hu, J., Gostinčar, C., & Gunde-Cimerman, N. (2013). Genome and transcriptome sequencing of the halophilic fungus *Wallemia ichthyophaga*: haloadaptations present and absent. *BMC Genomics*, 14(1), 617.
- Zalar, P., de Hoog, G. S., Schroers, H.-J., Crous, P. W., Groenewald, J. Z., & Gunde-Cimerman, N. (2007). Phylogeny and ecology of the ubiquitous saprobe *Cladosporium sphaerospermum*, with descriptions of seven new species from hypersaline environments. *Studies in Mycology*, 58, 157–183.
- Zaugg, C., Jousson, O., Léchenne, B., Staib, P., & Monod, M. (2008). *Trichophyton rubrum* secreted and membrane-associated carboxypeptidases. *International Journal of Medical Microbiology*, 298, 669–682.
- Zerbino, D. R., & Birney, E. (2008). Velvet: algorithms for de novo short read assembly using de Bruijn graphs. *Genome Research*, 18(5), 821–829.
- Zhang, J., Chiodini, R., Badr, A., & Zhang, G. (2011). The impact of next-generation sequencing on genomics. *Journal of Genetics and Genomics*, 38(3), 95–109.
- Zhang, Y., Crous, P. W., Schoch, C. L., & Hyde, K. D. (2012). Pleosporales. *Fungal Diversity*, 53(1), 1–221.
- Zhao, X., Mehrabi, R., & Xu, J.-R. (2007). Mitogen-activated protein kinase pathways and fungal pathogenesis. *Eukaryotic Cell*, 6(10), 1701–1714.
- Zhao, Z., Liu, H., Wang, C., & Xu, J.-R. (2014). Correction: Comparative analysis of fungal genomes reveals different plant cell wall degrading capacity in fungi. *BMC Genomics*, 15, 6.
- Zhdanova, N. N., Zakharchenko, V. A., Vember, V. V., & Nakonechnaya, L. T. (2000). Fungi from Chernobyl: mycobiota of the inner regions of the containment structures of the damaged nuclear reactor. *Mycological Research*, 104(12), 1421–1426.

LIST OF PUBLICATIONS AND PAPERS PRESENTED

Published manuscripts

- Yew, S. M.**, Chan, C. L., Ngeow, Y. F., Toh, Y. F., Na, S. L., Lee, K. W. ... Kuan, C. S. (2016). Insight into different environmental niches adaptation and allergenicity from the *Cladosporium sphaerospermum* genome, a common human allergy-eliciting Dothideomycetes. *Scientific Reports*, 6, 27008.
- Yew, S. M.**, Chan, C. L., Kuan, C. S., Toh, Y. F., Ngeow, Y. F., Na, S. L., ... Ng, K. P. (2016). The genome of newly classified *Ochroconis mirabilis*: Insights into fungal adaptation to different living conditions. *BMC Genomics*, 17(1), 91.
- Yew, S. M.**, Chan, C. L., Lee, K. W., Na, S. L., Tan, R., Hoh, C.-C., ... Ng, K. P. (2014). A Five-Year Survey of Dematiaceous Fungi in a Tropical Hospital Reveals Potential Opportunistic Species. *PLoS ONE*, 9(8), e104352.
- Yew, S. M.**, Chan, C. L., Soo-Hoo, T. S., Na, S. L., Ong, S. S., Hassan, H., ... Ng, K. P. (2013). Draft Genome Sequence of Dematiaceous Coelomycete *Pyrenochaeta* sp. Strain UM 256, Isolated from Skin Scraping. *Genome Announcements*, 1(3), e00158–13–e00158–13.
- Ng, K. P., **Yew, S. M.**, Chan, C. L., Chong, J., Tang, S. N., Soo-Hoo, T. S., ... Yee, W. Y. (2013). Draft Genome Sequence of the First Isolate of Extensively Drug-Resistant (XDR) *Mycobacterium tuberculosis* in Malaysia. *Genome Announcements*, 1(1), e00056–12–e00056–12.
- Ng, K. P., **Yew, S. M.**, Chan, C. L., Tan, R., Soo-Hoo, T. S., Na, S. L., ... Yee, W.-Y. (2013). Draft Genome Sequence of *Herpotrichiellaceae* sp. UM 238 Isolated from Human Skin Scraping. *Genome Announcements*, 1(1), 3–4.
- Ng, K. P., **Yew, S. M.**, Chan, C. L., Soo-Hoo, T. S., Na, S. L., Hassan, H., ... Yee, W. Y. (2012a). Genome sequence of an unclassified *Pleosporales* species isolated from human nasopharyngeal aspirate. *Eukaryotic Cell*, 11(6), 828.
- Ng, K. P., **Yew, S. M.**, Chan, C. L., Soo-Hoo, T. S., Na, S. L., Hassan, H., ... Yee, W.-Y. (2012b). Sequencing of *Cladosporium sphaerospermum*, a Dematiaceous fungus isolated from blood culture. *Eukaryotic Cell*, 11(5), 705–706.
- Ng, K. P., Ngeow, Y. F., **Yew, S. M.**, Hassan, H., Soo-Hoo, T. S., Na, S. L., ... Yee, W.-Y. (2012c). Draft genome sequence of *Daldinia eschscholzii* isolated from blood culture. *Eukaryotic Cell*, 11(5), 703–4.

- Ng, K. P., Chan, C. L., **Yew, S. M.**, Yeo, S. K., Toh, Y. F., Looi, H. K., ... Kuan, C. S. (2016). Identification and characterization of *Daldinia eschscholtzii* isolated from skin scrapings, nails, and blood. *PeerJ*, 4, e2637.
- Toh, Y. F., **Yew, S. M.**, Chan, C. L., Na, S. L., Lee, K. W., Hoh, C.-C., ... Kuan, C. S. (2016). Genome Anatomy of *Pyrenochaeta unguis-hominis* UM 256, a Multidrug Resistant Strain Isolated from Skin Scraping. *PLOS ONE*, 11(9), e0162095.
- Kuan, C. S., **Yew, S. M.**, Chan, C. L., Toh, Y. F., Lee, K. W., Cheong, W.-H., ... Ng, K. P. (2016). DemaDb: an integrated dematiaceous fungal genomes database. *Database*, 2016, baw008.
- Kuan, C. S., **Yew, S. M.**, Toh, Y. F., Chan, C. L., Lim, S. K., Lee, K. W., ... Ng, K. P. (2015). Identification and Characterization of a Rare Fungus, *Quambalaria cyanescens*, Isolated from the Peritoneal Fluid of a Patient after Nocturnal Intermittent Peritoneal Dialysis. *PLOS ONE*, 10(12), e0145932.
- Chan, C. L., **Yew, S. M.**, Ngeow, Y. F., Na, S. L., Lee, K. W., & Hoh, C. (2015). Genome analysis of *Daldinia eschscholtzii* strains UM 1400 and UM 1020, wood- decaying fungi isolated from human hosts. *BMC Genomics*, 1–14.
- Kuan, C. S., **Yew, S. M.**, Toh, Y. F., Chan, C. L., Ngeow, Y. F., Lee, K. W., ... Ng, K. P. (2015). Dissecting the fungal biology of *Bipolaris papendorffii*: from phylogenetic to comparative genomic analysis. *DNA Research*, 22(3), 219–232.
- Chan, C. L., **Yew, S. M.**, Na, S. L., Tan, Y.-C., Lee, K. W., Yee, W.-Y., ... Ng, K. P. (2014). Draft Genome Sequence of *Ochroconis constricta* UM 578, Isolated from Human Skin Scraping. *Genome Announcements*, 2(2), e00074–14.
- Looi, H. K., Toh, Y. F., **Yew, S. M.**, Na, S. L., Tan, Y.-C., Chong, P.-S., ... Kuan, C. S. (2017). Genomic insight into pathogenicity of dematiaceous fungus *Corynespora cassiicola*. *PeerJ*, 5, e2841.
- Kuan, C. S., Chan, C. L., **Yew, S. M.**, Toh, Y. F., Khoo, J.-S., Chong, J., ... Ng, K. P. (2015). Genome Analysis of the First Extensively Drug-Resistant (XDR) Mycobacterium tuberculosis in Malaysia Provides Insights into the Genetic Basis of Its Biology and Drug Resistance. *PloS One*, 10(6), e0131694.
- Kuan, C. S., Cham, C. Y., Singh, G., **Yew, S. M.**, Tan, Y. C., Chong, P. S., ... Ng, K. P. (2016). Genomic analyses of *Cladophialophora bantiana*, a major cause of cerebral phaeohyphomycosis provides insight into its lifestyle, virulence and adaption in host. *PLoS ONE*, 11(8), 1–31.

Kuan, C. S., Ismail, R., Kwan, Z., Yew, S. M., Yeo, S. K., Chan, C. L., ... Ng, K. P. (2016). Isolation and Characterization of an atypical *Metschnikowia* sp. Strain from the Skin Scraping of a Dermatitis Patient. *PLoS ONE*, 11(6), e0156119.

Attended conferences

Impact of Molecular approaches in Mycology Laboratory. Updates and Dilemmas in Pathology. 15th Annual Scientific Meeting, College of Pathologists, Academy of Medicine Malaysia, Hotel Pullman, Putrajaya, Malaysia (Poster presenter)

Characterization of newly classified *Ochroconis mirabilis* UM 578 genome, isolated from human sample reveals its adaptation to different living conditions. 7th World DNA and Genome Day 2016, Dalian International Conference Center (DICC), Dalian, China (Oral presenter)

The Draft Genome of *Ochroconis mirabilis* UM 578 isolated from human skin scraping. Infectious 2015 Conference, Putrajaya Marriott Hotel, Putrajaya, Malaysia (Poster presenter)

Draft Genome Sequencing of *Cladosporium sphaerospermum* isolated from blood culture. 17th Biological Sciences Graduate Congress (BSGC) 2012, Chulalongkorn University, Bangkok, Thailand (Oral presenter)

MOLECULAR IDENTIFICATION OF *CLADOSPORIUM* SPECIES FROM CLINICAL SPECIMENS. International Congress of the Malaysian Society for Microbiology 2011, Bayview Beach Resort, Penang, Malaysia (Poster presenter)